2008:39

LICENTIATE THESIS

FRP shear strengthening of RC beams and walls

Gabriel Sas

Luleå University of Technology
Department of Civil, Mining and Environmental Engineering
Division of Structural engineering

2008:39 | ISSN: 1402-1757 | ISRN: LTU-LIC -- 08/39 -- SE

LULEÅ
UNIVERSITY
OF TECHNOLOGY

Licentiate Thesis 2008

FRP shear strengthening of RC beams and walls

Gabriel Sas

Division of Structural Engineering
Department of Civil and Environmental Engineering
Luleå University of Technology
SE-971 87 Luleå
Sweden
http://www.cee.ltu.se/
http://construction.project.ltu.se/

Preface

The present licentiate thesis is the result of the work carried out between May 2006 and November 2008 at the Division of Structural Engineering, Department if Civil, Mining and Environmental Engineering at Luleå University of Technology, Sweden. The work presented in this thesis has been carried out in the research group "Innovative Materials and Structures".

First I would like to thank God for giving me strength and knowledge to carry this work.

I would like to acknowledge the European Network for Composite Reinforcement (εn.core) for providing the financial support for the work presented here.

I would like to thank my supervisor Dr. Anders Carolin for his invaluable scientific and moral support provided during this period. I know sometimes things did not go according to plan but you were always there to guide me on the right path. I really hope we will have the opportunity to work again in the close future. I will always be grateful to my co-supervisor Prof. Björn Täljsten for showing high interest for the shear strengthening work, for the practical applications that he got me involved in and for his positive way of motivating me.

I would also like thank my dear PhD student colleagues and friends: Alann André, Thomas Blanksvärd, Peter Simonsson, Markus Bergtröm and Anders Bennitz for the scientific discussions, deep chats and great parties we had together.

Many thanks for helping me in gathering the basic knowledge about FRP strengthening go to the fellow researchers at the Civil Engineering Department from the Politehnica University of Timişoara, România. I am looking forward to a fruitful and long collaboration.

To pass the long and cold winter days up north, close to the Arctic Circle, I have always had support from all my good friends that I made in Luleå. Since the list of names would be too long to mention here and I don not want to leave anyone out, I would just like to express my gratitude to all of you. You are the best!

Cu siguranţă cea mai importantă parte din viaţa mea e familia. Mamă, tată chiar dacă mii de kilometri ne despart, vreau să ştiti că v-am simţit prezenţa tot timpul. Sunteţi singurele persoane care mă iubesc şi sprijină necondiţionat şi pentru asta am să vă fiu recunoscător toata viaţa. Vă voi iubi mereu.

Luleå, November 2008

Gabriel Sas

Summary

The shear failure of Fibre Reinforced Polymers (FRP) strengthened reinforced concrete (RC) beams has not been studied to the same extent as bending failure mechanism over the past decade. The complex nature of the shear failure mechanism just for reinforced concrete beams is still being debated among scientists and not fully solved yet. If we add the FRP for shear strengthening to the already existing shear problems the failure mechanism becomes more complicated. In other words an extra uncertainty to the already existing ones is complicating more the problem of shear in concrete. It is of utmost importance to understand the shear failure mechanism of reinforced concrete beams and for this all the known theories for designing reinforced concrete beams subjected to shear are presented: truss analogy, theory of plasticity for concrete and modified compression field theory. The use of these theories in two of the most commonly used standards is also exemplified. Further on, a design model for the shear strengthening of concrete beams by using fibre-reinforced polymers (FRP) is presented in one of the appended papers, and the limitations of the truss model analogy are highlighted. The fracture mechanics approach is used in analyzing the bond behaviour between the FRP composites and concrete. The fracture energy of concrete and the axial rigidity of the FRP are considered to be the most important parameters. The effective strain in the FRP when debonding occurs is determined. The limitations of the anchorage length over the cross section are analyzed. A simple iterative design method for the shear debonding is finally proposed. Since the model's predictions are considered satisfactory but not really precise, a deep literature review has been performed. All the significant theoretical models for predicting the shear capacity of FRP strengthened RC beams developed during the years are analyzed, commented on and compared with an extensive experimental database. The database contains the results from more than 200 tests performed in different research institutions across the world. The results of the comparison are not very promising and the use of the additional principle in the actual shear design equations should be questioned. The large scatter between the predicted values of different models and experimental results is of real concern bearing in mind that some of the models are used in present design codes.

Furthermore, the influence of the FRP composites to strengthen openings in RC walls is analyzed. In the same manner as for RC beams the current design methods existing in two of the most commonly used standards are presented. Since the strengthening of RC walls was studied even less than FRP strengthened RC beams an up to date literature review of the experimental and theoretical work is presented. A concept, developed in collaboration with the Civil Engineering Department from Politehnica University of Timişoara, is presented for testing RC walls with openings subjected to

lateral and gravitational loads. From a matrix of 50 different practical configurations of openings 12 walls are selected which make the subject of an ongoing experimental program. Eight walls with different opening configurations are subjected to cyclic lateral loading under constant gravitational load to simulate the seismic behaviour of FRP strengthened walls with openings. Four walls with different opening configurations are to be tested to monotonic gravitational loading up to failure. The possibility for strengthening RC walls with opening is exemplified in a case study. A simplified design procedure for strengthening RC walls with openings is presented. This procedure is considered to be the basis for a future theoretical model that is intended to be derived.

Keywords: reinforced concrete, FRP, strengthening, shear, carbon fibre, model, comparison, walls.

Notations and symbols

General notation list

Roman letters

	Description	*Unit*
a	*Maximum aggregate size*	*[m]*
A_g	*Gross area of the wall panel*	*[m²]*
A_s	*Shear reinforcement area*	*[m²]*
A_{st}	*Tensile reinforcement area for beams*	*[m²]*
A_{sv}	*Steel vertical reinforcement area*	*[m²]*
b	*Width of the cross section*	*[m]*
b_w	*Minimum width of the T cross section*	*[m]*
d	*Lever arm*	*[m]*
D_{frp}	*Stress/strain distribution factor in the FRP*	*[-]*
E_{frp}	*Modulus of elasticity of FRP*	*[N/m²]*
e	*Eccentricity of the load*	*[m]*
e_a	*Additional eccentricity due do deflections in the wall*	*[m]*
f_1	*Principal tensile stress*	*[N/m²]*
f_2	*Principal compressive stress*	*[N/m²]*
f_c'	*Compressive strength of concrete*	*[N/m²]*
f_{cc}'	*Compressive strength of the confined concrete*	*[N/m²]*
f_{c0}	*Compressive strength of the unconfined concrete*	*[N/m²]*
f_{frp}	*Tensile strength of the FRP*	*[N/m²]*
f_y	*Yield stress of steel*	*[N/m²]*
f_{ys}	*Yielding stress of the shear reinforcement*	*[N/m²]*
f_x	*Stress in the longitudinal bars*	*[N/m²]*
f_v	*Stress in the stirrups*	*[N/m²]*

G_f	*Fracture energy of concrete*	*[N/m²xm]*
h	*height of the considered element*	*[m]*
$h_{frp,e}$	*Effective height of the FPR over the cross section*	*[m]*
H	*Height of the wall*	*[m]*
H_0	*Height of the opening in the wall*	*[m]*
H_{we}	*Effective height of the wall*	*[m]*
k_1*and* k_2	*Empirically determined factors for walls with openings*	*[m]*
k_c	*Coefficient depending on the quality of the concrete*	*[-]*
k_φ	*Coefficient depending on the slenderness of the column*	*[-]*
L	*Length of the wall*	*[m]*
L_0	*Length of the opening in the wall*	
L_{max}	*Maximum bond length of the FRP*	*[m]*
L_e	*Effective bond length of the FRP*	*[m]*
L_{cr}	*Critical anchorage length*	*[m]*
M	*Bending moment in the centre of gravity of the cross section*	*[Nm]*
M_d	*Design bending moment*	
M_p	*Yield moment in pure bending*	*[Nm]*
N	*Normal force in the centre of gravity of the cross section*	*[N]*
N_p	*Tension yield load*	*[N]*
N_{ps}	*Design axial load of a solid wall*	*[N/m]*
N_{p0}	*Ultimate load of a wall with opening*	*[N/m]*
N_h	*Horizontal projection of the shear force*	*[N]*
P_i	*Defines arbitrary loads on a rigid body*	*[N]*
Q_i	*Generalized stress*	*[N/m²]*
q_i	*Generalized strain*	*[-]*
$q_{1,2,...}$	*Plastic strains equivalent to the arbitrary loads* P_i	*[-]*
s	*Stirrups spacing*	*[m]*
$s_{m\theta}$	*Average spacing of the cracks*	*[m]*
s_{mx}	*Average crack spacing that would result if the member would be subjected to longitudinal tension*	*[m]*
s_{mv}	*Average crack spacing that would result if the member was*	*[m]*

	subjected to transverse tension	
s_{frp}	*Horizontal spacing of the FRP strips*	*[m]*
t_{frp}	*Thickness of the FRP*	*[m]*
t_w	*Thickness of the wall*	*[m]*
u_i	*Corresponding displacements of loads* P_i	*[m]*
V	*External shear force*	*[N]*
V_c	*Concrete contribution to the shear force capacity of a beam*	*[N]*
V_d	*Design shear force*	*[N]*
V_s	*Steel stirrups contribution to the shear force capacity of a beam*	*[N]*
V_p	*Axial load contribution to the shear force capacity of a beam*	*[N]*
V_i	*Other contributions to the shear capacity of a beam*	*[N]*
V_{frp}	*FRP contribution to the shear capacity*	*[N]*
W	*Work produced by the arbitrary loads* P_i	*[J]*
w_{frp}	*Width of the FRP*	*[m]*
γ_0	*Length of the compressed area used in Theory of Plasticity*	*[m]*
z_t	*Coordinate of the top end of the effective FRP*	*[m]*
z_b	*Coordinate of the bottom end of the effective FRP*	*[m]*

Greek letters

	Description	*Unit*
α	*Angle between shear reinforcement and the beam axis perpendicular to the shear force*	*[-]*
α_1	*Factor considering the bond characteristics of the reinforcement*	*[-]*
α_2	*Factor considering the load type*	*[-]*
α_w	*Experimentally determined factor considering the eccentricity effect*	*[-]*
β	*Fibre alignment angle with respect to the longitudinal axis of the beam*	*[°]*
β_w	*Experimentally determined factor considering the aspect ratio and the slenderness of the wall*	*[-]*
ε_x	*Longitudinal strain*	*[-]*
ε_t	*Transversals strain*	*[-]*
ε_1	*Principal tensile strain*	*[-]*

ε_2	*Principal compressive strain*	*[-]*
ε_{bond}	*Strain in fibre at debonding failure*	*[-]*
$\varepsilon_{c,max}$	*Strain in the fibre depending on the concrete contribution*	*[-]*
$\varepsilon_{frp,e}$	*Effective strain in the FRP*	*[-]*
$\varepsilon_{frp,u}$	*Ultimate strain in the FRP*	*[-]*
γ_{frp}	*Partial safety factor for FRP*	*[-]*
γ_{xy}	*Shear strain*	*[-]*
φ_{ef}	*Effective creep number*	*[-]*
θ	*Crack inclination angle with respect to the longitudinal axis of the beam*	*[°]*
λ	*Normalized maximum bond length*	*[-]*
λ_p	*Non dimensional factor used in defining the plasticity*	*[-]*
μ	*Proportionality factor used for determining the yield condition*	*[-]*
μ_π	*Proportionality factor when the yield condition is fulfilled*	*[-]*
η_{frp}	*Stress distribution factor in the FRP over the cross section of a beam, equals 0.6.*	*[-]*
η_0	*Position of the centre of gravity of the opening with respect to the left edge of the wall*	*[m]*
$\overline{\eta}$	*Position of the centre of gravity of a wall with opening with respect to the left edge of the wall*	*[m]*
ρ_{frp}	*FRP reinforcement ratio*	*[-]*
σ_ℓ	*confinement pressure provided by the FRP*	*[N/m²]*
$\sigma_{frp,max}$	*Maximum stress in fibres*	*[N/m²]*
υ_{ci}	*Shear stresses along the crack defined in the Compressive Field Theory*	*[N/m²]*
ω	*is the crack width*	*[m]*
χ	*Non dimensional factor accoutring for the geometrical properties of a wall with openings*	*[-]*
τ^2_{max}	*Shear stress of the concrete in a bonded element*	*[N/m²]*
ζ	*Factor considering the effective bonded area at the top and bottom of the beam*	*[-]*

Eurocode (2004a, b and 2005) notation list

Roman letters

	Description	*Unit*
A_{sl}	*is the area of tensile reinforcement, which extends beyond the section considered*	*[m²]*
A_C	*Area of concrete cross section*	*[m²]*

A_h	*is the horizontal area of the wall*	
A_{sw}	*Cross-sectional area of the shear reinforcement*	$[m^2]$
A_v	*Vertical area of the wall*	
a_v	*Clear span between the support and applied load*	*[m]*
b_{w0}	*The minimum width between tension and compression chords*	*[m]*
b_w	*The smallest width of the cross-section in the tensile area*	*[m]*
b_{wo}	*Thickness of the web of the wall*	*[m]*
e	*Eccentricity of P with respect to the centroid of stiffness*	*[m]*
f_{cvd}	*Concrete design strength in shear and compression*	$[N/m^2]$
f_{cd}	*Concrete design strength in compression*	$[N/m^2]$
f_{ck}	*Concrete characteristic compressive strength*	$[N/m^2]$
f_{ctd}	*Concrete design strength in tension*	$[N/m^2]$
f_{yd}	*Design value of the yield strength of the reinforcement*	$[N/m^2]$
$f_{yd,h}$	*Design value of the yield strength of the horizontal web reinforcement*	$[N/m^2]$
$f_{yd,v}$	*Design value of the yield strength of the vertical web reinforcement*	$[N/m^2]$
f_{ywd}	*Design yield strength of the shear reinforcement*	$[N/m^2]$
F_{td}	*Design value of the tensile force in the longitudinal reinforcement*	$[N/m^2]$
F_{cd}	*Design value of the concrete compression force in the direction of the longitudinal member axis.*	*[N]*
h_w	*Height of the wall*	*[m]*
k	*Geometrical factor*	*[-]*
k_1	*Partial safety factor equals to 0.15 or defined in National Annex*	*[-]*
k_{1w}	*Partial factor equals 1.0 or the value given in National Annex*	*[-]*
k_2	*Partial factor equals 0.85 or the value given in National Annex*	*[-]*
k_3	*Partial factor equals 0.75 or the value given in National Annex*	*[-]*
k_w	*Factor prevailing the prevailing failure mode*	*[-]*
l_w	*Length of the wall*	*[m]*
M_{Rd}	*Design flexural resistance at the base of the wall*	*[Nm]*

M_{Ed}	Design bending moment at the base of the wall	[Nm]
N_{Ed}	Axial force in the cross-section due to loading or prestressing (N_{Ed}>0 for compression)	[N]
P	Applied load	[N]
P_n	Lateral load on wall n	[N]
q	Behaviour factor used in design	[-]
q_0	Behaviour factor depending on the regularity in elevation of the wall structure	[-]
r_{frp}	Factor accounting for the type of strengthening configuration used	[-]
$S_e(T_c)$	Ordinate of the elastic response spectrum	[m]
s	Spacing of the stirrups	[m]
s_h	Spacing of the horizontal reinforcement	[m]
s_v	Spacing of the vertical reinforcement	[m]
s_l	Spacing of the vertical stirrups	[m]
s_b	Spacing of the inclined stirrups	[m]
T	Tensile force in a tie	[N]
T_1	Fundamental period of vibration of the building in the direction of shear forces VE_d	[s]
T_C	Upper limit period of the constant spectral acceleration region of the spectrum	[s]
V_{Ed}	Design shear force	[N]
V_{ccd}	Design value of the shear component of the force in the compression area, in the case of an inclined compression chord	[N]
V'_{Ed}	Design shear force determined form seismic analysis	[N]
$V_{Rd,c}$	Design shear resistance of the member without shear reinforcement	[N]
$V_{Rd,s}$	Design value of the shear force which can be sustained by the yielding shear reinforcement	[N]
$V_{Rd,max}$	Design value of the maximum shear force which can be sustained by the member, limited by crushing of the compression struts	[N]
V_{td}	Design value of the shear component of the force in the tensile reinforcement, in the case of an inclined tensile chord	[N]

Y_n	*is the distance of wall n from the centroid of stiffness*	*[m]*
z	*Inner lever arm, for a member with constant depth, corresponding to the bending moment in the element under consideration. In the shear analysis of reinforced concrete without axial force, the approximate value $z = 0.9d$ may normally be used.*	*[m]*

Greek letters

	Description	*Unit*
α	*Angle between shear reinforcement and the beam axis perpendicular to the shear force*	*[-]*
α_s	*Shear reinforcement ratio*	*[-]*
α_{cw}	*Coefficient taking account of the state of the stress in the compression chord*	*[-]*
ε	*Magnifying factor*	*[-]*
γ_c	*Partial safety factor equals 1.2 for persistent and transient loads and 1.5 for accidental loads*	*[-]*
γ_n	*Distance of wall n from the centroid of stiffness*	*[m]*
γ_{Rd}	*Factor to account for over strength due to steel strain-hardening; in the absence of more precise data, γ_{Rd} may be taken equal to 1.2*	*[-]*
θ	*Angle between the concrete compression strut and the beam axis perpendicular to the shear force*	*[-]*
ρ_l	*Longitudinal reinforcement area*	*[-]*
ρ_w	*Shear reinforcement ratio*	*[-]*
ρ_h	*Reinforcement ratio of horizontal web bars*	*[-]*
ρ_v	*Reinforcement ratio of vertical web bars*	*[-]*
σ_{cp}	*Mean compressive stress, measured positive, in the concrete due to the design axial force. This should be obtained by averaging it over the concrete section taking account of the reinforcement. The value of σ_{cp} shall not be calculated at a distance less than $0.5d \cot\theta$ from the edge of the support.*	*[N/m²]*
$\sigma_{Rd,max}$	*Design strength*	*[N/m²]*
ν_1	*Strength reduction factor for concrete cracked in shear*	*[-]*
f_{cp}	*= $N_{Ed}/A_c < 0,2\, f_{cd}$*	*[N/m²]*

ACI (2005) notation List

Roman letters

	Description	*Unit*
A_{cv}	*Gross area of concrete section bounded by web thickness and length of section in the direction of shear force considered*	
A_{cw}	*Area of concrete section of the coupling beam resisting shear*	
A_g	*Gross area of concrete section*	$[m^2]$
A_v	*Area of shear reinforcement*	
b_w	*Web width*	*[m]*
d	*Distance from extreme compression fibre to centroid of longitudinal tension reinforcement*	*[m]*
l_n	*Clear span of the coupling beam*	*[m]*
h	*Height of the wall*	*[m]*
h_b	*Clear height of the coupling beam*	*[m]*
l_w	*Overall length of the wall*	*[m]*
M_u	*Factored moment in the section*	*[Nm]*
M	*Nominal flexural moment in the coupling beam*	*[Nm]*
N_u	*Factored axial force*	*[N]*
s	*Stirrups spacing*	*[m]*
t_w	*Thickness of the wall*	*[m]*
V_c	*Nominal shear strength provided by concrete*	*[N]*
V_n	*Lateral load*	*[N]*
V_s	*Nominal shear strength provided by shear reinforcement*	*[N]*
V_u	*Factored shear force*	*[N]*

Greek letters

	Description	*Unit*
α	*Angle between inclined stirrups and longitudinal axis of the member*	*[-]*

α_c	*Coefficient defining the relative contribution of concrete strength to nominal shear strength*	*[-]*
ρ_t	*Steel transverse reinforcement area*	*[-]*
ρ_w	*Ratio of tension reinforcement to $b_w d$*	*[-]*

Betonghandboken (1997) notation list

Roman letters

	Description	*Unit*
A_c	*Area of the concrete*	*[m^2]*
A_{s0}	*Longitudinal tensile reinforcement*	*[m^2]*
b	*Width of the beam*	*[m]*
d	*Effective height of the beam*	*[m]*
e	*is the eccentricity*	*[m]*
E	*Modulus of elasticity of concrete*	*[N/m^2]*
f_{cc}	*Concrete compression strength*	*[N/m^2]*
f_{ck}	*Characteristic compression strength of concrete*	*[N/m^2]*
f_{ct}	*Concrete tensile strength, limited to the value 2.7 MPa*	*[N/m^2]*
f_{st}	*Steel tensile strength*	*[N/m^2]*
f_v	*Concrete formal strength determined according to:*	*[N/m^2]*
f_w	*Utilized stress in shear reinforcement*	*[N/m^2]*
I	*Moment of inertia*	*[m^4]*
M_2	*is the resulted bending moment due to eccentricity e and the reaction force R_2*	*[Nm]*
N_{sd}	*The design value of the pre-stressed force or other compression force*	*[N]*
R_2	*is the reaction force of the assumed frame*	*[N]*
s	*Stirrups longitudinal spacing*	*[m]*
V_2	*is the shear force acting on the assumed frame*	*[N]*
V_c	*Concrete contribution to the shear capacity*	*[N]*

V_{Rds}	*Shear reinforcement capacity*	*[N/m²]*
z	*Internal level arm of the steel reinforcement, set to be 0.9d if not other provisions*	*[m]*

Greek letters

	Description	*Unit*
β	*Inclination angle of the steel stirrups*	*[°]*
ρ	*Tensile reinforcement ratio*	*[-]*
θ	*Angle of the compression struts with respect to a beam axis perpendicular to the shear force direction*	*[°]*

Table of content

1 Introduction

With the evolution of the human society, the complexity of structures has undergone its own evolution too. Humans started using caves, then building tents, huts, igloos, castles multi-story buildings or skyscrapers, but regardless of our development all these buildings are still subjected to the laws of nature i.e. deterioration. In general, constructions are designed for a minimum life span and have a precise functionality. There are several causes other than natural forces which diminish the performance of constructions, such as change of functionality (eg. from an apartment building to an office building), structural intervention (eg. new openings are created or bearing elements are removed), design errors, construction faults or exceptional events (calamities or explosions). When one or more of these actions are present simultaneously, and no responsible action has been taken to re-establish the safe performance of the building, catastrophic consequences may result. The bearing capacity is of utmost importance for the safety of their users but, in some cases this is not enough to ensure good performance. The durability, the functionality or the aesthetics are important factors to consider. For example a bridge may have the necessary bearing capacity but can be too narrow, so it does not fulfil its main function. In general, for a structure all these three additional criteria have to be satisfied up to a certain level required for the main purpose of the building. For instance a school, beside load bearing capacity, needs to fulfil the function and durability demand at a higher level and the aesthetics at a lower level. The class rooms have to be large enough to host students and the corridors wide enough to allow emergency evacuations. Therefore it is of high interest to have durable structures with long life and low maintenance costs.

In the case of newly built constructions a high degree of complexity and long term performance is being achieved, but at the same time a large number of older structures are not performing according to the expectations. Sometimes, to prevent deterioration or possible collapse these structures are kept in service with partial or total restrictions to the usage until appropriate measures can be taken. Usually, when speaking about appropriate measures to apply to a structure the replacement of the structure or rehabilitation of the initial capacity through different methods of strengthening or retrofitting has to be considered. Normally an economical study leads to a decision to either replace a structure or retrofit it or vice versa.

For strengthening or retrofitting structural buildings several methods have been used with success in the past. Among these we can mention the new structural material added to an already existing structural element to increase the gross section, the post-tensioning technique, total replacement of some structural elements or changing the

structural system (Carolin, 2003). Although these methods can be viable and successful in some cases they are uneconomical or inefficient in terms of time. An alternative rehabilitation system to the ones mentioned above is the plate bonding technique. In its beginnings the rehabilitation was performed by attaching steel plates to a concrete surface. Nowadays the steel plates have been replaced by fibre reinforced polymers (FRP) and as bonding agent the epoxy resigns are used. Fibre reinforced polymers are the result of the conjugated effort of continuous improvement of construction materials and innovation in construction technology. Among others (aviation industry, car industry, medicine, etc.), FRP composites are used in the construction industry too, and are a real and viable solution to rehabilitate a structure. The outstanding mechanical properties combined with the low weight makes the FRP composites a real challenge for the classic strengthening techniques (Täljsten, 2006).

1.1 Aim

The overall aim of the present thesis is to investigate and improve the understanding of shear FRP strengthening of reinforced concrete beams and FRP strengthening of reinforced concrete walls with openings. This main goal was divided into four different sub-aims:

- To evaluate and analyse different methods of determining the shear capacity of RC beams and the capacity of RC walls with openings.
- To analyse, evaluate and compare the existing theoretical models for FRP shear strengthening of reinforced concrete beams.
- To develop a simple to use design model for strengthening concrete beams in shear.
- To assess the work performed on FRP strengthened reinforced concrete walls with openings and develop the bases for a theoretical model.

1.2 Method

To achieve the above mentioned goals a step by step procedure has been used. To understand the shear failure mechanism of the FRP strengthened reinforced concrete elements the behaviour of these elements has been studied. An important issue was to asses and understand the work done until and during the work carried for this research. This has been done through a literature review study. A very important aspect is considered to be the accuracy of the existing theoretical model to predict the shear capacity of strengthened structural elements. This was performed by comparing the predictions of different models found in the literature with a large database of experimental results and an analytical shear model for strengthening concrete elements has been derived based on the fracture mechanics approach. A literature survey has been performed to assess the design methods for RC walls with openings and FRP strengthened RC walls with openings. The static analysis of frames was used to develop the bases for a theoretical model for FRP strengthened RC walls with openings.

1.3 Limitations

The theoretical model for shear strengthening of RC beams involves derivations only for the debonding failure mechanism and is intended to complete the model derived by Carolin (2003) and Carolin and Täljsten (2005). The model does not present any details regarding the fibre failure. The weaknesses and unsafe predictions of the model emerge from the empirical determination of the fracture energy of the concrete. The fracture mechanics concept used for the derivations is limited and does not cover the non linear fracture approach. No advanced statistical analysis has been used to appraise the theoretical predictions of the theoretical models analyzed. A majority of the experimental database was not collected by the author. All the experimental values obtained from scaled tests have been removed from the database before performing the analysis.

The present work on walls does not include any experimental work walls at this stage and the theoretical work is limited. However, this is the subject and aim for the PhD research which will be continued after the licentiate thesis.

1.4 Content

The thesis is divided into an extended summary which gives an overall presentation of the area studied together with four appended papers, two journal papers and two conference papers. The extended summary is divided into six chapters which all, except the introductory chapter, are briefly presented below.

In *Chapter 2* the shear design principles are presented and exemplified.

Chapter 3 presents the fibre reinforced polymers and depicts the main components of the composites.

Chapter 4 is dedicated to the shear strengthening of RC beams and FRP strengthening of RC walls with openings. First the shear failure in beams and walls is presented followed by a description of the classical rehabilitation principles and ends with emphasizing the shear strengthening of RC beams and walls. Considerations for the design of FRP strengthening of RC walls with openings are also presented.

In *Chapter 5* a case study is presented for FRP strengthening of RC walls with openings.

Chapter 6 is summarizing the research significance of the topics presented and tries to identify the future work to be performed.

The content of the appended papers and the author's contribution to these papers is presented below.

Paper I consist of a manuscript titled "*Are available models reliable for predicting the FRP contribution to the shear resistance of RC beams?*" by G. Sas, B. Täljsten, J. Barros, J. Lima, A. Carolin. The paper is submitted to Journal of Composites for Construction.

Gabriel Sas's contribution to the paper is reviewing the literature, analyzing and evaluating both the theoretical models and the experimental data base (not collecting the database), concluding the paper and finally writing the paper including drawings and figures.

Paper II consists of a paper titled "*A model for predicting shear bearing capacity of FRP strengthened beams*" by G. Sas, A. Carolin and B. Täljsten and published in Mechanics of Composite Materials, Vol. 44, No. 3, 2008.

Gabriel Sas's contribution to the paper is the introduction, the literature review, the theoretical model derivations, partially the comparison with the experimental results, the conclusion and finally writing the paper and partially the figures.

Paper III consists of a paper titled "*Research Results on RC Walls and Dapped Beam Ends Strengthened with FRP Composites*" by T. Nagy-György, V. Stoian, D. Dan, C. Daescu, D. Diaconu, G. Sas, M. Mosoarca and published in Proceedings: FRPRCS-8, Patras, Greece, July, 2007, ISBN 978-960-89691-0-0.

Gabriel Sas's contribution to the paper is the literature review, participating in the planning of the experimental work and in the tests.

Paper IV consists of a paper titled "*FRP strengthened RC panels with cut-out openings*" by G. Sas, I. Demeter, A. Carolin, T. Nagy-György, V. Stoian and B. Täljsten, published in Proceedings: Challenges for Civil Construction, Porto, Portugal, ISBN: 978-972-752-100-5, April 2008.

Gabriel Sas's contribution to the paper are the literature review study, partial planning of the tests, formulating the conclusions, partially drawing the figures and writing the paper.

2 Shear design

The main subject of this thesis is shear strengthening of beams and walls, and the current shear design methods are presented in this chapter. However, it must be mentioned that because of the complicated nature of the shear behaviour the development of viable theoretical philosophies for reinforced concrete shear walls is limited, their design being adapted from the theoretical methods applied for beams and columns. In the following subchapters a general description of the three most used theoretical approaches for shear design of structurally reinforced concrete are presented.

2.1 Shear design principles

2.1.1 Truss model

The truss model was presented by Ritter (1899), to explain the flow of forces in cracked reinforced concrete beams.

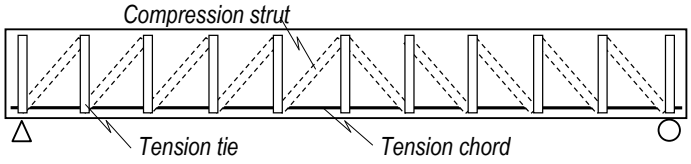

Figure 2-1: Ritter's truss analogy for shear (adapted from Collins, 1991)

The principle of the truss model is based on the following assumptions;

- The longitudinal tension reinforcement acts as a bottom chord of the truss while the flexural compressive zone of the beam acts as the top chord.
- The diagonal compressive stresses (dashed line in Figure 2-1) act as diagonal members and the stirrups (solid vertical lines in Figure 2-1) are considered as vertical tension members.

Later on Mörsch (1902) gave insight into the theory, pointing out that compression diagonals do not have to go from the top of one stirrup to the bottom of the next stirrup, and they represent a continuous field of stresses rather than discrete diagonal compressive struts (Mörsch, 1922).The tensile stress in cracked concrete was neglected by both Ritter and Mörsch assuming only that after cracking the diagonal compression stresses would remain at 45°.

The truss model is derived using the equilibrium condition between the external and internal forces as presented in Figure 2-2. The shear stresses are assumed to be uniformly distributed over an effective shear area b_w wide and d deep (Figure 2-2a). Between the external shear force V, and the total diagonal compressive force the next

relation can be written, from which the principle compressive stress, f_2, can be determined, assuming a crack angle of 45°:

$$f_2 b_w d / \sqrt{2} = \sqrt{2} V \tag{2-1}$$

From Figure 2-2b, the longitudinal component of the diagonal compressive force is considered equal to the external shear force, V. The tensile stress in stirrups is determined considering equation (2-2).

$$\frac{A_s f_{ys}}{s} = \frac{V}{d} \tag{2-2}$$

Allowing only the use of the 45° crack angle the method is robust and gives conservative results, and it is widely used by the designers because of its simplicity.

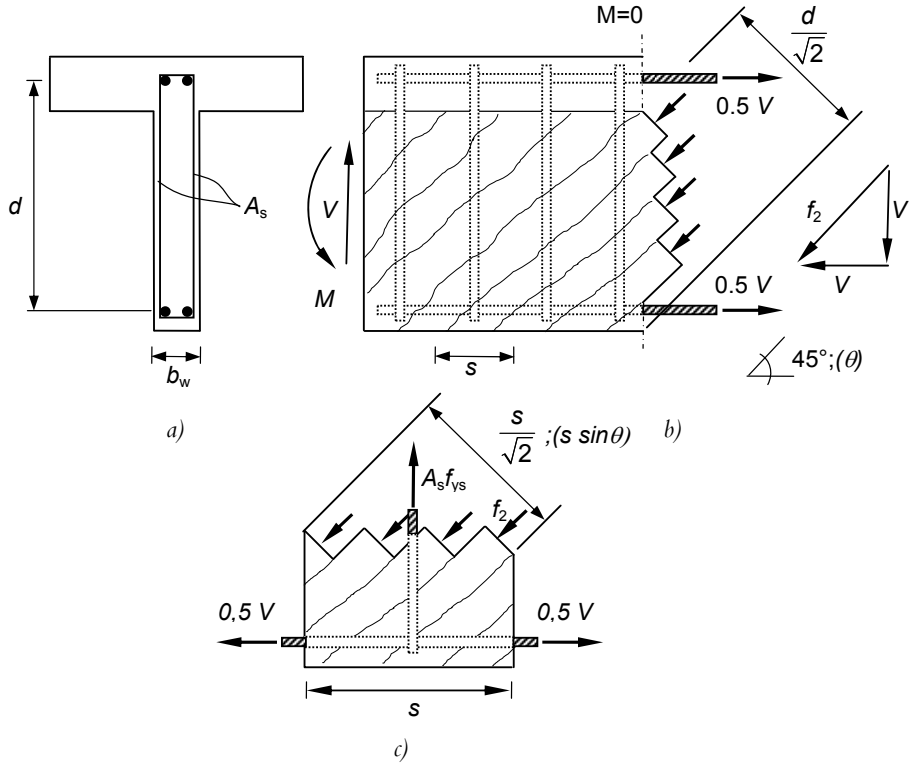

Figure 2-2: Equilibrium conditions for the truss model

Derived from the Mörch (45°) truss model is the variable truss angle model which adds a "concrete contribution" to compensate for the conservative nature of this model, and accounting for a variable angle of the crack, θ. The principle is similar to the one presented in Figure 2-2. In this case the required magnitude of the principal

compressive stress, f_2, is determined from the equality between the resultant D of the diagonal stresses and the projection of the shear force (Eq. (2-3).

$$f_2 = \frac{V}{b_w d}(\tan\theta + \cos\theta) \tag{2-3}$$

The tensile force in the longitudinal reinforcement due to shear will be equal to the horizontal projection of the shear force (Eq. (2-4).

$$N_h = V\cos\theta \tag{2-4}$$

The tensile stress in stirrups (the right term in equation (2-2), has to be multiplied with the factor $\tan\theta$ (Eq. 2-5).

$$\frac{A_s f_{ys}}{s} = \frac{V}{d}\tan\theta \tag{2-5}$$

Since the equilibrium equations are three (Eqs. (2-3, (2-4 and (2-5) and we have four unknowns (i.e. principle compressive stress, the tensile force in the longitudinal reinforcement, the stress in stirrups, and the inclination, θ, of the principal compressive stress), the stresses in a beam caused by a given shear cannot be explicitly determined. So, for design considerations, the shear force can be predicted assuming the crack angle at 45° and the tensile stress in stirrups reaches the tensile strength of steel. Rather than assuming the crack angle, the compressive stress in concrete f_2,can be assumed and then the crack angle can be determined (Eq. (2-4) and the shear force can then be predicted (Eq. (2-5). Collins (1991) had an interesting comment for this method saying: *"These approaches, which consider the mechanism of failure, are referred to as plasticity methods"*. Particular specifications were given for different parameters during time after more tests were available for the "effective" compressive strength should be $0.6f_c'$, and $\tan\theta$, recommended to be less than 0.5.

The truss model is also the starting point of the shear friction model, also known as Loov's theory (1998), in which the shear forces are carried by stirrups and shear friction in concrete crack. The method comprises the calculation of the shear capacity from all possible crack angles by identifying the weakest plane of failure.

2.1.2 Limit Analysis and Concrete Plasticity

The concrete plasticity method treats the shear problem based on the classical methods: strut and tie and diagonal compression field. The difference consists in using coefficients that consider the interaction between the materials, geometry of the elements or loading type, using this theory. To assure a good understanding of the plasticity theory for shear the basic assumptions and the defining limitations are given next according to Nielsen (1999).

First a rigid body material is defined as a material in which no deformation occurs (at all) for stresses up to a certain limit, i.e. the yield point. This definition is used in order to validate the Von Mises's Flow Rule (Eq. (2-6).

$$q_i = \lambda_p \frac{\partial f}{\partial Q_i} \quad i = 1,2,...,n \tag{2-6}$$

Where λ is an undetermined factor, Q_i is the generalized stress, q_i is the generalized strain and f is the yield condition. In accordance with this hypothesis, the stresses corresponding to a given strain field assume such values that the work per unit volume, area, or length becomes as large a possible. For example let us consider a beam with a rectangular cross section (bh) of rigid plastic material. The cross section is loaded by a bending moment (M) and a normal force (N) in the centre of gravity. The load-carrying capacity is determined from the stress distribution shown in Figure 2-3.

$$\left(h - 2\gamma_0\right) b f_\gamma = N \Rightarrow \frac{\gamma_0}{h} = \frac{1}{2}\left(1 - \frac{N}{N_p}\right) \tag{2-7}$$

where N_p being the tension yield load given as:

$$N_p = bhf_\gamma \tag{2-8}$$

We then have:

$$M = \gamma_0 b f_\gamma \left(h - \gamma_0\right) = \frac{1}{4} b h^2 \left[1 - \left(\frac{N}{N_P}\right)^2\right] = M_P \left[1 - \left(\frac{N}{N_P}\right)^2\right] \tag{2-9}$$

and M_p the yield moment in pure bending is:

$$M_P = \gamma_0 b f_\gamma \left(h - \gamma_0\right) = \frac{1}{4} h N_P \tag{2-10}$$

The yield condition is found to be:

$$f(m,n) = m + n^2 - 1 = 0 \tag{2-11}$$

where $m=M/M_p$ and $n=N/N_p$.

For rigid plastic materials it is assumed that as long as the stresses in a body are below the yield point no deformations occur. This idealization induces the consequence of not being able to determine the stress field in such a body when stresses are below the yield point. A body is considered to be subjected to collapse by yielding when the load is reaching a point where the material may carry only yielding stresses and unlimited deformations are possible without changing the load, if the strains correspond to a geometrically possible displacement field.

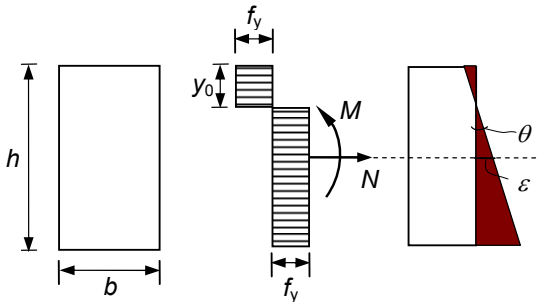

Figure 2-3: Stress and strain distribution in a rectangular beam

With the above definitions of the stress flow and the failure criterion now boundaries are defined:

- For the load magnitude at which it is possible to find a stress distribution corresponding to stresses within the yield surface and satisfying the equilibrium conditions, then this load will not be able to cause collapse of the body. If the external load is determined by one parameter $\mu>0$ in such way that the individual loading components are proportional to μ, we have a proportional loading. The theorem can be used to find values of the load that are lower than the collapse load corresponding to $\mu=\mu_p$, hence the name *the lower bound theorem*. For all the loads where safe and admissible stress distribution can be found we have $\mu<\mu_p$.
- *The upper bound theorem* states that if various geometrically possible strain fields are considered, the work equation (2-12) can be used to find values of the load carrying capacity that are greater than or equal to the collapse load. If for the values of μ determined from equation (2-12), then the smallest increase in load cannot be carried by the material, that is $\mu>\mu_p$.

$$\mu \sum P_i u_i = \int_V W(q_1,\ldots) dV \tag{2-12}$$

Where P_i and u_i are the loads and their corresponding displacement effect, W is the work and q_1 is the plastic strain.

- The uniqueness theorem has to satisfy the following two conditions simultaneously:

  a) There is a statically admissible stress distribution corresponding to stresses on or within the yield surface.

  b) The strains corresponding to the stresses according to the flow rule can be derived from a geometrically possible displacement field.

The plasticity theory can be applied to reinforced concrete structures as it has been proven by Nielsen (1999). The most obvious application refers to the application of the lower bound theorem when designing the reinforcement. If a statically admissible stress

field is selected, the necessary reinforcement may be calculated using this stress field, and at the same time the stresses in concrete which leads to a safe structure can be calculated. In particular, it is easy to determine the complete group of statically admissible stress fields for beams. If the beam is *n* time statically undetermined, *n* moments or forces may be chosen arbitrarily and then the entire stress field may be calculated using statics only.

Nevertheless the appliance of the method was limited for reinforced concrete structures, because the acceptance of plasticity in concrete is still a topic of debate among scientist However, the design construction codes in Canada, Demark and parts of the Eurocode (2004) formulas are based on this theory.

2.1.3 Modified Compression Field Theory

A key factor in the compressive field theory is the angle inclination of the diagonal tension. The first hint on this was given in 1929 by Wagner who treated the problem in studying the post-buckling shear resistance of thin-webbed metal girders. He assumed that after local buckling the thin webs will not carry any compression, the resisting mechanism being based on the field of diagonal tension. In order to determine the angle inclination, the deformation of the system was considered and the next assumption has to be valid: the angle of the diagonal tensile stress has to coincide with the inclination angle of the principle tensile strain. This assumption was defined as the tension field theory.

The tension field theory can be applied for reinforced concrete, assuming after cracking the concrete carries no tension and that the shear is carried by a field of diagonal compression. The angle of inclination of the diagonal compression can be determined from equation (2-13). Also when using the Mohr circle the principle tensile strain in the web is given as in equation (2-14) and the shear strain in the web in equation (2-15).

$$\tan^2\theta = \frac{\varepsilon_x - \varepsilon_2}{\varepsilon_t - \varepsilon_2} \tag{2-13}$$

$$\varepsilon_1 = \varepsilon_x + \varepsilon_t - \varepsilon_2 \tag{2-14}$$

$$\gamma_{xy} = 2\left(\varepsilon_x - \varepsilon_2\right)\cot\theta \tag{2-15}$$

Where: ε_x is the longitudinal strain of the web, tension positive; ε_t is the transverse strain, tension positive; ε_2 is the principal compressive strain, negative quantity. If the strains in three directions are known, the strain in any other direction can be determined according to Mohr's circle. For cracked concrete average strains have to be used, that is strains covering more cracks. For cracked concrete these compatibility relations are applied on "average" strains, so that the measured values include several cracks (Figure 2-4). Based on the same principle, the compressive field theory (CFT) has been presented by Collins and Mitchell (1991).

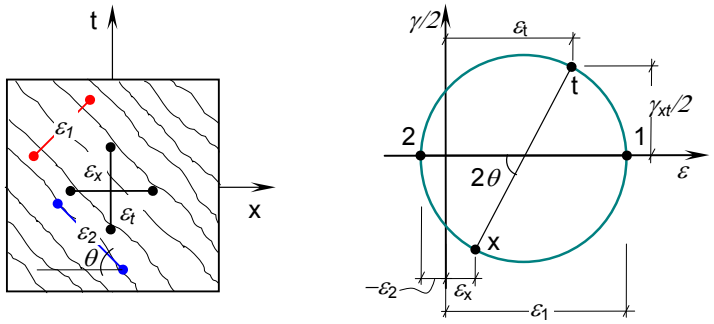

a) Average strains in cracked element

b) Mohr's circle for average strains

Figure 2-4: Mohr's circle for average strains and stresses in concrete (from Collins and Mitchell, 1991)

Let us consider a symmetrically reinforced concrete beam subjected to shear. For a given level of shear there are a total of four unknowns: the stress in the longitudinal bars, f_x; the stress in the stirrups f_v; the diagonal compressive stress in concrete f_2 and the inclination of the diagonal compressive stresses, θ. In this case it is assumed that the cracked concrete cannot transmit any tension force and the diagonal compressive fields carry all the forces. To find these unknowns we have three equilibrium equations (2-16), (2-17) and (2-18) and the constitutive laws for the materials and one compatibility equation (2-13).

$$f_2 = \frac{V}{b_w jd}\left(\tan\theta + \cot\theta\right) \tag{2-16}$$

$$A_x f_x = \frac{V}{\tan\theta} \tag{2-17}$$

$$\frac{A_v f_v}{s} = \frac{V}{jd}\tan\theta \tag{2-18}$$

In general the compressive stress-strain relation is defined from the response of a standard concrete cylinder. But this value might not correctly describe the shear behaviour for the cracked concrete in the web of an element. Vecchio and Collins (1982) tested reinforced concrete elements in pure shear and discovered that the principle compressive stress in the concrete, f_2, is not only dependent on the principal compressive strain ε_2, but also on the corresponding tensile strain ε_1. Based on these test results, the following stress strain relation was recommended afterwards.

$$f_2 = f_{2\max}\left[2\left(\frac{\varepsilon_2}{\varepsilon_c'}\right) - \left(\frac{\varepsilon_2}{\varepsilon_c'}\right)^2\right] \quad \text{where} \quad \frac{f_{2\max}}{f_c'} = \frac{1}{0.8 + 170\varepsilon_1} \le 1.0 \tag{2-19}$$

The compressive field theory is an iterative method of calculating the stresses when shear failure occurs and needs several steps before the shear capacity is calculated. Since the tensile strength is neglected the predictions are conservative. To overcome this uneconomical drawback, Vecchio and Collins (1986) developed the theory further, also known as Modified Compressive Field Theory (MCFT) by subtracting the tensile principal stress f_1 (Eq. (2-20), from equation (2-16). The value of the tensile stress is limited to the value given in equation (2-21). The evolution of the stresses is presented in Figure 2-5. Before cracking, the shear is carried equally by diagonal tensile and compressive stresses acting at 45° (Figure 2-5a). After cracking the tensile stresses are substantially reduced but different than zero (Figure 2-5c) while in the compressive field theory it is considered zero (Figure 2-5b).

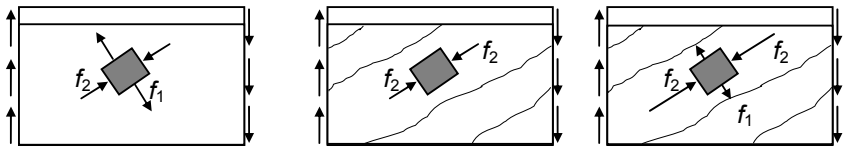

(a) Before cracking $f_1=f_2$, $\theta=45°$ | *(b) Compression field theory,* $f_1=0$ | *(c) Modified compression field theory,* $f_1\neq 0$

Figure 2-5: Stress fields in web of reinforced concrete beams (after Collins and Mitchell, 1991)

$$f_1 = \begin{cases} \varepsilon_1 E_c & \text{if } \varepsilon_1 \le \varepsilon_{cr} \\ \dfrac{\alpha_1 \alpha_2 f_{cr}}{1+\sqrt{500\varepsilon_1}} & \text{if } \varepsilon_1 > \varepsilon_{cr} \end{cases} \qquad (2\text{-}20)$$

$$\upsilon_{ci} = \frac{0.18\sqrt{f_c'}}{0.3+\dfrac{24\omega}{a+16}} \qquad (2\text{-}21)$$

Where α_1, α_2 are factors accounting for the bond characteristics of the reinforcement and the type of loading and a is the maximum aggregate size. When using equation (2-20) the average values of the tensile stress and strains are considered as in Figure 2-6b but the local stresses (Figure 2-6c) that occur at a crack location will differ from calculated average values. This was explained by Collins and Mitchell (1991) in the following way: "At low shear values, tension is transmitted across the crack by local increases in reinforcement stresses. At a certain shear force the stress in the web reinforcement will just reach yield at the crack locations. Higher shear forces transmitting tension across the crack will require shear stresses, υ_{ci} Eq. (2-21), on the crack surface (see Figure 2-6c)". The equilibrium conditions between these two sets of stresses (when the same vertical force is applied) will limit the tensile stress to the value defined in equation (2-22). If the crack width is not limited, in most of the cases the shear capacity of a member is restricted by the ability of the member to transmit forces across the crack.

$$f_1 = \upsilon_{ci} \tan\theta + \frac{A_v}{sb}\left(f_{yv} - f_v\right) \tag{2-22}$$

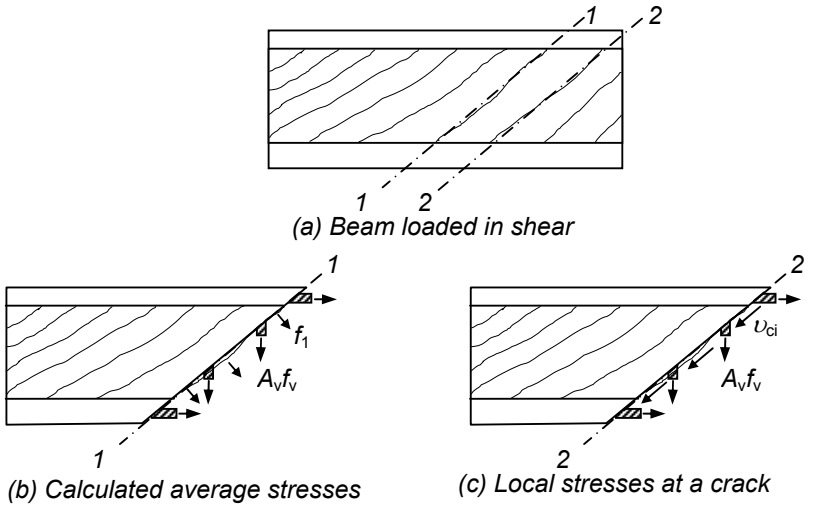

Figure 2-6: Forces transmitted across a crack

ω is the crack width defined as the product between the principle tensile strain and the average spacing of the cracks:

$$\omega = \varepsilon_1 s_{m\theta} \text{ and } s_{m\theta} = \frac{1}{\left(\frac{sin\theta}{s_{mx}} + \frac{cos\theta}{s_{mv}}\right)} \tag{2-23}$$

Where s_{mx} is the average crack spacing that would result if the member would be subjected to longitudinal tension while s_{mv} is the average crack spacing that would result if the member was subjected to transverse tension. For details on how to determine these values see Collins and Mitchell (1991). After defining the above quantities equilibrium equations are applied for the cross section considered and the shear capacity is determined iteratively. The MCFT is refers mainly to the design of beams but other types of elements can be designed respecting the same principle. Since the procedure is iterative and requires several steps of computation its use has been limited among the designers. However, in the past years the potential of the computer assisted design has increased its application. A summary of the method is presented in Figure 2-7.

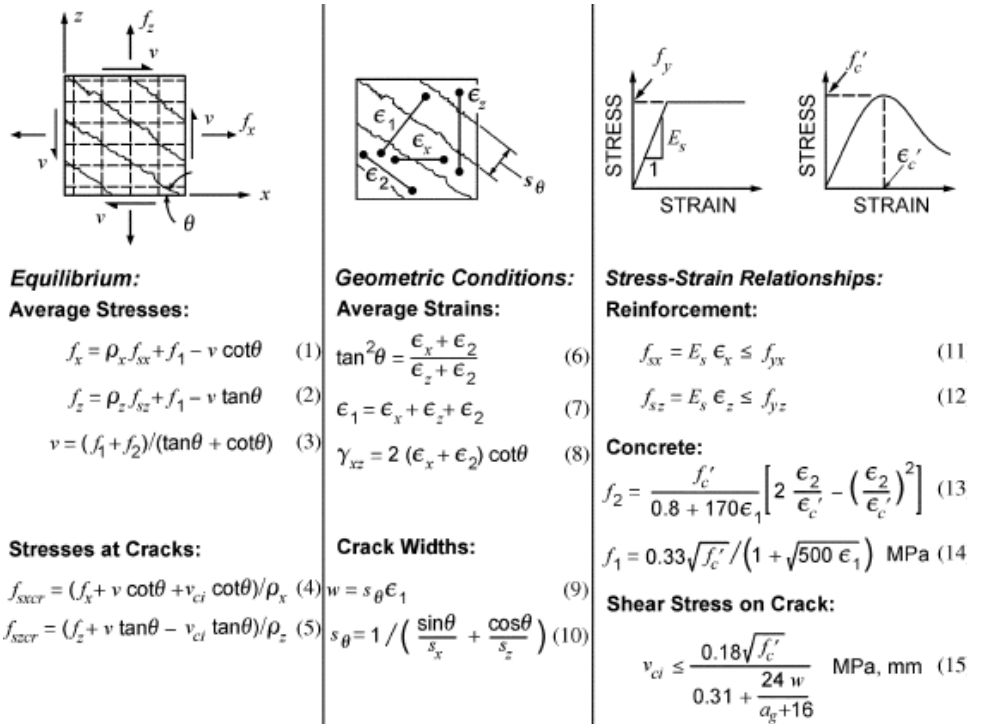

Figure 2-7: Summary of Compression Filed Theory (from Collins and Mitchell, 1991)

2.2 Shear design in Standards

2.2.1 Eurocode (2004a, b)

The general procedure for shear design of reinforced concrete members is presented in chapter 6.2 in Eurocode (2004a). The shear resistance of a member with shear reinforcement is based on the variable truss angle and is calculated using the addition principle:

$$V_{Rd} = V_{Rd,s} + V_{cd} + V_{td} \tag{2-24}$$

From this point the design is separated in two calculating routines in function of the relation between V_{Ed}, the design shear force resulted from external loading and prestressing (if present) and the design shear resistance of the concrete member without shear reinforcement, $V_{Rd,c}$.

Members not requiring design shear reinforcement

These include the members for which $V_{Ed} \leq V_{Rd}$. The design value for the shear resistance is given by:

$$V_{Rd,c} = \left[C_{Rd,c} k (100 \rho_l f_{ck})^{1/3} + k_1 \sigma_{cp} \right] b_w d \tag{2-25}$$

with a minimum of

$$V_{Rd,c} = \left(V_{\min} + k_1 \sigma_{cp} \right) b_w d \tag{2-26}$$

The values for k, k_1, $C_{rd,c}$, V_{min} can be found in the National Annex for each country or the values recommended: $k = 1 + \sqrt{200/d} \leq 2.0$ with d in mm, $C_{rd,c}$=$0.18/\gamma_c$; k_1=0.15 V_{min}=$0.035 k^{3/2} f_{ck}^{1/2}$. The origin and further details of these factors where not further discussed in Eurocode, thus making the interpretation harder to understand. The partial factor γ_c is given in Eurocode (2004a) chapter 2.4.2.4 and can be equal to 1.2 or 1.5 for persistent and transient design situation or accidental design situation respectively.

For members on which loads are applied within a distance $0.5 \leq a_v \leq 2d$ from the edge of the support (Figure 2-8), the contribution of this load to the shear force V_{Ed} should be multiplied by the factor $a_v/2d$. This condition is only valid if the longitudinal reinforcement is properly anchored at the support.

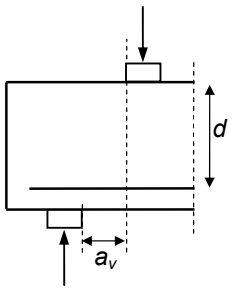

Figure 2-8: Load near support

Even if the factor $a_v/2d$ is not applied the shear force V_{Ed} should always satisfy equation (2-27).

$$V_{Ed} \leq 0.5 b_w d \nu f_{cd} \tag{2-27}$$

Where, the value of ν is recommended to be taken as in equation (2-28) or the National Annex.

$$\nu = 0.6 \left[1 - \frac{f_{ck}}{250} \right] \tag{2-28}$$

Members requiring design shear reinforcement

These include the members for which $V_{Ed} > V_{Rd,c}$. The design is based on a truss model (Figure 2-9), where the angle of the inclined struts in the web θ, should respect the condition $1 \leq \cot\theta \leq 2.5$.

When vertical reinforcement is used, the shear resistance is the smaller value determined from equations (2-29) and (2-30).

$$V_{Rd,s} = \frac{A_{sw}}{s} z f_{yd} \cot\theta \tag{2-29}$$

$$V_{Rd,\max} = \alpha_{cw} b_w z \nu_1 f_{cd} \left(\cot\theta + \tan\theta\right) \tag{2-30}$$

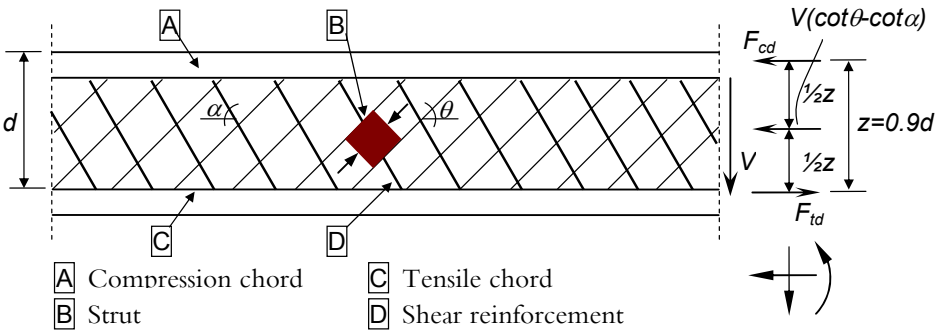

Figure 2-9: Truss model and notation for shear reinforced members

The values for the coefficient ν_1 are given for a value of the design stress in the reinforcement smaller than 80% of the characteristic yield stress f_{yk} as:

$$\nu_1 = \begin{cases} 0.6 & for \quad f_{ck} \leq 60\ MPa \\ 0.9 - f_{ck}/200 > 0.5 & for \quad f_{ck} \geq 60\ MPa \end{cases}$$

The recommended value for α_{cw} is as follows:

$$\alpha_{cw} = \begin{cases} 1 & for \quad non-prestressed\ strucutres \\ (1+\sigma_{cp}/f_{cd}) & for \quad 0 < \sigma_{cp} \leq 0.25 f_{cd} \\ 1.25 & for \quad 0.25 f_{cd} < \sigma_{cp} \leq 0.5 f_{cd} \\ 2.5(1-\sigma_{cp}/f_{cd}) & for \quad 0.5 f_{cd} < \sigma_{cp} \leq 1.0 f_{cd} \end{cases}$$

The maximum effective cross sectional area of the shear reinforcement is determined from equation (2-31).

$$\frac{A_{sw,\max} f_{ywd}}{b_w s} \leq \frac{1}{2} \alpha_{cw} \nu_1 f_{cd} \tag{2-31}$$

When inclined shear reinforcement is used the shear resistance is determined as the minimum from equations (2-32) and (2-33).

$$V_{Rd,s} = \frac{A_{sw}}{s} z f_{ywd} \left(\cot\theta + \cot\alpha\right) \sin\alpha \tag{2-32}$$

$$V_{Rd,\max} = \alpha_{cw} b_w z \nu_1 f_{cd} \left(\cot\theta + \cot\alpha\right) \Big/ \left(1 + \cot^2\theta\right) \tag{2-33}$$

Here, the maximum effective shear reinforcement takes a similar form as in equation (2-31) being only affected by the inclination of the stirrups.

$$\frac{A_{sw,\max} f_{ywd}}{b_w s} \le \frac{\frac{1}{2}\alpha_{cw}\nu_1 f_{cd}}{\sin\alpha} \tag{2-34}$$

Specifications are given for the dowel effect, considering the additional tensile force ΔF_{td} in the longitudinal reinforcement due to shear V_{Ed} as:

$$\Delta F_{td} = 0.5 V_{Ed} \left(\cot\theta - \cot\alpha\right) \tag{2-35}$$

Please note, the shear design resistance presented in Eurocode (2004a) does not allow the concrete contribution (Eq. (2-26) and the steel reinforcement contribution (Eq. (2-31) to be considered simultaneously. This leads to a conservative design prediction.

2.2.2 ACI (2005)

In Chapter 11 of the ACI (2005) the shear strength design is presented. Two methods are used for the design of reinforced concrete elements, the strut-and-tie model and the addition principle to calculate the shear capacity of the steel and concrete. The strut-and–tie model is presented in a similar form as for Eurocode (2004a) so it will not be detailed further, while for the addition principle the equation (2-36) is used to compute the nominal shear strength.

$$V_n \ge V_c + V_s \tag{2-36}$$

The shear strength is based on an average shear stress on the full effective cross section $b_w d$. For members with shear reinforcement the shear capacity is divided between concrete and steel stirrups, while for members without shear reinforcement the shear is assumed to be carried by the concrete web only. The concrete shear strength is assumed to be the same for elements with and without shear reinforcement and is determined for members subjected to shear and flexure (Eq. (2-37), and for members subjected to axial compression (Eq. (2-38).

$$V_c = 0.17\sqrt{f_c'} b_w d \tag{2-37}$$

$$V_c = 0.17\left(1 + \frac{N_u}{14 A_g}\right)\sqrt{f_c'} b_w d \tag{2-38}$$

A more detailed calculation of the concrete shear strength can be performed incorporating the effect of shear and flexure for both members subjected to shear and flexure (Eq. (2-39) and axial compression (Eq. (2-40) respectively.

$$V_c = \left(0.16\sqrt{f_c'} + 17\rho_w \frac{V_u d}{M_u}\right) b_w d \le 0.29\sqrt{f_c'} b_w d \text{ and } V_u d/M_u \le 1.0 \quad (2\text{-}39)$$

$$V_c = \left(0.16\sqrt{f_c'} + 17\rho_w \frac{V_u d}{M_m}\right) b_w d \le 0.29\sqrt{f_c'} b_w d \sqrt{1 + \frac{0.29N_u}{A_g}}; \quad (2\text{-}40)$$

$$M_m = M_u - N_u \frac{(4h - d)}{8}$$

For members subjected to significant axial tension the concrete shear contribution is computed as:

$$V_c = 0.17\left(1 + \frac{0.29N_u}{A_g}\right)\sqrt{f_c'} b_w d \text{ and } V_u d/M_u \le 1.0 \quad (2\text{-}41)$$

A minimum area of shear reinforcement (Eq. (2-42) has to be provided in all reinforced concrete elements even if it did not result from shear design as being necessary.

$$A_{v,\min} = 0.062\sqrt{f_c'} \frac{b_w s}{f_{yt}} \ge 0.35 \frac{b_w s}{f_{yt}} \quad (2\text{-}42)$$

When factor shear force in the section exceeds the concrete shear strength the shear capacity of steel reinforcement has to be added using equation (2-43).

$$V_s = \frac{A_v f_{yt} (\sin\alpha + \cos\alpha) d}{s} \quad (2\text{-}43)$$

2.3 Shear in beams

2.3.1 Introduction

Shear failure of reinforced concrete beams is a complicated mechanism depending on the combination of different effects. The stresses in the shear span of a beam are usually developed in inclined critical planes. Depending on the amount of shear reinforcement, steel reinforcement, concrete strength, aggregate size, dowel effect, and position of loading the shear plane of failure may be generated between 30-60°. The typical failure modes of a beam are presented in Figure 2-10 and can be identified as:

- Shear failure of the web

This occurs usually in locations not affected by bending cracks or in regions located close to the supports but not more than one third of the beams for normally shear reinforced beams. It usually starts in the middle of the section (high strains or high shear

stresses) and propagates outwards. When the principle tensile stress (σ_2) outruns the concrete's tensile strength the element failure emerges. Shear failure of the web is most of the time a consequence of the poor shear reinforcing (e.g. steel stirrups) or the lack of it.

- Bending – Shear failure

This is located usually between a third and a half of the beam (for normally shear reinforced concrete beams) the failure initiates from bending cracks to inclined shear cracks. Cracks propagate from the tensile zone toward the compression zone of the structural element. The final failure can be induced by crushing of the concrete (reaching the compressive strength of the concrete) either by splitting of the concrete zone (reaching the shear strength). Using elements of a truss model as comparison we can describe the components as:

  - Tensile bars – ties – shear and bending reinforcement
  - Compressive bars – struts – the concrete between the cracks from the tensile zone and the concrete from the compression zone.

- Compressive failure in the web

This arises in regions similar to the shear failure in the web. Compression failure in the inclined concrete struts in the truss is the main failure in this case. It is determined when the element is over dimensioned in shear and the concrete compressive strength is reached before the steel reinforcement reaches the yield limit.

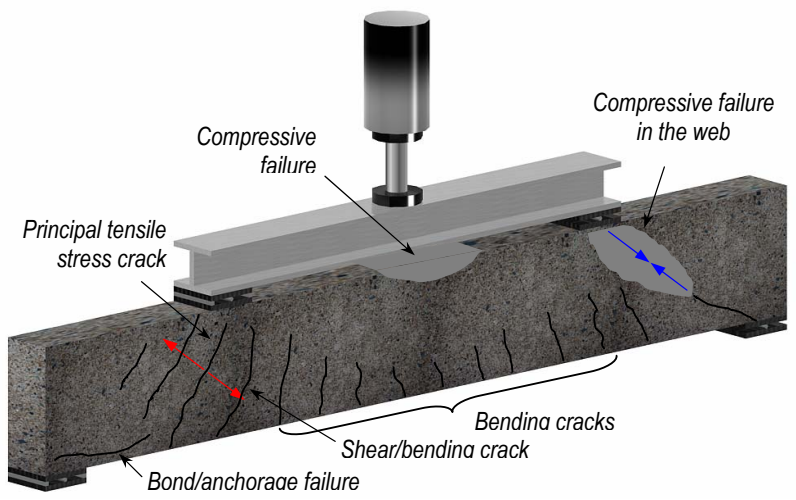

Figure 2-10: Shear failure modes in a beam (after Täljsten, 2006)

2.3.2 Shear in beams according to Eurocode (2004a, b)

The general shear design procedure presented in the previous paragraph (2.2.1) is applied for the beam design along with specific detailing of the reinforcement. The next clauses are applied for detailing the shear reinforcement:

- The shear reinforcement should form an angle α between 45° and 90° to the longitudinal axis of the structural element
- The shear reinforcement can take the form of links enclosing the tensile reinforcement, bent-up bars, cages, ladders and has to be properly anchored in the compression and tension zones
- The ratio of the shear reinforcement is determined using equation (2-44) and it has to always be larger than the minimum shear reinforcement ratio expressed in equation (2-45).

$$\rho_w = A_{sw} \Big/ \left(s b_w \sin\alpha \right) \tag{2-44}$$

$$\rho_{w,\min} = \left(0.08\sqrt{f_{ck}} \right) \Big/ f_{yk} \tag{2-45}$$

- The maximum longitudinal spacing between vertical steel stirrups is calculated according to equation (2-46), while if bent up bars are used it should not exceed the value given in the equation (2-47).

$$s_{l,\max} = 0.75d\left(1 + \cot\alpha\right) \tag{2-46}$$

$$s_{b,\max} = 0.6d\left(1 + \cot\alpha\right) \tag{2-47}$$

2.3.3 Shear in beams according to ACI (2005)

The design for shear of beams is based on the paragraph 2.2.2.

2.3.4 Shear in beams according to Betonghandbok (1997)

The shear design of reinforced concrete beams is based on empirical formulations presented in Betonghandbok (1997) and is calculated by considering independently the concrete contribution and the steel stirrups contribution (Blanksvärd, 2007).

Concrete contribution

The concrete contribution to the shear capacity is given as:

$$V_c = bdf_v \tag{2-48}$$

where

$$f_v = \xi(1+50\rho)0.3f_{ct} \tag{2-49}$$

$$\xi = \begin{cases} 0,5 & for\ d \le 0.2m \\ 1.6-d & for\ 0.2 < d \le 0.5m \\ 1.3-0.4d & for\ 0.5 < d \le 1.0m \\ 0.9 & for\ d > 1.0m \end{cases} \tag{2-50}$$

and the tensile reinforcement ratio is:

$$\rho = \frac{A_{s0}}{bd} < 0.02 \tag{2-51}$$

The value of the tensile strength f_{ct} is limited to 2.7 MPa for design.

Steel contribution

The steel contribution to the shear capacity (Eq. (2-52) is calculated based on the truss model (Blanksvärd, 2007) and considers the minimum between the equation (2-53) and equation (2-54).

$$V_s = \min\left\{V_{Rds}, V_{Rd,\max}\right\} \tag{2-52}$$

The shear reinforcement is given by the following equation

$$V_{Rds} = A_{sw} f_{sw} \frac{z}{s}\left(\cot\theta + \cot\beta\right)\sin\beta \tag{2-53}$$

The compressive failure in concrete compression struts

$$V_{Rd,\max} = \alpha_c \nu b z f_{cc} \frac{\cot\theta + \cot\beta}{1+\cot^2\theta} \tag{2-54}$$

Where θ is the angle of the compression struts with respect to a beam axis perpendicular to the shear force direction, having values $21.8<\theta<45$ for non pre-stressed reinforcement and $18.4<\theta<$for pre-stressed reinforcement. The factor for pre-stressed or other compression forces is given in eq. (2-55) and the utilized part of the concrete compressive strength, ν, is given in eq. (2-56)

$$\alpha_c = \begin{cases} 1+\dfrac{\sigma_{cn}}{f_{cc}} & for \quad 0 < \dfrac{\sigma_{cn}}{f_{cc}} \le 0.25 \\ 1.25 & for \quad 0.25 < \dfrac{\sigma_{cn}}{f_{cc}} \le 0.5 \\ 2.5\left(1-\dfrac{\sigma_{cn}}{f_{cc}}\right) & for \quad 0.5 < \dfrac{\sigma_{cn}}{f_{cc}} < 1.0 \end{cases} \tag{2-55}$$

Where the prestressing force contribution is determined as $\sigma_{cn}=N_{sd}/A_c$ with N_{sd} being the design value of the pre-stress force or other compression force and A_c the area of concrete.

$$\nu = \begin{cases} 0.6\left(1-\dfrac{\sigma_{cn}}{f_{cc}}\right) & for \quad f_{sv} = f_{st} \\ 0.6 & for \quad f_{sv} = 0.8 f_{st} \end{cases} \tag{2-56}$$

2.3.5 Calculation example for beams

The shear capacity of a beam is computed according to the design standards presented in section 2.2. As an example a beam is chosen from the experimental tests performed by Blanksvärd (2007). The test setup and the geometrical characteristics of the beam are presented in Figure 2-11. The internal lever arm d=419 mm. The stirrups spacing is 300 mm. The concrete compressive and tensile strength reported are 73.3 MPa and 3.7 MPa, respectively. The dominant shear crack was formed at 32°. The design yield strength of the steel is 500 MPa.

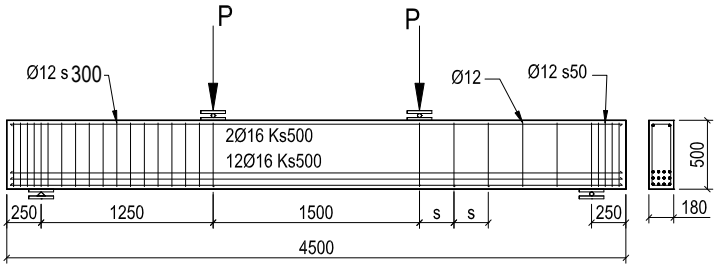

Figure 2-11: Experimental test set-up of a RC beam (from Blanksvörd, 2007)

Eurocode (2004a)

In this case the design should be performed respecting the conditions for members requiring shear reinforcement presented in paragraph 2.2.1. Although the Eurocode does not simultaneously consider the concrete contribution and the steel contribution both are presented in the followings for the sake of comparison presented in

Table 2-1.

Members not requiring shear reinforcement

$$C_{Rd,c} = \frac{0.18}{\gamma_c} = \frac{0.18}{1.5} = 0.12$$

$$\rho_l = \frac{A_{sl}}{b_w d} = \frac{12 \times \pi \times 8^2}{180 \times 419} = 0.03 > 0.02 \Rightarrow \rho = 0.02$$

$$k = 1 + \sqrt{\frac{200}{419}} = 1.69$$

$\sigma_{cp} = 0$, since no prestressing force is applied

$$V_{Rd,c} = \left[C_{Rd,c} k (100 \rho_l f_{ck})^{1/3} + k_1 \sigma_{cp} \right] b_w d = \left[0.12 \times 1.69 \times \left(100 \times 0.02 \times 73.3 \right)^{1/3} + 0 \right] \times 180 \times 419 = 80.7 \; kN$$

Members requiring shear reinforcement

The steel stirrups capacity is calculated according to eq. (2-29).

$$V_{Rd,s} = \frac{A_{sw}}{s} z f_{yd} \cot\theta = \frac{2 \times 113.04}{300} \times 0.9 \times 419 \times 500 \times \cot 32^\circ = 227.4 \; kN$$

ACI (2005)

Concrete contribution

$$V_c = 0.17 \sqrt{f_c'} b_w d = 0.17 \times \sqrt{73.3} \times 180 \times 419 = 99.314 kN$$

Steel contribution

$$V_s = \frac{A_v f_{yt} \left(\sin\alpha + \cos\alpha \right) d}{s} = \frac{2 \times 113.04 \times 500 \times \left(\sin 32^\circ + \cos 32^\circ \right) \times 419}{300} = 217.6 kN$$

The shear capacity of the beam is

$$V_n = V_c + V_s = 99.31 + 217.6 = 316.9 kN$$

Betonghandboken (1997)

Concrete contribution

$$\rho = \frac{A_{s0}}{bd} = \frac{12 \times \pi \times 8^2}{180 \times 419} = 0.03 > 0.02 \Rightarrow \rho = 0.02$$

$$\xi = 1600 - 419 = 1181 \; mm$$

$$f_v = \xi (1 + 50\rho) 0.3 f_{ct} = 1181 \times \left(1 + 50 \times 0.02 \right) \times 0.3 \times 2.7 = 1913.2 \; N/mm^2$$

$$V_c = bdf_v = 180 \times 419 \times 1913.2 = 144.3 \; kN$$

Steel contribution

$$V_{Rds} = A_{sw} f_{sw} \frac{z}{s} \left(\cot\theta + \cot\beta \right) \sin\beta = 2 \times 113.04 \times 500 \times \frac{0.9 \times 419}{300} \times \left(\cot 32^\circ + \cot 90^\circ \right) \sin 90^\circ =$$

$$= 227.4 \; kN$$

$$V = V_c + V_s = 144.3 + 227.4 = 371.7 \; kN$$

Table 2-1. Summary of the shear force design calculation

Design standard	*Concrete contribution*	*Steel contribution*	*Total shear capacity*	*Experimental value⋆*
	[kN]	*[kN]*	*[kN]*	*[kN]*
Eurocode	*80.7⋆*	*227.4*	*227.4*	
ACI	99.3	217.6	316.9	*318.9*
Betonghandboken	144.3	227.4	371.7	

⋆value displayed only for comparison purposes

The results displayed in table 2-1 are outlining the differences between the three analyzed standards. ACI has the best prediction in terms of total capacity; this may be attributed to the large number of tests used to derive the theoretical model. Eurocode underestimated the total shear capacity since is not considering simultaneously the contribution and the steel contribution. The concrete contribution calculated according to the Swedish Betonghandboken (1997) is much higher than the one presented in Eurocode and ACI although the tensile strength is limited making the prediction unsafe. The reason may partly found in be the empirical derivation of geometrical factor ξ, and also that no factored value has been used for the splitting strength, f_{ct}, of concrete

2.4 Reinforced concrete walls

2.4.1 Introduction

Reinforced concrete walls are vertical structural elements designed to withstand gravitational and lateral loading. A wall can be characterised in function of its geometrical features by: slenderness ratio (H/t), aspect ratio (H/L) and thinness ratio (L/t) (Fragomeni et al., 1994).

The walls can be loaded perpendicular to the median plane or along the median plane. These different loading systems can produce different failure modes. The perpendicular loading produces an out of plane bending failure while the in plane loading may induce diagonal compressive failure, diagonal tensile failure, or concrete crushing due to bending failure. When a wall is subjected to a gravitational load the most common failure is the compressive failure if the load is not eccentric. All theses modes of failure are depicted in Figure 2-12. Of course these general modes of failure can be present almost simultaneously if both loading systems are present, and may take different forms depending on how the walls' boundary conditions are.

Since the topic of the thesis covers the strengthening of walls with openings subjected to gravitational load a brief description of the work performed in the past years is presented below.

Doh and Fragomeni (2006) described clearly the response of the walls under axial loading in function of the boundary conditions as being: one-way action for walls supported at the top and bottom and two-way action for walls supported on al side edges (Figure 2-13).

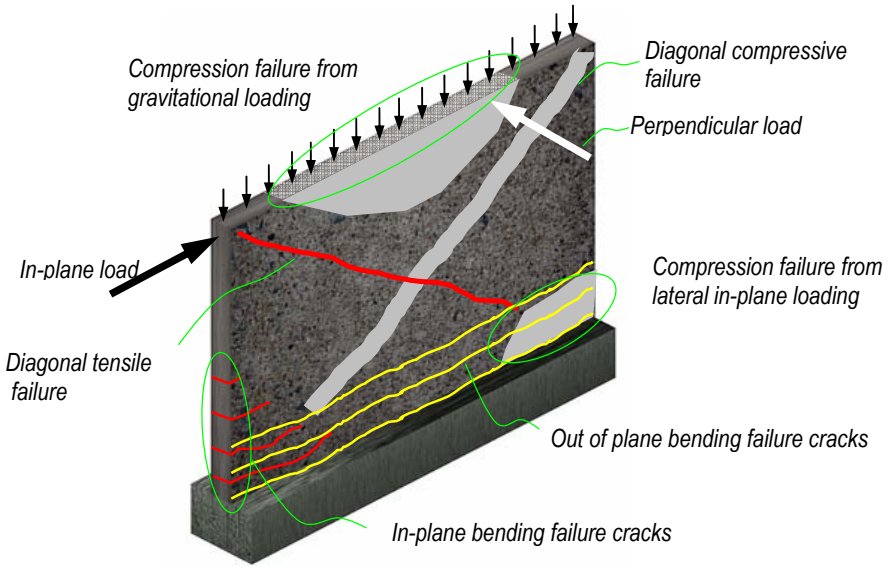

Figure 2-12: Different failure modes in walls

Work on one-way and two-way action solid walls has been carried at great extent Seddon (1956), Oberlender, (1973), Zielinski et al. (1982, 1983), Wallace et al. (1992, 1994) for example. Fragomeni et al. (1994) inventoried design formulas related to the ACI 318 design standard and several other theoretical research publications and concluded that the code failed to recognize any contribution to load capacity from restraints provided to side edges, hence the design is uneconomical. It was found that empirical design formulas developed are leading to very conservative predictions. The German code (1988, by Fragomeni et al., 1994) leads to a more realistic prediction, but is too difficult to adopt in design because it is not versatile enough for practical applications (Fragomeni et al., 1994).

A deep statistical analysis of the performed experimental results and theoretical predictions for reinforced concrete squat (height less than twice the length) walls subjected to lateral cyclic loading was presented by Gulec et al. (2008). The effectiveness of five predictive equations was evaluated using data from 120 rectangular walls. Among the conclusions of this report it is worth mentioning the large scatter between the peak shear strength predicted by all the equations. It is also reported that the equation proposed by Wood gives the best predictions.

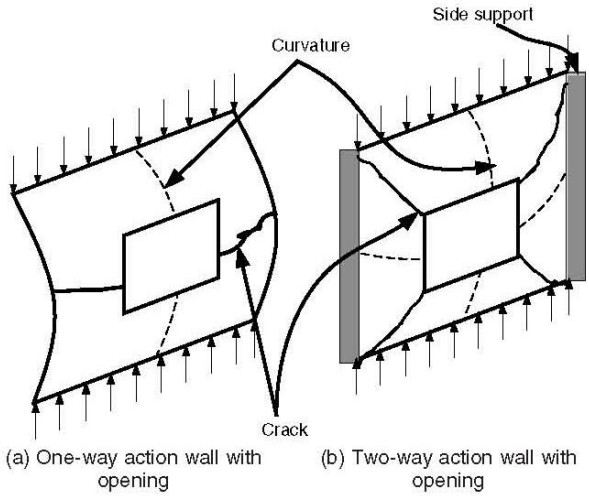

Figure 2-13: Response of walls in function of the boundary conditions (after Doh and Fragomeni, 2005)

2.4.2 Reinforced concrete walls according to Eurocode (2004a, b)

The design of reinforced concrete walls is not presented in a specific chapter in Eurocode (2004a) and the design is suggested to be performed using the variable inclination truss model, the column design method or the strut-and-tie modelling. However, detailing of members and particular rules for elements with a length to thickness ratio of 4 or more are given in section 9.6. Openings in walls are not presented and very few specifications are given in this case.

The *strut-and-tie model* is presented in general form with no particular specification for different types of elements and will be presented in the following since it can be applied also to the walls with openings.

The method is appropriate for the design in ultimate limit state (ULS) of continuous or discontinuous regions where a non linear distribution exists (i.e. supports, near concentrated loads or plain stress). The compressive stress fields are represented by the struts while the ties represent the reinforcement and being joined in nodes. The ties of the strut-and-tie should coincide in position and direction with the corresponding reinforcement. For a suitable model, the adoption of stress trajectories distribution from linear elastic analysis theory or the load path can be used.

The concrete *struts* are calculated according to equation (2-57) for regions without transverse compressive stress (Figure 2-14a) or with transverse compressive stress (Figure 2-14b). If cracks exist in the compression zones the design strength calculated with formula (2-57) is affected by the factor 0.6ν.

$$\sigma_{Rd,\max} = f_{cd} \tag{2-57}$$

Where f_{cd} is the design compressive stress and $\nu=1-f_{ck}/250$ or can be found in the National Annex.

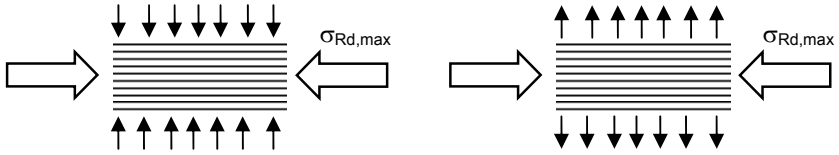

Figure 2-14: Design strength of concrete struts without (a) and with (b) transverse tension (reproduced after Eurocode 2004a)

The *ties* design is subjected to the same general rules as the steel reinforcement. The reinforcement required for the tie is calculated based on the tensile force determined from equations (2-58) and (2-59) considering the existence of discontinuities in the element.

$$T = \frac{1}{4}\frac{b-a}{b}F \text{ for partial discontinuity regions } \left(b \le \frac{H}{2}\right) \text{ (see Figure 2-15a)} \tag{2-58}$$

$$T = \frac{1}{4}\left(1-0.7\frac{a}{h}\right)F \text{ for full discontinuity regions } \left(b > \frac{H}{2}\right) \text{ (see Figure 2-15b)} \tag{2-59}$$

The rules for *the nodes* are applied for the regions where concentrated forces are transferred in a member and which are not designed by the strut-and-tie method (i.e. where point loads are applied, at supports, in anchorage zones with concentration of reinforcement or prestressing tendons, at bends in reinforcing bars or at the connection and corners of members). The main assumption beside the design is the equilibrium of all the forces acting in the node (including transverse tensile forces).

- If no ties are anchored at the node the design value for the compressive stresses within the node is determined in the same way as for the concrete struts:

$$\sigma_{Rd,\max} = k_{1w}\nu f_{cd} \tag{2-60}$$

For the factor k_{1w} it is recommended to take the value 1.0 or the value defined in the National Annex.

- In compression - tension nodes with anchored ties provided in one direction are designed according to equation (2-60) only replacing the factor k_{1w} with k_2=0.85
- In compression-tension nodes with anchored ties provided in more than one direction are designed according to the same equation (2-60) only replacing the factor k_1 with k_3=0.75.

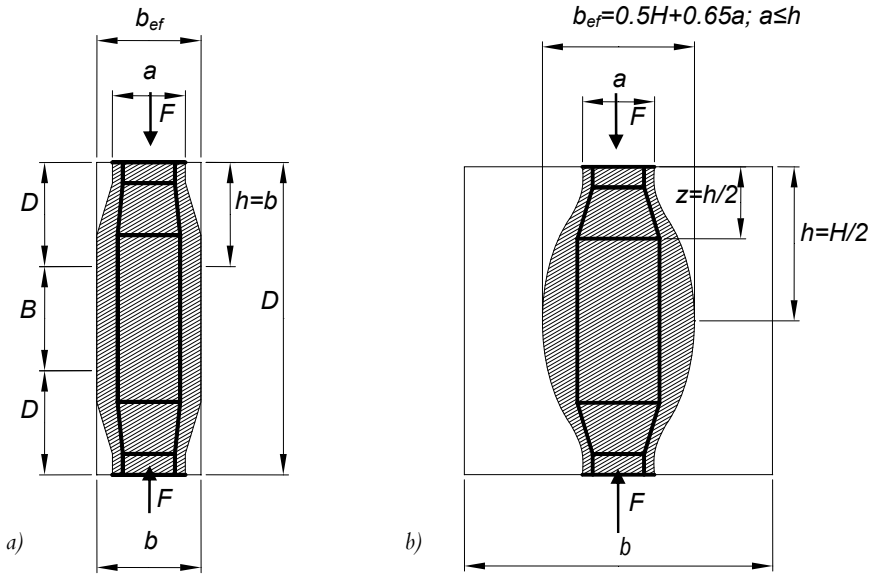

Figure 2-15: Parameters for the determination of transverse tensile forces in compression field with smeared reinforcement for a) partial discontinuity b) full discontinuity (after Eurocode 2004a)

For all three cases mentioned above the design values of the compressive stress have to be increased with 10% if:

- triaxial compression is assured,
- all angles between struts and ties are ≥ 55°,
- the stresses applied at supports or at point loads are uniform, and the node is confined by stirrups,
- the reinforcement is arranged in multiple layers,
- the node is reliably confined by means of bearing arrangement or friction.

For plain concrete or where the reinforcement is less then the minimum required the maximum stresses induced by the shear force V_{Ed} and normal force N_{Ed} should satisfy the conditions:

$$\tau_{cp}=V_{Ed}/A_{\alpha}\leq f_{cvd} \tag{2-61}$$

Where:

- if $\sigma_{cp}\leq \sigma_{c,lim}$ $\qquad f_{cvd}=\sqrt{f_{ctd}^2+\sigma_{cp}f_{ctd}}$

or

- if $\sigma_{cp} > \sigma_{c,lim}$ $\qquad f_{cvd} = \sqrt{f_{ctd}^2 + \sigma_{cp} f_{ctd} - \left(\frac{\sigma_{cp} - \sigma_{c,\lim}}{2}\right)^2}$

and $\sigma_{cp} = N_{Ed}/A_c \leq f_{cvd}$, $\sigma_{c,\lim} = f_{cd} - 2\sqrt{f_{ctd}\left(f_{ctd} + f_{cd}\right)}$

In addition to the Eurocode (2004a) a short description of the shear walls is given in Annex I of Eurocode (2004b). The shear walls are defined as being plain or reinforced concrete walls which contribute to the lateral stability of the structure. The lateral load resisted by each shear wall in a structure should be obtained from a global analysis of the entire structure (Figure 2-16). For design purposes the combined effect of axial loading and shear has to be considered. Furthermore a simple design equation (2-62) for the lateral load resisted by a shear wall is given for buildings not exceeding 25 storeys where the plan layout of the walls is reasonably symmetrical and walls have no openings causing significant global shear deformation. Where *EI* is the rigidity of the considered walls, *e* is the eccentricity of the load P with respect to the centroid and Y_n is the relative distance of the n-th wall to the centroid.

$$P_n = \frac{P(EI)_n}{\sum(EI)} \pm \frac{(Pe)\gamma_n (EI)_n}{\sum(EI)Y_n^2} \tag{2-62}$$

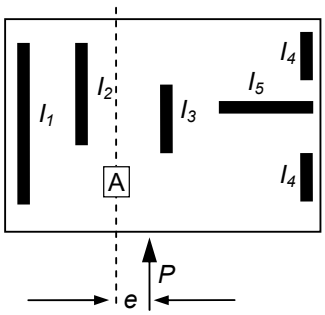

Figure 2-16: Eccentricity of load from centroid of shear walls

For a successful design, a building subjected to vertical loads and lateral loads, such as wind or earthquakes, needs to have adequate capacity to dissipate energy without substantial reduction of its overall resistance against horizontal and vertical loading (Eurocode 2004b). As an example concrete buildings may alternatively be designed for low dissipation capacity and low ductility, by applying only the rules of Eurocode (2004a) for the seismic design situation. The overall ductile behaviour is considered to be assured if the ductility demand involves globally a large volume of the structure spread to different elements and locations of all its storeys. The order of the failure modes is considered of outmost importance. The ductile failure (e.g. flexure) should precede the brittle failure modes (e.g. shear). Structures may be classified in two ductility classes DCM (medium ductility) and DCH (high ductility) depending on their

hysteretic dissipation capacity. For both ductility classes different provisions are given for the elements of the structure.

Since walls may have different behaviour as parts of different structural systems they can be classified as:

- *ductile wall* – wall fixed at the base so that the relative rotation of the base with respect to the rest of the structural system is prevented, and that is designed and detailed to dissipate energy in a flexural plastic hinge zone free of openings or large perforations, just above its base.
- *large lightly reinforced wall* – wall with large cross-sectional dimensions, that is, a horizontal dimension l_w at least equal to 4.0 m or two-thirds of the height h_w of the wall, whichever is less, which is expected to develop limited cracking and inelastic behaviour under the seismic design situation.
- *coupled wall* – structural element composed of two or more single walls, connected in a regular pattern by adequately ductile beams ("coupling beams"), able to reduce by at least 25% the sum of the base bending moments of the individual walls if working separately.
- *wall system* – structural system in which both vertical and lateral loads are mainly resisted by vertical structural walls, either coupled or uncoupled, whose shear resistance at the building base exceeds 65% of the total shear resistance of the whole structural system.

The design for shear resistance is presented for both ductility classes (i.e. DCM and DCH) for ductile walls and large lightly reinforced wall as follows.

DCM (medium ductility)

The DCM (medium ductility) walls should be designed according to the general design procedure for shear (variable truss angle or strut-and-tie model) to which special provisions for allowing local ductility are provided.

For large lightly reinforced walls a clause that ensures flexural yielding before the shear failure is introduced (Eq. (2-63). This requirement is considered to be satisfied if at every storey of the wall the design shear force V_{Ed} is obtained from the shear force calculated from the analysis, V'_{Ed}.

$$V_{Ed} = V'_{Ed} \frac{q+1}{2} \tag{2-63}$$

where $q = q_0 k_w \geq 1.5$ is the behaviour factor depending on the type of structural system and on its regularity in elevation (q_0) and the factor reflecting the prevailing failure mode k_w. If the value calculated with equation (2-63) is smaller than the value obtained from equation (2-25) the minimum shear reinforcement ratio $\rho_{w,min}$ in the web is not required, else the shear reinforcement should be calculated on the basis of the variable inclination truss model or strut-and-tie model.

DCH (high ductility)

The design shear force for ductile DCH (high ductility) is determined according to equation (2-64).

$$V_{Ed} = \varepsilon V_{Ed}^{'} \tag{2-64}$$

where $V_{\mathrm{Ed}}^{'}$ is the shear force from the analysis and ε is the magnification factor determined from equation (2-65) but never smaller than 1.5.

$$\varepsilon = q\sqrt{\left(\frac{\gamma_{Rd}}{q}\frac{M_{Rd}}{M_{Ed}}\right)^2 + 0.1\left(\frac{S_e(T_c)}{S_e(T_c)}\right)^2} \le q \tag{2-65}$$

The value of the shear resistance, when *diagonal compression failure of the web* occurs outside the critical region, is calculated from equation (2-33) in which the internal lever arm, z=0.8l_{w} and the inclination of the compression strut to the vertical, tanθ=1. When the failure is located inside the critical region 40% of the value outside the critical region is used.

When the *diagonal tension failure of the web* is considered the web reinforcement for the ULS verification in shear has to consider the value of the shear ratio defined in equation (2-66).

$$\alpha_s = M_{Ed}/(V_{Ed}l_w) \tag{2-66}$$

- If α_{s}≥2

The general equations (2-29) to (2-35) are used with the internal lever arm, z=0.8l_{w} and the inclination of the compression strut to the vertical, tanθ=1.

- If α_{s}<2

For the horizontal web bars equation (2-44) is modified to account the horizontal reinforcement in the web and is applied as:

$$V_{Ed} \le V_{Rd,c} + 0.75\rho_h f_{yd,h} b_{wo} \alpha_s l_w \tag{2-67}$$

If the axial force is tensile than the concrete contribution $V_{Rd,c}$ should be zero in the critical regions.

The amount of vertical web bars should be larger than the horizontal web bars, if anchored and spliced according to the clauses from Eurocode (2004a):

$$\rho_h f_{yd,h} b_{wo} z \le \rho_v f_{yd,z} b_{wo} z + \min N_{Ed} \tag{2-68}$$

In primary seismic walls with a height to length ratio, $h_{\mathrm{w}}/l_{\mathrm{w}}$, not greater than 2.0 (squat walls), there is no need to modify the bending moments from the analysis. Shear magnification due to dynamic effects may also be neglected. The shear force $V_{\mathrm{Ed}}^{'}$ from the analysis needs to be increased as follows in equation (2-69).

$$V_{Ed} = \gamma_{Rd}\left(\frac{M_{Rd}}{M_{Ed}}\right)V'_{Ed} \le qV'_{Ed} \tag{2-69}$$

2.4.3 Reinforced concrete walls according to ACI (2005)

The wall design is presented in summarized form in Chapter 14 in ACI (2005) and is performed according to tree types of solicitation: axial, flexural and shear. A direct method for the computation of the walls under axial loading is given also. The flexural design of wall is addressed in Chapter 10, and as in Eurocode is given in general terms. The specifications given in Chapter 14 are the ones concerning the minimum reinforcement. Special provisions are given in Chapter 21 for walls subjected to seismic loading where the design of the walls boundary elements and coupling beams are described. The design of perforated walls is performed considering the sub-elements (pier walls and coupling beams), each being designed individually. The efficiency and the unitary behaviour of the walls with openings is assured by providing anchorage length of the reinforcement and assuring the redistribution of stresses. Otherwise the method for deriving the formulas is semi empirical, as for the beam design, and uses the addition principal and plasticity theory (as upper bound and lower bound limits are introduced).

The method used for calculating the walls with a height not exceeding two times the length of the wall is the strut and tie model, presented in detail in Appendix A in ACI. The general formula presented to calculate a cross section subjected to shear is based on the general design for shear equation (2-36). The nominal concrete strength V_c shall be permitted to be the lesser of the values computed from equation (2-70) and (2-71).

$$V_c = 0.27\sqrt{f'_c}t_w d + \frac{N_u d}{4l_w} \tag{2-70}$$

$$V_c = \left[0.05\sqrt{f'_c} + \frac{l_w\left(0.1\sqrt{f'_c} + 0.2\frac{N_u}{l_w t_w}\right)}{\frac{M_u}{V_u} - \frac{l_w}{2}}\right]hd \tag{2-71}$$

If the denominator in equation (2-71) is negative, the equation shall not apply. When a detailed calculus, according to equations (2-70) and (2-71) is not performed the nominal shear strength V_c is limited to the value $0.17\sqrt{f'_c}hd$ for walls subjected to axial compression, or it should not be taken to be greater than the value given in equation (2-72) for walls subjected to axial tension.

$$V_c = 0.17\left(1 + \frac{0.29N_u}{A_g}\right)\sqrt{f'_c}b_w d \tag{2-72}$$

Both, equation (2-70) and (2-71) may be used to determine the inclined cracking strength at any section through a shear wall.

The reinforcement provided in the walls is determined according to the formula (2-43) in which A_v is the area of horizontal shear reinforcement with spacing s and $d=0.8l_w$. The provisions for the horizontal reinforcement area are given as the ratio of the steel to gross concrete area in vertical and horizontal directions.

$$\rho_t > 0.0025 \tag{2-73}$$

$$\rho_l > 0.0025 + 0.5\left(2.5 - \frac{t_w}{l_w}\right)\left(\rho_t - 0.0025\right) \tag{2-74}$$

The spacing of both vertical and horizontal reinforcement should not exceed the smallest of $l_w/3$, 3h and 450 mm for vertical and $l_w/5$, 3h and 450 mm for horizontal.

The special provisions for seismic design in Chapter 21 (ACI, 2005) address more restrictive design. At least two curtains (layers) of reinforcement should be used if $V_u > 0.17A_{cv}\sqrt{f_c}$. Specific development of the reinforcement in the wall is given to account for the alternation of the sagging and hogging moment. The shear strength equation (2-75) presented here considers the vertical gross area of concrete (A_{cv}) and the steel transverse reinforcement area (ρ_t).

$$V_n = A_{cv}\left(\alpha_c\sqrt{f_c'} + \rho_t f_y\right) \tag{2-75}$$

α_c, the coefficient defining the relative contribution of concrete strength to nominal shear strength is given in function of the ratio of the entire height of the wall h_w to the length of the wall l_w (Eq. (2-76).

$$\alpha_c = \begin{cases} 0.25 & for \quad h_w/l_w \le 1.5 \\ 0.17 & for \quad h_w/l_w \ge 2.0 \end{cases} \tag{2-76}$$

For values between 1.5 and 2.0 of α_c a linear variation is assumed.

The shear reinforcement has to be distributed in the plane of the wall in two orthogonal directions and if the ratio h_w/l_w does not exceed 2.0 the longitudinal ratio reinforcement ρ_l cannot be less than the transversal reinforcement ratio ρ_t.

The *wall with opening* is considered a "wall segment (…) as a part of a wall bounded by openings or by openings and an edge. Traditionally, a vertical wall segment bounded by two window openings has been referred as piers" (ACI, 2005). When wall piers share a common lateral force V_n shall not be taken larger than $0.66A_{cv}\sqrt{f_c}$. The individual pier wall's shear strength is also limited to the value $0.83A_{cv}\sqrt{f_c}$. The average unit shear strength for the total available cross-sectional area is limited to $0.66\sqrt{f_c}$ if the factored shear force at a given level in the structure is greater then the nominal shear

strength. Furthermore to any single pier, a maximum limit of $0.83\sqrt{f_c}$ for the unit shear strength is imposed to limit the degree of redistribution of shear force.

To determine whether boundary elements are needed two methods are used in function of the construction method. The first, considers if the walls or piers are "effectively" continuous from base of structure to top of wall, and designed to have a single critical section for flexural and axial loads, also known as the displacement-based analysis. Limitations are introduced (restricting the neutral axis movement as displacement increases) for the compression zones and the extension length of the reinforcement from the critical section. The second category is more general and is referred to as "structural walls not designed to the previous section" (ACI, 2005). The boundary elements shall be applied for walls or piers at boundaries or edges around openings where the maximum extreme fibre compressive stress or loads effect from earthquake exceeds $0.2f_c$. In this case the wall is considered to be acted on by gravity loads and the maximum shear and moment induced by an earthquake in a given direction. The boundary elements are permitted to be interrupted only in the sections where the compressive stress is less than $0.15f_c^{'}$. Few specifications are given as to how to calculate the aforementioned compressive stress. A linear elastic analysis considering the gross section properties is only suggested. If from the above two mentioned methods a need of boundary elements results, specification are given for the reinforcement design. Where special boundary elements are not required, minimum reinforcement ratio and anchorage length is prescribed.

Two or more piers of walls are connected by coupling beams. The design of coupling beams has to be performed in function of the ratio of the clear span (l_n) and height (h_b) of the beam:

- If $l_n/h_b \geq 4$ the provisions from flexural members (beams) of special moments are applied (Paragraph 21.3 in ACI)
- If $l_n/h_b < 4$ shall be permitted to be reinforced with two intersecting groups of diagonally placed bars symmetrical about the mid span. No other details are given in this case.
- If $l_n/h_b < 2$ and V_u is exceeding $0.33\sqrt{f_c}A_{cw}$ the coupling beams are reinforced with two intersecting groups of diagonally placed bars symmetrical about the mid span.

When intersecting groups of diagonally placed bars symmetrical about the mid span are used, they need to satisfy several assembling criteria. The nominal shear strength is determined according to equation (2-77):

$$V_n = 2A_{vd}f_y \sin\alpha \leq 0.83\sqrt{f_c}A_{cw} \qquad (2\text{-}77)$$

In plus, the diagonally placed bars shall be developed for tension in the wall and contribute to the nominal flexural strength M_n of the coupling beam.

2.4.4 Walls with openings

When mentioning the design of walls with openings, Doh and Fragomeni (2005) stated that the current design codes Australian Standard AS3600-01 and ACI318-02 (quoted in Doh and Fragomeni, 2005) do not include any provisions for it. Moreover theoretical work is not covered for elements with slenderness ratio (height to thickness ratio) less than 30. Analyzing the latest release of ACI 318-05 and Eurocode (2004a, b), the same conclusion can be drawn.

Consistent work performed on one-way acting wall panels has been reported by Seddon (1956). After several tests it was concluded that the opening in the wall changed the global mode of failure as the parts above and below the aperture caused beam element behaviour and the potions adjacent to the opening had a column element action. The panels failed "through one of the column elements due to cracks extending to the corners of openings". The necessity of appropriate reinforcement in the "beam elements" was also reported.

Zielinski et al. (1982, 1983) undertook experimental investigations on ribbed panels with window openings under axial uniformly distributed loading. Failure was localized in areas of abrupt changes in cross section and concentration of stresses. Vertical cracking emerged from the top and bottom corners of the openings and extended to the bearing ribs.

Tremendous effort was involved in investigating the influence of openings in walls by Saheb and Desayi (1989, 1990a). 12 panels were tested to in-plane vertical loading at an eccentricity representing a possible accidental loading (Figure 2-17). Half of the specimens tested considered a one-way action and the other half consider the two-way action. Proper reinforcement was provided at 45° in the corners to avoid premature cracking failure. For one-way walls, the failure consisted in buckling influenced by bending of the slender column strips adjacent to openings. The two-way walls had a slightly more rigid performance, but the ultimate load was nearly equal for both cases. Based on these experimental results two empirical formulas were developed with the recommendation of caution in use since some factors needed more calibration.

Four reduced scaled structural walls were tested by Ail and Wight (1991) under constant vertical load and horizontal cyclic load. Three of the specimens were designed with openings and one was solid. All the specimens were assembled in a multi-story structure. It was investigated the damage at different levels of drifts for each story and the effectiveness of the staggered-opening concept. It was found that story drift of 1% was not producing significant damage and the staggered-opening positioning is a viable alternative to the in-line door opening that creates coupled walls. The experimental tests showed that door openings located to close to the edge of the boundary column remove the in-plane confinement and can trigger an early shear compression failure. Based on basic mechanics theory and reinforced concrete principles a the envelope for all four walls was presented

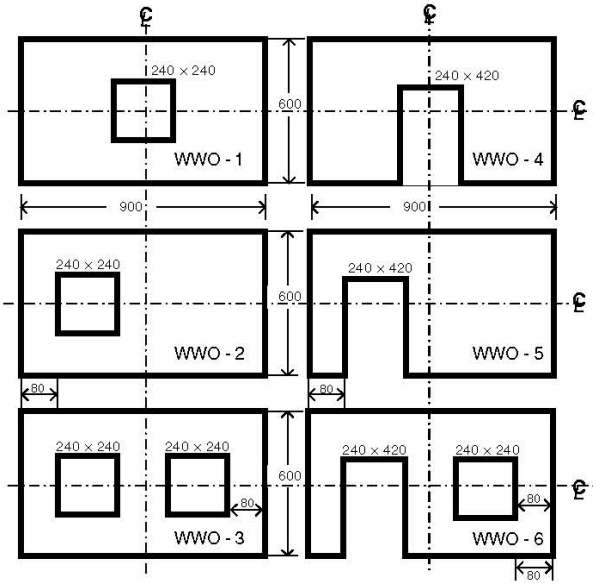

Figure 2-17: Details example of Saheb and Desayi (1990b) walls with openings (from Doh and Fragomeni, 2006)

More recently Doh et al. (2002), Doh and Fragomeni (2005) and Doh and Fragomeni (2006) conducted an intensive experimental and theoretical program on one-way and two-ways walls with and without openings. These walls were half scaled and loaded with an eccentricity of $t_w/6$. The slenderness ratio varied between 30 and 40 and the test results indicated that axial strength ratio gradually decreases with the increase of the slenderness. The study was finalized with a theoretical model based on empirical derivations from the tests found in the literature. With the experience accumulated from the work carried out during the year Doh and Fragomeni (2006) recommended more work on this subject since "the research on high strength concrete wall panels with various openings remains relatively unexplored and needs more focused research in the future".

Numerical analysis of one-way and two-way reinforced concrete walls with openings has been carried out by Hallinan and Guan (2007). After establishing a benchmark model a parametric survey was carried out on 54 wall panels investing the slenderness ratio and the effects of eccentricity on the ultimate load capacity. The results from the non linear analysis are compared with the experimental results and found satisfactory. Also, from the parametric study it is concluded that as a wall panel becomes more slender its axial strength ratio decreases and openings have decreasing axial strength for low slenderness ratio rather than high slenderness. The eccentricity is found to affect more the one-way walls more than the two-way walls. Hallinan and Guan (2007) concluded that more experimental tests would be needed to validate the finite element analysis used.

2.4.5 Theoretical models for walls with openings

A full study including experimental and theoretical work on reinforced concrete walls with openings was conducted in very few cases. The complex mechanism of failure restricted analytical models and the derivations for these theoretical formulations have empirical background. The models for predicting bearing capacity of walls with openings found in the literature are presented below. The use of these models is presented in paragraph 2.5.6.

Saheb and Desayi (1990b)

The intensive experimental work performed (Saheb and Desayi 1989, 1990a) was evaluated, and two design formulas were presented for walls with openings (Saheb and Desayi, 1990b).The ultimate load is determined using equation (2-78):

$$N_{u0} = \left(k_1 - k_2 \chi\right) N_{us} \tag{2-78}$$

The design axial load N_u is the ultimate load of an identical solid wall and can be calculated for one-way action according to equation (2-79) and for two-way action assuming equation (2-80).

$$N_{us} = 0.55\left[A_g f_c^{'} + \left(f_y - f_c^{'}\right) A_{sw}\right]\left[1 - \left(\frac{H}{32 t_w}\right)^2\right] \tag{2-79}$$

$$N_{us} = 0.67 f_c^{'} A_g \left\{1 - \left[L / \left(120 t_w\right)\right]^2\right\}\left\{1 + 0.12\left(H / L\right)\right\} \tag{2-80}$$

where:

$$k_1 = \begin{cases} 1.25 & \text{for one - way action} \\ 1.02 & \text{for two - way action} \end{cases}$$

$$k_2 = \begin{cases} 1.22 & \text{for one - way action} \\ 1.00 & \text{for two - way action} \end{cases}$$

The non-dimensional factor χ is determined as:

$$\chi = \left(\frac{A_0}{A} + \frac{\eta}{L}\right), \text{ where } \eta = \left(\frac{L}{2} - \bar{\eta}\right)$$

The parameter $\bar{\eta}$ is the distance from the left vertical edge to the centre of gravity of the cross section of the wall with openings (see Figure 2-18) given as:

$$\bar{\eta} = \left(\frac{\frac{1}{2} t_w L^2 - t_w L_0 \eta_0}{L t_w - L_0 t_w}\right) \tag{2-81}$$

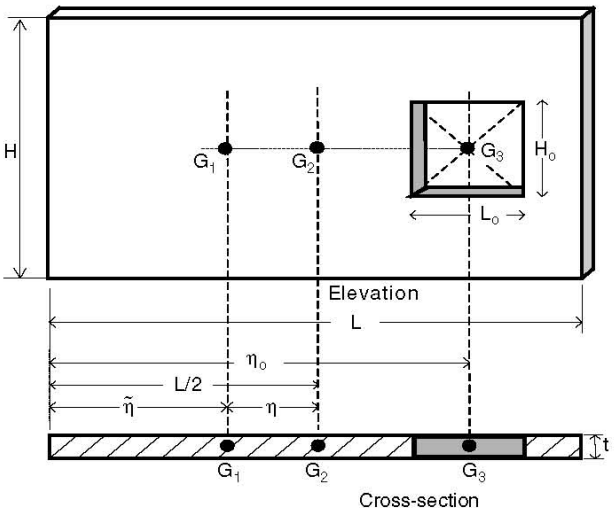

Figure 2-18: Geometry of a wall with openings for Saheb and Desayi (1990b) (from Doh and Fragomeni, 2006)

Please note that this method for calculating the capacity of the wall with openings is not applicable in all situations and is valid for the concrete walls with slenderness ration H/t_w<12 and normal strength concrete. In the calculation example presented in the next paragraph the capacity of the wall with openings is actually higher than for the same wall without opening.

Doh and Fragomeni (2006)

The equation (2-82), suitable only for solid walls with slenderness ratio less than 25, has presented first in Australian Standard AS3600-01 (2001), has modified based on the experimental work (Doh and Fragomeni, 2002, 2005).

$$N_{us} = 2.0\left(f_c^{'}\right)^{0.7}\left(t_w - 1.2e - 2e_a\right) \tag{2-82}$$

where e_a, is an additional eccentricity due to deflections in the wall (mm) defined by equation (2-83). In equation (2-83) a 0.6 safety factor is suggested to be used.

$$e_a = \frac{\left(H_{we}\right)^2}{2500t_w} \tag{2-83}$$

The effective height of the wall, H_{we}, is defined as:

$$H_{we} = \beta_w H \tag{2-84}$$

And the effective height factor can be determined for one-way walls using equation (2-85) or two-way walls by equation (2-86).

$$\beta_w = \begin{cases} 1 & for \quad H/t_w < 27 \\ \dfrac{18}{\left(\dfrac{H}{t_w}\right)^{0.88}} & for \quad H/t_w \geq 27 \end{cases} \tag{2-85}$$

$$\beta_w = \begin{cases} \alpha_w \dfrac{1}{1+\left(\dfrac{H}{L}\right)^2} & for \quad H \leq L \\ \alpha_w \dfrac{L}{2H} & for \quad H > L \end{cases} \tag{2-86}$$

The eccentricity factor α in equation ((2-86) can be calculated as:

$$\alpha_w = \begin{cases} \dfrac{1}{1-\dfrac{e}{t_w}} & for \quad H/t_w < 27 \\ \dfrac{1}{1-\dfrac{e}{t_w}} \times \dfrac{18}{\left(\dfrac{H}{t_w}\right)^{0.88}} & for \quad H/t_w \geq 27 \end{cases} \tag{2-87}$$

One year later Doh and Fragomeni (2006) published a new model in which they combined the model presented in Doh and Fragomeni (2005) with the model Saheb Desayi (1990b). The parameter N_u in the ultimate load capacity of a wall with openings Eq. (2-78) is calculated using the solid wall capacity defined in equation (2-82). A new set of factors, k_1 and k_2, had to be introduced by using the newly combined equation. A regression analysis has been undertaken from the merged experimental set of values (Figure 2-19) and it was found that k_1=1.188 and k_2=1.175 for one-way action walls, and k_1=1.004 and k_2=0.933 for two-way action walls. Omitting any reinforcement from the calculation is the major drawback of the model since the predictions are unrealistic (see paragraph 2.5.6).

Betonghandboken (1997)

The design of the solid walls in Betonghandboken (1997) is presented as a particular case of the column design. The openings in walls are not specifically addressed and the design recommendations are based on the calculations of the deep beams, therefore this method is discussed and presented here.

It is clear that opening can change the stresses in a wall panel radically. Since Betonghandboken (1997) is developed for engineering purposes an easy to use and clear method to determine the bending moment close to openings in deep beams is presented. The design consists in verifying the moment capacity in several sections as depicted in Figure 2-20a) and refers only to openings close to the edge of a deep beam. In this case Betonghandboken (1997) considers the sections adjacent to the opening as a

frame (Figure 2-20b). The shear force through the section of the opening is entirely supported by the beam over the opening. The moment distribution presented in Figure 2-20c) is determined according to the elastic theory in which the next simplifications are adopted, $V_2=R_2$ and $M_2 = e\ R_2$.

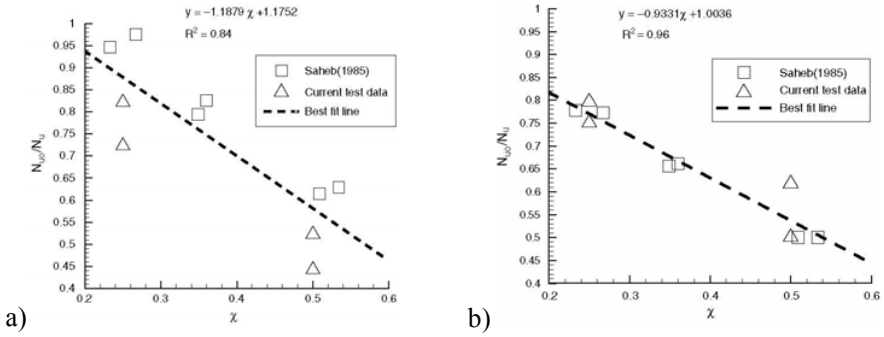

Figure 2-19: Calibration of the load capacity from experimental values for a) one-way action walls b) two-way action walls (from Doh and Fragomeni, 2006)

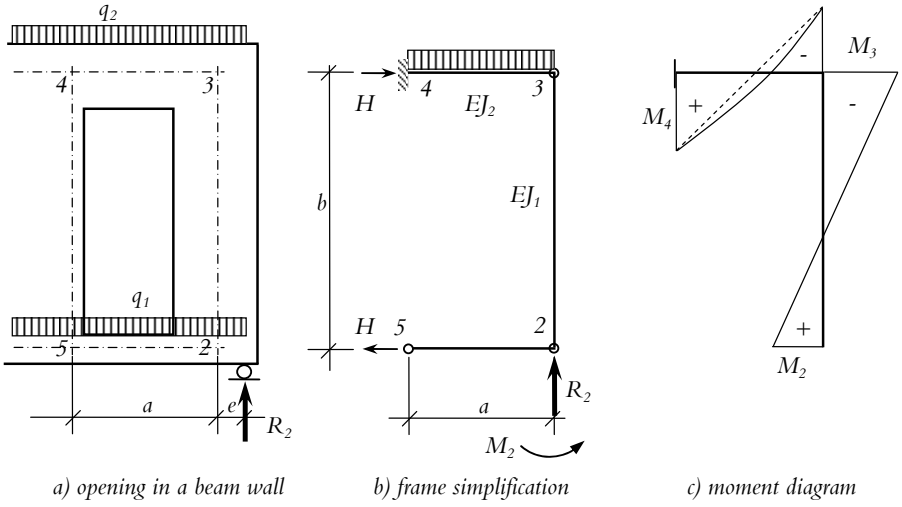

Figure 2-20: Methodology used in Betonghandboken for designing openings in wall (after Betonghandbok, 1997)

Another simplification is introduced as the moment resistance for bars 2-5 is set to be equal to zero, since in reality the opening is cutting the bar. The frame consisting of bars 2-3, 2-5 and 3-4 is once static undetermined. The moments in points 3 and 4 are determined as.

$$M_3 = \frac{-3R_2a - q_2a + M_2k}{2k+6} \text{ and } k = \frac{EI_2}{EI_1}\frac{b}{a} \tag{2-88}$$

$$M_4 = R_2a - q_2a^2/2 + M_3 \tag{2-89}$$

The horizontal force H is determined from the following equation

$$H = \frac{M_2 - M_3}{b} \tag{2-90}$$

2.4.6 Calculation example for walls

A reinforced concrete walls with openings consider the wall in Figure 2-21. A concrete of 20MPa compressive strength has been used. An in plane mesh reinforcement is provided into the wall Ø4/200/200. The strength of the reinforcement is 400MPa. No eccentricity is considered here. The wall is calculated for both one-way action and two-way action respectively.

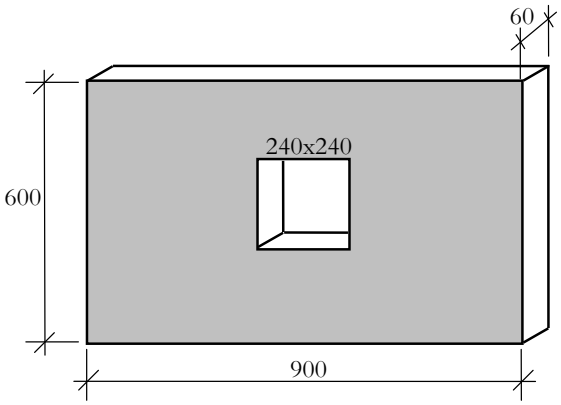

Figure 2-21: Geometrical characteristics of the wall with opening in mm

Saheb and Desayi (1990b) model prediction

$A_g = 900 \times 600 = 540000\ mm^2$

$A_{sv} = 9 \times \pi \times r^2 = 30 \times \pi \times 2^2 = 113.04\ mm^2$

Capacity for one-way action solid wall

$$N_{us} = 0.55\left[A_g f_c^{'} + \left(f_y - f_c^{'}\right)A_{sv}\right]\left[1 - \left(\frac{H}{32t_w}\right)^2\right] =$$

$$= 0.55 \times \left[900 \times 60 \times 20 + \left(400 - 20\right) \times 113.04\right]\left[1 - \left(\frac{600}{32 \times 60}\right)^2\right] = 557.35\ kN$$

Capacity for two-way action of the wall

$$N_{us} = 0.67 f_c^{'} A_g \left\{1 - \left[L / \left(120 t_w\right)\right]^2\right\}\left\{1 + 0.12\left(H / L\right)\right\} =$$

$$= 0.67 \times 20 \times 900 \times 60 \times \left\{1 - \left[900/\left(120 \times 60\right)\right]^2\right\}\left\{1 + 0.12 \times \left(600/900\right)\right\} = 769.28\ kN$$

$$\overline{\eta} = \left(\frac{\frac{1}{2}t_w L^2 - t_w L_0 \eta_0}{L t_w - L_0 t_w}\right) = 450\ mm \quad \text{(the opening is in the centre of the wall)}$$

$$\eta = \left(\frac{L}{2} - \overline{\eta}\right) = 0$$

$$\chi = \left(\frac{A_0}{A} + \frac{\eta}{L}\right) = \frac{240 \times 60}{54000} + 0 = 0.267$$

The capacity of the wall with opening for one-way action is:

$$N_{u0} = \left(k_1 - k_2 \chi\right) N_{us} = (1.25 - 1.22 \times 0.267) \times 557.35 = 515.14\ kN$$

The capacity of the wall with opening for two-way action is:

$$N_{u0} = \left(k_1 - k_2 \chi\right) N_{us} = (1.02 - 1.00 \times 0.267) \times 769.3 = 579.3\ kN$$

From the above calculations it is noted that an opening in a wall is affecting more the two way action walls rather than the one way action walls.

Doh and Fragomeni (2006) model prediction

The slenderness ratio is calculated first.

$H/t_w = 600/60 = 10$, so the coefficients for determining the effective height are:

$\beta_w = 1$ for one-way action

$$\beta_w = \frac{1}{1 + \left(\frac{600}{900}\right)^2} = 0.693 \quad \text{for two-way action}$$

$\alpha_w = 1$ since no eccentricity is assumed in this example only the additional eccentricity due to deflections in the wall will be calculated.

$H_{we} = \beta_w H = 600\ mm$ for one-way action

$H_{we} = \beta_w H = 0.693 \times 600 = 415.8\ m$ for two-way action

$e_a = \frac{\left(H_{we}\right)^2}{2500 t_w} = \frac{600^2}{2500 \times 60} = 2.4\ mm$ for one-way action

$e_a = \frac{\left(H_{we}\right)^2}{2500 t_w} = \frac{415.8^2}{2500 \times 60} = 1.15\ mm$ for two-way action

For one way action the solid wall's capacity is:

$$N_{us} = 2.0\left(f_c^{'}\right)^{0.7}\left(t_w - 1.2e - 2e_a\right) = 2.0 \times \left(20\right)^{0.7} \times \left(60 - 2 \times 2.4\right) =$$
$$= 898\ N/mm \times 900mm = 808.97\ kN$$

For two way action the solid wall's capacity is:

$$N_{us} = 2.0\left(f_c^{'}\right)^{0.7}\left(t_w - 1.2e - 2e_a\right) = 2.0 \times 20^{0.7} \times \left(60 - 2 \times 1.15\right) =$$
$$= 939.56\ N/mm \times 900mm = 845.61\ kN$$

The wall with opening is calculated similarly as in Saheb and Desay (1990) only using the new experimental coefficients proposed by Doh and Fragomeni (2006).

And the total capacity of the wall with openings is:

for one-way action:

$$N_{u0} = \left(k_1 - k_2 \chi\right) N_{us} = (1.1885 - 1.175 \times 0.267) \times 808.97 = 707.67 kN$$

for two-way action:

$$N_{u0} = \left(k_1 - k_2 \chi\right) N_{us} = (1.004 - 0.933 \times 0.267) \times 845.61 = 638.34\ kN$$

Table 2-2 summarizes the predictions calculated with the above models. As a general remark it can be mentioned the quite large difference between the values predicted by the two models although the Doh and Fragomeni (2006) model is using the same general equation from Saheb and Desayi (1990b). These variations might appear because the values determined using Saheb and Desayi (1990b) model do not consider any eccentricity and the derivations used are partially empirical. The Doh and Fragomeni (2006) model is derived entirely from experimental results.

Table 2-2. Summary of the shear force design calculation

Models	*Solid wall*		*Wall with opening*	
	One-way action [kN]	*Two-way action [kN]*	*One-way action [kN]*	*Two-way action [kN]*
Saheb and Desayi (1990)	*557.35*	*769.28*	*515.14*	*579.3*
Doh and Fragomeni (2006)	809.97	845.61	707.67	638.34

3 Fibre reinforced polymers

Fibre reinforced polymers (FRP) are a composite material. The first known composite material made by man is a floor made of red lime, sand, and gravel found in Serbia and dated 5600BC (Wild, 2007). Etymologically the word composite has its origin in the Latin language, *componere*, which means to put together. Composite materials are made from two ore more constituent materials with significantly different physical and/or chemical properties which remain separate and distinct on a microscopic level. In this thesis composites will refer to fibre reinforced materials. The FRP composites have two constituent materials: the fibres and the matrix. Embedding the fibres, the matrix has the role to support and keep the relative position. The composites are well known and have been widely used in sports equipment, aeronautics, vehicle industry or medicine for a long time.

3.1 Composites

In civil engineering, composites used have different shapes and configurations. The acronyms used to distinguish the composites for strengthening structures are defined by the type of fibre used: AFRP (Aramid Fibre Reinforced Polymers), CFRP (Carbon Fibre Reinforced Polymers) or GFRP (Glass Fibre Reinforced Polymers). From these three above mentioned composites CFRP covers 90-95% of the rehabilitation and strengthening market. The AFRP and GFRP are mainly used in seismically active regions where their high strength and relatively ductile behaviour is preferred (Täljsten, 2006). When considering the manufacturing process, the composites are made by: hand lay-up, pultrusion, moulding and filament winding. The aforementioned processes are influencing the fibre content in the volume of the composite. The fibre content by volume is between 25-70%, depending on the manufacturing process used. If pulstrusion is used, as for laminates, the volume fraction of FRPs equals about 50-70%, while for hand lay-up applied sheets the value ratio is significantly lower, 25-35%. The mechanical properties of the composites are dependent on the fibres, matrix properties, fibre direction and fibre amount. The composites developed for strengthening purposes can have different shapes, i.e. sheets, laminates, grids or bars (Figure 3-1a). The fibres may be placed in one, two or multiple directions, the composite being unidirectional, bi or multi directional, respectively (Figure 3-1b).

3.1.1 Components of the composites

3.1.2 Fibres

The mechanical performance of the composites is highly dependent on the fibres. Fibres are a class of material made from continuous filaments or are in discrete elongated pieces similar to threads. Based on the primary material used in the

manufacturing process, three types of fibres are commonly utilized for the composites in the construction industry: carbon, glass, and aramid. During the last decade also basalt fibres have become an alternative for building and civil applications. In Table 3-1 the material characteristics of the fibres are presented along with common steel and concrete.

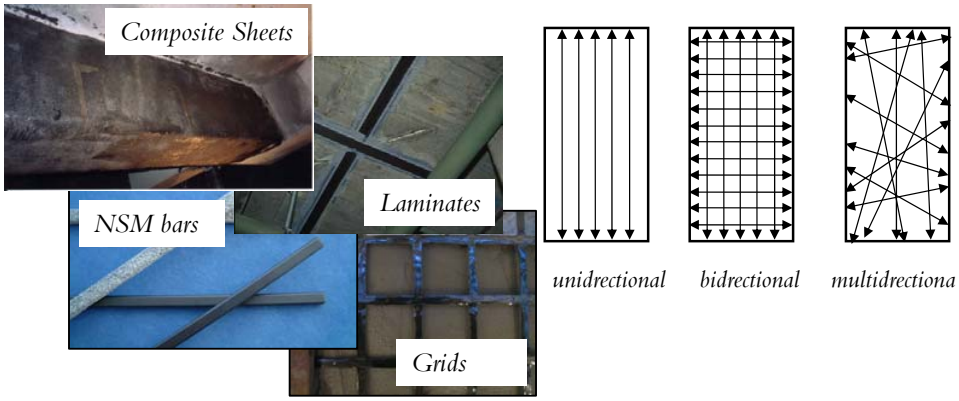

a) Various composite materials a) Fibre directions in composites

Figure 3-1*: FRP composites used for strengthening*

Table 3-1. Mechanical properties of common materials (after Carolin, 2003)

Material	*Elastic modulus [GPa]*	*Compressive strength [MPa]*	*Tensile strength [MPa]*	*Density [kg/m³]*
Concrete	20-40	5-60	1-3	2400
Steel	200-210	240-690	240-690	7800
Carbon fibre★	200-800	0★★	2500-6000	1750-1950

★ Given values are for plain carbon fibre. The characteristics of the composites will vary with amount and property of the used matrix

★★ The value is commonly too low compared to the tensile strength and thus is set to zero

The most important mechanical properties of the fibres are the stiffness and the tensile strain. The fibres have anisotropic linear elastic behaviour until failure developing outstanding performance in one direction and poor in the other two directions (Figure 3-2). Unfortunately the main advantage becomes also the main disadvantage. Because of the linear elastic behaviour (Figure 3-3) the failure occurs suddenly without or little or no forewarning.

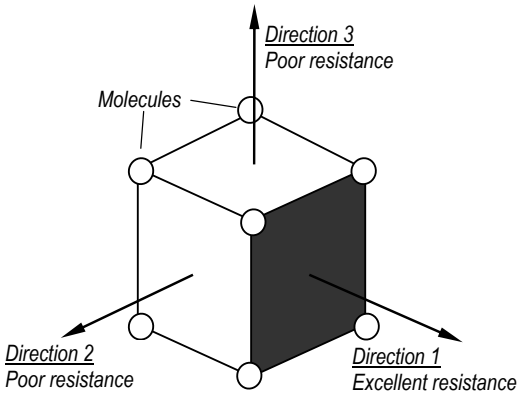

Figure 3-2: Unit material of fibre

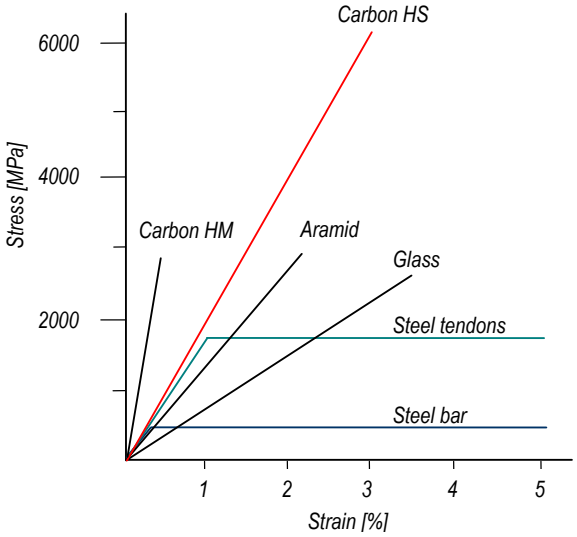

Figure 3-3: Properties of different fibres and typical reinforcing steel (after Carolin, 2003)

Carbon

Carbon fibres are made by oxidation, carbonisation and graphitisation at high temperatures (2500-3000°) from carbon precursor materials (e.g. pitch, cellulose, polyacrylonitrile). The diameter of transversal section varies between 5 and 15 μm (Figure 3-4). Two types of fibres are normally used for strengthening of structures, high modulus (HM) and high strength (HS), properties depending on the production temperature. The modulus of elasticity can take values between 200-800 GPa and the elongation is 0.3-2.5%, the lower value corresponding for high strength and vice versa.

Properties for common fibres are presented in Table 3-2. Carbon fibres behave excellently in fatigue loading; do not show creep relaxation, are resistant to multiple chemical agents and are water proof. Because of their high content of carbon, they are electrically conductive and might produce galvanic corrosion in direct contact with steel (Carolin, 2003).

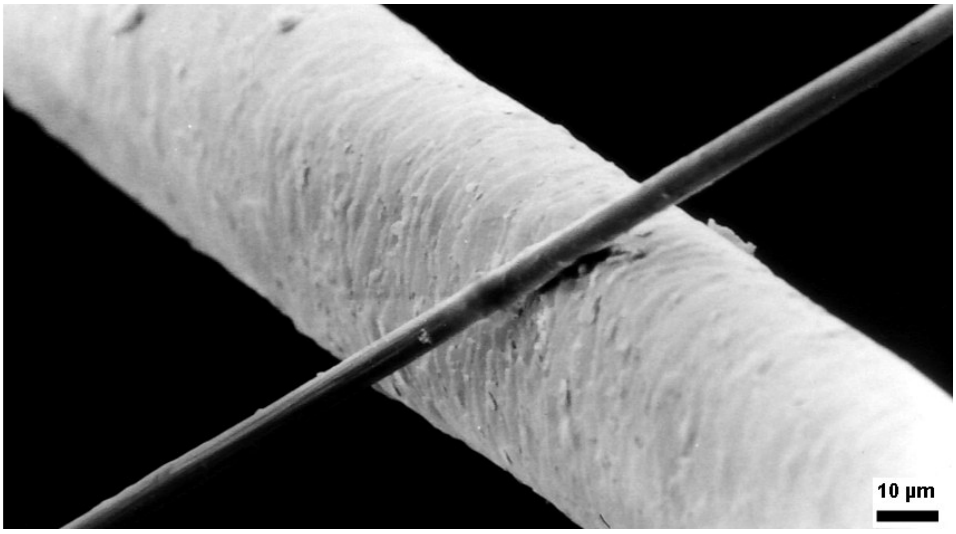

Figure 3-4: Carbon fibre filament compared to human hair (www.wikipedia.org)

Glass

The glass fibres are one of the strongest materials if we consider the strength to weight ratio. Glass fibres are obtained from the mixture of sand, kaolin, limestone and colemanite treated to high temperatures (1600°). The mixture can have different proportions of each material resulting in different types of glass fibres with different properties. The most well known types are the E-glass fibres, S-glass and alkali resistant AR-glass fibres. The E type contains aluminoborosilicate and has a maximum alkali content of 2.0%, and the dominant characteristics are the electrical and heat resistance, and the low resistance to alkali environment; these are most used for structural applications. The S-glass has higher strength, modulus and heat resistance. They contain magnesium aluminosilicate compositions and have a better resistance to acids like H_2SO_4, HCl and HNO_3 but still no resistance to alkali. The alkali resistance has been solved by adding zircon and this is how AR-glass emerged. The AR-glass has similar mechanical properties to E-glass. The diameter of transversal section varies between 5 and 24 µm. The Young modulus varies from 70 to 90 GPa with ultimate elongation of 2-5%. Glass fibres are cheaper than carbon fibres so they have a wider utilization in the world. Different problems have been observed for glass fibres like such as stress corrosion at high stress levels, moisture sensitivity or fatigue loading.

Table 3-2. Fibre properties (after André, 2007 and Sudaglass, 2008)

Fibres	E_{axial}/ E_{radial} *[GPa]*	σ_{max} *[MPa]*	ε_{max} *[%]*	ν *[-]*	ρ *[g/cm³]*	*Price [€/kg]*
HM Carbon	380/12	2400	2.6	0.2	1.95	20-60
HS Carbon	230/12	3400	1.1	0.2	1.75	20-60
Glass	76/76	2000	2.6	0.22	2.6	1.5-3
Aramid	130/10	3000	2.3	0.35	1.45	20-35
Basalt	89/NA	4800	3.15	NA	2.75	NA

3.1.3 Matrices

The main functions of the matrices are to protect the fibres from the external environment and transfer forces between the fibres. For this, the ultimate strength, and the capacity to develop high strains are of high importance. The matrices are classified in two categories:

a) thermoplastic-they can be melted again and remoulded. They have a glassy state when cooled sufficiently.

b) thermosetting-the matrices irreversibly cure to a stronger form. For strengthening purposes, thermosets vinylester, and to greater extent, thermosets epoxy matrices are used. Epoxy's pot life can be set using different additives and is shorter as the temperature increases; in normal conditions it is around 30 minutes at 20°C. The main mechanical properties are presented in Table 3-3.

Table 3-3. Properties of matrices used for composites (after André, 2007)

Fibres	E_{axial} *[GPa]*	σ_{max} *[MPa]*	ε_{max} *[%]*	ν *[-]*	ρ *[kg/m³]*	*Price [€/kg]*
Thermoplastics						
Polypropylene	1.0-1.4	20-40	300	0.3	0.9	NA
Polyetheretheketone	3.6	170	50	0.3	1.3	NA
Polyamide	1.4-2.8	60-70	40-80	0.3	1.14	5
Thermosets						
Epoxy	2-5	35-100	1-6	0.35-0.4	1.1-1.4	6.5

Polyester	2-4.5	40-90	1-4	0.37-0.39	1.2-1.5	1.5
Vinylester	3	70	5	0.35	1.2	2.5

4 Shear strengthening

4.1 General rehabilitation principles

Four characteristics are defining a structure: load carrying capacity, durability, functionality and aesthetics. From these the first three are considered the most important, mainly for safety and comfort reasons. When one of these functions is not fulfilled, a construction may be in need of:

- maintenance – keep the structure at a desired performance level, e.g. a steel bridge has to be periodically painted to avoid corrosion
- repair – upgrade the structure to its original design level, e.g. a structure damaged from an earthquake has to be structurally repaired to be at the same performance level as before the earthquake
- upgrading – to increase the performance of a structure to a higher level, e.g. if the traffic load on a bridge has increased, so the load bearing capacity has to be increased

The actions mentioned above, are called rehabilitation methods in this chapter and refer to reinforced concrete structures. The concrete, by definition, is a composite material which has very good compressive properties but low tensile strength. When steel reinforcement is added the tensile properties are increased but up to a limit, usually when steel yields. The rehabilitation of a structure can be performed by means of different methods which may involve: hand applied repairs with concrete mortar, shotcrete, injection techniques, concrete casting, post-tensioning or plate bonding (Figure 4-1).

One technique for rehabilitation is the *increase of the cross section* with different materials by means of, for example hand repaired concrete mortar, shotcrete, casted concrete, (see Figure 4-1a and c). In some cases adding or replacing different new structural elements, such as beams or columns, may fall into the same category. This method is suitable for the case when enough compressive capacity is not provided by the structural element in the present form. Different successful techniques have been developed during time for implementing this method, but it has to be mentioned that when extra material is added to a structure, redistribution of the stiffness of a structure may occur. The interface between the new and old material is a very complex problem that in some cases has no solution yet. These two issues have to be treated with caution and experienced engineers are needed for a proper design. Effectively, the method is rather economical, common construction materials are used and the workmanship does not require more skills than for a normal construction. Nevertheless, when rehabilitation work is done using this method the functional use of the structure is drastically limited or even stopped which in most of the cases means a financial loss.

Plated bonding (Figure 4-1d) started to be considered a solution for rehabilitating structures in the middle of the 1970s (Täljsten, 1994). The method consists of adding a material with high stiffness and tensile strength to the tension side of an element through a bonding agent, to serve as external reinforcement. The first studies were carried out in France by L'Hermite (1967) and Breson (1971) on reinforced concrete beams strengthened with steel plates. Several drawbacks have been observed in utilizing steel plates for bonding. One is that in some cases they are too heavy to mount on the work site requiring extra pressure during curing if applied upside down. Another one is the high risk of corrosion, which involves high costs of maintenance in order to prevent it. Also considered a drawback is the limitation of the maximum dimension for transporting and the fact that steel cannot be adapted easily on a site to different uneven shapes. It was mainly to avoid the steel plate bonding limitations that fibre reinforced polymers started to be used. The FRP plate bonding gathered wide acceptance all over the world. Meier et al. (1992), Täljsten (1994), van Gemert (1996), Burgoyne (1998), Karbhari and Sieble (1999), are some of the pioneers in this field but also many more have reported successfully applied FRP. The use and application of the FRP will be thoroughly described in the next section.

Prestressing is a method to reinforce concrete to counteract the internal stresses produced by the action of the externally applied loads during the service life of a structural member. Two methods are commonly used for this. The first is called *pre-tensioning*; here the steel is stressed before the concrete is cast, and is not applicable for rehabilitation purposes. The second method is called *post tensioning* and is used in some cases for rehabilitating structures which are in need of an increased serviceability limit state. The procedure involves the stressing of the steel after the concrete is cast and consists in tensioning different high tensile resisting tendons, e.g. steel reinforcement, FRP bars, to a desired level. For this, proper anchorages have to be ensured. A fixed anchorage system is attached to the structure and the tendon is set into it. Next, the strands are prestressed to the level desired with the help of hydraulic jacks and anchored in the structure. After the final anchorage point has been set the jacks are released and the strengthening is completed. A key factor for this method is to ensure proper anchorage since large parts of the tensioning force can be lost by excessive deformation or failure of the anchorage. It has to be mentioned also that these anchorage systems can have local effects on the element, since in most of the cases different types of holes are drilled in the structure to fix the anchorage system. The post tensioning systems can be imbedded in concrete (Figure 4-1e) or be applied externally (Figure 4-1 b and f) and can be either bonded or unbonded. For some bridges and in most rehabilitation applications the post tensioning systems are mounted outside the structural members and are referred to as post tensioned systems (PSI, 2006).

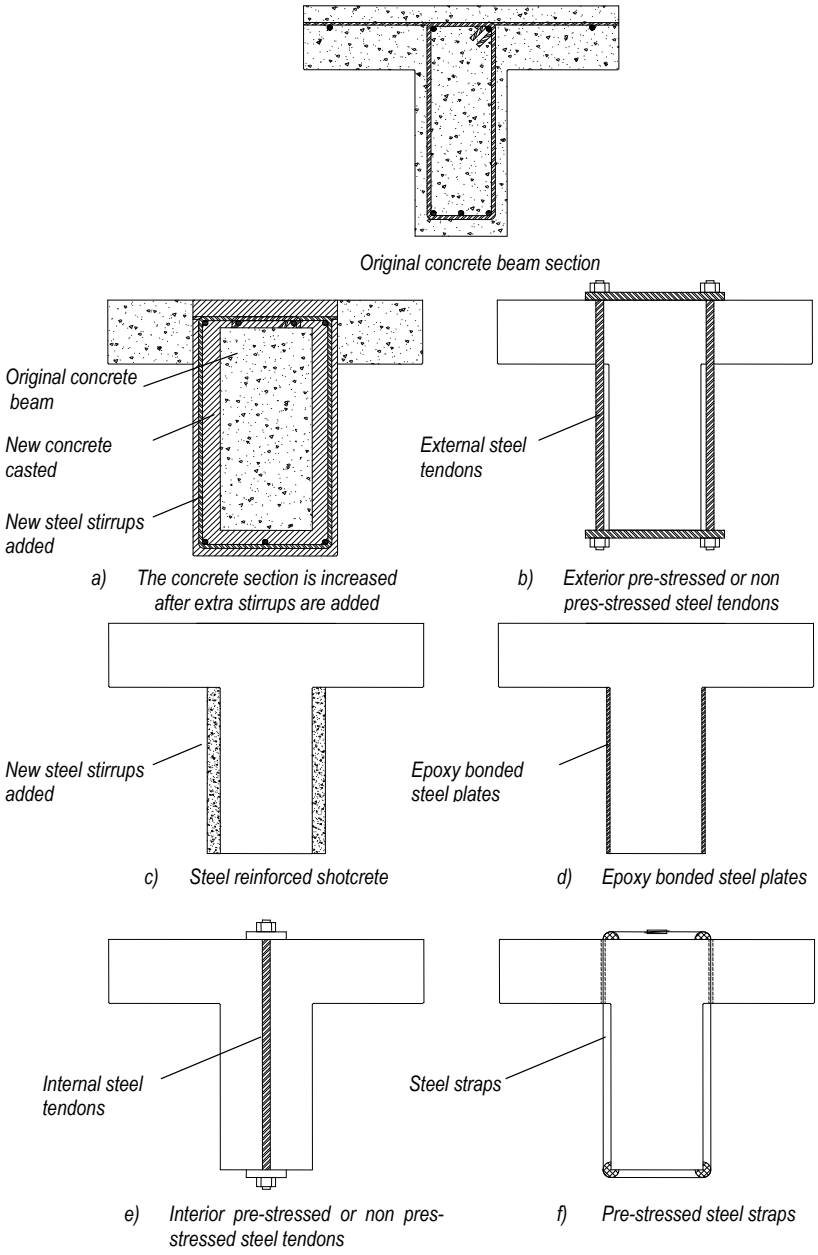

Figure 4-1: Rehabilitation solutions for beams

4.2 FRP strengthening

4.2.1 General

Most of the elements of a structure can be strengthened with FRP composite materials as it can be seen in Figure 4-2). This means in fact that FRP composites can take up the majority of the forces developed in a structure as long as they are transmitted by the strengthened element to the composite as tensile stresses. As shown in chapter 3, the compressive strength of the fibres is insignificant, but that does not mean that members in compression cannot be strengthened. In fact the confinement of columns using FRP has been proven to be a very reliable solution to improve the compressive behaviour along with the flexural response. Although a strengthening method is recommended because an element is susceptible to a failure mode, the other possible modes of failure have to be checked too, and a brittle failure should be avoided. A simple example can be given when strengthening a beam for flexure. Since the new flexural capacity is now higher and considering the interaction between the shear force and the bending moment, the beam may change its mode of failure.

Masonry walls and RC walls can be strengthened for in plane state of stress by using FRP sheets, plates or NSM bars, while for out of plane state of stress sheets are used for their shape fitting properties. The slabs can be strengthened using sheets, plates, bars or grids by simply bonding these materials to the surface of the concrete. FRPs are appropriate for the very sensitive issue that represents the openings created in slabs and walls.

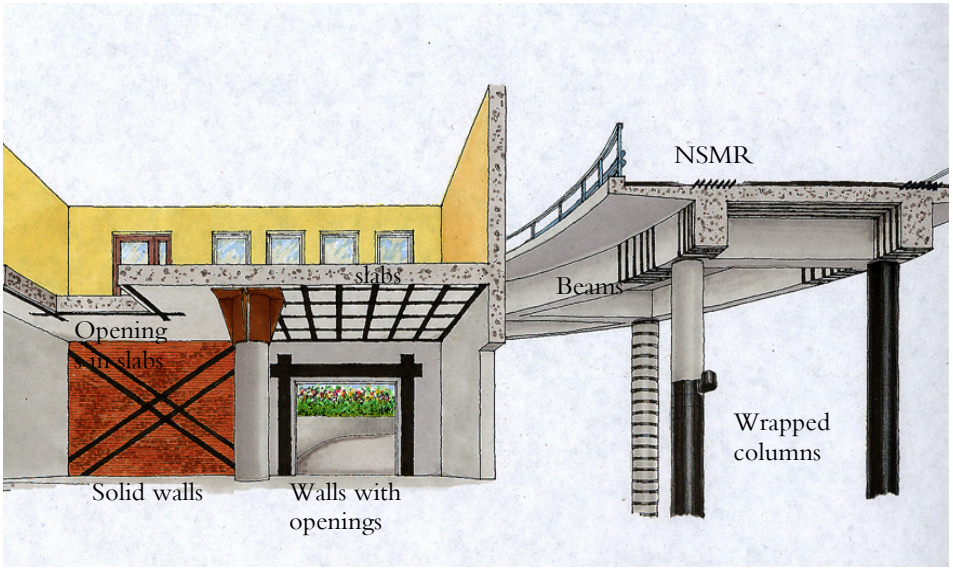

Figure 4-2: Applied FRP to structural elements (from Täljsten, 2006)

Compared to the traditional methods i.e. material addition or frame boarding of the element the FRPs are practically "invisible" from the aesthetical point of view and if the design of the strengthening is correct the element will show no weaknesses in behaviour.

When performing a strengthening three rules have to be respected (Täljsten, 2006):

- The surface has to be prepared for the strengthening. This demand is fulfilled when the area is cleared of any other materials and the concrete is revealed. The surface has to be clean of water, grease or dust.
- With the intention of applying the strengthening system the temperature of the environment surrounding the area to be strengthened has to be a minimum 10°C. This condition must be fulfilled so that the adhesive will harden in optimum state. For temperatures below 10°C an external heat source should be applied.
- After installation is performed the composite need to be protected, where applicable, against fire, vandalism or intense heat radiation. Several commercial materials can be used for this such as fire-resistant paint, plaster or other systems considered appropriate.

The three systems used widely in the FRP strengthening industry today are presented below, but it must be mentioned that other systems such as pre stressed laminates, pre stressed bars or automated wrapping system for columns are used too.

Sheet system

The typical sheet system (Figure 4-4a) consists of epoxy primer, putty, dry or pre-impregnated fibre and a resin system. The installation is preceded by the concrete surface preparation as described above. The primer is applied afterwards and in case of large unevenness the putty is used to level the surface. The following step involves the application of a thin layer of low viscosity epoxy adhesive to the concrete surface. The carbon fibre sheet is rolled and easily stretched over the impregnated surface. The possible air voids from the contact area are removed with the help of a roller and a new layer of adhesive is applied. The sheets used usually have a width of 200-400 mm and a weight of 200-400g/m^2. The most used sheets are made of unidirectional fabrics but bi-directional weaves are also used. Because sheets can be modelled to almost any geometrical shape they can be used for rounded sections or where full wrapping is needed.

Laminate system

The laminate systems (Figure 4-3a) have the following components: primer, adhesive and a composite laminate. While the primer can be similar to the one used for the sheet system and has the role of enhancing the bond of the adhesive to the concrete surface, the adhesive is different. Here, a high viscosity filled paste is used such as epoxy

adhesive applied in a thickness of 1-2 mm. The laminates have a thickness of 1.2 mm and can be obtained in different widths: 50, 70, 100, 150 mm or other requested dimensions. Theoretically the length can be unlimited but for practical reasons such as transport or handling they are distributed in pieces not longer than 20 m. The installation of the laminate system is less time consuming than the sheets system and involves the application of the primer, followed by the application of the adhesive on the laminate with a slightly thicker thickness in the longitudinal axes. The next step is to apply the laminate on the surface (usually with a roller) with enough pressure that the adhesive thickness has a constant thickness over the entire surface. This system is appropriate for flat surfaces such as beams, walls and slabs.

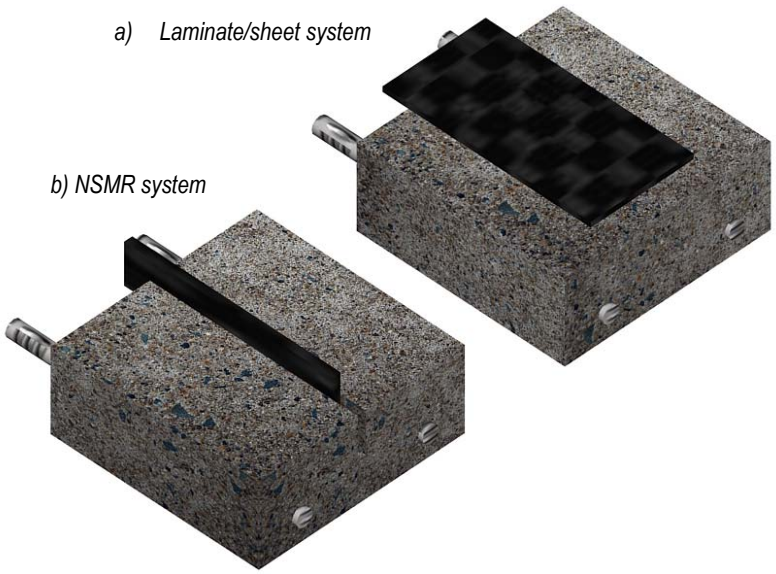

Figure 4-3: Techniques to apply FRP composites

NSMR System

The NSMR system consists of adhesive and rods. The adhesive used may be of two types epoxy or high quality cement grout. The rods can have different section configurations, and the most commonly used are the rectangular and round sections. The cross sectional area of the bars is about 100-300 mm^2 and the length is limited to 200 m, deliverable in rolls. The main characteristic of this system is the positioning of the rod inside a sawed slot (Figure 4-3b). A very important factor for the NSMR system is the quality and thickness of the concrete cover. This must be checked before sawing the slots, since 25 mm are normally needed. After sawing the slots the surface must be cleaned from dust, wet concrete or concrete ashes. When epoxy adhesive is used the slot surface must be dry, while for cement grout the surface need to be

moisturized and the surface must be cleaned. This system can be applied to all types of plane surfaces and is not sensitive to irregularities. The system is recommended to be used where high impact loads from car accidents or blasts are a risk.

4.2.2 Shear strengthening of beams

State of the art

Shear strengthening of concrete structures using FRP is a topic that has been studied intensively, both theoretically and experimentally for more than a decade. For engineering design purposes an easy to use design approach is needed so the majority of the researchers assumed that externally bonded FRP materials behave like internal stirrups. Most of the models use the additional principle where the contribution from the FRP can be added to the ones derived from the stirrups and concrete, not considering any influence of existing strain fields or interaction between steel stirrups. Since the predictions of the models based on this approach were not considered satisfactory, studies started to be focused on developing new theories that take into account the strain field formed in the FRP systems. During the years many theoretical studies have been carried out. One of the first models to predict the shear contribution of FRP was proposed by Chaallal et al (1998). The corresponding formulation is based on the assumption that the composite and the stirrups have similar behaviour. The model assumes that the FRP tensile strength is reached when the composite is intersected by the shear failure crack if sufficient bond length is not provided. Malek and Saadatmanesh (1998a and 1998b) introduced the anisotropic behaviour of the FRP considering the fibre orientation. Triantafillou (1998) and Triantafillou and Antonopoulos (2000), based on the computation of an effective FRP strain with the help of truss theory, derived a model supported from experimental fitting. Khalifa et al. (1998, 1999) modified Triantafillou's (1998) model introducing strain limitations due to shear crack opening and loss of aggregate interlock. The performance of the proposed model was assessed by considering more tests. From the performed tests, Deniaud and Cheng (2001, 2003) stated that the FRP strains are uniformly distributed among the fibres crossing the crack. A design model was derived combining the strip method and the shear friction approach, based on the failure mechanism observed of the tested specimens. A refined model was proposed in Deniaud and Cheng (2004). Pellegrino and Modena (2006) suggested a modified reduction factor for the model of Khalifa et al. (1998). According to the experimental results, the ratio between the steel stirrup and the FRP shear reinforcement percentages has a significant effect on the strengthening effectiveness of FRP systems. Carolin (2003) and Carolin and Täljsten (2005) presented an equation for predicting the contribution of Externally Bonded Reinforcement (EBR) composites for the shear strengthening. Comparisons between the results recorded from experimental tests and obtained from theoretical models (using measured strains) showed good agreement. The non-uniform distribution of the strains in FRP over the cross section was stated. It must be noticed that anchorage failure was not considered in the present design. Chen and Teng (2001, 2003a, and 2003b) analyzed the shear failure of reinforced concrete (RC) beams strengthened with FRP and

reached the conclusion that the stress (strain) distribution in the FRP along the crack is non-uniform. They presented a model for reinforced concrete beams strengthened with FRP based on the fibre rupture and debonding. Stress limitation is introduced by bond length coefficient and strip width coefficient. Based on the works of Chen and Teng (2003a and 2003b), new design proposals have been formulated using reduction factors for the ultimate tensile strength and for the spacing between FRP strips. Aprile and Benedetti (2004) presented a new flexural – shear design model for RC beams strengthened with EBR FRP systems. Ianniruberto and Imbimbo (2004) derived a model based on the modified compression field theory combined with the variable angle truss model (that takes into account the influence of the FRP systems), in order to predict the contribution of FRP sheets to the shear capacity of RC beams. Although the derivations are coherent, the model has some limitations, since it can only be used for a fully wrapped strengthening scheme, hence the debonding failure mechanism for side bonding strengthening configuration cannot be predicted. Furthermore, the model does not simulate the strain concentration at the composite-crack intersection, so it is unable to foresee the potential rupture of the composite at cracking regions for U wrapping or fully wrapped schemes. Theoretical predictions were compared with experimental results and unfortunately found to be incompatible. Cao et al. (2005) proposed an empirical model to predict the FRP contribution to the shear strengthening of RC beams strengthened with FRP wraps failing by FRP debonding. The strain distribution modification factor gave uncertain results because of the large scatter of the test data. The comparison of the theoretical prediction with the experimental results has shown "a general agreement between the two" with "a significant scatter" (Cao et al., 2005). The shear bond model proposed by Zhang and Hsu (2005) followed two approaches: model calibration by curve fitting and bond mechanism. The smallest reduction factor for the effective strain obtained from the two methods was suggested to be used. The model for the shear debonding strength developed by Ye et al. (2005) has its theoretical starting point in Chen and Teng's model (2003b), and is now used in the Chinese Design Code. Aspects regarding lateral concrete peeling failure, under shear loading, of FRP were studied by Pellegrino and Modena (2006). This model follows the truss approach and describes the concrete, steel and FRP contribution to the shear capacity of RC beams based on the experimental observations made. Monti and Liotta (2007) proposed a debonding model for the FRP-based shear strengthening of RC beams. The features of the model are divided in three steps: generalized constitutive law for the FRP-concrete bond, boundary limitations and shear crack opening provisions. A generalized failure criterion of FRP strips/sheets is introduced. Two cases are considered: straight strip/sheet and strip/sheet wrapped around a corner. The design proposal described in this model is used currently in the Italian design code CNR (2005).

Two main modes of failure are recognized by the research society now for FRP strengthened beams (Figure 4-4). These are:

- Fibre failure in the FRP

It occurs when the tensile stress in the fibres exceeds the tensile strength. It is characterized by a rapid progressive fibre failure in the composite, especially for sheets, but the failure is in most of the cases brittle. The orientation of the fibres with respect to the principal strain in concrete affects the ductility of the composite.

- Anchorage failure

Also known as bond failure is governed by the properties of the weakest materials in contact, i.e. concrete and adhesive. When the shear strength of one of these two exceeds the force then transfer cannot be ensured anymore and a "slip" is produced. The debonding can take place in concrete, between the concrete and adhesive, in the adhesive, between the adhesive and the fibres. The most common debonding failure observed is at the surface of the concrete, which is an explicable phenomenon since the concrete is the weakest element in this "interaction chain". The anchorage failure is considered as more dangerous than tensile failure because it cannot be foreseen and can almost not be controlled at all.

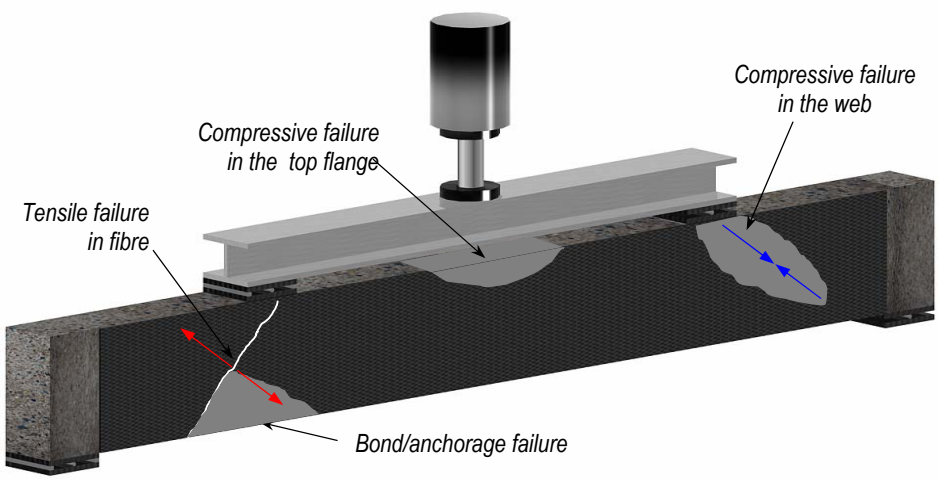

Figure 4-4: Shear failure of a strengthened beam

The failure mode of a strengthened beam depends also on the configuration of the strengthening used (Figure 4-5). From the configurations used the one to be avoided is the side bonded because it is the most exposed to debonding failure due to its limited anchorage length. The fully wrapped configuration is the safest since is the failure is controlled by fibre rupture, but it is quite uncommon with this type of free bound configuration for a beam in a structure. Probably the most used configuration is the U wrapped system. Since the beams are connected to slabs, consequently T section behaviour, this configuration is safer than the side bonding but still has critical regions, i.e. bellow the slab, where mechanical anchorage is recommended Care must be taken when strengthening continuous beams because of the variation and interaction of efforts, and especially over the support regions where the tensile side will be just beneath the slab.

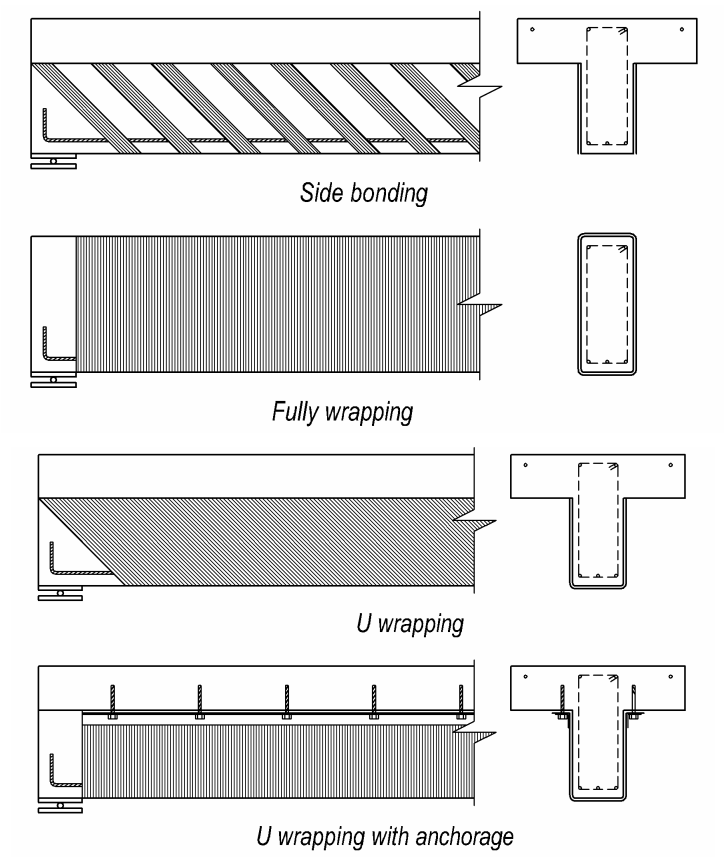

Figure 4-5: Shear strengthening configurations using FRP, (after Täljsten, 2006)

Existing theoretical models

Certainly beams can be successfully strengthened for shear using FRP composites. This has been proven during the years by the tremendous, both experimental and theoretical work performed from which we can mention Täljsten (1994, 2003), Khalifa et al. (1998), Triantafillou (1998, 2000), Chen and Teng (2001, 2003a, b), Deniaud and Cheng (2001, 2003), Monti and Liotta (2008) etc. In the following section some used design models are presented since most of the models are analyzed and compared with an extensive database in Paper I.

Triantafillou (1998) and Triantafillou and Antonopoulos (2000) model

Triantafillou's model (1998) is one off the first models proposed and is based on the truss analogy. The derivations are based on the regression analysis of experimental tests

performed and refined after two years with more experimental results (Triantafillou and Antonopoulos, 2000). The equations presented, Eqs. (4-1), (4-2) and (4-3), are adapted for simple and fast engineering design, but due to limited data available at that moment the model's predictions are unsatisfactory in some cases. Unfortunately the model is not considering the side bonded strengthening configuration. The strain defined in equation (4-2) is the effective strain in the fibres for CFRP rupture for a fully wrapped beam, while the strain in equation (4-3) is the effective strain in the fibres for CFRP debonding for a U wrapped beam. Care must be taken when applying these two equations since the regression on the axial rigidity has been performed using the GPa units.

$$V_{frp} = \frac{0.9}{\gamma_{frp}} \rho_{frp} E_{frp} \varepsilon_{frp,e} b_w d \left(1 + \cot\beta\right) \sin\beta \tag{4-1}$$

$$\varepsilon_{frp,e} = 0.17 \varepsilon_{frp,u} \left(\frac{f_c^{2/3}}{E_{frp} \rho_{frp}} \right)^{0.30} \tag{4-2}$$

$$\varepsilon_{frp,e} = \min \left[0.65 \left(\frac{f_c^{2/3}}{E_{frp} \rho_{frp}} \right)^{0.56} \times 10^{-3}; 0.17 \varepsilon_{frp,u} \left(\frac{f_c^{2/3}}{E_{frp} \rho_{frp}} \right)^{0.30} \right] \text{ U shaped CFRP} \tag{4-3}$$

Chen and Teng (2001, 2003a, b) model

An extensive work performed by Chen and Teng (2001, 2003a and 2003b) resulted in one of the most used shear models. The general equation (4-4) is based on the truss model theory, with the remarks that discrete FRP strips were modelled as equivalent continuous FRP sheets/plates, and a reduction factor for the stress is used (4-5).

$$V_{frp} = 2 f_{frp,e} t_{frp} w_{frp} \frac{h_{frp,e} \left(\cot\theta + \cot\beta\right) \sin\beta}{s_{frp}} \tag{4-4}$$

$$f_{frp,e} = D_{frp} \sigma_{frp,\max} \tag{4-5}$$

When deriving the effective shear stress, for both fibre and debonding failure, Chen and Teng (2003a and 2003b) used the non uniform distribution of stresses along the crack. The stress distribution factor is determined analytically by integrating the stresses/strains over the cross section of the beam (Eq. (4-6).

$$D_{frp} = \frac{\int_{z_t}^{z_b} \sigma_{frp,z} dz}{h_{frp,e} \sigma_{frp,\max}} \; or = \frac{\int_{z_t}^{z_b} \bar{\varepsilon}_z dz}{h_{frp,e} \bar{\varepsilon}_{\max}} \tag{4-6}$$

For fibre rupture different shapes of non linear distribution of the stresses are analyzed and the final form is expressed in function of geometrical limitations as in equation (4-7).

$$D_{frp} = \frac{1+\zeta}{2} \text{ where } \zeta = z_t / z_b \tag{4-7}$$

$z_t = (0.1d + d_{frp,t}) - 0.1d = d_{frp,t}$, coordinate of the top end of the effective FRP (4-8)

$z_b = 0.9d$, coordinate of the bottom end of the effective FRP (4-9)

The shear failure was considered to occur when the maximum tensile stress in the FRP reached the ultimate tensile strength. Also the loss of aggregate interlocking was mentioned as a shear mode of failure of a beam although the ultimate tensile stress is not reached.

The debonding model developed outlines the importance of the effective bond length defined as the length" beyond which an extension of the bond length cannot increase the bond strength" (Chen and Teng, 2003b). The maximum stress in the FRP at debonding is considered to be:

$$\sigma_{frp,\max} = \begin{cases} f_{frp} \\ 0.427\beta_w\beta_L\sqrt{\dfrac{E_{frp}\sqrt{f_c'}}{t_{frp}}} \end{cases} \quad (4\text{-}10)$$

where:

$$\beta_L = \begin{cases} 1 & if\ \lambda \geq 1 \\ \sin\left(\dfrac{\pi\lambda}{2}\right) & if\ \lambda < 1 \end{cases} \quad (4\text{-}11)$$

$$\beta_w = \sqrt{\frac{2 - w_{frp}/(s_{frp}\sin\beta)}{1 + w_{frp}/(s_{frp}\sin\beta)}} \quad (4\text{-}12)$$

The model has a dimensional inconsistency of the maximum stress expressed in this mathematical form but the reasons can be found in the regression analysis on the ultimate bond strength. The two coefficients β_w, β_L, reflect the effective bond length and the effect of FRP to concrete width ratio, respectively. The parameters normalized maximum bond length λ, the maximum bond length $L_{\max}$ and the effective bond length L_e are given as:

$$\lambda = \frac{L_{\max}}{L_e};\ L_{\max} = h_{\mathrm{frp,e}}/\sin\beta \text{ for U jacketing,} \quad (4\text{-}13)$$

$$L_{\max} = h_{\mathrm{frp,e}}/(2\sin\beta) \text{ for side bonding}$$

$$L_e = \sqrt{\frac{E_{frp}t_{frp}}{\sqrt{f_c'}}} \quad (4\text{-}14)$$

In this model it was assumed that all the FRP crossing the shear crack can develop full bond strength. Under this assumption the stress distribution factor for debonding failure was derived, (Eq. (4-15). It must be noted as equally important that the bond strength of a strip depends on the distance from the shear crack relative to the ends of the strip. For design purposes a simplified formula was proposed in which 95% characteristic bond strength given by the analytical model is used (Eq. (4-16).

$$D_{frp} = \begin{cases} \dfrac{2}{\pi\lambda}\dfrac{1-\cos\dfrac{\pi}{2}\lambda}{\sin\dfrac{\pi}{2}\lambda} & if\ \lambda \le 1 \\ 1-\dfrac{\pi-2}{\pi\lambda} & if\ \lambda > 1 \end{cases} \tag{4-15}$$

$$\sigma_{frp,\max} = \begin{cases} 0.8 f_{frp} / \gamma_{frp} \\ \dfrac{0.3}{\gamma_b}\beta_w\beta_L\sqrt{\dfrac{E_{frp}}{t_{frp}}\sqrt{f_c}} \end{cases} \tag{4-16}$$

Carolin and Täljsten (2005) and Sas et al.(2008) model

This shear strengthening model has been presented in Carolin (2003), Carolin and Täljsten (2005) and Sas et. al (2008). The superposition principal has been used to derive the equations of the model in which the total shear capacity of the beam is considered to be:

$$V_{Rd} = V_c + V_s + V_p + V_i + V_{frp} \tag{4-17}$$

Where: V_c is the capacity of the concrete, and can be determined according to the current standards, V_s is the stirrups contribution also can determined according the current standards, V_p contribution from axial loads as prestressing, V_i other contributions (e.g. inclined compression cords), V_{frp} the contribution of the externally bonded composite.

The contribution from the externally bonded composite has been addressed using the following formula.

$$V_{FRP} = \eta_{frp} \cdot \varepsilon_{cr} \cdot E_{frp} \cdot t_{frp} \cdot r_{frp} \cdot z \cdot \frac{\sin(\theta+\beta)}{\sin\theta} \tag{4-18}$$

The reduction factor η_{frp} introduced here, is considering the non uniform distribution of the stresses over the cross section and was initially derived by Popov (1998) (Eq. (4-19). A value from 0.6 was suggested to be used.

$$\eta_{frp} = \frac{\int_{-h/2}^{h/2} \varepsilon_{frp}(y)\,dy}{\varepsilon_{frp,\max} \cdot h} \tag{4-19}$$

$$\varepsilon_{cr} = \min\begin{Bmatrix} \varepsilon_{frp,u} \\ \varepsilon_{bond} \cdot \sin^2(\theta+\beta) \\ \varepsilon_{c,\max} \cdot \sin^2(\theta+\beta) \end{Bmatrix} \tag{4-20}$$

$$\varepsilon_{bond} = \frac{1}{E_{frp} t_{frp}} \sqrt{2 E_{frp} t_{frp} G_f} \begin{cases} \sin(\omega L_{cr}) & for\ L_{cr} \le \dfrac{\pi}{2\omega} \\ 1 & for\ L_{cr} > \dfrac{\pi}{2\omega} \end{cases} \text{ where } \omega = \sqrt{\frac{\tau_{max}^2}{2 E_{frp} t_{frp} G_f}} \qquad (4\text{-}21)$$

The critical strain in fibres (Eq. (4-20) is a factored effective strain accounting for:

- the ultimate limit strain in fibres, $\varepsilon_{frp,u}$, usually defined by rupture of the composite. Normally the value of the ultimate strain provided by the producers is adopted in design
- the strain in fibre, ε_{bond} (Eq. (4-21) when debonding failure occurs. A full derivation of this strain is presented in Paper II. The background of the derivations is the linear fracture mechanics theory for concrete.
- the strain in concrete, $\varepsilon_{c,max}$, is a strain in the fibre depending on the concrete contribution (aggregate interlocking)

The reduction $sin^2(\theta+\beta)$ in formula (4-20) is applied to consider a possible deviation of the principal strains in the fibres from the direction of the strains developed in the crack . In formula (4-21) the critical length L_{cr} is the bonding length at which the cracking at the interface FRP-concrete is stably propagating during debonding process. If this length is increased the debonding process will conduct to progressive failure. The term G_f is the fracture energy of concrete in mode II (shear). Since the fracture mechanic is a field of science still under development the adopted value of the fracture energy value is the major drawback of the model. The factor r_{frp} identifies the effect of the continuous or discontinuous strengthening configuration (Eq. (4-22).

$$r_{frp} = \begin{cases} \sin\beta & \text{continuous wrapping} \\ \dfrac{w_{frp}}{s_{frp}} & \text{discrete strips} \end{cases} \qquad (4\text{-}22)$$

4.2.3 Calculation example for FRP strengthened beams

To exemplify the design of a RC beam strengthened in shear using FRP composites the models presented in the previous paragraph are used. A similar procedure has been carried out also for the analysis performed in Paper I.

The beam presented in Figure 4-6: Test set-up of strengthened beam (after Hägglund, 2003) is similar to the one presented in chapter 2.4 but without shear reinforcement. This beam has been tested by Hägglund (2003) accompanied by a reference beam without strengthening. The strengthening configuration consisted of 50 mm discrete strips applied at 45° with a spacing of 50 mm. The strengthened beam failed by rupture of the CFRP sheets at 247 kN while the beam without strengthening failed at 125 kN, hence the fibre contribution can be considered the difference between the two values, i.e. 122 kN. Although the fibre rupture has been reported in the test the calculation examples presented bellow will include also the debonding failure to exemplify better the use of the models. The properties of the materials used are presented in Table 4-1.

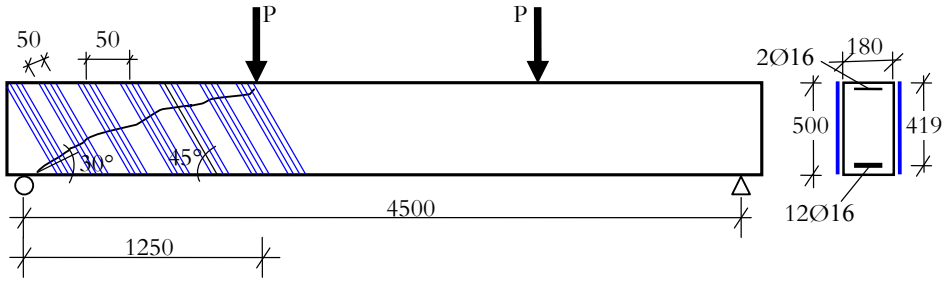

Figure 4-6: Test set-up of strengthened beam (after Hägglund, 2003)

Table 4-1. Properties of tested beam, from Hägglund (2003)

	Notation	*Size*	*Unit*
Concrete			
Compressive strength	f_c	67	*[MPa]*
Tensile strength	f_{ct}	2.8	*[MPa]*
Modulus of elasticity	E_c	30	*[GPa]*
Cross section area	A_c	90000	*[mm²]*
Shear crack surface	$A_{c,shear}$	169837	*[mm²]*
Reinforcement			
Yield strength	f_y	500	*[MPa]*
Modulus of elasticity	E_{ct}	210	*[GPa]*
Area of compressive reinforcement	$A_{s,c}$	402	*[mm²]*
Area tensile reinforcement	$A_{s,t}$	2413	*[mm²]*
Steel compressive reinforcement ratio	$\rho_{s,c}$	0.00447	-
Steel tensile reinforcement ratio	$\rho_{s,t}$	0.02681	-
CFRP			
Tensile strength	$f_{frp,u}$	3150	*[MPa]*
Modulus of elasticity	E_{frp}	234	*[GPa]*
Fibre rupture strain	$\varepsilon_{frp,u}$	1.5	*[%]*
Thickness	t_{frp}	0.09	*[mm]*

Width of the strip	w	50	*[mm]*
Strip distance	s	50	*[mm]*
Fibre alignment	β	45	*[°]*
Shear crack area	$A_{frp,shear}$	170	*[mm²]*
FRP reinforcement ratio	ρ_{frp}	0.001	-

Triantafillou model

Fibre rupture

Although the model is not fully applicable for this case study since it refers to fully wrapped beams and the beam is side bonded the calculation example will be presented to exemplify its use.

Fibre rupture

First the axial rigidity is determined:

$$\rho_{frp} E_{frp} = 0.001 \times 234 = 0.234\,GPa$$

The effective strain at fibre failure is determined using equation (4-2):

$$\varepsilon_{frp,e} = 0.17\varepsilon_{frp,u}\left(\frac{f_c^{2/3}}{E_{frp}\rho_{frp}}\right)^{0.30} = 0.17 \times 0.015 \times \left(\frac{67^{2/3}}{0.234}\right)^{0.3} = 0.00915\,\text{strains}$$

The CFRP contribution for fibre rupture failure is determined according to equation (4-3):

$$V_{frp} = \frac{0.9}{\gamma_{frp}}\rho_{frp} E_{frp} \varepsilon_{frp,e} b_w d\left(1+\cot\beta\right)\sin\beta = \frac{0.9}{1} \times 0.243 \times 0.00915 \times 180 \times 419 \times (1+\cot 45^\circ) \times \sin 45^\circ = 213.5\,kN$$

Debonding failure

The effective strain at debonding is checked in accordance with equation (4-3), where the second parameter has been already computed for the case of fibre rupture.

$$\varepsilon_{frp,e} = 0.65\left(\frac{f_c^{2/3}}{E_{frp}\rho_{frp}}\right)^{0.56} \times 10^{-3} = 0.65 \times \left(\frac{67^{2/3}}{0.234}\right)^{0.56} \times 10^{-3} = 0.007\,\text{strains}$$

The contribution of the composite to the shear capacity is then determined:

$$V_{frp} = \frac{0.9}{\gamma_{frp}}\rho_{frp} E_{frp} \varepsilon_{frp,e} b_w d\left(1+\cot\beta\right)\sin\beta = \frac{0.9}{1} \times 0.243 \times 0.00915 \times 180 \times 419 \times (1+\cot 45^\circ) \times \sin 45^\circ = 164.3\,kN$$

Chen and Teng model

For a better understanding on how to apply this model on the beam presented in Figure 4-6 several additional parameters need to be added. These parameters are depicted in Figure 4-7.

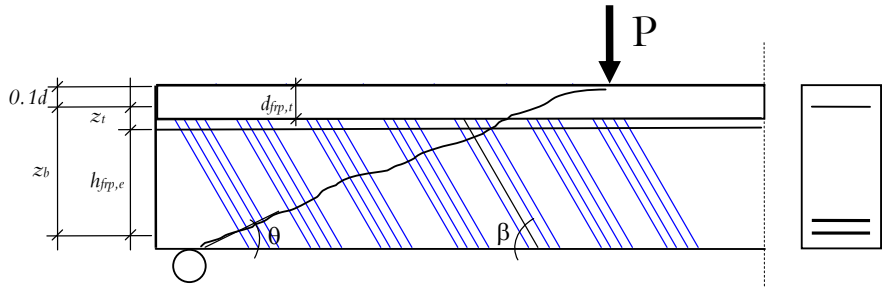

Figure 4-7: Geometrical parameters used in derivations

Fibre rupture

To determine the distribution factor of the strain in equation (4-7) first the geometrical coordinates are determined from equations (4-8) and (4-9):

$$z_t = \left(0.1d + d_{frp,t}\right) - 0.1d = d_{frp,t} = \left(0.1\times 419 + 0\right) - 0.1\times 419 = 0$$

$$z_b = 0.9d = 0.9\times 419 = 377.1\,\text{mm}$$

$$h_{frp,e} = z_b - z_t = 377.1$$

$$D_{frp} = \frac{1+\zeta}{2} = \frac{1+\frac{0}{377.1}}{2} = 0.5$$

The effective stress in the fibres is determined according to equation (4-5).

$$f_{frp,e} = D_{frp}\sigma_{frp,\max} = 0.5\times 4500 = 2250\ \text{MPa}$$

So the shear capacity at rupture should be calculated as in equation (4-4) where the similar partial factor γ_{frp}=1.5 has been applied.

$$V_{frp} = 2 f_{frp,e} t_{frp} w_{frp} \frac{h_{frp,e}\left(\cot\theta + \cot\beta\right)\sin\beta}{s_{frp}} =$$

$$= 2\times 0.5\times 3150\times 0.09\times 50\times \frac{377.1\times\left(\cot 30^\circ + \cot 45^\circ\right)\times\sin 45^\circ}{50} = 206.36\,\text{kN}$$

Debonding failure

The calculation procedure starts with the following parameters:

- maximum bond length (Eq. (4-13) for side bonding

$$L_{\max} = \frac{h_{frp,e}}{2\sin\beta} = \frac{377.1}{2\times\sin 45^{\circ}} = 266.65\,\text{mm}$$

- effective bond length (Eq.(4-14)

$$L_e = \sqrt{\frac{E_{frp}t_{frp}}{\sqrt{f_c'}}} = \sqrt{\frac{234\times10^3\times0.09}{\sqrt{67}}} = 50.73\,\text{mm}$$

- It yields the maximum bond length

$\lambda = L_{max}/L_e = 5$

To calculate the distribution factor of the stresses for debonding failure the coefficients for effective bond length and the geometrical distribution of the fibres along the side of the beam have to be determined. According to equations (4-11) and (4-12) the values are:

$$\beta_L = 1$$

$$\beta_w = \sqrt{\frac{2 - w_{frp}/(s_{frp}\sin\beta)}{1 + w_{frp}/(s_{frp}\sin\beta)}} = \sqrt{\frac{2-50/(50\times\sin 45^{\circ})}{1+50/(50\times\sin 45^{\circ})}} = 0.4925$$

Than the maximum stress in fibres is computed according to eq. ((4-10):

$$\sigma_{frp,\max} = 0.427\beta_w\beta_L\sqrt{\frac{E_{frp}\sqrt{f_c'}}{t_{frp}}} = 0.427\times1\times0.4925\times\sqrt{\frac{234\times10^3\times\sqrt{67}}{0.09}} = 970\,\text{MPa}$$

Finally, the contribution of the fibres at debonding failure is determined

$$V_{frp} = 2f_{frp,e}t_{frp}w_{frp}\frac{h_{frp,e}\left(\cot\theta+\cot\beta\right)\sin\beta}{s_{frp}} =$$

$$= 2\times970\times0.09\times50\times\frac{377.1\times\left(\cot 30^{\circ}+\cot 45^{\circ}\right)\times\sin 45^{\circ}}{50} = 127.1\,\text{kN}$$

Carolin, Täljsten and Sas model

The strain limitation presented in equation (4-20) will disregard the strain accounting for concrete contribution, $\varepsilon_{c,max}$ since V_c has been subtracted from the total shear capacity.

Fibre rupture

The strain distribution factor over the cross section defined in equation (4-19) is chosen to be 0.6.

The fibre contribution to the shear capacity when fibre rupture occurs is determined according to equation (4-18).

$$V_{FRP} = \eta_{frp} \cdot \varepsilon_{cr} \cdot E_{frp} \cdot t_{frp} \cdot r_{frp} \cdot z \cdot \frac{\sin(\theta + \beta)}{\sin\theta} =$$

$$= 0.6 \times 0.015 \times 234 \times 10^3 \times 0.09 \times \frac{50}{50} \times 0.9 \times 419 \times \frac{\sin(30^\circ + 45^\circ)}{\sin 30^\circ} = 138.1 kN$$

Debonding failure

If the bond failure is considered than the fracture energy and the corresponding shear strength have to be computed first. For this a model of your choice can be chosen. Here the model proposed by Nakaba et al.(2001) is adopted.

$$G_f = 0.644 f_c^{0.19} = 0.644 \times 67^{0.19} = 1.43 \,\text{MPa} \times \text{mm}$$

$$\tau_{\max} = 3.5 f_c^{0.19} = 3.5 \times 67^{0.19} = 7.78 \text{ MPa}$$

$$\omega = \sqrt{\frac{\tau_{\max}^2}{2E_{frp} t_{frp} G_f}} = \sqrt{\frac{7.78^2}{2 \times 234 \times 10^3 \times 0.09 \times 1.43}} = 0.010052$$

The critical length is determined,

$$L_{cr} = \frac{\pi}{2\omega} = \frac{\pi}{2 \times 0.01005} = 156.3 \,\text{mm}$$

The critical bond strain is determined using equation (4-21.

$$\varepsilon_{bond} = \frac{1}{E_{frp} t_{frp}} \sqrt{2E_{frp} t_{frp} G_f} = \frac{1}{234 \times 10^3 \times 0.09} \sqrt{2 \times 234 \times 10^3 \times 0.09 \times 1.43} = 0.0116 \text{ strains}$$

Finally, the shear contribution of the fibre would be,

$$V_{FRP} = \eta_{frp} \cdot \varepsilon_{cr} \cdot E_{frp} \cdot t_{frp} \cdot r_{frp} \cdot z \cdot \frac{\sin(\theta + \beta)}{\sin\theta} =$$

$$= 0.6 \times 0.0116 \times 234 \times 10^3 \times 0.09 \times \frac{50}{50} \times 0.9 \times 419 \times \frac{\sin(30^\circ + 45^\circ)}{\sin 30^\circ} = 106.8 kN$$

A summary of the calculation is presented in Table 4-2, since the models predictions are calculated just for one beam an unbiased analysis and conclusion cannot be formulated. Instead, a deeper discussion is presented in Paper I, where the most used models are presented analyzed and compared.

Table 4-2. Summary of the FRP strengthening contribution to the shear capacity

	V_{frp}		
Design model	*Fibre rupture*	*Debonding failure*	*Experimental value*
	[kN]	*[kN]*	*[kN]*
Triantafillou	213.5	164.3	
Chen and Teng	206.36	127.1	122
Carolin, Täljsten and Sas	138.1	106.8	

4.2.4 Strengthening of RC walls with openings

Discontinuity regions in reinforced concrete can create stresses that cannot be classified in known patterns making the design difficult. One solution can be considered the use of the FRP systems for strengthening these regions. Experimental work presented in Paper III has proved that this system is a viable method but more work is needed to investigate the discontinuity regions. For this, the experimental program presented in Paper IV, concerning the RC walls with openings strengthened with FRP system, has been initiated and is undergoing.

State of the art

One of the first FRP strengthening of RC shear walls was reported by Ehsani et al. (1997). A tilt-up concrete building was retrofitted using glass fibres following the '94 Northridge earthquake. Out-of-plane flexural failure was recorded as the primary mode of failure immediately after the earthquake. The major cause of the failure was considered the horizontal forces acting perpendicular to the in-plane as wall stiffness redistribution of the structure occurred. The strengthening effectiveness was emphasized considering the moment capacity from the self weight of a unit width of wall. After strengthening the parameter has increased to 74%; which before retrofitting was 13.8%. The strengthening effect was expressed also as ground motion acceleration capacity. Relative ground motion capacity increased from 0,138g to 0,74g.
Bond properties between CFRP and concrete on adjacent RC wall panels connected though CFRP were experimentally studied by Volnyy and Pantelides (1999). A series of nine tests on full scale precast RC walls under in-plane horizontal cyclic quasi-static load were conducted. Influence of the parameters: surface preparation technique and contact area of the composites with concrete, were investigated. Three main modes of failure were reported: fibre failure of the composites, "cohesive failure" (delamination of the fabric from the concrete surface) and concrete surface shear failure. The 3rd mode was considered to be the most influential and more likely to occur. In terms of strains, the measurements showed a low utilization of the fibres i.e. 1200 microstrains. The

experimental effective length of 125 mm was considered in good agreement with the theoretical values.
The feasibility of CFRP strengthening and rehabilitation of reinforced concrete shear wall was studied by Lombard et al. (2000). Four walls were tested in a quasi-static cyclic load sequence (Figure 4-8) in load control up to yielding and displacement control up to failure, respectively.

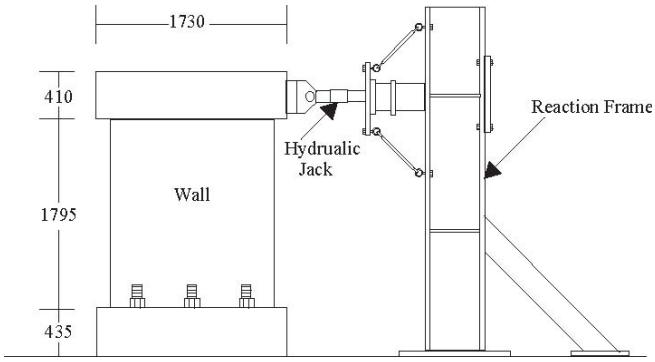

Figure 4-8: Test set-up of RC walls (from Lombard, 2000)

Two unstrengthened walls were tested and used as reference, retrofitted with CFRP and then retested. Parameters measured during tests were lateral load applied, horizontal displacement, elastic stiffness, yield load level of vertical steel reinforcement and ultimate load capacity.
A strengthening system was applied to the next two walls prior to testing. The configuration of the CFRP strengthened system consisted of one or three sheets with fibres applied in vertical or vertical and horizontal directions. For all the walls CFRP was applied on both faces. A mechanical anchorage at the basis of the wall was provided in all the cases to ensure sufficient bond length (Figure 4-9). Flexural failure with yielding of steel reinforcement was observed at the base of the walls. When stiffness changed, horizontal and diagonal cracks developed merged. As ultimate failure different modes were reported i.e. concrete crushing, fracture of vertical steel reinforcement, anchorage slippage and tearing of the CFRP sheet at the base of the wall. A substantial increase of the ultimate bearing capacity of the strengthened walls it was reported. Based on the experimental observations an empirical theoretical model was developed to predict the load-displacement envelope of reinforced concrete shear walls strengthened by CFRP. The expression addresses design aspects for shear reinforced concrete walls with aspect ration greater than 1.0 and are considered to fail in ductile manner. The flexural and shear deflection at the top of the wall are considered as the most important parameters. A correlation between the cantilever beam's behaviour and the shear wall's behaviour is made to derive the model. A partial factor is introduced to account for the inelastic behaviour of the concrete, the non-linear distribution in the wall and the load resistant effect of the carbon fibre sheets. Model predictions are in good agreement with experimental result obtained.

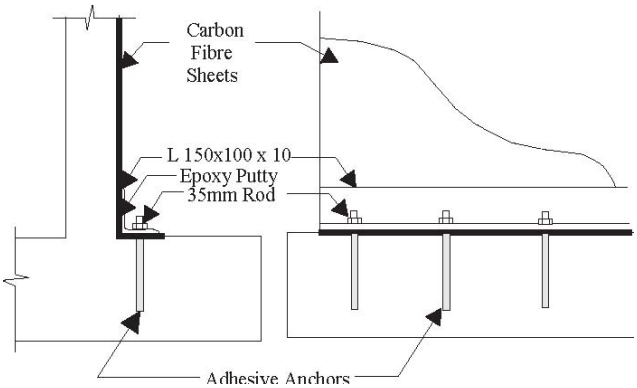

Figure 4-9: Anchoring system for the carbon fibre sheets (from Lombard, 2000)

Sixteen scaled specimens of RC columns with wing walls were tested by Iso et al. (2000) simulating seismical loading (in – plane cyclic storey drift control and vertical load) to investigate the shear reinforcing effect of the externally bonded carbon and aramid FRP sheets. Four types of unstrengthened specimens were tested first. One of the tested specimens was strengthened and retested. Based on the observations from initial tests the remaining eleven were first strengthened and tested. Shear diagonal crack was observed as a general failure mode for all specimens. The unstrengthened specimens failed in shear with progressive diagonal crack propagation, followed by lateral bar yielding and concrete crushing in the compressive zone of the wing walls (Figure 4-10). The strengthened specimens failed in the same manner, shear, with debonding of FRP. It has been reported a linear increase of the shear capacity with the increase of composites layers. However, a limitation of retrofitting effects of FRP sheets on the ultimate shear strength was found. A theoretical model has been derived to evaluate the bearing capacity of FRP strengthened RC columns with wing walls. The predictions were considered to be within the safe margins.

Seismic behaviour of non-structural reinforced concrete walls with openings, strengthened using FRP composite sheets, was studied by Sugiyama et al. (2000). A series of tests was conducted on eight 1:3 scale specimens. Six specimens each had door and window openings while the other two had only door a opening. Three walls with openings were tested without strengthening as reference specimens. Different CFRP configuration arrangements and layers were applied before testing for the rest of the walls (Figure 4-11). The static scheme considers the cantilever wall behaviour. Walls were subjected to in- plane cyclic horizontal force and constant vertical force. The non-structural reinforced concrete walls were compared with a shear reinforced concrete wall. It was concluded that even if the bearing capacity of the non-structural walls increased the global behaviour of the frame remained the same. For serviceability limit state (the deflection angle of doors and the residual crack width) a good enhancement was provided by the FRP strengthening.

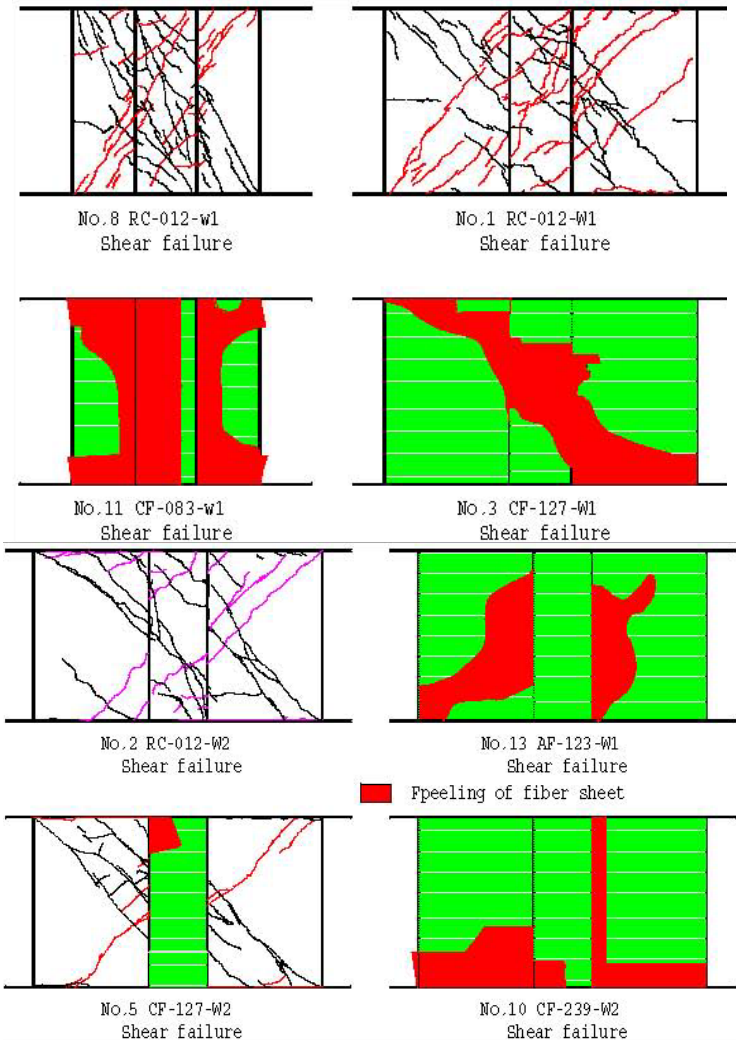

Figure 4-10: Example of final crack pattern (from Iso, 2000)

The efficiency of the FRP strengthening on RC walls subjected to lateral loading (Hiotakis et al., 2003) has been proven in a series of tests. First, four tests were performed on three elements constructed with 40 MPa strength concrete and 400 MPa yield strength reinforcement. The dimensions of a specific element are 100x1500mm and 2000 mm height. Even if during testing large torsion effects are observed for all three elements, the effect of the strengthening was considered successful. The ultimate load of the wall repaired with one layer of FRP sheets on each face increased by 80%. Two new undamaged walls were tested: a) with one layer of FRP sheets on both faces mechanically anchored; b) two vertical layers of FRP sheets and one horizontal on

both faces. For these strengthening schemes the increase in ultimate load was 46% for a) element and 132% for b) compared to the control specimen. For the a) element failure of the anchorage system has been reported. In the second phase a reconfiguration of the stand setup was considered in order to prevent torsion and five additional tests were performed on four walls. The control element was tested, repaired with FRP and then retested. The configuration of the retrofitted elements was changed for the second and third elements of this series. Now a double and a triple vertical layer on both sides were applied. Beside the increase of the ultimate load for the strengthened and retrofitted elements of about 55% compared to the control element it is important to mention that all the specimens in this set had a higher failure load compared to the first set, proving also the negative influence of the torsion effect.

In two series of tests Antoniades et al. (2003, 2005) analyzed the results of seismic loading on low-medium slenderness cantilever reinforced concrete walls strengthened with FRP. The walls, designed according to modern code provisions, were subjected to cyclic loading up to failure. After a conventional repair consisting of replacement of damaged concrete and lap-welding of fractured reinforcement FRP retrofitting was performed to increase both flexural and shear capacity. CFRP strips with fibres orientated along the vertical direction were applied on the lateral sides of the walls for bending capacity. For the shear strengthening GFRP sheets with fibres aligned along the horizontal direction were used (see Figure 4-12). Special attention was given to the FRP anchorage system: GFRP tows, U-shaped strips, C-shaped strips and metal plates, steel angles fixed with resin and metal bolts. A new series of tests was performed on the strengthened specimens. A comparison between initial specimens and retrofitted ones was used to show the effect of FRP strengthening. The dominant failure mode in all cases was flexural with local anchorage failure. Appropriate confinement of the compressed concrete could not be reached even if visible damage such as concrete crushing or reinforcement buckling was not observed. In terms of strength capacity the strengthened walls showed an increase between 2-48% with respect to unstrengthened repaired walls and a lost of 6% compared to initial undamaged walls (Figure 4-13).
Paterson and Mitchell (2003) conducted an experimental program on four cantilever reinforced concrete walls in order to investigate the effectiveness of the combined strengthening using FRP wrapping, headed reinforcement and reinforced concrete collars. Two walls were tested as reference specimens without strengthening and two companion walls were retrofitted prior to testing. For one wall from the first pair confinement effect was provided through a reinforced concrete collar with headed bars in longitudinal, transverse and through-wall reinforcements. The initial transverse reinforcement anchorage was provided by headed bar end pins at the side edges of the walls. At the end, FRP strips orientated horizontally above the reinforced concrete collar was applied to increase the shear capacity. FRP was anchored with longitudinal headed bars. For the companion wall from the second pair, the procedure was similar excepting the concrete collar application. The tests showed a flexural failure in all four cases. The difference was made in the type of failure; unstrengthened walls by brittle lap splice failure while companion specimens had gradual strength degradation. An increase of 54% of the bearing capacity was observed for the first pair and 6% for the second pair.

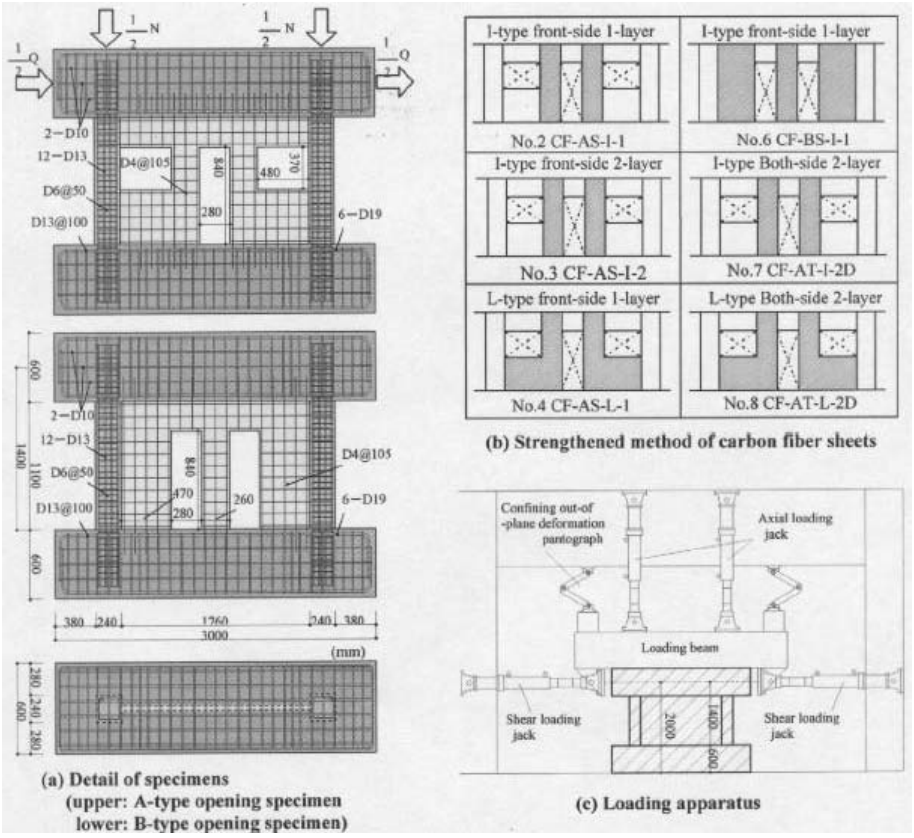

Figure 4-11: Strengthening configuration of walls with openings and test set-up (from Sugiyama, 2000)

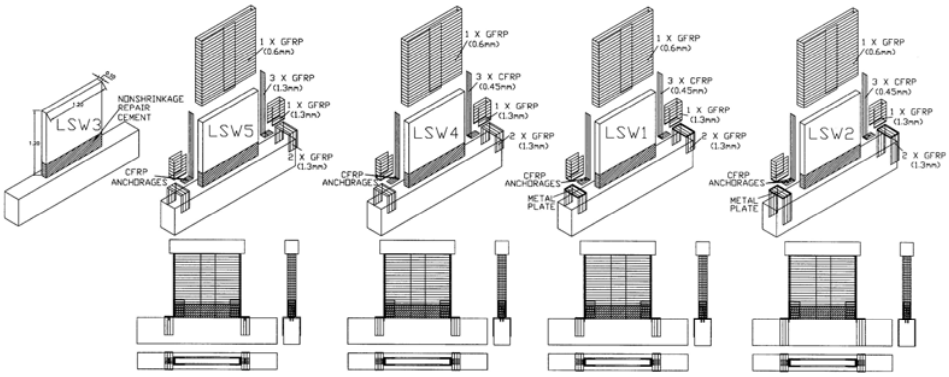

Figure 4-12: Repair and strengthening procedures (from Antoniades, 2003)

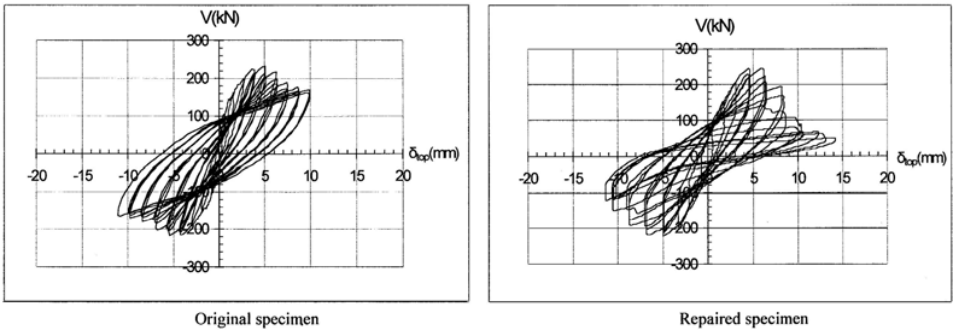

Figure 4-13: Example of hysteresis loops comparison for element LSW4 before and after strengthening (from Antoniades, 2003)

An experimental investigation on the behaviour of RC structural walls strengthened with FRP has been performed by Khalil and Ghobarah (2005). The potential of the plastic hinges retrofitted with composite materials under earthquake loading was studied on the large scale models. The three specimens replicate the plastic hinge of a ten storeys structure, 33 m high and 3 m long wall. According to the design methods when the building was constructed the plastic hinge region is considered at 3 m from the bottom of the real structural wall. Due to technical limitations the specimens are cast on a scale 1:3 with a 0.12 m thickness. The shear to moment ratio was chosen to be 2.25, as it is considered a flexural wall. The first specimen is tested as a reference specimen without any strengthening. The second wall is retrofitted for shear using two layers of bidirectional fibres sheets anchored by wrapping with unidirectional fibres; while for the third element an extra mechanical anchorage with steel bolts anchored on both sides of the walls with steel plates is used for the same configuration as the second element. As failure mechanism, the diagonal crack has been reported for the control element at 363KN, diagonal debonding of the FRP with crushing of concrete at the bottom for the second element. The third element had a more complex failure mechanism as a result of the conjugated tensile failure of the steel bolts and debonding of the FRP with crushing of the concrete. It is important to notice the large displacement of this specimen. It was reported that the wall was shortened by 100mm as a result of the crushing. Both strengthened walls developed larger resistance forces, 515KN and 571 KN, respectively.

An innovative strengthening method of reinforced concrete walls using Aramid fibre reinforced polymers (AFRP) was performed by Kobayasi (2005). AFRP bundles were passed through drilled holes on a diagonal path. Two series of scaled RC shear wall specimens were investigated in order to evaluate the strengthening effect. All the walls had the same size and test setup and were loaded according to a cyclic pattern. Three walls were tested in a pilot program: (1) original specimen, (2) original specimen up to failure strengthened and retested and (3) strengthened original specimen and tested. Another set of four walls was added to previous tests. One of them was loaded as a control specimen. The remaining three, were initially strengthened with different amounts of AFRP and tested. Shear failure was reported in all the cases. A 25% increase

of the shear load was noted. The author considered the research as having a valuable significance also from an economical point of view due to a low consumption of material and the easier application.
In order to validate finite element analysis (FEA) Li et al. (2005) tested a 1:5 scale reinforced concrete shear wall strengthened with GFRP. After an initial test of the wall the strengthening was applied and subjected to a cyclic loading. The FEA was based on three key parameters for the material behaviour. Concrete was defined using damaged plasticity criterion. GFRP was implemented using SPRING elements. The reinforcing steel rebars were supposed to behave as a perfect elasto-plastic material. All the material constants were introduced after material tests. A good correlation between the FEA and the experimental test was reported. Shear failure was observed as the dominant failure mode followed by GFRP debonding and rupture. As secondary failure mode flexure at the toe edges were reported in the real test represented by concrete spalling, concrete crushing and horizontal cracks development. The comparison between the experimental work and the FEA is presented in Figure 4-14.

Following a pattern of a real four-levels building arrangement (i.e. different positions of doors and windows), five 1:4 scale reinforced concrete walls specimens, strengthened with FRP were tested by Nagy-György et al. (2005). Initially all the walls were seismically tested up to failure in cyclic loading. The FRP strengthening system was applied on one face of the walls after a standard repair of the damaged specimens i.e. replacing the crushed concrete with mortar and filling the cracks with epoxy resins. The FRP was anchored at the toe of the walls using steel angle profiles fixed with bolts through resin. Different configurations of strengthening were used in function of the openings pattern in the walls. The effect of the strengthening was evaluated by average values (relative to baseline records). The elastic limit increased by 47%, average failure load increased by 45%, average stiffness decreased by 53% and average ductility decreased by 60%. Since three out of five specimens had an unsymmetrical geometry the test results were dependent on the loading direction.

Although the strengthening of walls structures with FRP has been proven to be a viable solution (Hiotakis et al. 2003, Khalil and Ghobarah 2005, Nagy et al. 2005, etc.) theoretical research is still in the beginning of its development but lacks specifications for the walls with openings.

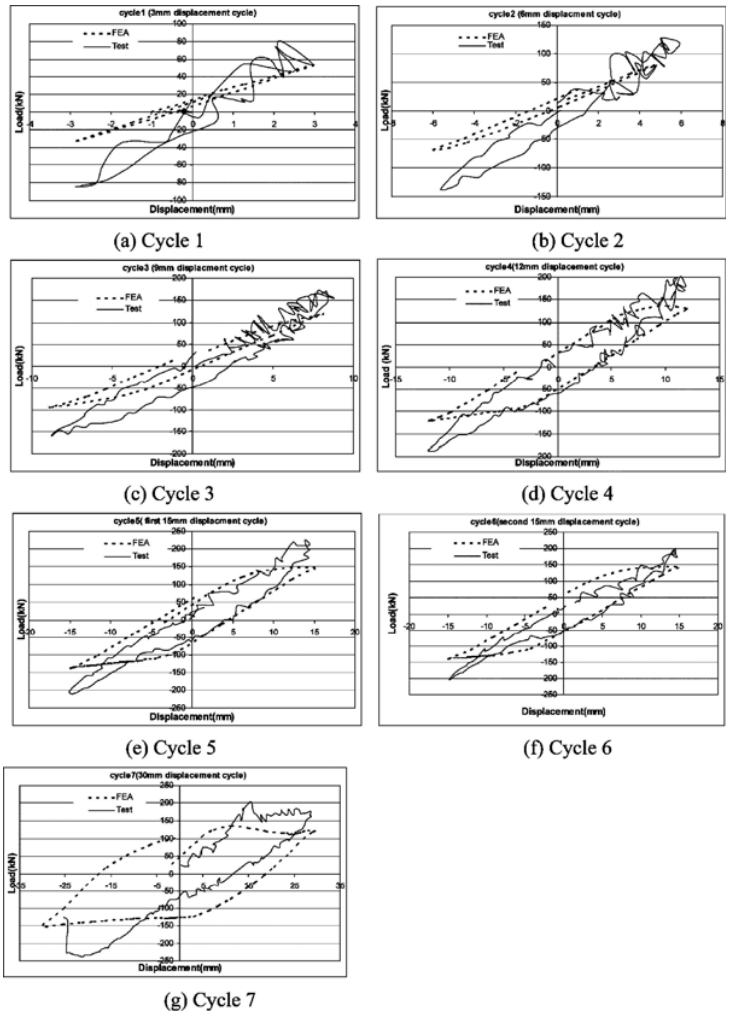

Figure 4-14: Cycle by cycle comparison between experiment and the FEA performed by Li et al. (from Li et al., 2005)

4.3 Calculation procedure for walls with openings FRP strengthened

To the best knowledge of the author, the effect of the FRP strengthening of a wall with openings has not been presented in theoretical form. This paragraph is trying to outline several aspects that might lead to a safe calculation procedure for FRP strengthened walls with openings axially loaded. However this simple model is under development and here some general aspects are presented only.

The total capacity of a wall is not possible to be computed using Betonghandbok (1997), but the efforts surrounding the opening can be determined in a simple to use manner as it has been shown in paragraph 2.5.5. Trough these efforts the necessary reinforcement area surrounding the opening can be determined. A similar procedure for deriving the design efforts is adopted in this chapter too.

Let's consider a solid one-way action loaded with an initial axial load q acting on the top, as in (Figure 4-15). The wall is assumed to be reinforced with a uniformly distributed mesh of steel reinforcement in the middle plane. Now we assume a door opening is created in the wall. The objective is to determine the necessary FRP strengthening system to rehabilitate the wall considering the new created opening.

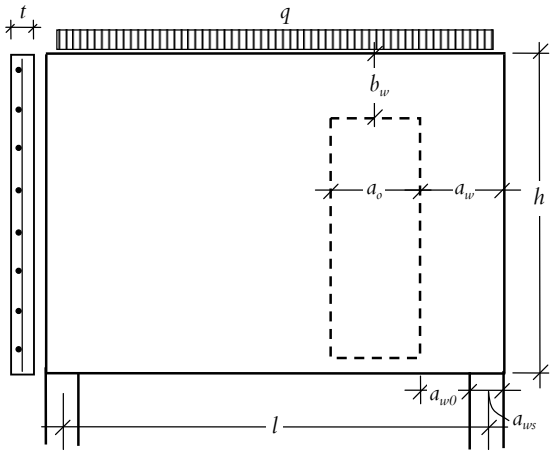

Figure 4-15: Wall with opening

In order to simplify the calculation procedure the section surrounding the opening (Figure 4-16a) is considered to act as a frame (Figure 4-16b). The elements of the frame are considered to pass trough the centre of gravity of the each element (dashed line in Figure 4-16a).This assumption is based on the similar approach found in Betonghandbok (1997) for the design of the steel reinforcement. The distribution of the bending moments, shear forces and axial forces are presented in Figure 4-16 c, Figure 4-16d and Figure 4-16e.

The following assumptions are made:

- The resultant of the axial load acting on the assumed frame is equal to the reaction force in the support $V_2=R_2$ and the bending produced by the eccentricity e, is determined as in equation (4-24).

$$V_2 = \frac{ql}{2} \tag{4-23}$$

$$M_2 = e\, R_2 \tag{4-24}$$

- The moment resistance for bars 2-5 is set to be equal to zero, since in reality for making the opening the bar is sectioned.
- The horizontal reaction force H is determined from the following equation.

$$H = \frac{M_2 - M_3}{b} \tag{4-25}$$

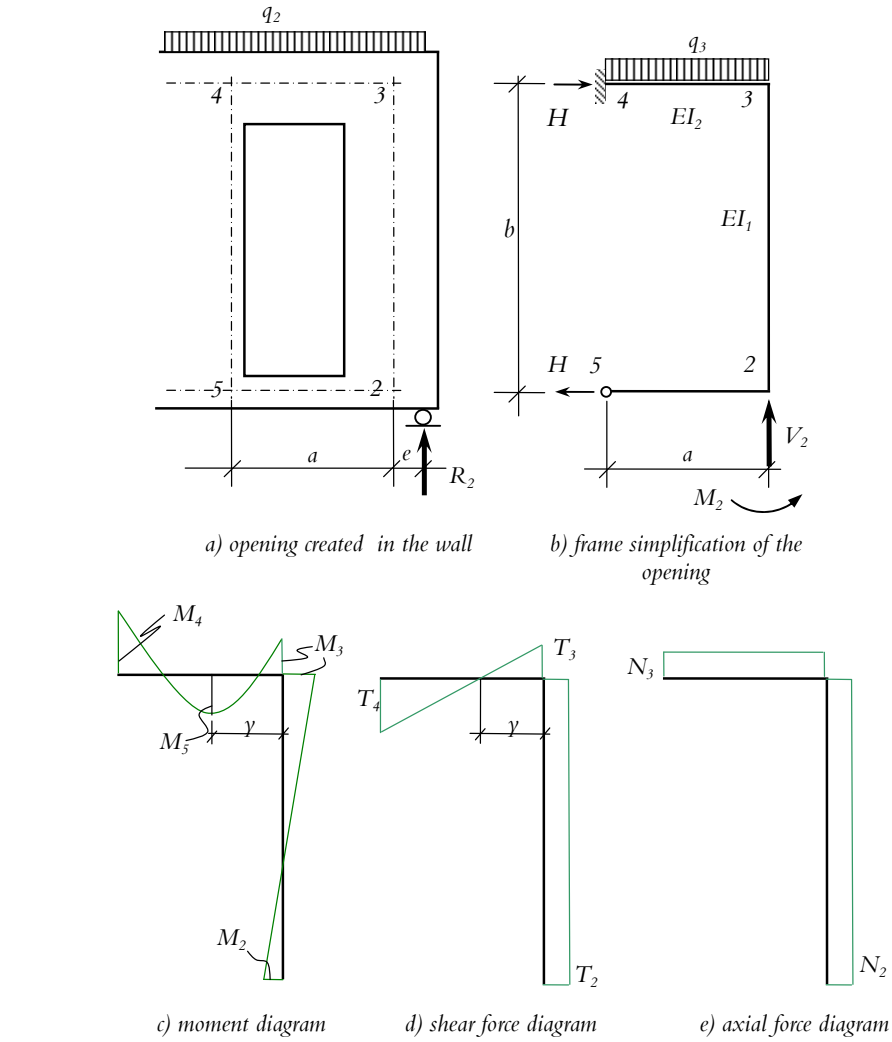

a) opening created in the wall *b) frame simplification of the opening*

c) moment diagram *d) shear force diagram* *e) axial force diagram*

Figure 4-16: Static analysis simplifications

4.3.1 Determining the efforts in the frame

The unknown design efforts are derived considering the static analysis of the frame (Langesten, 1999) following. The bar 3-4 is considered fixed in node 4 and hinged in node 3, while the bar 2-3 is simply supported (Figure 4-17). According to these assumptions the rotation condition of node 3 ($\theta_{23}=\theta_{34}$) is used to determine the design moment M_3 (Eq. (4-26).

$$\theta_{32} = M_3 \frac{b}{3EI_1} + M_2 \frac{b}{6EI_1}$$

$$\theta_{34} = M_3 \frac{a}{4EI_2} + \frac{q_2 a^3}{48EI_2}$$

$$\theta_{32} = \theta_{34}$$

$$M_3 \frac{b}{3EI_1} + M_2 \frac{b}{6EI_1} = -M_3 \frac{a}{4EI_2} + \frac{q_2 a^3}{48EI_2}$$

$$M_3 \left(\frac{b}{3EI_1} + \frac{a}{4EI_2} \right) = -M_2 \frac{b}{6EI_1} + \frac{q_2 a^3}{48EI_2} \Bigg| \times 12 \frac{EI_2}{a}$$

$$M_3 \left(2k + 3\right) = -4kM_2 + \frac{q_2 a^2}{4} \quad where\ k = \frac{EI_2}{EI_1} \frac{b}{a}$$

$$M_3 = \frac{\frac{q_2 a^2}{4} - 4kM_2}{\left(2k + 3\right)} \tag{4-26}$$

$$M_4 = \frac{q_2 a^2}{8} + \frac{M_3}{2} \tag{4-27}$$

The shear forces are determined using the basic formulas provided in static tables.

$$H_2 = \frac{M_3 - M_2}{b} \tag{4-28}$$

$$H_3 = \frac{M_2 - M_3}{b} \tag{4-29}$$

$$V_3 = \frac{3q_2 a}{8} + \frac{3M_3}{2a} \tag{4-30}$$

$$V_4 = \frac{5q_2 a}{8} - \frac{3M_3}{2a} \tag{4-31}$$

The design moment M_5 is determined in the section γ (see Figure 4-16 c and Figure 4-17).

$$V_3 - q_2\gamma = 0 \Rightarrow \gamma = \frac{V_3}{q_2} \tag{4-32}$$

$$M_5 = V_3\gamma - q_2\frac{\gamma^2}{2} - M_3 \tag{4-33}$$

The axial forces H and V_2 were already defined in equation (4-23) and (4-25).

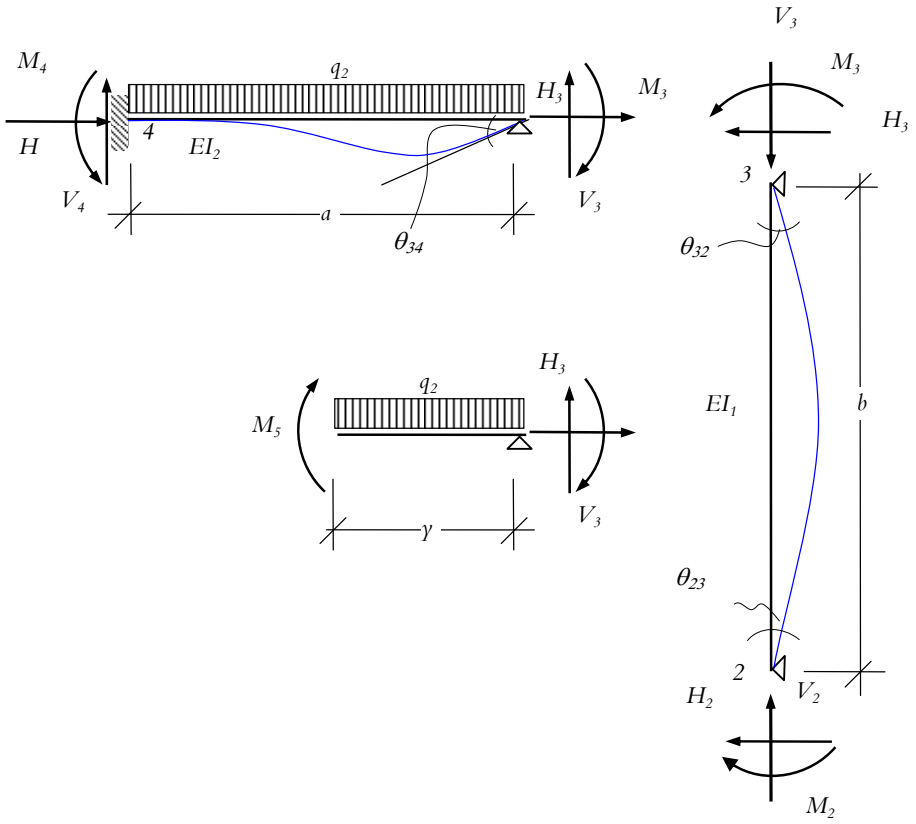

Figure 4-17: Assumed beam behaviour for the derivations

4.3.2 FRP strengthening design

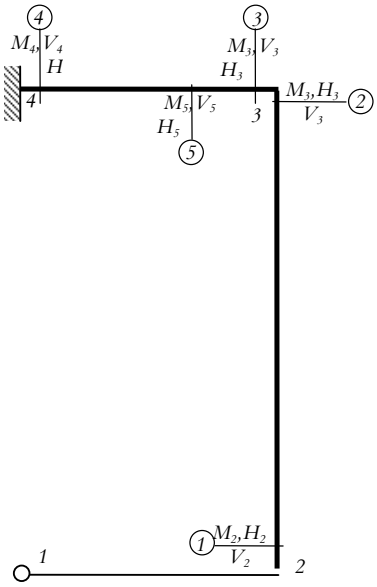

Figure 4-18: Sections considered for design

Design of elements

The design is carried out in the sections depicted in Figure 4-18. It should be noted that no contribution from the concrete is considered in this analysis for the elements subjected to bending or shear, all forces are transmitted to the composite material.

Design for bending moment

The design for bending is similar for all elements the frame is performed considering the approach found in Täljsten (2006).

$$A_{frp,b} = \frac{M_d / 0.9 - A_{st} f_y}{\varepsilon_{frp} E_{frp}} \tag{4-34}$$

where the steel area A_{st} and the yield strength of the steel, f_{st}, should not be accounted if no steel is present in the section.

Design for shear

The shear contribution attributed to the strengthening material is determined as (Täljsten, 2006).

$$t_{frp} = \frac{V_d}{0.6\varepsilon_{frp} E_{frp} b_{frp}} \tag{4-35}$$

Design for axial load

A simple check adopted from Täljsten (2006) is considered for the axial load design of the column element 2-3. The equation (4-36) defines the increase in axial compression strength of FRP confined concrete.

$$\frac{f_{cc}^{'}}{f_{c0}} = 1 + 2.0\frac{\sigma_\ell}{f_{c0}} \tag{4-36}$$

where $f_{cc}^{'}$ is the compressive strength of the confined concrete, f_{c0} is the compressive strength of the unconfined concrete and σ_ℓ is the confinement pressure provided by the FRP determined as in equation (4-37).

$$\sigma_\ell = \frac{2\varepsilon_{frp} E_{frp} A_{frp}}{\sqrt{h^2 + t^2}} \tag{4-37}$$

The compressive strength of the unconfined concrete is determined based on the next formulation found given in BBK (2004).

$$N_d = k_c \frac{A_c f_{cc}^{'}}{1 + k_\varphi \varphi_{ef}} + k_s A_s f_{sc} \tag{4-38}$$

where A_c is the cross section area of the concrete and A_s is the longitudinal steel reinforcement. φ_{ef} is the effective creep number equal 2 (BBK, 2004). k_c and k_φ are coefficients depending on the concrete quality and the slenderness of the column considered (l_c/h), normally given in tables (Täljsten, 2006). Since no steel is considered in this analysis equation (4-38) gives.

$$N_d = k_c \frac{A_c f_{cc}^{'}}{1 + k_\varphi \varphi_{ef}} \Rightarrow f_{cc}^{'} = \frac{N_d \left(1 + k_\varphi \varphi_{ef}\right)}{A_c k_c} \tag{4-39}$$

Substituting equation (4-39) in equation (4-36) results the confinement pressure provided by the FRP.

$$\sigma_\ell = \frac{1}{2}\left[\frac{N_d \left(1 + k_\varphi \varphi_{ef}\right)}{k_c A_c} - f_{c0}\right] \tag{4-40}$$

The necessary strengthening area is determined as:

$$A_{frp,c} = \frac{1}{2}\left[\frac{N_d \left(1 + k_\varphi \varphi_{ef}\right)}{k_c A_c} - f_{c0}\right]\frac{\sqrt{h^2 + t^2}}{2\varepsilon_{frp} E_{frp}} \tag{4-41}$$

4.3.3 Concluding remarks and research questions

At this stage the design procedure can be regarded as a guideline on how to strengthen RC walls with openings due to simplifications adopted and the omission of the contribution from the steel reinforcement provided in the middle plane of the wall. If walls with existing openings are the subject of an investigation the presence of structural steel reinforcement cannot be disregarded. In what manner existing reinforcement in the wall is influencing the strengthening effect is a subject of a further research.

The real behaviour of a structural wall with openings is not always covered by the simplification assumed in this design procedure because large variation of the efforts can occur if different static frame models are selected. To avoid these situations critical aspects such as support system and boundary condition of the wall should not be disregarded in the analysis. Until further investigations of the behaviour of FRP strengthened walls with opening are performed mechanical anchorages are suggested to be used to ensure full utilization of the strengthening and avoiding the loss of bond. However, the strain in the FRP ε_{frp} can be calculated considering different theoretical approaches as presented in Chapter 4 or available in the literature.

The design efforts determined analytically in this model can be viewed as a specific case but the principle is similar for other configurations too. More detailed analysis will be carried out to investigate a general loading configuration. The interaction between the efforts (bending moment-axial force and bending moment-shear force) in a section of an element is another topic to be followed. Further more for different types of openings the configuration of the efforts can change also. Of high interest is to determine in what manner is influencing the size of the opening the structural behaviour of the walls. In other words when stops the wall to act like a single element or starts to behave partially or totally like a frame (Figure 4-19a, b). A fast solution for determining the efforts acting on the wall can be provided by simple finite element analysis. In normal cases this should be carried out considering different support systems and an envelope of the maximum efforts can be used for design considerations.

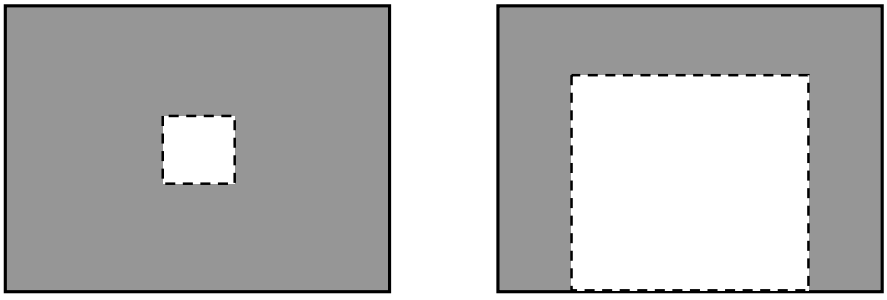

a) small opening *b) large opening*

Figure 4-19: Walls with different types of opening

5 Case study for walls with openings FRP strengthened

5.1 General description

The general plan presented in Figure 5-1 is the plan of a building 2 stories high with basement, used as the local city hall of Sävsjö (Sweden). The entire edifice is divided in 3 main parts. The infrastructure is formed by continuous foundations and reinforced concrete (RC) walls. The superstructure is made of transversal and longitudinal RC walls and RC slabs. The roof structure is made of timber columns and beams as a truss structural system. A new configuration of the offices was intended to be created and for this RC walls were modified by enlarging existing openings. For doing this the influence of the new openings on the capacity of the walls had to be checked and a rehabilitation principle suggested. A special request of the client was to minimize the visibility of the rehabilitation and thus the applicability of the FRP technique was investigated, i.e. NSMR.

5.2 Available data for analysis and simplifications

As in other cases of practical applications, complete technical information is missing for this case. The reinforcing plans of the walls were not available but visual contact had certified the existence of a one layer mesh of steel reinforcement in the mid plane. However the reinforcement was disregarded in the analysis. Moreover information about the existing reinforcement in the coupling beam between the two parts of the wall was not accessible, so it cannot be considered in the analysis. Compressive tests on concrete specimens revealed a compressive strength of 30 MPa corresponding tensile strength assumed from Eurocode (2004a), 2.0 MPa. The materials used for the strengthening are given in Table 5-1 and Table 5-2.

The distributions of the walls combined with different loading situations were evaluated and the section presented in Figure 5-2 was identified as being critical. From this section the 1st level wall is analyzed. Geometrical characteristics are presented in Figure 5-3. The axial load of 29 kN/m acting on this wall, accounted for the weight of the slab, the weight of the top wall and the live load for an office building. All have been determined according to BBK (2004).

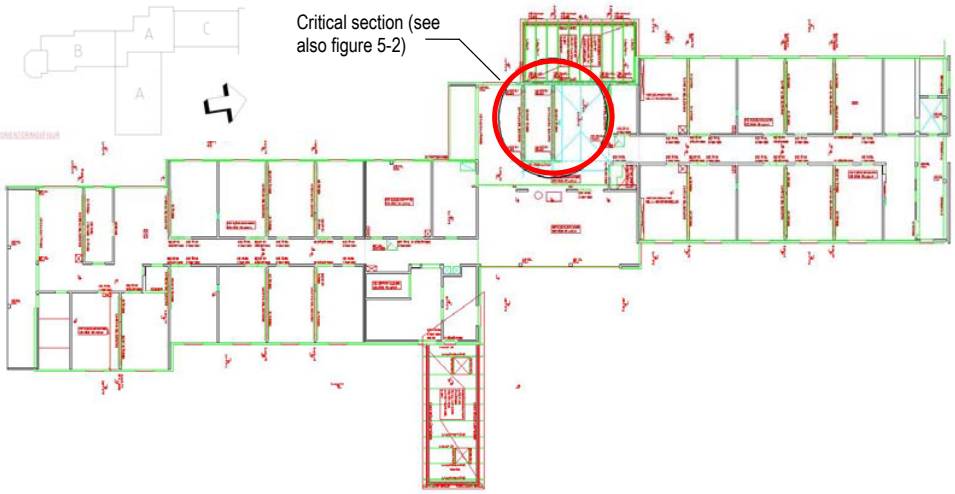

Figure 5-1: RC wall with opening

Table 5-1. Carbon fibre materials considered in the analysis

	f_{yk} [MPa]	E_{frpk} [GPa]	E_{frp} [GPa]	ε_{frpu} [%]	ε_{frp} [%]	A_{frp} [mm^2]
Sto FRP Bar E10C	2200	160	112	1.1	0.5	100*
Sto FRP Sheet S300C300	3500	230	130	1.5	0.5	51**

*for one bar, **for one sheet

Table 5-2. Adhesive recommended for bonding the carbon fibre

	ρ [kg/m3]	f_{ck} [MPa]	f_{ct} [MPa]	E_{frp} [GPa]	$\varepsilon_{adh\ m}$ [%]	Pot life [min]
Sto BPE Lim 417A/417B	1095	80	50	2	3	30
Sto BPE Lim 465/464	1498	103	31	7	-	90
Sto BPE Primer 50	1050	-	-	-	-	45

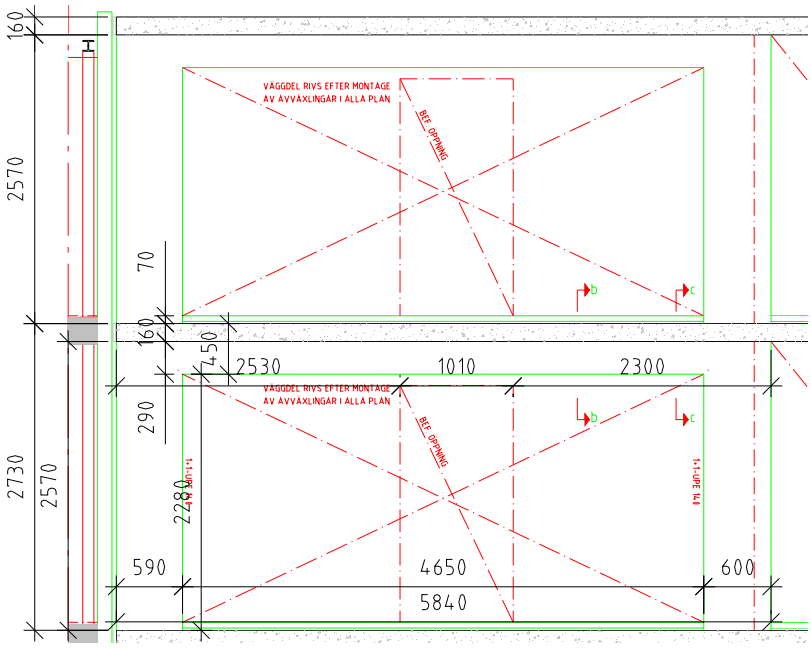

Figure 5-2: Identified section for analysis

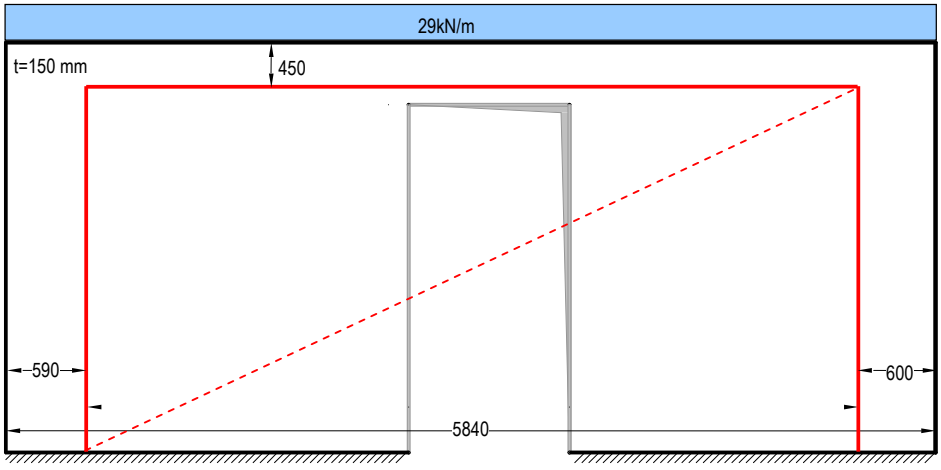

Figure 5-3: Geometrical characteristics of the wall with opening in mm

5.3 Analysis and evaluations

To evaluate the effect of the NSMR strengthening first a check of the actual capacity of the wall with opening was intended to be performed.. The slenderness ration, H/t_w=18.6 is larger then 12 the maximum slenderness used for Saheb and Desayi (1990b). The concrete strength of 30 MPa is not in accordance with the minimum compressive strength used in the model proposed by Doh and Fragomeni (2005). Hence the capacity was possible to be calculated according to the models presented the paragraph 2.5.5. Due to this a finite element analysis has been performed to evaluate the stresses distribution in the wall.

The distribution of principal stresses has been determined for the wall before enlarging the opening (Figure 5-4) and after creating the opening (Figure 5-5). A maximum value of principal tensile stress 0.33 MPa is found for the first case and 5.5 MPa in the second case. It is important to mention that this analysis did not consider the T cross section created by the slab and the coupling beam of the wall, since the most unfavourable structural behaviour was intended to be analyzed. Hence, the analysis is carried out on the safe side.

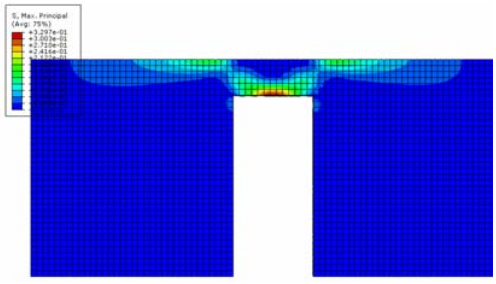

Figure 5-4: Principal stresses in the initial wall

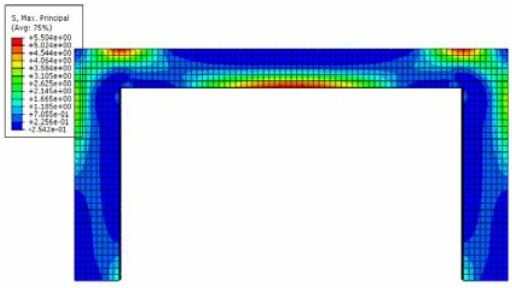

Figure 5-5: Principal stresses in the wall after creating the opening

The stress flow in the wall was changed with the enlarged opening and had increased values compared to the initial wall structure. It was observed that enlarging the opening in the wall imposes an effect similar to frame structure behaviour. Based on this observation a static analysis was conducted to identify the design efforts in the structure. The distributed load of 29 kN/m is considerably reduced when the openings in the

walls from both levels (Figure 5-2) are created. However, in the static analysis the same value of 29 kN/m has been used. This decision was based on the assumption that the wall from the first level is strengthened first.

The frame (Figure 5-7) was analyzed using a commercial finite element software. This analysis considered different configurations for the support systems and the maximum efforts were determined when the supports are fixed (Figure 5-7). The bending moment was found to be 52 kNm in the clear span and 79 kNm at the junction of the column with the beam. The maximum shear force in the beam is 87 kN and 42 kN in the column. The axial load values were 42 kN in the beam and 87 kN in the column. To cover all possible failure cases the beam of the frame was analyzed as a simple supported beam for wich the maximum bending moment is 130.5 kNm.

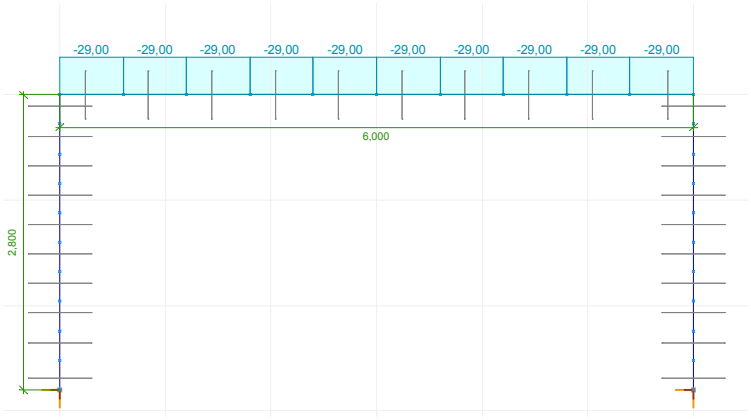

Figure 5-6: Characteristics of the frame considered in design

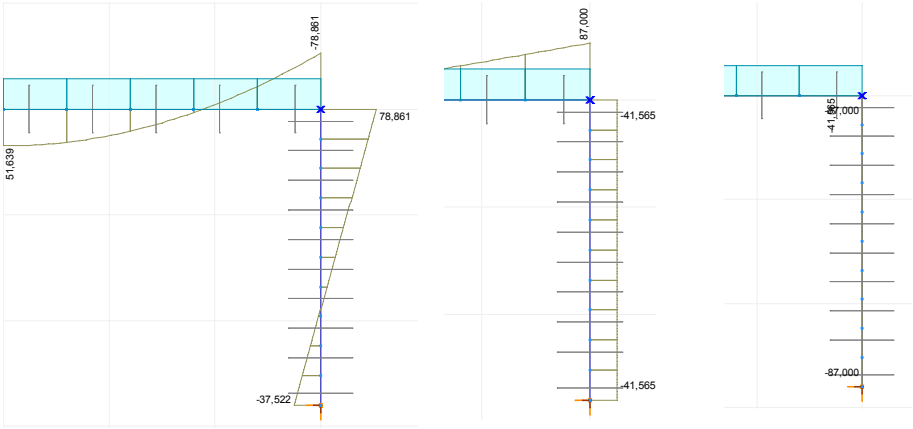

Figure 5-7: Design efforts: left-bending moment, centre-shear force, right-axial load

5.4 Design of the FRP strengthening

The design of the strengthening was carried out as presented in paragraph 4.3.2, where all elements are design considering no interaction between the efforts.

The necessary fibre quantity for strengthening the beam for bending can be determined from:

$$A_{frp} = \frac{M/0.9 - A_s f_{st}}{\varepsilon_{frp} \cdot E_{frp}} = \frac{130.5 \cdot 10^6 / 0.9 - 0}{5 \cdot 10^{-3} \cdot 121 \cdot 10^3} = 199 \text{mm}^2$$

The strengthening system recommended was 2 bars of Sto FRP bar E10C. A minimum anchorage length of 500 mm had to be provided, or else a mechanical anchorage had to be ensured. The NSM bars provided by the manufacturer have a nominal cross section area on 100 mm^2 for each individual bar and the strengthening system has to be applied symmetrically on both sides of the wall. The bending moments acting in the columns are smaller that the ones considered on the beams so applying the same strengthening configuration is considered on the safe side.

The necessary fibre quantity for shear strengthening can be determined from:

$$t_{frp} = \frac{V}{0.6\varepsilon_{frp} E_{frp} b_{frp}} = \frac{87 \times 10^3}{0.6 \times 5 \times 10^{-3} \times 130 \times 10^3 \times 300} = 0.49 \text{ mm}$$

Resulting from the above calculation, 3 layers of Sto FRP sheet S300C300 (0.17 mm thickness/sheet) system were recommended to strengthen the beam. A U strengthening configuration with mechanical anchorage was also recommended to be used.

The shear strengthening of the columns results from:

$$t_{frp} = \frac{V}{0.6\varepsilon_{frp} E_{frp} b_{frp}} = \frac{42 \times 10^3}{0.6 \times 5 \times 10^{-3} \times 130 \times 10^3 \times 590} = 0.19 \text{ mm}$$

So 2 layers of Sto FRP sheet S300C300 (0.17 mm thickness/sheet) are recommended for both columns. For the column on the right fully wrapped system was recommended to be applied. For the column on the left the U wrapped system was proposed since the initial wall is connected with a transversal wall (Figure 5-2). Also a mechanical anchorage should be provided to ensure the bond capacity of the FRP sheet system.

The axial capacity of the concrete columns is checked as:

$$N = k_c \frac{A_c f_{c0}}{1 + k_\varphi \varphi_{cf}} = 0.92 \frac{0.15 \times 600 \times 150 \times 30}{1 + 0.02 \times 2} = 372 \; kN > 87 \; kN$$

From the above calculation it results no need of confinement of the columns.

The principle for the strengthening configuration of a wall is presented in Figure 5-8 and details of application in Figure 5-9. Similar strengthening procedure is applied for the rest of the walls.

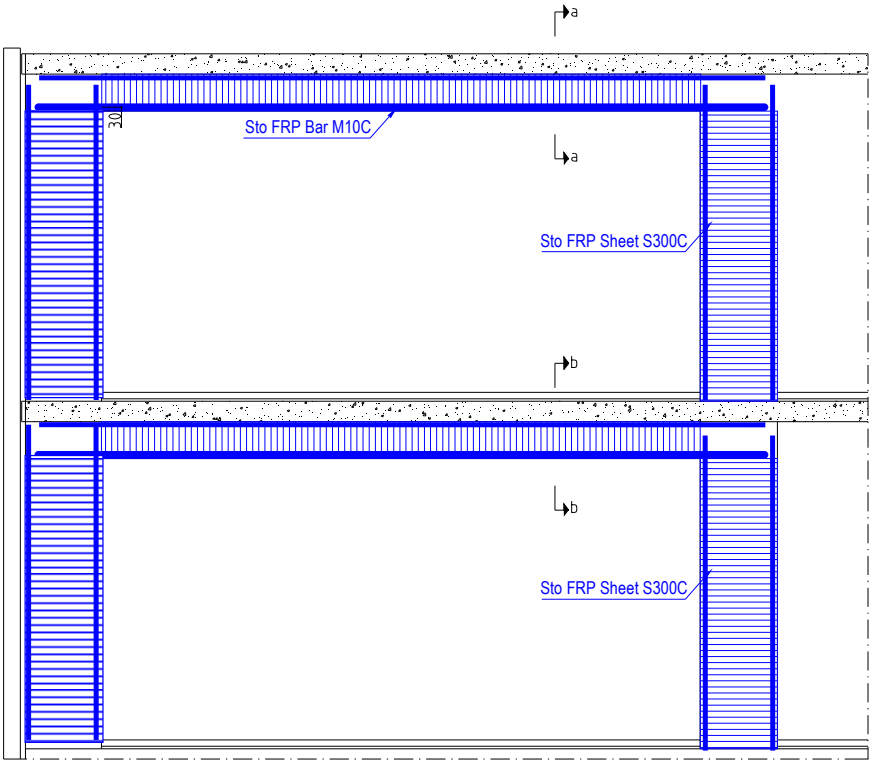

Figure 5-8: Principle strengthening configuration for wall with openings

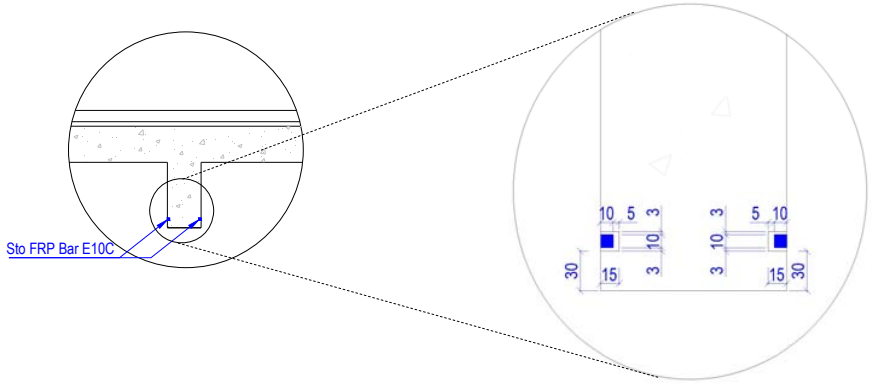

Figure 5-9:Details of NSMR application

5.5 Concluding remarks

It is worth to notice that the strengthening proposal was accepted and successfully applied. Although, a few comments regarding the field application have to be mentioned. The strengthening is successful from a technical point of view. However, due to limited experience of the contractor regarding the strengthening systems, the practical strengthening procedure was much more complicated than necessary. The handling of the adhesive was not always in agreement with the standard procedures applied by experienced contractors. Yet, a control on site showed that that the instructions regarding bonding temperature and humidity had been followed since no areas with bond problems were discovered. Aesthetic of the strengthened walls was not relevant since gypsums boards were intended to be applied from the beginning, although many messy areas with hardened adhesive, as in the right photo in figure 5-9, have been reported. A few photographs of the strengthening are presented in Figure 5-10.

Figure 5-10: Photographs from the application of the strengthening system

6 Conclusions and future research

Shear strengthening of RC elements using FRP materials are certified to be a successful and viable alternative to traditional strengthening methods. However attention must be given when shear design models are used for calculating the FRP contribution to total shear capacity of the RC beams.

The shear strength of concrete beams according to the design standard analyzed in this thesis presents weaknesses which may lead to unsafe design. The use of the simple truss model analogy in ACI (2005) does not comprise the complex behaviour in shear making the calculations robust and the predictions inaccurate. The European design standard Eurocode (2004a, b and 2005) is conservative for design purposes since the contribution of the steel stirrups and concrete cannot be considered simultaneously. The Swedish design standard BBK (2004) provides a design method for shear strength of concrete beams based on empirical derivations, which makes the design unpredictable. If we add a new parameter to these uncertainties the shear aspect in FRP strengthened RC beams is found to be more complicated.

A large amount of tests on RC beams strengthened with FRP materials has been performed across the world. The reports of these experimental results were collected and assembled in a large database. Although the number of experiments that have been performed is much higher than those selected for the database, the information presented in it contains only valid outputs of the test. The reasons for not including more tests are as follows: in several cases key factors were missing (i.e. tensile strength of FRP, modulus of elasticity of FRP, concrete compressive strength, etc.); the beams in shear are highly dependent on size effect so the scaled beams used for tests were removed. It is interesting to note that although T beams are more commonly used in actual structures, only a small number of T beams in comparison to rectangular beams have been tested. For further reliability and development more tests should be conducted on strengthened T beams.

Using the database presented in paper I the efficiency of the theoretical models with high impact in design (popular among the researchers, used in design guidelines) was investigated and found to be unsatisfactory to a high degree. These models were thoroughly analyzed and their predictions were compared with the test results and all of them were found to be inaccurate for predicting the actual behaviour of a FRP strengthened RC beam. Moreover from being inaccurate some of the predictions were highly unsafe giving reasons for concern in their use for design purposes. These weaknesses emerge from the truss model analogy used in the majority of the theoretical models for predicting the shear capacity of strengthened beams. The regression analysis, used in several models, can be a powerful tool in deriving an equation, but here a too

large variability of material characteristics or number of parameters are used to cover a small number of experimental tests. In addition it is important to mention the uncertain test results for some models used for derivation. Also it is doubtful whether using tests performed on rectangular beams to calibrate T section beams is reliable since the behaviour between these two types of beams can be different.

The theoretical model derived and presented in this thesis respects the same trend as for the rest of the models when used to compare the predicted values with the experimental results. The model is derived based on the linear fracture mechanics theory. The use of the fracture energy is the model's weakness since the fracture mechanic field is still under development. Until further progress is made in theoretically expressing the fracture energy in concrete the values based on the experimental tests can be used in this model. In the model a mode II of fracture has been assumed but it is still unclear what fracture mode is dominant at the interface concrete-composite. Understanding this can be considered a future research area along with the application of non-linear fracture mechanics theory.

The author considers that real progress in deriving accurate models for FRP strengthened beams in shear is hard to be accomplished until the behaviour of the simple RC beams in shear is solved. The corroborating action of influential factors such as: tensile reinforcement, shear span ration, size effect, aggregate size, steel stirrups–concrete interaction or crack propagation process must be studied deeply. In this sense more attention should be given to Modified Compressive Field Theory and Theory of Plasticity, because the truss model analogy used is a simplified method and its limitations have been proven.

The need for strengthening RC elements with openings is a demand emerging from the dynamic changes of the society, i.e. functionality of buildings modified in a large number of cases. In this thesis openings in RC walls and possibilities of strengthening have been analyzed. The design of solid walls is performed according to the RC columns design or strut-and-tie analysis. Direct calculus procedures for walls with openings are not provided in the standards analyzed here. Only two empirical models to calculate the bearing capacity of walls with openings have been found, but the predictions are not reliable and their use in design is limited. To the best knowledge of the author, theoretical models for RC walls strengthened with FRP materials are missing.

Therefore a simple theoretical model has been derived based on the assumption that the elements boarding the opening behave as a frame. The necessary FRP strengthening quantity is determined using the addition principal. For this, the actual capacity of the wall is determined and if the bearing capacity of the elements surrounding the opening is exceeded the difference is supplemented with FRP reinforcement. The derivations presented here do not consider out of plane eccentricities and the effect of FRP strengthening on a wall eccentrically axially loaded, but this is considered to be a possible subject of future work. Furthermore a question to be answered is how large an opening should be in order to have the assumed behaviour. The influence of boundary conditions such as restraints on the vertical sides

of the walls should be another subject to be discussed. An answer to these topics could be provided by a future finite element analysis. The experimental tests which are the subject of an ongoing research program should be able to clarify some aspects but more experimental work is needed to estimate also more complex loading conditions such as lateral loading, the influence of the existing reinforcement in the wall or the properties of the materials. The research on walls with openings presented in this thesis must be considered at the basic level since no interaction between walls or system of walls has been considered and the theoretical basis of the derived model relies on the elastic analysis on the frames.

It must also be noted that the studies on FRP strengthened RC walls is a relatively new subject and more questions to be answered could arise as a result.

References

ACI Committee 318 (2002). "Building code requirements for reinforced concrete." American Concrete Institute, Detroit, pp. 111.

ACI Committee 318 (2005). "Building code requirements for structural concrete (ACI 318-05) and commentary (318M-05)." American Concrete Institute, Farmington Hills, (MI, USA).

ACI Committee 440 (2002). "Guide for the design and construction of externally bonded FRP systems for strengthening concrete structures (ACI 440.2R-02)." American Concrete Institute, Farmington Hills, (MI, USA).

Adhikary, B. B., Mutsuyoshi, H., and Ashraf, M. (2004). "Shear strengthening of reinforced concrete beams using fiber-reinforced polymer sheets with bonded anchorage." ACI Structural Journal, 101(5), 660-668.

Ali, A. and Wight, J. K. (1991). "RC structural walls with staggered door opening.", Journal of Structural Engineering, 117(5), 1514-1531.

André, A. (2007). "Strengthening of timber structures with flex fibres" Luleå University of Technology, Licentiate thesis 2007:61.

Antoniades, K., K., Salonikios, T., N., and Kappos A., J. (2003). "Cyclic tests on seismically damaged reinforced concrete walls strengthened using fiber-reinforced polymer reinforcement". ACI Struct. J., 100(4), pp. 510-518.

Antoniades, K., K., Salonikios, T., N., and Kappos A. J. (2005). Tests on seismically damaged reinforced concrete walls repaired and strengthened using fiber-reinforced polymers, J. Compos. for Constr., Vol. 9, No. 3, 236-246, 2005.

Antoniades, K., K., Salonikios, T., N., and Kappos, A., J., (2007). "Evaluation of hysteretic response and strength of repaired R/C walls strengthened with FRPs". Engineering Structures 29, pp. 2158-2171.

Aprile, A., Benedetti, A. (2004). "Coupled flexural-shear design of R/C beams strengthened with FRP", Composites: Part B Engineering, 35, 1–25.

BBK 04 (2004). "Boverkets handbook-About concrete structures" (in Swedish). ISBN: 91-7147-816-7.

Betonghandboken (1997). "Konstruktion" Svenskt tryck AB, issue nr 2, ISBN 91-7332-533-3.

Blanksvärd, T. (2007). " Strengthening of concrete structures by the use of mineral based composites", Luleå University of Technology, Licenciate thesis, 2007:15.

Bresson, J. (1971). "Nouvelles rechercher et applications concernant l'utilisation des collages dans les structures". Betton plaque annales de l'institut technique, No. 278.

Burgoyne, C. J. (1999). "Advance composites in civil engineering in Europe". Structural Engineering International, Journal of IABSE, 9(4), pp. 267-273.

Cao, S. Y., Chen, J. F., Teng, J. G., Hao, Z., and Chen, J. (2005). "Debonding in RC beams shear strengthened with complete FRP wraps." Journal of Composites for Construction, 9(5), 417-428.

Carolin, A. (2003) "Carbon fiber reinforced polymers for strengthening of structural elements", Luleå University of Technology, Doctoral thesis 2003:18.

Carolin, A., and Täljsten, B. (2005). "Theoretical study of strengthening for increased shear bearing capacity." Journal of Composites for Construction, 9(6), 497-506.

Gulec, K., C., Whittaker, A., S. and Stojandinovic, B. (2008). "Shear strength of squat rectangular reinforced concrete walls.", ACI Structural Journal 105(4), 488-497.

Chaalla,l O., Nollet, M-J., and Perraton, D. (1998). "Strengthening of reinforced concrete beams with externally bonded fibre-reinforced-plastic plates: design guidelines for shear and flexure." Canadian Journal of Civil Engineering, 25, 692-708.

CEN (2004a). "Eurocode 2: Design of concrete structures-Part 1-1: General rules and rules for buildings". European Committee for Standardization. Brussels (Belgium).

CEN (2004b). "Eurocode 8: Design of structures for earthquake resistance – Part 1: General rules, seismic action and rules for buildings". European Committee for Standardization. Brussels (Belgium).

CEN (2005). "Eurocode 8: Design of structures for earthquake resistance-Part 3: Assesment and retrofitting of buildings". European Committee for Standardization Brussels (Belgium).

Chen, J. F., and Teng, J. G. (2001). "Anchorage strength models for FRP and steel plates bonded to concrete." Journal of Structural Engineering, 127(7),784-791.

Chen, J. F. and Teng, J. G. (2003a). "Shear capacity of fibre-reinforced polymer-strengthened reinforced concrete beams: fibre reinforced polymer rupture." Journal of Structural Engineering, 129(5), 615-625.

Chen, J. F., and Teng, J. G. (2003b) "Shear capacity of FRP-strengthened RC beams: FRP debonding." Construction and Building Materials, 17, 27-41.

CNR, (2005). "Instructions for design, execution and control of strengthening interventions through fiber reinforced composites (English version). CNR-DT 200/04, Consilglio Nazionale delle Ricerche, Rome, Italy.

Collins, M. P., Mitchell, P. (1991). "Prestressed concrete structures". Prentice-Hall, New Jersey, USA. ISBN 0-13-691635-X.

Deniaud, C., and Roger Cheng, J. J. (2001). "Shear behaviour of reinforced concrete T-beams with externally bonded fibre-reinforced polymer sheets." ACI Structural Journal, 98(3), 396-394.

Deniaud, C., and Roger Cheng, J. J. (2003). "Reinforced Concrete T-Beams Strengthened in Shear with Fibre Reinforced Polymer Sheets." Journal of Composites for Construction, 7, No. 4, 302-310.

Deniaud, C., and Roger Cheng, J. J. (2004). "Simplified shear design method for concrete beams strengthened with fibre reinforced polymer sheets." Journal of Composites for Construction, 8 (5), 425-433.

Dias, S. J. E., and Barros, J. A. O. (2008). "Behaviour of RC beams shear strengthening with NSM CFRP laminates." Proceedings CCC 2008 - Challenges for Civil Construction, Torres Marques et al. (Eds) FEUP, Porto.

Doh, J.H., Fragomeni, S. and Loo, Y.C.(2002). "Evaluation of experimental behaviour of normal and high strength reinforced concrete walls in two-way action", Proceedings of the 17th Advanced in Mechanics of Structures and Materials, Gold Coast, Australia, June, pp. 169–173.

Doh, J.H. and Fragomeni, S. (2005). "Evaluation of experimental work on concrete walls in one and two-way action", Australian Journal of Structural Engineering, Vol. 6, No. 1, pp. 37–52.

Doh, J.H. and Fragomeni, S. (2006). "Ultimate load formula for reinforced concrete wall panels with openings." Advances in Structural Engineering, 9(1), 103-115.

Ehsani, M., M., and Saadatmanesh, H. (1997). "Fiber composites: An economical alternative for retrofitting earthquake-damaged precast-concrete walls". Earthquake Spectra, 13(2), 225-241.

fib Task Group 9.3, (2001). "Externally bonded FRP reinforcement for RC Structures." fib Bulletin 14, Lausanne, Switzerland.

fib Task Group 9.3, (2003). "Seismic assessment and retrofit of RC Buildings." fib Bull. 24, Lausanne, Switzerland.

Fragomeni, S., Mendis, P. A. and Grayson, W. R. (1994). "Review of reinforced concrete wall design formulas", ACI Structural journal, 91(5), 521-529.

van Gemert, D. (1996). "Design applications and durability of plate bonding technique" Proceedings of the International Conference on Concrete Repair, Rehabilitation and Protection, Scotland. London: Chapman & Hall. pp. 559-569. ISBN 0 419 21490 9.

Hallinan, P. and Guan, H., (2007). "Layered finite analysis of one-way and two-way concrete walls with openings." Advance is Structural Engineering, 10(1), 55-72.

Hiotakis, S., Lau, D., Z., Londono, J., C., Lombard, J., C., and Humar, J., L. (2003). "Retrofit and repair of reinforced concrete shear walls with externally epoxy bonded carbon fiber sheets." Annual Conference of the Canadian Society for Civil Engineering, Moneton, Nouveau-Brunswick, Canada.

Holzenkämpfer, P. (1990). "Strengthening of structural members by bonding steel plates". International seminar: Structural Repair/Strengthening by the Plate Bonding Technique, University of Schefield.

Hägglund, A. (2003). "Concrete beams strengthened with carbon fibre composites – shear" (in Swedish). Master thesis 2003:177. Luleå University of Technology , Division of Structural Engineering.

Ianniruberto, U., and Imbimbo, M. (2004). "Role of fibre reinforced plastic sheets in shear response of reinforced concrete beams: Experimental and analytical results." Journal of Composites for Construction, 8(5), 415-424.

Iso, M., Matsuzaki, Y., Sonobe, Y., Nakamura, H., and Watanabe, M. (2000). "Experimental study on reinforced concrete columns having wing walls retrofitted with continuous fiber sheets". Proc. Twelfth World Conf. on Earthquake Engineering, (CD-ROM), New Zealand Society for Earthquake Engineering, Silverstream, New Zealand, Paper No. 1865.

Japan Concrete Institute (1998). Technical report on continuous fiber reinforced concrete. Tokyo (Japan).

Karbhari, V. and Seible, F. (1999). "Fribre reinforced polymer composites for civil infrastructure in USA". Structural Engineering International, Journal of IABSE, 9(4), pp. 274-277.

Khalifa, A., Gold, W., Nanni, A., and Abdel Aziz, M. J. (1998). "Contribution of externally bonded FRP to shear capacity of RC flexural members." Journal of Composites for Constructions, 2(4), 195–202.

Khalifa, A., and Nanni, A. (1999). "Improving shear capacity of existing RC T-section beams using CFRP composites." Cement and Concrete Composites, 22(3), 165–174.
Khalifa, A. and Ghobarah, A. (2005). "Behaviour of rehabilitated structural walls." Journal of Earthquake Engineering, 9(3), pp. 371-391.

Kobayashi, K. (2005). "Innovative application of FRPs for seismic strengthening of RC shear wall." Proc., Fiber-Reinforced Polymer (FRP) Reinforcement for Concrete Structures, (CD-ROM), ACI, Farmington Hills, Mi., Paper No. 72.

Langesten, B. (1999). "Byggkonstruktion1. Byggnadsstatik" (In Swedish). Elanders Gummessons, Laköping. ISBN 91-47-00810-5.

Li, Z., J., Balendra, T., Tan, K., H., and Kong K. H. (2005). "Finite element modelling of cyclic behaviour of shear wall structure retrofitted using GFRP." Proc., Fiber-Reinforced Polymer (FRP) Reinforcement for Concrete Structures, (CD-ROM), ACI, Farmington Hills, Mi., Paper No. 74.

Lima, J.L.T., and Barros, J.A.O. (2007)"Design models for shear strengthening of reinforced concrete beams with externally bonded FRP composites: a statistical vs reliability approach", Proceedings FRPRCS-8, Patras, Greece, July 16-18 (CD ROM).

L'Hermite, (1967). "L'application des colles et resins dans la construction", La bateong a coffrage portant, Annales linstitute technique, No. 239.

Lombard, J., Lau, D., T., Humar, J., L., Foo, S., and Cheung, M., S. (2000). "Seismic strengthening and repair of reinforced concrete shear walls" Proc., Twelfth World Conf. on Earthquake Engineering, (CD-ROM), New Zealand Society for Earthquake Engineering, Silverstream, New Zealand, Paper No. 2032.

Loov, R. E. (1998). "Review of A23.3-94 simplified method of shear design and comparison with results using shear friction". Canadian Journal of Civil Engineering, 25, pp. 437-450.

Maeda, T., Asano, Y., Sato, Y., Ueda, T. and Kakuta, Y., (1997). "A study on bond mechanism of carbon fiber sheet", Non metallic (FRP) Reinforcement for Concrete Struct., Proc., 3rd Symp., vol. 1, Japan 279-286,

Malek, A. M., and Saadatmanesh, H. (1998a). "Analytical study of reinforced concrete beams strengthened with web bonded fibre reinforced plastic plates or fabrics." ACI Structural Journal, 95(3), 343-352.

Malek, A. M. and Saadatmanesh, H. (1998b). "Ultimate shear capacity of reinforced concrete beams strengthened with web-bonded fibre reinforced plastic plates." ACI Structural Journal, 95(4), 391-399.

Meier, U. Deuring M., Meier, H., and Scwegler, G. (1992). "Strenghtening of structures with CFRP laminates, research and application in Switzerland". Advance Composites Materials in Bridges and Structures, pp. 243-251.

Miller, B.D. (1999). "Bond between carbon fiber reinforced polymer sheets and concrete." MSc Thesis, Department of Civil Engineering, The University of Missouri, Rolla, MO.

Monti, G., and Liotta, M'A. (2007). "Tests and design equations for FRP-strengthening in shear." Construction and Building Materials, 21, pp. 799-809.

Mörsch, E. (1902). "Concrete-steel constructions", McGraw-Hill Book Company, New York, 1909, pp. 368 (English translation by E.P. Goodrich of 3rd edition of Der Eisenbetonbau, 1st edition, 1902).

Mörsch, E. (1922). "Der Eisenbetonbau (Reinforced concrete construction). Verlag von Konrad Wittwer, Stuttgart, West Germany, pp. 460.

Nagy-György, T., Mosoarca, M., Stoian, V., Gergely, J., and Dan, D. (2005). "Retrofit of reinforced concrete shear walls with CFRP composites". Proc., Keep Concrete Attractive, Hungarian Group of fib, Budapest, Hungary, vol. 2, pp. 897-902.

Nakaba, K., Kanakubo, T., Furuta, T. and Yoshizawa, H. (2001). "Bond behavior between fiber-reinforced polymer laminates and concrete," ACI Struct. J., 98(3), pp. 359-367 .

Nielsen, M., P. (1999). "Limit Analysis and Concrete Plasticity". Second edition. ISBN 0-8493-9126-1.

Oberlender, G.D. (1973). Strength Investigation of ReinforcedConcrete Load Bearing Wall Panels, PhD thesis, University of Texas, Arlington.

PCI Committee Report (1997). State-of-the –art of precast/prestressed sandwich wall panels. PCI Journal, pp. 92-134.

Paterson, J., and Mitchell, D. (2003). "Seismic retrofit of shear walls with headed bars and carbon fiber wrap." J. Struct. Eng., 129(5) pp. 606-614.

Paulay, T., (1969). "Reinforced concrete shear walls." New Zeeland Engineering, October, pp. 315-321.

Pellegrino, C., and Modena, C. (2002). "Fiber reinforced polymer shear strengthening of reinforced concrete beams with transverse steel reinforcement." Journal of Composites for Constructions, 6(2), 104-111.

Pellegrino, C., and Modena, C. (2006). "Fibre-reinforced polymer shear strengthening of reinforced concrete beams: Experimental study and analytical modelling." ACI Structural Journal, 103(5), 720-728.

Popov, E. G. (1998). Engineering mechanics of solids, second edition, Prentice Hall, ISBN 0-13-726159-4.

PSI (2006). "Post tensioning manual – sixth edition." Post-Tensioning Institute, ISBN 0-9778752-0-2.

Ritter, W. (1899). "Die bauweise Hennebique (Construction techniques of Hennebique)". Schweizeriche Bauzeitung, Zurich, Switzerland.

Saheb, S. M. and Desayi, P. (1989). "Ultimate strength of RC wall panels in one-way in plane action", Journal of Structural Engineering", ASCE, 115(10), 2617-2629.

Saheb, S. M. and Desayi, P. (1990a). "Ultimate strength of RC wall panels in two-way in plane action", Journal of Structural Engineering", ASCE, 116(5), 1384-1402.

Saheb, S. M. and Desayi, P. (1990b). "Ultimate strength of RC wall panels with openings", Journal of Structural Engineering", ASCE, 116(6), 1565-1578.

Seddon, A.E. (1956). "Strength of concrete walls under axial and eccentric loads", Symposium on Strength of Concrete Structures, Cement and Concrete Association, May, London, UK.

Sudaglass Fiber Technoglogy (2008), http://www.sudaglass.com/chars.html.

Sugiyama, T., Uemura, M., Fukuyama, H., Nakano, K., and Matsuzaki, Y. (2000). "Experimental study on the performance of the RC frame infilled cast-in-place non-structural RC walls retrofitted by using carbon fiber sheets". Proc. Twelfth World Conf. on Earthquake Engineering, (CD-ROM), New Zealand Society for Earthquake Engineering, Silverstream, New Zealand, Paper No. 2153.

Standard Australia, (2001). "Australian standard 3600, Concrete Structure, Sydney.

Sway , R. N. and Jones R. (1988). "Bridge strengthening by epoxy bonding of steel plates-structural behaviour and design aspect". Proc. Syno. On Strengthening and Repair of Bridges, Leamington Spa., England, pp 22-35.

Taylor, C., P., Cote, P., A., and Wallace, J., W. (1999). "Design of slender reinforced concrete walls with openings." ACI Structural Journal, 95(4) pp. 422-433.

Täljsten, B. (1994). "Plate bonding: Strengthening of existing concrete structures with epoxy bonded plates of steel or fibre reinforced plastics." Doctoral thesis, Luleå University of Technology, Sweden.

Täljsten, B. (1997). "Defining anchor lengths of steel and CFRP plates bonded to concrete", Int. J. Adhesion and Adhesives, 17, No. 4, 319–327.

Täljsten, B. (2003). "Strengthening concrete beams for shear with CFRP sheets." Construction and Building Materials, 17, 15-26.

Täljsten, B. (2006). "FRP strengthening of existing concrete structures." Design guideline fourth edition, ISBN 91-89580-03-6.

Täljsten, B. (1991). "Strenghtening of existing concrete structures with glued steel plates". Analysis of Concrete Structures by Fracture Mechanics, Chapman and Hall, RILEM, ISBN 0 412 36980, pp. 208-219.

Triantafillou, T. C. (1998). "Shear strengthening of reinforced concrete beams using epoxy-bonded FRP composites." ACI Structural Journal, 95(2), 107-115.

Triantafillou, T. C., and Antonopoulos, C. P. (2000). "Design of concrete flexural members strengthened in shear with FRP." Journal of Composites for Constructions, 4(4), 198–205.

Triantafillou, T. C. (2003). "Strengthening of reinforced concrete structures using FRPs." [in Greek],Patras (Greece).

Teng, J. G., Chen, J. F., Smith, S. T., and Lam, L. (2002). "FRP strengthened RC structures.", John Wiley & Sons, LTD, ISBN 0-471-48706-6.

Vecchio, F., and Collins, M. P. (1986). "The modified compressive field theory for reinforced concrete element subjected to shear". ACI Structural journal. 14(2), pp. 219-231.

Volnyy, V., and Pantelides, C., P. (1999). "Bond length of CFRP composites attached to precast concrete walls", J. Compos. for Constr., 3(4), 168-176.

Wagner, H. (1929). "Ebene blecwandträger mit sehr dunnem stegblech (Metal beams with very thin webs)", Zeitschrift fur flugtechnik und motorluftschiffahr. 20(8-12).

Wallace, J. W. and Moehle, J. P. (1992). "Ductility and detailing requirements of bearing wall buildings." Jorunal of Structural Engineering, ASCE, 118(6), 1625-1644.

Wallace, J. W. (1994). "New methodology for seismic design of RC shear walls." Journal of Structural Engineering, ASCE, 120(3).

Wild, S. (2007). "Concrete evidence". New Scientist (2588):21.

Ye, L. P., Lum X. Z., and Chen, J. F. (2005). "Design proposals for debonding strengths of FRP strengthened RC beams in the Chinese Design Code", Proceedings of International Symposium on Bond Behaviour of FRP in Structures , Hong Kong, China.

Zielinski, Z.A., Troitski, M.S. and Christodoulou, H. (1982). "Full-scale bearing strength investigation of thin wall-ribbed reinforced concrete panels", American Concrete Institute Journal, Vol.79,pp. 313–321.

Zielinski, Z.A., Troitski, M.S. and El-Chakieh, E. (1983). "Bearing capacity tests on precast concrete thin-wall ribbed panels",Prestressed Concrete Institute Journal, Chicago, (28,3), 89–103.

Zhang, Z., and Hsu, C-T. T. (2005). "Shear strengthening of reinforced concrete beams using carbon-fibre-reinforced polymer laminates." Journal of Composites for Construction 9(2), 158-169.

Publications

Paper I

"*Are available models reliable for predicting the FRP contribution to the shear resistance of RC beams?*"

By:
G. Sas, B. Täljsten, J. Barros, J. Lima and A. Carolin

Submitted for publication in:
Journal of Composites for Construction

Are available models reliable for predicting the FRP contribution to the shear resistance of RC beams?

Gabriel Sas[1], Björn Täljsten[2], Joaquim Barros[3], João Lima[4], and Anders Carolin[5]

Abstract: In this paper the trustworthiness of the existing theory for predicting the FRP contribution to the shear resistance of reinforced concrete beams is discussed. The most well-known shear models for EBR (External Bonded Reinforcement) are presented, commented on and compared with an extensive experimental database. The database contains the results from more than 200 tests performed in different research institutions across the world. The results of the comparison are not very promising and the use of the additional principle in the actual shear design equations should be questioned. The large scatter between the predicted values of different models and experimental results is of real concern bearing in mind that some of the models are used in present design codes.

Subject headings: Bearing capacity; Concrete beams; Fiber reinforced polymers; Shear strength; State-of-the-art reviews.

Introduction

Shear strengthening of reinforced concrete (RC) beams using fiber reinforced polymers (FRP) has been studied intensively in the last decade, even if shear for simple reinforced concrete beams is not actually fully understood. The design equations for reinforced concrete beams used in the main current design guidelines are based on semi empirical approaches, e.g. ACI 318-05 (2005) and Eurocode 2 (2004). The shear capacity of the beams is computed by adding the contribution of the concrete (V_c) and the steel stirrups (V_s). In most of the cases, using the same procedure, the shear strength of the RC beams strengthened with composite materials is computed by adding the contribution of the FRP (V_{frp}). While the empirical design equations for reinforced concrete beams were validated with extensive experimental results, the equations for predicting the shear resistance of FRP strengthened RC beams are often compared with a small number of experiments, and, in some cases, using test series of questionable rigor. Three main configurations of FRP strengthening may be used for externally bonded reinforcement (EBR): side bonding, U-wrapping and complete wrapping (ACI Committee 440 2002; *fib* Task Group 9.3 2001), see Figure 1. The near surface mounted reinforcement (NSMR) has been also used for shear strengthening (Dias and Barros 2008) but the application is limited to side bonding technique.

The development of theoretical models began using the assumption that FRP materials behave like internal stirrups. Later, studies were focused on developing new theories based on the real strain field distribution. Even if a large effort has been focused on theoretical studies, the shear strength models are almost as many as the research studies performed.

Chaallal et al. (1998) proposed the equation for calculating the shear contribution of FRP based on the assumption that the composite and the stirrups behave similarly.

Malek and Saadatmanesh (1998a, b) introduced in their formulation the anisotropic behavior of the FRP. Studies have revealed that the inclination angle of the critical shear crack is influenced by the plate thickness, FRP percentage and orientation angle, percentage of existing steel hoops, concrete quality and percentage and diameter of the tensile longitudinal steel bars.

A model, obtained by experimental fitting, was derived by Triantafillou (1998), and Triantafillou and Antonopoulos (2000). The contribution of the FRP is limited by the effective strain in the composite. Further on,

[1] Phd Student, Division of Structural Engineering Luleå University of Technology, 971 87 Luleå, Sweden, e-mail: gabriel.sas@ltu.se.

[2] Professor, Division of Structural Engineering, Technical University of Denmark DK-2800 Kgs. Lyngby, Denmark, e-mail: bt@byg.dtu.dk.

[3] Assistant Professor, ISISE, School of Engineering, University of Minho Campus de Azurem, 4800-058 Guimarães, Portugal, e-mail: barros@civil.uminho.pt, joaolima@civil.uminho.pt.

[4] Phd Student, ISISE, School of Engineering, University of Minho Campus de Azurem, 4800-058 Guimarães, Portugal e-mail :joaolima@civil.uminho.pt

[5] Lecturer, Division of Structural Engineering Luleå University of Technology, 971 87 Luleå, Sweden, e-mail: anders.carolin@ltu.se.

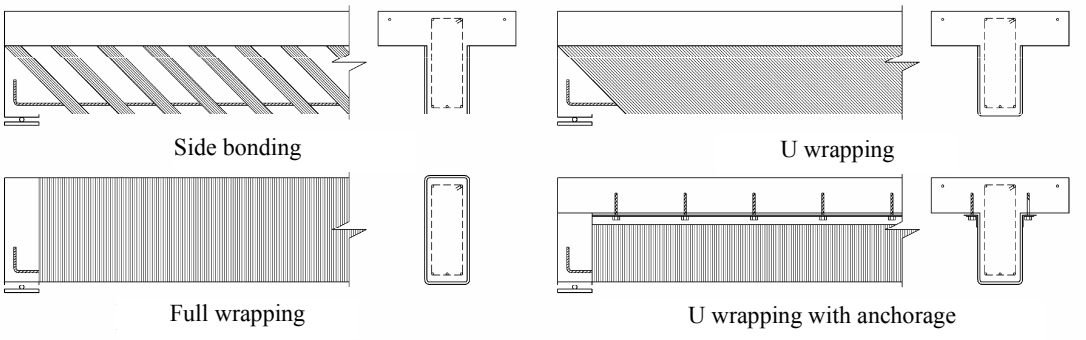

Fig. 1. Strengthening schemes for reinforced concrete beams

Khalifa et al. (1998, 1999) modified Triantafillou's (1998) model introducing strain limitations due to shear crack opening and loss of aggregate interlock. The proposed model was appraised by considering more tests.

By combining the strip mand shear friction approach Deniaud and Cheng (2001, 2003) stated that the FRP strains are uniformly distributed among the fibers crossing the critical shear crack. A design model was developed based on the failure mechanism observed on the tested specimens. The evaluation showed a good agreement between model predictions and test results. A refined model was proposed later by Deniaud and Cheng (2004).

Continuing the Khalifa model, Pellegrino and Modena (2002) suggested a modified reduction factor for the ratio of the effective strain to ultimate strain in FRP. According to the experimental studies performed, the stiffness ratio between transversal shear reinforcement and FRP shear reinforcement has a significant effect on the effectiveness of shear strengthening. Available information is restricted to side-bonded beams strengthening configurations. Aspects regarding lateral concrete peeling failure under shear loading of FRP were studied later by Pelegrino and Modena (2006). The model of these authors follows the truss model approach and describes the concrete, steel and FRP contribution to the shear capacity of RC beams based on the experimental observations.

Carolin (2003) and Carolin and Täljsten (2005) proposed an equation to predict the contribution of EBR composites for the shear strengthening, limiting the tensile failure of the fiber. The non-uniform distribution of the strains in FRP over the cross section was stated. A 55% to 65% of the maximum measured strain value was recommended for engineering design. The equations are used today in the Swedish Design Guideline for FRP strengthening (Täljsten, 2006).

Chen and Teng (2003a, b, 2004) analyzed the shear failure of the reinforced concrete beams strengthened with FRP and concluded that the stress distribution in the FRP along the crack plane is non-uniform. They proposed a model for reinforced concrete beams strengthened with FRP that takes into account the fiber rupture and debonding failure modes. The model also assumes a non-uniform stress distribution in the FRP along the shear crack. Stress limitation is introduced by bond length coefficient and strip width coefficient.

Using an adapted compression field theory, Ianniruberto and Imbimbo (2004) developed a theoretical model to predict the contribution of FRP sheets for the shear capacity of RC beams. Although the authors have made a coherent derivation, the model has some limitations, since it can be used only for wrapping strengthening schemes; hence it is not prepared to predict debonding failure mechanism for side bonding and U configurations. Furthermore, the model does not simulate the strain concentration at the composite-crack intersection, so the potential rupture in the composite at cracking regions cannot be captured. Theoretical predictions were compared with experimental results and, unfortunately found to be incompatible.

Adhikary et al. (2004) proposed two equations to determine the shear strength of CFRP and ARFP strengthened RC beams, calibrating the model proposed by Triantafillou (1998). These authors suggested that the two proposed equations should be checked with other test results available in the literature, since the effective strain in FRP was not yet clearly defined, and depends on many factors.

Introducing some adjustments to the model of Chen and Teng (2003b), Cao et al. (2005) proposed an empirical model to predict the FRP contribution to the shear strengthening of RC beams strengthened with complete wrapping of FRP strips failing by FRP debonding. The strain distribution modification factor gave uncertain results due to the large scatter of the test data. The comparison of the theoretical prediction with the experimental results has shown "a general agreement between the two" with "a significant scatter".
The shear bond model proposed by Zhang and Hsu (2005) followed two approaches: model calibration by curve fitting and bond mechanism. The smallest reduction factor for the effective strain obtained from the two methods was suggested to be used.
The model for the shear debonding strength developed by Ye et al. (2005) has its theoretical starting point in Chen and Teng's model, and it is being used in the Chinese Design Code.
Monti and Liotta (2006) proposed a debonding model for the FRP-based shear strengthening of RC beams. The features of the model are divided in three steps: a) generalized constitutive law of FRP layer bonded to concrete, b) boundary limits – function of the strengthening scheme and shear crack opening provisions, c) stress field in the FRP crossing a shear crack, analytically determined. A generalized failure criterion of FRP strips/sheets is introduced. Two cases are considered: straight strip/sheet and strip/sheet wrapped around a corner. This model is currently used in the Italian design code CRN (2005).

Database description

A full database containing 211 experiments (Table 1), collected by Lima and Barros (2007), was used to compare the theoretical predictions of the FRP contribution to shear. Nevertheless more experiments have been performed in the period covered by this research program, they were not included in this database since critical parameters are missing in their description. The database contains values from experiments performed on 34 beams with T cross sections and 177 beams with rectangular cross sections. The most used strengthening configuration was the U-wrapped with 101 elements, from which 6 include mechanical anchorages. From the remaining 110 beams, 72 were side-bonded without any mechanical anchorages. The other 38 identified beams were fully wrapped. The beams containing different anchorage systems are considered in the present study only for the models that are addressing specifically a theoretical approach for those strengthening system. Most of the available theoretical models do not simulate the effect of the anchorage systems and, consequently, failure predictions are unrealistic. In this case the beams considering anchorage systems are removed from the comparison. The specimens having dimensions smaller than 100×200mm were also removed from the comparison, since due to the scale effect, the obtained results might be not representative of the real behavior of FRP-based shear strengthened beams. The effective anchorage length of the FRP has been determined to be approximately 200-250mm (Täljsten 1994, Brosens and van Gemert, 1997), hence sufficient anchorage length cannot be assured in shallow beams, resulting in an inefficient strengthening. Furthermore, beams with inappropriate material characteristics reported, i.e. of too low strength concrete, were also removed.
After removing the beams from the database that did not correspond to the above criteria, the theoretical predictions of the models will be plotted for each model.

Shear models predictions

Even if the strengthening method has been used for more than a decade, the main part of the theoretical research has been focused on the flexural behavior of strengthened elements. Research on shear behavior has not been studied to the same extent. The shear models presented below are the models most commonly used in practical design. An exception from this rule was made for models introduced in national design guidelines, since they have a greater use in practical design.
For the theoretical predictions the models, in general, assume that shear failure crack has a 45° inclination angle, but experimental works have shown that this inclination can vary between 30 to 60 degrees, depending on the parameters already mentioned (Carolin, 2003).
The researchers define the contribution of the FRP to the shear strength as the product between the effective stress in FRP, the area of the FRP, partial reduction factors that intend to take into account the quality of material

and/or workmanship quality, and a geometrical factor depending on the type of strengthening system used, as well as fiber inclination with respect to the beams longitudinal axis. In general, the scientists are in agreement about the type and relevance that these parameters have in the prediction performance of a model, but the way that these parameters are defined is not the same, and relatively important differences can be found. The main differences appear on the evaluation of the stresses/strains in fibers. Based on the method of analysis, two different types of constitutive models have been proposed: empirical and semi empirical.

In a previous work, Lima and Barros (2007), based on the results of the same database, had already verified that none of the *fib* (2001), ACI (2002), CNR (2005) and CIDAR (2006) analytical formulations predicts with enough accuracy the contribution of the EBR CFRP systems for the shear strengthening of RC beams. In the present work this type of appraisal is extended to a larger set of models, published in reputed journals and conference proceedings

The models presented in this section are used to calculate the contribution of the FRP only for the strengthening configurations for which they were devised. A plot representing the shear contribution of the fibers for rectangular beams and T beams is presented for each model for a better visualization and a realistic evaluation of the results by the reader. For the sake of simplicity all the equations are presented using the same notation. A detailed notation list is appended at the end of the paper.

Chaallal (1998)

The proposed equation for calculating the shear contribution of FRP assumes that composites stirrups have similar functioning principle, Eq. (1). The model assumes that the FRP tensile strength is reached when the composite is intersected by the shear crack, as long as sufficient bond length is guaranteed. At the moment the model was derived the non-uniform distribution of the stresses over the cross section of the beam was not stated by any researcher, making this assumption unrealistic.

$$V_{frp} = 2\left[\tau_{avg}\left(\frac{b_{frp}h_{frp}}{2}\right)\right]\frac{(\sin\beta+\cos\beta)d}{s_{frp}} \tag{1}$$

The debonding problem is treated in a simplified form using the average shear stress (Eq. 2) between the FRP and concrete, even if the authors were aware of the non uniform distribution of the stresses.

$$\tau_{avg} = \frac{1}{2}\tau_{\max}^{debonding} \tag{2}$$

where $\tau_{\max}^{debonding}$ is the maximum shear stress given by:

$$\tau_{\max}^{debonding} = \frac{5.4}{1+k_1\tan 33^\circ} \text{ and } k_1 = t_{frp}\left[\frac{k_n}{4E_{frp}I_{frp}}\right]^{1/4} \text{ with } k_n = E_a b_a/t_a \tag{3}$$

The use of the average shear stress may be interpreted as: if sufficient bond length is assured then the tensile strength of FRP can be fully mobilized. Actually, the stress level will not increase by increasing the bond length if the effective bond length was already provided. The accuracy of this model cannot be checked since the values of the thickness and strength of the adhesive in parameter k_1 are not reported in most of the experimental studies presented in the database (Table 1).

Triantafillou (1998) and Triantafillou and Antonopoulos (2000)

According to Triantafillou (1998), and Triantafillou and Antonopoulos (2000), an accurate estimation of the FRP contribution to the shear capacity is quite difficult to obtain, due to the influence that too many factors has on the failure mode. The formulation is based on the Eqs. (4, 5 and 6):

$$V_{frp} = \frac{0.9}{\gamma_{frp}}\rho_{frp}E_{frp}\varepsilon_{frp,e}b_w d(1+\cot\beta)\sin\beta \tag{4}$$

$$\varepsilon_{frp,e} = 0.0119 - 0.0205\rho_{frp}E_{frp} + 0.0104(\rho_{frp}E_{frp})^2 \qquad 0\le\rho_{frp}E_{frp}\le 1 \tag{5}$$

$$\varepsilon_{frp,e} = -0.00065\rho_{frp}E_{frp} + 0.00245 \qquad \rho_{frp}E_{frp} > 1 \tag{6}$$

The model was derived using the truss analogy based on a semi – quantitative approach. The key parameter of the analytical expression, $\varepsilon_{frp,e}$, was obtained from regression of experimental data of beam tests, which may

suggest a narrow coverage solution for the shear problem. This effective strain has been found dependent both on the axial rigidity of the composite and effective bond length, and is used as the minimum of: maximum strain to control crack opening, strain limiting due to debonding, and strain corresponding to shear failure combined or followed by FRP rupture.
At that moment no clear distinction was made between the different types of strengthening on the application of the formula. The research was then extended, using a larger data base of available test reports (Triantafillou and Antonopoulos 2000). The model evolved still based on the regression analysis, but with a specifically defined effective strain for detailed failure types, different strengthening schemes and materials, Eqs. (7, 8 and 9).

- Wrapped with CFRP

$$\varepsilon_{frp,e} = 0.17\varepsilon_{frp,u}\left(\frac{f_c^{2/3}}{E_{frp}\rho_{frp}}\right)^{0.30} \tag{7}$$

- U – shaped CFRP jackets

$$\varepsilon_{frp,e} = \min\left[0.65\left(\frac{f_c^{2/3}}{E_{frp}\rho_{frp}}\right)^{0.56}\times 10^{-3}; 0.17\varepsilon_{frp,u}\left(\frac{f_c^{2/3}}{E_{frp}\rho_{frp}}\right)^{0.30}\right] \tag{8}$$

- Wrapped with AFRP

$$\varepsilon_{frp,e} = 0.048\varepsilon_{frp,u}\left(\frac{f_c^{2/3}}{E_{frp}\rho_{frp}}\right)^{0.47} \tag{9}$$

However, this model cannot simulate the FRP effective strain of the side bonding shear strengthening configuration, which is a limitation of its use. Due to the limited data available at the moment of the model's derivation, its prediction accuracy is unsatisfactory, but the similar distribution around the bisector can point out regression as being an acceptable method for deriving a viable model (Fig. 2).

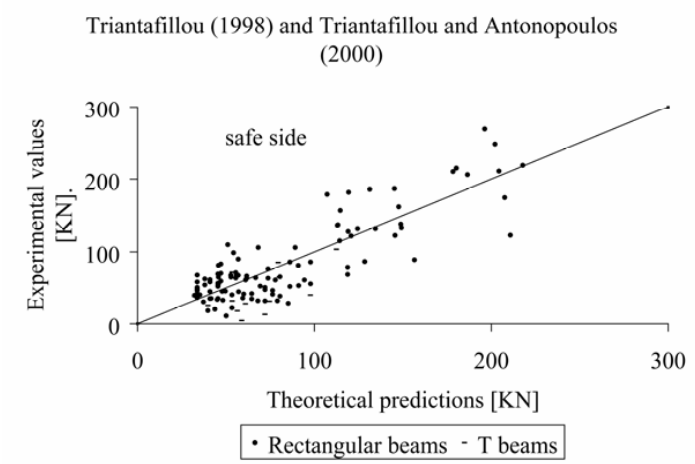

Fig. 2. Triantafillou (1998) and Triantafillou and Antonopoulos (2000) model comparison

Khalifa et al. (1998) and Khalifa and Nanni (2000)

Based on the Triantafillou model (1998), Khalifa *et al.* (1998) recommended a modified effective strain both for fiber rupture and debonding failure. A similar equation of the FRP contribution to the shear strength to the one of Triantafillou (1998) was derived (Eq. 10).

$$V_{frp} = \frac{A_{frp} f_{frp,e} (\sin\beta + \cos\beta) d_{frp}}{s_{frp}} \text{ where } f_{frp,e} = R f_{frp,u} \quad (10)$$

The effective stress in fibers was established as a function of FRP stiffness, and ultimate strain is obtained by regression of experimental data (Eq. 11). The equation is valid only for CFRP continuous sheets or strips and is suitable if the failure mechanism is controlled by FRP sheet rupture. The effective ratio is limited at $R \leq 0.5$.

$$R = 0.5622(\rho_{frp} E_{frp})^2 - 1.2188\rho_{frp} E_{frp} + 0.778 \quad (11)$$

Since Eq. (11) is not valid for debonding mechanism, the effective stress/strain R factor was derived considering a bond mechanism model (Eq. 12).

$$R = \frac{(f_c)^{2/3} w_{frp,e}}{\varepsilon_{frp,u} d_{frp}} \left[738.93 - 4.06(E_{frp} t_{frp}) \right] x10^{-6} \quad (12)$$

The real width of the FRP, w, was replaced by an effective width $w_{frp,e}$ (Eqs. 13 and 14) to account for the several effects, such as: shear crack angle (assumed to be 45°); effective bond and configuration of the strengthening, i.e. wrapped, U-jacketing or side bonded. The effective length proposed by Maeda (1997) was adopted in this case (Eq. 15). Due to its empirical deduction and the lack of test data at that moment, the effective bond length is limited to the value of 75 mm proposed by Miller (1999), and Khalifa and Nanni (2000).

$$w_{frp,e} = d - L_e \text{ for U-jacketing} \quad (13)$$

$$w_{frp,e} = d - 2L_e \text{ for side bonding} \quad (14)$$

$$L_e = e^{6.134 - 0.58\ln(t_{frp} E_{frp})} \quad (15)$$

Finally, a reduction factor of 0.7 for the FRP contribution to the shear capacity is prescribed. This model can be considered as the first complete formulation of the CFRP shear design strengthening, since it considers all three main types of strengthening configurations. Like in Triantafillou (1998), and Triantafillou and Antonopoulos (2000) models, this one presents the same weaknesses due to its empirical nature (Fig. 3).

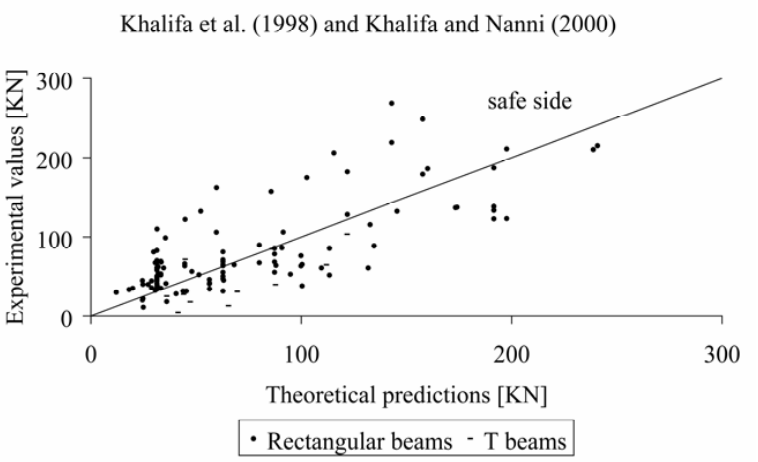

Figure 3. Khalifa et al. (1998) Khalifa and Nanni (2000) model comparison

Chen and Teng model (2001 and 2003a, b)

An extensive work performed by Chen and Teng (2001 and 2003a, b) resulted in one of the most widely-used shear models. The general equation (16) is based on the truss model theory, with the remark that discrete FRP strips were modeled as equivalent continuous FRP sheets/plates and a reduction factor for the stress is used instead of strain, as in the previous models. Since the authors of the model considered continuous sheets as a special case of strips, the equations of Chen and Teng's models are established in terms of strips.

$$V_{frp} = 2 f_{frp,e} t_{frp} w_{frp} \frac{d_{frp}\left(\cot\theta + \cot\beta\right)\sin\beta}{s_{frp}}, \text{ where } f_{frp,e} = D_{frp}\sigma_{frp,\max} \tag{16}$$

The average stress of the FRP intersected by the shear crack, $f_{frp,e}$, is determined based on the assumption that stress distribution in the FRP along the shear crack is not uniform at the ultimate limit state for both rupture and debonding failure modes. The key factors of the model are considered to be the stress distribution factor, D_{frp}, and the maximum stress that can be reached in the FRP intersected by the shear crack, $\sigma_{frp,max}$. The stress distribution factor is determined for both failure modes by integrating the stresses or strains over the cross section (Eq. 17).

$$D_{frp} = \frac{\int_{z_t}^{z_b} \sigma_{frp,z}\, dz}{d_{frp}\sigma_{frp,\max}} \; or = \frac{\int_{z_t}^{z_b} \bar{\varepsilon}_z\, dz}{d_{frp}\bar{\varepsilon}_{\max}} \tag{17}$$

FRP Rupture

Different shapes of non linear distribution of the strains over the crack are considered in the model similar to the approach found in Carolin (2003). For a general strengthening scheme, the stress distribution has been expressed as a dimensionless factor (Eq. 18) depending on geometrical boundary conditions (Eqs. 19 and 20).

$$D_{frp} = \frac{1+\zeta}{2}, \text{ where } \zeta = \frac{z_t}{z_b} \tag{18}$$

$z_t = (0.1d + d_{frp,t}) - 0.1d = d_{frp,t}$ is the coordinate of the top end of the effective FRP (19)

$z_b = \left[d - (h - d_{frp})\right] - 0.1d$ is the coordinate of the bottom end of the effective FRP (20)

When fiber rupture occurs, the maximum stress in the FRP is considered to be the ultimate tensile strength. The Authors advised that, due to the loss of aggregate interlocking, the ultimate tensile failure of the fiber may be reached before the shear failure of the beam has being attained.

FRP Debonding

The debonding model developed by Chen and Teng (2003b) considers "an effective bond length beyond which an extension of the bond length cannot increase the bond strength" of utmost importance. The maximum stress in the FRP at debonding is considered to be:

$$\sigma_{frp,\max} = \min\begin{cases} f_{frp,u} \\ 0.427\beta_w\beta_L\sqrt{\dfrac{E_{frp}\sqrt{f_c}}{t_{frp}}} \end{cases} \tag{21}$$

By analyzing the model one can notice the unit inconsistency of the maximum stress expressed in this mathematical form. The reason might be considered the fracture mechanic approach and regression analysis on the ultimate bond strength and the FRP width ratio (Chen and Teng, 2001). The two coefficients β_L, β_w (Eqs. 22a and 22b) reflect the effective bond length and the effect of FRP to concrete width ratio, respectively,

$$(a)\,\beta_L = \begin{cases} 1 & if\ \lambda \ge 1 \\ \sin\left(\dfrac{\pi\lambda}{2}\right) & if\ \lambda < 1 \end{cases}; \quad (b)\,\beta_w = \sqrt{\frac{2 - w_{frp}/(s_{frp}\sin\beta)}{1 + w_{frp}/(s_{frp}\sin\beta)}} \tag{22a, b}$$

The normalized maximum bond length parameter, λ, the maximum bond length, L_{max}, and the effective bond length, L_e, are given as:

$$\lambda = \frac{L_{\max}}{L_e}; \; L_{\max} = h_{frp,e}/\sin\beta \text{ for U jacketing, } L_{\max} = h_{frp,e}/(2\sin\beta) \text{ for side bonding and } L_e = \sqrt{\frac{E_{frp}t_{frp}}{\sqrt{f_c}}} \tag{23}$$

In this model it was assumed that all the FRP crossing the shear crack can develop full bond strength. Under this assumption, the stress distribution factor for debonding failure was derived (Eq. 24a). It must be noted as

equally important that the bond strength of a strip depends on the distance from the shear crack relative to the ends of the strip. For design purposes a simplified formula was suggested (Eq. 24b) in which 95% characteristic bond strength given by the analytical model is used. The plot of the theoretical predictions versus the experimental values from the database is presented in Fig. 4. The prediction of the FRP shear contribution shows a large scatter, in several cases drastically underestimating or overestimating the capacity for rectangular beams. The T beams show a fairly safe prediction, but a conclusion cannot be drawn due to lack of sufficient experimental data.

$$\text{(a) } D_{frp} = \begin{cases} \dfrac{2}{\pi\lambda}\dfrac{1-\cos\frac{\pi}{2}\lambda}{\sin\frac{\pi}{2}\lambda} & if\ \lambda \le 1 \\ 1-\dfrac{\pi-2}{\pi\lambda} & if\ \lambda > 1 \end{cases}; \text{(b) } \sigma_{frp,\max} = \min\begin{cases} 0.8 f_{frp}/\gamma_{frp} \\ \dfrac{0.3}{\gamma_b}\beta_w\beta_L\sqrt{\dfrac{E_{frp}}{t_{frp}}\sqrt{f_c}} \end{cases} \quad \text{(24a, b)}$$

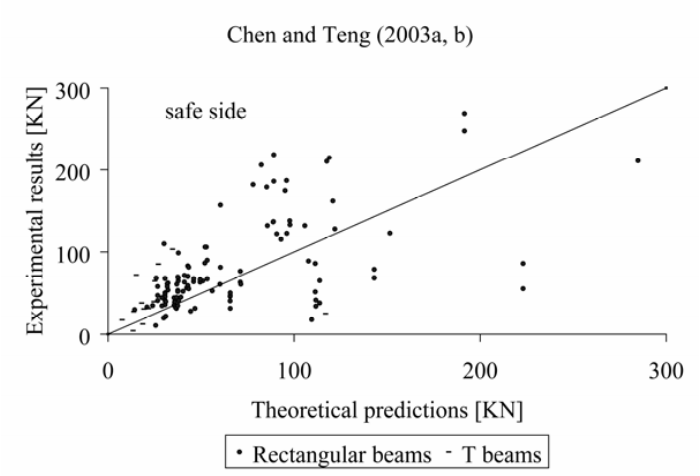

Figure 4. Chen and Teng (2003a, b) model comparison

Deniaud and Cheng model (2001 and 2004)

The model proposed by Deniaud and Cheng (2001, and 2004) has its origins in the modified friction method as a combination of Loov's (1998) shear friction method for RC beams and a strip method for computing the contribution of FRP strips. It must be noted the different approach used for concrete and steel contributions in Eq. (25). A different crack pattern is used for flange and web of the T beam, which might lead to a more accurate prediction of the total shear capacity. The last term of Eq. (25) represents the contribution of FRP sheets in the case of U-jacketing configuration. When discrete strips are used the FRP contribution can be computed from Eq. (26) (Deniaud and Cheng 2001).

$$V_n = 0.25k^2 f_c (A_{cf}\tan\theta_f + A_{cw}\tan\theta_w) + T_v n_s + \frac{d_{frp}t_{frp}E_{frp}\varepsilon_{frp,e}R_L}{\tan\theta_w} \quad (25)$$

$$T_{frp} = d_{frp}t_{frp}E_{frp}\varepsilon_{frp,e}R_L\left(\frac{w_{frp}}{s_{frp}}\right)^2\left(\frac{s}{d_s}\sin\beta+\cos\beta\right)\sin\beta \quad (26)$$

The method consists of an iterative procedure of evaluating the shear capacity of the beam with all potential crack patterns. The continuous debonding of the FRP is tracked until the maximum load is reached. The method is using an experimental curve for the interface shear stress from which the bond strength and the maximum allowable strain was determined. Based on experimental observations, linear and uniform distribution of the load

among the fiber was considered. The effective bond length is calculated according to the Eq. (15), initially proposed by Maeda et al. (1997) (Eq. 15).
Assuming that the ultimate load does not increase after the specified effective length, Deniaud and Cheng (2004) investigated in depth the shear stress field at the interface between concrete and FRP, and proposed a curve to determine the maximum bond strength. The factor accounting for the concrete bond shear resistance, ν=0.23, was obtained by fit regression evaluated at L/Le=1. As a function of the available effective length, the shear stress, τ, can be determined according to Eqs. (27a and 27b).

$$\frac{\tau}{\sqrt{f_c}} = \left(2 - \frac{L}{L_e}\right)\nu \text{ when } L<L_e \text{ and } \frac{\tau}{\sqrt{f_c}} = \frac{L}{L_e}\nu \text{ when } L \geq L_e \quad (27a, b)$$

Large discrepancies and scattering between different interfaces shear strength curves proposed in literature and Deniaud and Cheng's interface shear strength curve were found.
By regression and using the strip method the equation (28) was obtained that can determine the maximum FRP strain for sheets side bonded and beams "wrapped underneath the web".

$$\varepsilon_{\max} = \frac{3\sqrt{f_c}\, d_{frp}^{0.16}}{(t_{frp} E_{frp})^{0.67} (k_a \sin\beta)^{0.1}} (\%) \quad (28)$$

The remaining bonded width over initial width ratio was determined in a similar way as for the maximum strain, i.e. regression (Eq. 29):

$$R_L = 1 - 1.2 \exp\left[-\left(\frac{d_{frp}}{k_e L_{eff} \sin\alpha} \right)^{0.4} \right] \quad (29)$$

For this model, the degree of unsafe predictions is higher than for most of the other models for both T and rectangular beams (Fig. 5). One of the reasons may be the incompatibility of the effective length adopted from Maeda (1997) with the modified friction method.

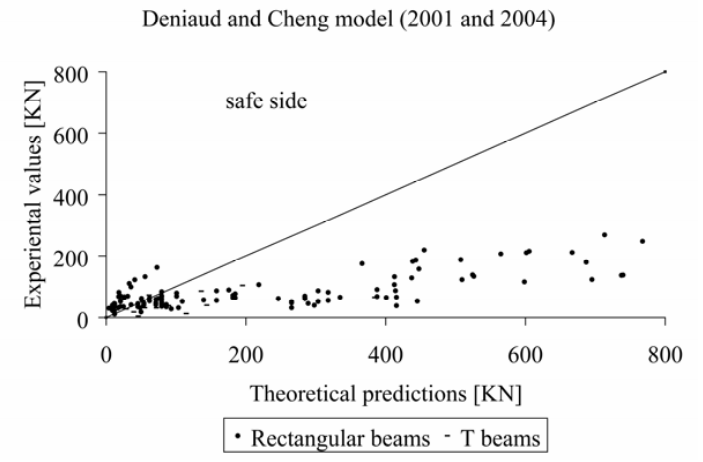

Figure 5. Deniaud and Cheng (2001 and 2004) model

Adhikary et al. model (2004)

After a series of tests with RC beams strengthened with U – wrapped and U – wrapped with different anchorage lengths on top of the beam, Adhikary et al. proposed two equations to predict the contribution of CFRP and AFRP systems for the shear resistance of RC beams. The effective strain when debonding occurs is evaluated by

Eqs. (30a and 30b) that were defined by calibrating Triantafillou and Antonopoulos model (2000) with data available in the literature.

$$\text{(a)}\ \frac{\varepsilon_{frp,e1}}{\varepsilon_{frp,u}} = \frac{0.038 f_c^{\frac{1}{3}}}{\sqrt{\rho_{frp} E_{frp}}}\ \text{for CFRP; (b)}\ \frac{\varepsilon_{frp,e1}}{\varepsilon_{frp,u}} = \frac{0.034 f_c^{\frac{1}{3}}}{\sqrt{\rho_{frp} E_{frp}}}\ \text{for AFRP} \qquad \text{(30a, b)}$$

The second equation of the model takes into account "the bonded anchorage provided to the top of the surface of the beam". It can be assumed that this quote refers to a provided mechanical anchorage, since no other specifications are given in the paper. The effective strain in the FRP is assumed to increase due to this anchorage, so, in this case the effective strain at failure is the sum of the effective strain in the FRP in the debonding mode ε_{fe1} and the increase in effective strain in FRP due to bond anchorage $\varepsilon_{frp,e2}$.

$$\text{(a)}\ \frac{\varepsilon_{frp,e}}{\varepsilon_{frp,u}} = \frac{0.038 f_c^{\frac{1}{3}}}{\sqrt{\rho_{frp} E_{frp}}} + 0.0043 \times f_c^{\frac{2}{3}}\ \text{for CFRP; (b)}\ \frac{\varepsilon_{frp,e}}{\varepsilon_{frp,u}} = \frac{0.034 f_c^{\frac{1}{3}}}{\sqrt{\rho_{frp} E_{frp}}} + 0.0046 \times f_c^{\frac{2}{3}}\ \text{for AFRP} \qquad \text{(31a, b)}$$

Eqs. (31a and 31b) can be interpreted as: the effective strain at debonding when mechanical anchorages are used is the sum of the effective strain at debonding from Eqs. (30a and 30b), and an empirically determined value of the concrete strength.

Adhikary et al. (2004) considered their proposed equations as valid only for the case when the axial rigidity is in the interval $0<\rho_{frp}E_{frp}\leq 1.0$, since for larger values of the axial rigidity the scatter of the collected data used for the calibration gave unsafe predictions.

To compute the shear contribution provided by FRP bonded sheets, Adhikary proposed the Eq. (32).

$$V_{frp} = \rho_{frp} E_{frp} \varepsilon_{frp} d_{frp} b_w (\sin\beta + \cos\beta) \qquad (32)$$

The comparison for the model proposed by Adhikary et al. (2004) led to the highest unsafe predictions, since it has been stated for large axial rigidities. For the sub unitary values of the axial rigidity the values are more realistic but still inadequate for a design model (Fig. 6).

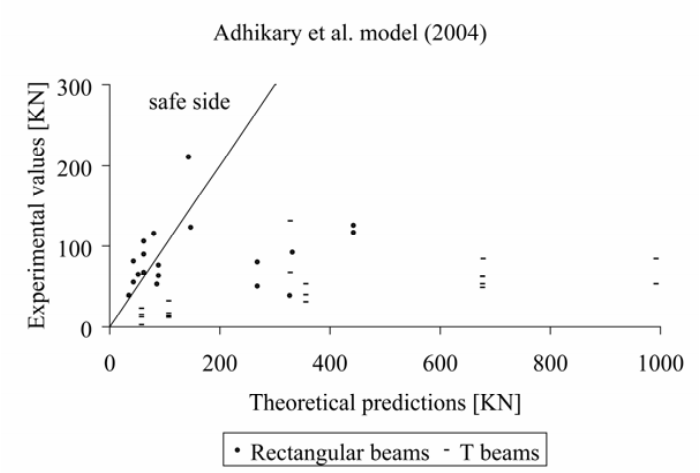

Figure 6. Adhikary et al. (2004) model comparison

Ye et al. model (2005)

The model for the shear debonding strength developed by Ye et al. (2005) has its theoretical starting point in Chen and Teng's model (2003 a, b), and it has been proposed in the Chinese Design Code. The FRP contribution to the shear capacity is obtained from Eq. (16), replacing $f_{frp,e}$ by $\varepsilon_{frp,e}E_f$. Here the simplified proposal of Lu

(2004, by Ye et. al) for the average FRP strain $\varepsilon_{frp,e}$ when debonding is a dominant failure mode (Eq. 33) has been adopted.

$$\varepsilon_{frp,e}=k_v\varepsilon_{frp,inf} \text{ with } K_v=\begin{cases}0.77(1-e^{-\lambda/0.79}) & \text{for side plates}\\ 0.96(1-e^{-\lambda/0.62}) & \text{for U jacketing}\end{cases} \quad (33)$$

A new formulation of the bond length ratio λ (Eq. 34) is expressed in this model, as the ratio of the FRP effective bond height, $h_{frp,e}$, to the FRP effective bond length L_e:

$$\lambda=\frac{h_{frp,e}}{2L_e\sin\beta} \text{ and } L_e=1.33\frac{\sqrt{E_{frp}t_{frp}}}{f_t} \quad (34)$$

A new term is introduce in this model, the FRP strain for an infinite bond length, $\varepsilon_{f,inf}$, which is determined from Eq. (35). Compared to Chen and Teng's equation (Eq. 21) this term does not account for the bond length coefficient, but it is obtained in the same way, by regression analysis.

$$\varepsilon_{f,\inf}=\beta_w\sqrt{\frac{0.616\sqrt{f_t}}{E_{frp}t_{frp}}} \text{ with } \beta_w=\sqrt{\frac{2.25-w_{frp}/s_{frp}}{1.25+w_{frp}/s_{frp}}} \quad (35)$$

In the equation that evaluates the contribution of the FRP for the shear resistance of RC beams (Eq. 36), an inclination angle of 45° was assumed for the critical crack, and the average bond strength between the FRP and concrete is directly taken into account.

$$V_{frp}=\gamma_{frp}K_f\tau w_{frp}\frac{h_{frp,e}^2(\sin\beta+\cos\beta)}{s_{frp}} \text{ where } K_f=\phi_{frp}\frac{\sin\beta\sqrt{E_{frp}t_{frp}}}{\sin\beta\sqrt{E_{frp}t_{frp}}+0.3h_{frp,e}f_t} \text{ and } \tau=1.2\beta_w f_{td} \quad (36)$$

Ye et al. (2005) compared the model with the experimental results. Predictions were considered to be in good agreement with test data and conservative. When compared with a larger database the predictions have a large spreading with a tendency for precarious predictions as a consequence of its empirical deduction (Fig. 7).

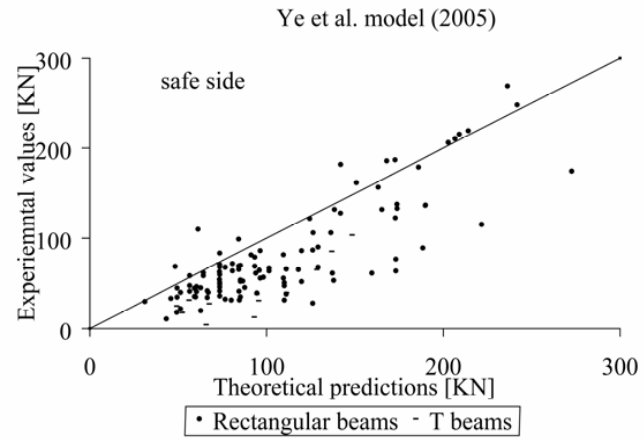

Figure 7. Ye et al. (2005) model comparison

Cao et al. model (2005)

Cao et al. (2005) proposed a simple model to predict the contribution of FRP to the shear capacity of beams where "complete debonding of the critical strips occurs". This model is also based on the previous work performed by Chen and Teng (2003a, b), and is intended to improve the strain distribution factor D_{frp} for discrete

strips. The general definition proposed by Chen and Teng (2003 b) in Eq. (17) was adopted and expressed as the average strain in all FRP strips divided by the maximum strain (Eq. 37).

$$D_{frp} = \frac{\sum_{i=1}^{n} \varepsilon_{frp,i}}{n\varepsilon_{frp,\max}} \approx \frac{\int_{0}^{l} \varepsilon_{frp}(x)\,dx}{l\varepsilon_{frp,\max}} \tag{37}$$

The model requires strain measurements (for the maximum strain and to determine the average strain, "which are mostly dependent on the test errors") in the strips intersected by the shear crack. The average and maximum strains along the critical shear crack were also determined by regression analysis, taking the discrete strain observations.

Eq. (24a), proposed by Chen and Teng (2003b), was refined considering the effect of the shear span-to-effective depth ratio on the strain distribution factor D_{frp},. Cao et al. (2005) admitted that the modified Eq. (38) does not really improve the theoretical predictions compared with the test data.

$$D_{frp} = \left(1 - \frac{\pi - 2}{\pi\lambda_{frp}}\right)(1.2 - 0.1\lambda) \quad \text{for } 1.4<\lambda<3 \tag{38}$$

In order to estimate the contribution of FRP to the shear resistance at debonding, the interaction between the shear span-to-effective depth ratio and the critical shear crack angle was analyzed, resulting in the following equation:

$$D_{f\theta} = \left(1 - \frac{\pi - 2}{\pi\lambda_{frp}}\right) \times \begin{cases} 1 & for\ \lambda \le 1.4 \\ \dfrac{1}{1 - 0.2(\lambda - 1.4)^2} & for\ 1.4 < \lambda < 3 \\ 2.05 & for\ \lambda \ge 3 \end{cases} \tag{39}$$

Furthermore, the maximum strain in the FRP at debonding was analyzed, and an equation similar to the one proposed by Ye et al. (2004) was determined (Eq. 40).

$$\varepsilon_{frp,\max} = 0.427\beta_w \frac{\sqrt{f_c L_e}}{E_{frp} t_{frp}} = 0.427\beta_w \frac{\sqrt[4]{f_c}}{\sqrt{E_{frp} t_{frp}}} \tag{40}$$

From the comparison of the theoretical predictions of the Cao et al. (2005) model with the experimental results of the collected data base, depicted in Fig. 8, a significant scatter and unsafe predictions were obtained.

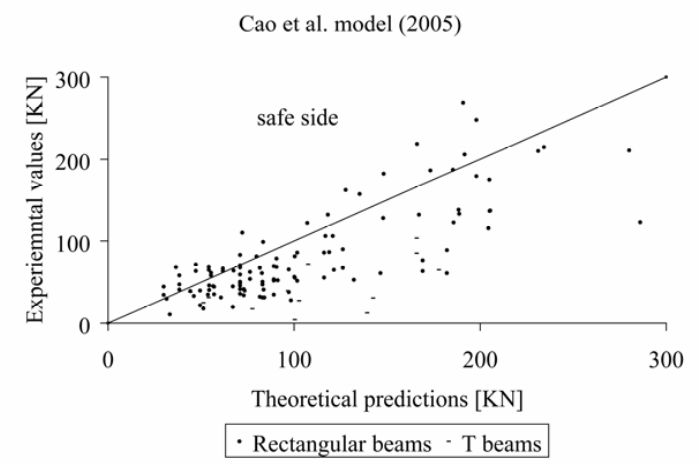

Figure 8. Cao et al. (2005) model comparison

Zhang and Hsu model (2005)

The shear bond model proposed by Zhang and Hsu (2005) was derived in two steps: model calibration by curve fitting and bond mechanism. The smallest reduction factor, obtained using the two methods, was suggested to be used for the evaluation of the effective strain.

Curve fitting model

To determine the reduction factor for the evaluation of the effective strain when debonding failure occurs, the initial model proposed by Khalifa et al. (1998) was used (see Eq. 12).
Having collected more data from test results, the authors used a power regression line to determine the reduction factor, *R*. The power regression gave higher R-square values than the polynomial, which led to the conclusion that the power regression line gives a more realistic prediction of the FRP contribution (Eq. 41a)

$$\text{(a) } R = 0.1466\left(\rho_{frp} E_{frp}\right)^{-0.8193}\text{; (b) } R = 1.8589\left(\rho_{frp} E_{frp} / f_c\right)^{-0.7488} \qquad \text{(41a, b)}$$

Separate analysis was performed for the debonding and fiber rupture failure modes. A large scatter between the two failure modes was observed. Fiber rupture occurred at $0 < \rho_{frp}E_{frp} < 0.55$ GPa, while debonding occurred at $0<\rho_{frp}E_{frp}<1.2$ GPa. Zhang and Hsu (2005) concluded that debonding dominates over the tensile rupture of the CFRP laminates as they become thicker and stiffer, thus the effective strain needs to be consequently reduced. According to Zhang and Hsu (2005) the effective strain in fibers is influenced by the concrete strength, i.e. when concrete strength increases the effective strain increases too. Based on the influence of the concrete strength another model was derived, also adopting a power regression line to evaluate the reduction factor (Eq. 41b). The new reduction factor was obtained by dividing the axial rigidity to the concrete compressive strength. The new model was considered to have better results in terms of R-square, when compared to the results obtained using the other reduction factors.

Bond mechanism model

Proposed for design purposes, the model uses a triangular shape distribution of the shear stresses. Using a simple equilibrium equation for the pure shear stress transfer (not including normal stresses) the total force that can be transferred on two sides is computed according to Eq. (42a). The force when the beam fails in shear failure is given in Eq. (42b). Applying the equilibrium condition for the two equations the strain (stress) reduction factor is determined (Eq. 42c).

$$\text{(a) } T = \frac{1}{2}\cdot\tau_{\max}\cdot L_e\cdot\left(2\cdot w_{frp,e}\right)\text{; (b) } T = 2\cdot t_{frp}\cdot w_{frp,e}\cdot f_{frp,e}\text{; (c) } R = \frac{f_{frp,e}}{f_{frp,u}} = \frac{\tau_{\max}\cdot L_e}{2\cdot t_{frp}\cdot f_{frp,u}} \le 1 \qquad \text{(42a, b, c)}$$

The effective bond length, L_e, of the FRP sheets was proposed to be 75 mm.
The maximum shear stress was computed as a best-fit polynomial function of the concrete compressive strength (Eq. 43).

$$\tau_{\max} = \left(7.64\cdot 10^{-4}\cdot f_c^{\,2}\right) - \left(2.73\cdot 10^{-2}\cdot f_c\right) + 6.38 \qquad (43)$$

Aware of the empirical nature of the model, Zhang and Hsu (2005) suggested adjustments to the model when more experimental data are available. The comparisons plot (Fig. 9) shows a large scatter of the predicted values, but slightly safer then the previous models.

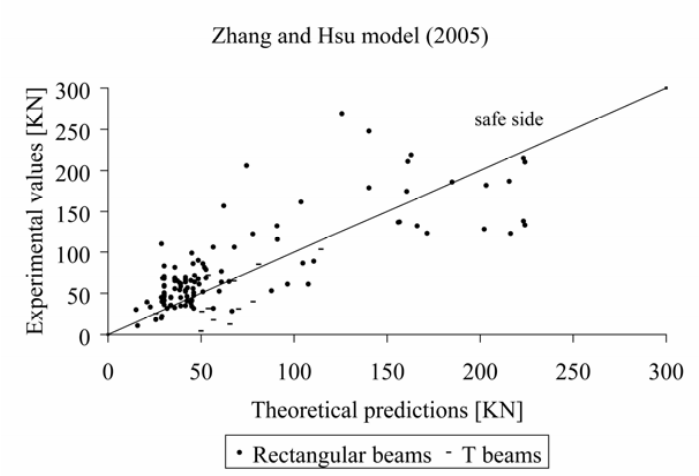

Figure 9. Zhang and Hsu model (2005) model comparison

Carolin (2003) and Carolin and Täljsten (2005)

The design model is based on the superposition principle of the shear contributions of the strengthening and the strut and tie model. A calibration factor to consider the non uniform strain distribution over the cross section, derived by Popov (1998) was proposed. This factor, η, expresses the average strain in the fibers over the height of the beam in relation to the strain in the most stressed fiber (Eq. 44).

$$\eta = \frac{\int_{-h/2}^{h/2} \varepsilon_{frp}(y)\,dy}{\varepsilon_{frp,\max} \cdot h} \tag{44}$$

The factor includes the relative stiffness between concrete in compression, cracked reinforced concrete in tension and lightly reinforced concrete in tension. The proposed design model by Carolin and Täljsten (2005) is given in Eq. (45).

$$V_{FRP} = \eta \cdot \varepsilon_{cr} \cdot E_{frp} \cdot t_{frp} \cdot r_{frp} \cdot z \cdot \frac{\sin(\theta+\beta)}{\sin\theta} \tag{45}$$

The critical strain, ε_{cr}, is limited by a minimum value of the ultimate allowable fiber capacity, $\varepsilon_{frp,ult}$, the maximum allowable strain without achieving anchorage failure ε_{bond} (Eq. 46b), and maximum allowable strain to achieve concrete contribution, $\varepsilon_{c,max}$, e.g. concrete contribution due to aggregate interlocking.

$$\text{(a)}\ \varepsilon_{cr} = \min\begin{Bmatrix} \varepsilon_{frp,u} \\ \varepsilon_{bond} \cdot \sin^2(\theta+\beta) \\ \varepsilon_{c,\max} \cdot \sin^2(\theta+\beta) \end{Bmatrix},\ \text{(b)}\ \varepsilon_{bond} = \frac{1}{E_{frp} t_{frp}} \sqrt{2 E_{frp} t_{frp} G_f} \begin{cases} \sin(\omega L_{cr}) & \text{for } L_{cr} \le \dfrac{\pi}{2\omega} \\ 1 & \text{for } L_{cr} > \dfrac{\pi}{2\omega} \end{cases} \tag{46a, b}$$

In Eq. (46b) G_f is the concrete fracture energy and ω is defined as in Täljsten (1994):

$$\omega = \sqrt{\frac{\tau_{\max}^2}{2 \cdot E_{frp} \cdot t_{frp} \cdot G_f}} \tag{47}$$

The reduction of $\sin^2(\theta+\beta)$ to the anchorage and concrete contribution comes from the anisotropic behavior of the composite. If the concrete contribution is not included in the shear bearing capacity the limiting parameter $\varepsilon_{c,max}$ can be ignored. The critical strain times the reduction factor gives the effective strain, $\varepsilon_{frp,e}$, described

earlier. The r_{frp} factor in Eq. (45) depends on the layout of the strengthening system and is given in Eqs. (48a and 48b):

$$\text{(a) } r_{rfp}=\sin\beta \text{ for continuous wrapping; (b) } r_{frp}=\frac{w_{frp}}{s_{frp}} \text{ for discrete strips} \tag{48}$$

When the theoretical predictions are compared to the experimental results (Fig. 10) a safer estimation of the FRP contribution to shear capacity is found but still with a large scatter. The cause of this might be the definition of fracture energy of concrete, which is still a challenge for the research, since it is not clear which fracture mode is dominant, i.e. fracture mode I, fracture mode II, fracture mode III or a combination of both.

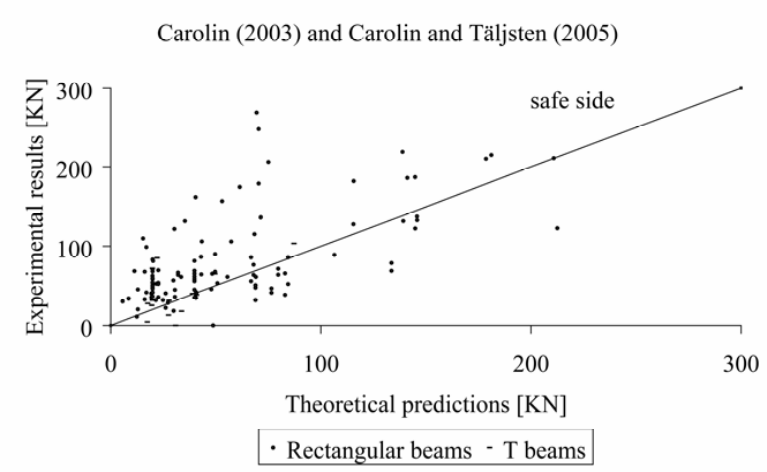

Figure 10. Carolin (2003) and Carolin and Täljsten (2005) model comparison

Monti and Liota (2007)

A complete design method was developed by Monti and Liotta (2008) considering all the strengthening schemes and failure modes known at that time. The model was derived by considering the three following main aspects: a) a generalized FRP-concrete bond constitutive law is defined; b) boundary limitations are considered; and c) the stress field in the FRP crossing a shear crack is analytically determined. Also the following assumptions are considered: the cracks are evenly spaced along the beam axis with an inclination of θ, the crack depth is equal to the internal lever arm $z = 0.9d$ for the ultimate limit state, the resisting shear mechanism is based on the truss analogy for wrapping and U-jacketing. For side bonding, the development of a "crack-bridging" resistance mechanism was considered, due to the missing tensile diagonal tie in the truss analogy. The last two assumptions yield that, for wrapping and U-jacketing the truss resisting mechanism can be activated, while for side bonding the role of the FRP is that of "bridging the crack". The effective bond length (Eq. 51) and the debonding strength are defined for side bonding (Eq. 52).

$$L_e=\sqrt{\frac{E_{frp}t_{frp}}{2f_{ctm}}} \tag{49}$$

$$f_{frp,dd}=\frac{0.80}{\gamma_{frp}}\sqrt{\frac{2E_{frp}\Gamma_{Fk}}{t_{frp}}} \text{ where } \Gamma_{Fk}=0.03k_b\sqrt{f_c f_{ctm}} \text{ and } k_b=\sqrt{\frac{2-w_{frp}/p_{frp}}{1+w_{frp}/400}}\geq 1 \tag{50}$$

When sufficient bond length (l_b) can not be provided due to the strengthening scheme and the apparent shear crack alignment, the bond strength is reduced according to Eq. (53).

$$f_{frp,dd}(l_b) = f_{frp,dd}\frac{l_b}{L_e}\left(2-\frac{l_b}{L_e}\right) \tag{51}$$

According to the authors knowledge, Monti and Liota (2007) were the first researchers to introduce a reduction coefficient considering the radius of the corner of the beam when U-jacketing and wrapping is used (Eq. 54).

$$\phi_R = 0.2 + 1.6\frac{r_c}{b_w} \text{ for } 0 \le \frac{r_c}{b_w} \le 0.5 \tag{52}$$

The ultimate strength of the FRP for all types of strengthening is defined using the following function:

$$f_{frp,ult}(l_b, \delta_e, r_c) = f_{frp,dd}(l_b) + \left\langle \varphi_R \cdot f_{frp,ult} - f_{frp,dd}(l_b) \right\rangle \cdot \delta_e \tag{53}$$

If the term in ‹·› of this function becomes negative it should be considered null. Also, a generalized stress-slip constitutive function, $\sigma_{frp}(u,l_b,\delta_e)$, was proposed. The stress-slip law is denoted as a function of the applied slip, u, at the loaded end of the available bond length, l_b, and the end restraint, δ_e. To define the crack width a coordinate system was proposed with the origin placed at the tip of the shear crack and with the abscissa axis along the shear crack. In this way, the crack width, w, can be considered perpendicular to the crack axis. The crack opening is considered to be governed by a linear relationship depending on the crack opening angle and distance of the strip/sheet to the crack tip:

$$w(x) = \alpha \cdot x \tag{54}$$

Symmetry, with respect to the coordinate system defined above, is considered at both sides of the crack to impose a slip to the FRP. The slip function is given as:

$$u(\alpha, x) = \frac{w(x)}{2}\sin(\theta+\beta) = \frac{1}{2}\alpha x \sin(\theta+\beta) \tag{55}$$

Boundary conditions are imposed as a function of the strengthened scheme adopted, i.e. side bonding, U jacketing or wrapping. With the compatibility (crack width) and boundary conditions, the stress profile in the FRP along the crack $\sigma_{frp,e}(x)$ is determined. In order to determine the FRP contribution to the shear capacity an effective stress along the shear crack length $z/\sin\theta$ is defined by:

$$\sigma_{frp,e}(\alpha) = \frac{1}{z/\sin\theta}\int_0^{z/\sin\theta} \sigma_{frp,cr}\left[u(\alpha,x), l_b(x)\right]dx \tag{56}$$

The effective debonding strength, $f_{frp,ed}$, is given by Eqs. (57a, 57b and 58) for side bonding, for U-jacketing, and for wrapping, respectively.

$$\text{(a) } f_{frp,ed} = f_{frp,dd}\frac{z_{rid,eq}}{\min\{0.9d, h_w\}}\left(1-0.6\sqrt{\frac{l_{eq}}{z_{rid,eq}}}\right)^2 \text{; (b) } f_{frp,ed} = f_{frp,dd}\left(1-\frac{1}{3}\cdot\frac{L_e\sin\beta}{\min\{0.9d, h_w\}}\right) \tag{57a, b}$$

$$f_{frp,ed} = f_{frp,dd}\left(1-\frac{1}{6}\frac{L_e\sin\beta}{\min\{0.9d, h_w\}}\right) + \frac{1}{2}\left(\phi_R f_{frp,u} - f_{frp,dd}\right)\left(1-\frac{L_e\sin\beta}{\min\{0.9d, h_w\}}\right) \tag{58}$$

$$z_{rid,eq} = \min\{0.9d, h_w\} - \left(l_e - \frac{s_f}{f_{frp,dd}/E_{frp}}\right)\sin\beta \tag{59}$$

The FRP contribution to the shear capacity is computed considering two approaches: the Mörsch resisting mechanism for U jacketing and wrapped strengthening schemes computed according to Eq. (60a), while for side bonding, the "bridging" of the shear crack principle is used (Eq. 60b).

$$\text{(a) } V_{frp} = \frac{1}{\gamma_{frp}}0.9d \cdot f_{frp,ed}\, 2t_{frp}\left(\cot\theta+\cot\beta\right)\frac{w}{p_{frp}} \text{; (b) } V_{frp} = \frac{1}{\gamma_{frp}}\min\{0.9d, h_w\} f_{frp,ed}\, 2t_{frp}\frac{\sin\beta}{\sin\theta}\frac{w}{p_{frp}} \tag{60a, b}$$

The predictive performance of the model was originally appraised using results from an experimental program composed of beams manufactured with a concrete of too low compressive strength. When applied to the collected data base, Fig. 11 shows that the model generally allows safety estimations, but the safety factor is too high and it seems to increase with the increase of the contribution of the FRP shear strengthening configurations.

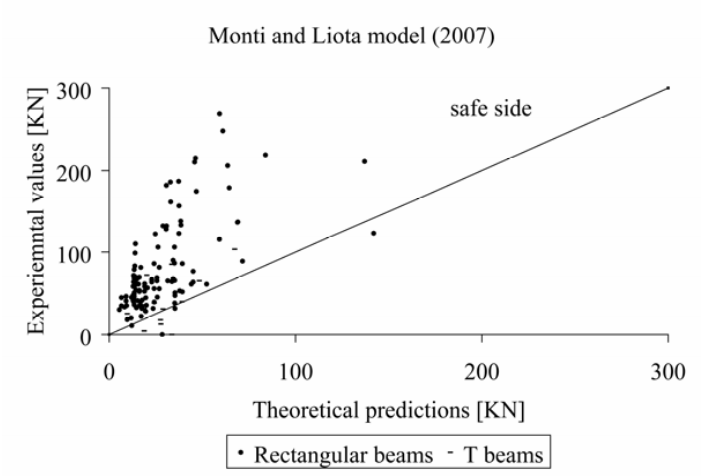

Figure 11. Monti and Liota (2007) model comparison

Conclusions

The prediction of the shear resistance of RC beams is still a big challenge in structural engineering domain. This complexity is even augmented when FRP materials are used to increase the shear capacity of RC beams. Therefore, it is not strange that differences are observed between the available models for the prediction of the FRP contribution to the shear resistance of RC beams, as well as the use of several and distinct parameters, which, in general, were calibrated from a reduced amount of experimental results. This can partially justify the distinct predictive performance of these models, as well as the large dispersion observed when the analytical results determined from these models were compared to results of the biggest data base collected up to the moment in this topic.

Scientists focused their attention on the properties of the composites when deriving the equations, but it is quite clear that existing shear models for FRP strengthening, at least in their present form, do not predict the shear failure very well. From the literature it can also be found that many researchers have calibrated their models from unrealistic geometric conditions on their laboratory specimens. If calibration of experimental results should be done, it is suggested that a Round Robin test procedure should be followed.

Another important concern is the fact that a major part of the experimental programs is composed of rectangular cross section beams, in spite of the fact that T cross section beams represent the real situation.

The theoretical approach for the T beams is treated as a special case of the rectangular beams with bonded fibers over a fraction of the cross section. It is also of concern that in some cases theoretical work on T beams has been validated with experimental data obtained from rectangular cross sections. This direction can be misleading since the two types of cross section have different behavior. One model, as the authors are aware of, considers the interaction between the existing steel stirrups and the FRP wrap (Pellegrino and Modena, 2006), however, since critical parameters to determine the shear contribution of the FRP are missing it was not included in the comparison.

Consequently, before a more thorough understanding of FRP shear strengthened beams has been obtained, a conservative approach is suggested. The question is now how to proceed from here. A well planned International Round Robin test with T cross section beams, where the main factors that influence this structural problem are carefully considered, seems to be the right path to define a well accepted formulation to predict the contribution of FRP configurations for the shear resistance of RC beams. The quality of monitoring systems (in particular, the ones for measuring the strains in the FRP) and correct evaluation of the properties of the intervening materials need to have a strict control.

Acknowledgments

The first, the second and the fifth authors wishes to acknowledge the financial assistance of the European Union for the Marie Curie Research Training Network En-Core.

The third and fourth authors wish to acknowledge the support provided by the research program "SmartReinforcement - Carbon fibre laminates for the strengthening and monitoring of reinforced concrete structures" supported by ADI-IDEIA, Project nº 13-05-04-FDR-00031.

Notation List

A_{cf} = effective flange concrete area
$A_{c,p}$ = area of peeled concrete
A_{cw} = concrete web area
A_{frp} = area of FRP shear reinforcement
D_{frp} = the stress distribution factor in FRP
$D_{frp,\theta}$ = modified distribution factor in FRP accounting the shear crack angle □
E_a = Young's modulus of the adhesive
E_{frp} = Young's modulus of the FRP
I_{frp} = moment of inertia of the FRP plate
L_{cr} = critical bond length
L_e = effective bond length
L_f = active length of FRP
G_f = fracture energy of concrete
R = ratio of effective stress or strain in FRP to its ultimate strength or elongation
R_{ck} = concrete characteristic cube strength
R_L = remaining bonded length over initial length ratio
T = force transferred by FRP
T_v = tension force in the stirrups
W_{frp} = width of FRP
$W_{frp,e}$ = effective width of FRP
b_a = the width of the adhesive
$b_{c,v}$ = vertical arm measured from center of peeled area
b_f = is the sum of concrete cover and half stirrup
b_w = minimum width of CS over the effective depth
d = effective depth of the cross section
d_{frp} = effective depth of the FRP shear reinforcement (usually equal to d for rectangular sections and d-thickness of the slab for T sections
$d_{frp,t}$ = distance from the compression face to the top edge of the FRP
d_s = height of the stirrups
f_c = compressive strength of concrete
f_{ctm} = mean tensile strength of concrete $0.27R_{ck}^{2/3}$
f_{frp} = tensile strength of FRP
$f_{frp,dd}$ = bond strength of FRP
$f_{frp,u}$ = ultimate strength of FRP
$f_{frp,ed}$ = effective debonding strength of FRP
$f_{frp,d}$ = design ultimate strength of FRP
$f_{frp,e}$ = effective tensile stress in FRP
$f_{frp,u}$ = ultimate tensile strength of FRP in direction of principle stresses
f_t = average tensile strength of concrete
f_{td} = design tensile strength of concrete
h = height of the beam
$h_{frp,e}$ = effective height of FRP

h_w = height of the web
k = experimentally determined factor equal to 0.5 for normal concrete strength
$k_a = k_e$ = coefficient for anchorage end condition equals 2, 1, 0.79 for Side bonded, U shape bonded and fully wrapped
k_b = covering/scale coefficient
k_n = normal stiffness of the adhesive
k_v = the FRP bond length effect factor
l_a = anchorage length provided on the top of the beam
l_b = sufficient bond length
l_{eq} = equivalent length
n_f = number of fully contributing stirrups
n_s = total number of stirrups crossing concrete shear crack
p_{frp} = FRP spacing measured orthogonally to □
r_c = corner radius
s = stirrups spacing
s_{frp} = spacing of FRP strips measured along longitudinal axis
t_a = the thickness of the adhesive
t_{frp} = thickness of FRP shear reinforcement
z = length of the vertical tension tie in the truss, normally expressed as $0.9d$. When composites are bonded over the entire height, can be equated to the beam height, h.
Γ_{Fk} = specific fracture energy of the FRP to concrete bond interface
ϕ_{frp} = FRP material reduction factor
α = crack opening angle
β = fiber angle direction with respect to the longitudinal axis of the beam
β_L =bond length coefficient
β_w = strip width coefficient
γ_{frp} = partial safety factor for FRP
γ_b = partial safety factor for bond strength, equals 1.25
ρ_{frp} = FRP shear reinforcement ratio
$\varepsilon_{frp,e}$ = effective FRP strain in principal fiber direction
$\varepsilon_{frp,u}$ = ultimate tensile strain in FRP
$\varepsilon_{frp,e1}$ = effective strain in FRP at debonding
$\varepsilon_{frp,e2}$ = effective strain in FRP with bonded anchorage
$\varepsilon_{frp,inf}$ = the FRP strain when the bond length is infinite
$\varepsilon_{frp,max}$ = maximum strain in FRP at debonding
ε_{cr} = critical strain in FRP
ε_{bond} = maximum allowable strain without achieving anchorage failure
$\varepsilon_{c,max}$ = maximum allowable strain to achieve concrete contribution
λ = normalized maximum bond length
θ = crack angle direction with respect to the longitudinal axis of the beam
θ_f = shear plane angle in flange
θ_w = shear plane angle in web
$\sigma_{frp,max}$ = maximum stress in FRP
τ = average concrete bond strength
τ_{max} = maximum shear stress in concrete
ν = concrete bond shear resistance factor
η = average strain in fibers, the value varies between 0.6 and 0.7
ϑ = angle of conventional roughness of interface

References

ACI Committee 318 (2005). “Building code requirements for structural concrete (ACI 318-05) and commentary (318R-05).” *American Concrete Institute*, Farmington Hills, Mich., pp 430.
ACI Committee 440 (2002). “Guide for the design and construction of externally bonded FRP systems for strengthening concrete structures (ACI 440.2R-02).” *American Concrete Institute*, Farmington Hills, Mich., pp 45.
Adhikary, B. B., Mutsuyoshi, H., and Ashraf, M. (2004). “Shear strengthening of reinforced concrete beams using fiber-reinforced polymer sheets with bonded anchorage.” *ACI Struct. J.*, 101(5), 660-668.
Brosens, K., and van Gemert, D. (1997). ‘‘Anchoring stresses between concrete and carbon fibre reinforced laminates.’’ *Non-Metallic (FRP) Reinforcement for Concrete Struct., Proc., 3rd Int. Symp., Japan Concrete Institute*, Sapporo, 1, 271–278.
Cao, S. Y., Chen, J. F., Teng, J. G., Hao, Z., and Chen, J. (2005). “Debonding in RC beams shear strengthened with complete FRP wraps.” *J. Compos. Constr.*, 9(5), 417-428.
Carolin, A. (2003) “Carbon fiber reinforced polymers for strengthening of structural elements”, Doctoral thesis 2003:18, Luleå University of Technology.
Carolin, A., and Täljsten, B. (2005). “Theoretical study of strengthening for increased shear bearing capacity." *J. Compos. Constr.*, 9(6), 497-506.
Chaalla,l O., Nollet, M-J., and Perraton, D. (1998). “Strengthening of reinforced concrete beams with externally bonded fibre-reinforced-plastic plates: design guidelines for shear and flexure.” *Can. J. Civ. Eng.*, 25, 692-708.
Chen, J. F., and Teng, J. G. (2001). “Anchorage strength models for FRP and steel plates bonded to concrete.” *J. Struct. Engrg.*, 127(7),784-791.
Chen, J. F. and Teng, J. G. (2003a). “Shear capacity of fibre-reinforced polymer-strengthened reinforced concrete beams: fibre reinforced polymer rupture.” *J. Struct. Engrg.*, 129(5), 615-625.
Chen, J. F., and Teng, J. G. (2003b) “Shear capacity of FRP-strengthened RC beams: FRP debonding.” *Constr. Build. Mater.*, 17, 27-41.
CIDAR (2006). “Design guideline for RC structures retrofitted with FRP and metal plates: beams and slabs” Draft 3 - *submitted to Standards Australia*, The University of Adelaide.
CNR (2005). “Instructions for design, execution and control of strengthening interventions through fiber-reinforced composites.” CNR-DT 200/04, *Consiglio Nazionale delle Ricerche*, Rome, Italy (English version).
Deniaud, C., and Roger Cheng, J. J. “(2001). “Shear behaviour of reinforced concrete T-beams with externally bonded fibre-reinforced polymer sheets.” *ACI Struct. J.*, 98(3), 396-394.
Deniaud, C., and Roger Cheng, J. J. (2004). “Simplified shear design method for concrete beams strengthened with fibre reinforced polymer sheets.” *J. Compos. Constr.*, 8(5), 425-433.
Dias, S.J.E.; Barros, J.A.O., “Shear strengthening of T cross section reinforced concrete beams by near surface mounted technique”, Journal Composites for Construction, 12(3), 300-311, Maio/Junho, 2008.
European Standard EN 1992 (2004), “Eurocode 2: Design of concrete structures”, European Committee for Standardization, B-1050 Brussels.
fib Task Group 9.3, 2001, “Externally bonded FRP reinforcement for RC Structures.” fib Bulletin 14, Lausanne, Switzerland.
Ianniruberto, U., and Imbimbo, M. (2004). “Role of fibre reinforced plastic sheets in shear response of reinforced concrete beams: Experimental and analytical results.” *J. Compos. Constr.*, 8(5), 415-424.
Khalifa, A., Gold, W., Nanni, A., and Abdel Aziz, M. J. (1998). “Contribution of externally bonded FRP to shear capacity of RC flexural members.” *J. Compos. Constr.*, 2(4), 195–202.
Khalifa, A., and Nanni, A. (1999). “Improving shear capacity of existing RC T-section beams using CFRP composites.” *Cement and Concrete Composites*, 22(3), 165–174.
Lima, J. L. T., and Barros, J. A. O. (2007)”Design models for shear strengthening of reinforced concrete beams with externally bonded FRP composites: a statistical vs reliability approach”, *Proceedings FRPRCS-8*, Patras, Greece, July 16-18 (CD ROM).
Loov, R. E. (1998). “Review of A23.3-94 simplified method of shear design and comparison with results using shear friction”. *Canadian Journal of Civil Engineering*, 25, pp. 437-450.
Malek, A. M., and Saadatmanesh, H. (1998a). “Analytical study of reinforced concrete beams strengthened with web bonded fibre reinforced plastic plates or fabrics.” *ACI Struct. J.*, 95(3), 343-352.

Malek, A. M. and Saadatmanesh, H. (1998b). “Ultimate shear capacity of reinforced concrete beams strengthened with web-bonded fibre reinforced plastic plates.” *ACI Struct. J.*, 95(4), 391-399.
Miller, B.D. (1999). “Bond between carbon fiber reinforced polymer sheets and concrete.” MSc Thesis, Department of Civil Engineering, The University of Missouri, Rolla, MO.
Monti, G., and Liotta, M’A. (2007). “Tests and design equations for FRP-strengthening in shear.” *Constr. Build. Mater.*, 21, 799-809.
Pellegrino, C., and Modena, C. (2002). “Fiber reinforced polymer shear strengthening of reinforced concrete beams with transverse steel reinforcement.” *J. Compos. Constr.*, 6(2), 104-111.
Pellegrino, C., and Modena, C. (2006). “Fibre-reinforced polymer shear strengthening of reinforced concrete beams: Experimental study and analytical modeling.” *ACI Struct. J.*, 103(5), 720-728.
Popov, E. G. (1998). *Engineering mechanics of solids, second edition*, Prentice Hall, ISBN 0-13-726159-4.
Täljsten, B. (1994). “Plate bonding: Strengthening of existing concrete structures with epoxy bonded plates of steel or fibre reinforced plastics.” Doctoral thesis, Luleå University of Technology, Sweden.
Täljsten, B. (1997). “Defining anchor lengths of steel and CFRP plates bonded to concrete”, *Int. J. Adhes. Adhes.*, 17, No. 4, 319–327.
Täljsten, B. (2006) “FRP strengthening of existing concrete structures.” Design guideline fourth edition, ISBN 91-89580-03-6.
Täljsten, B. (2003). “Strengthening concrete beams for shear with CFRP sheets.” *Constr. Build. Mater.*, 17, 15-26.
Triantafillou, T. C. (1998). “Shear strengthening of reinforced concrete beams using epoxy-bonded FRP composites.” *ACI Struct. J.*, 95(2), 107-115.
Triantafillou, T. C., and Antonopoulos, C. P. (2000). “Design of concrete flexural members strengthened in shear with FRP.” *J. Compos. Constr.*, 4(4), 198–205.
Teng, J. G., Chen, J. F., Smith, S. T., and Lam, L. (2002). “FRP strengthened RC structures.”, John Wiley & Sons, LTD, ISBN 0-471-48706-6.
Ye, L. P., Lum X. Z., and Chen, J. F. (2005). “Design proposals for debonding strengths of FRP strengthened RC beams in the Chinese Design Code”, *Proceedings of International Symposium on Bond Behaviour of FRP in Structures* , Hong Kong, China.
Zhang, Z., and Hsu, C-T. T. (2005). “Shear strengthening of reinforced concrete beams using carbon-fibre-reinforced polymer laminates.” *J. Compos. Constr.* 9(2), 158-169.

Tabel 1. Experimental database

Citation Reference	Original numbering	Beam Cross Section				Concrete properties				FRP properties									
		Type	$B_{slab\ T}$	b_{web}	h	$h_{slab\ T}$	f_{cm}	f_{ck}	f_{ctm}	E_c	E_{frp}	$\varepsilon_{frp,u}$	$f_{frp,u}$	Config.	Disc vs Cont	t_{frp}	w_{frp}	s_{frp}	β	V_{frp}
	-	R-T	(mm)	(mm)	(mm)	(mm)	(MPa)	(MPa)	(MPa)	(MPa)	(MPa)	%	(Mpa)	S-U-W	D-C	(mm)	(mm)	(mm)	°	(KN)
Uji (1992)	3	R	0	100	200	0	32,60	24,60	2,54	3,136E+04	230000	0,0115	2645	W	C	0,097	1	1	90	34,5
	5	R	0	100	200	0	32,60	24,60	2,54	3,136E+04	230000	0,0115	2645	S	C	0,097	1	1	90	20,5
	6	R	0	100	200	0	35,40	27,40	2,73	3,215E+04	230000	0,0115	2645	S	C	0,137	1	1,41	45	33
	7	R	0	100	200	0	35,40	27,40	2,73	3,215E+04	230000	0,0115	2645	S	C	0,195	1	1	90	20,5
Satto et al. (1996)	S2	R	0	200	300	0	53,20	45,20	3,81	3,632E+04	230000	0,0151	3473	S	D	0,24	20	80	90	68,4
	S3	R	0	200	300	0	49,30	41,30	3,58	3,550E+04	230000	0,0151	3473	U	D	0,24	20	80	90	110
	S4	R	0	200	300	0	45,50	37,50	3,36	3,466E+04	230000	0,0151	3473	S	C	0,12	1	1	90	64,2
	S5	R	0	200	300	0	47,70	39,70	3,49	3,515E+04	230000	0,0151	3473	U	C	0,12	1	1	90	106,1
Araki et al. (1997)	CF045	R	0	200	400	0	32,80	24,80	2,55	3,142E+04	230000	0,0151	3473	W	D	0,11	20	84,62	90	35
	CF064	R	0	200	400	0	32,90	24,90	2,56	3,145E+04	230000	0,0151	3473	W	D	0,11	20	48,89	90	61
	CF097	R	0	200	400	0	33,20	25,20	2,58	3,153E+04	230000	0,0151	3473	W	D	0,11	20	28,57	90	106
	CF131	R	0	200	400	0	33,40	25,40	2,59	3,159E+04	230000	0,0151	3473	W	C	0,11	1	1	90	157
	CF243	R	0	200	400	0	33,60	25,60	2,61	3,165E+04	230000	0,0151	3473	W	C	0,22	1	1	90	206
Funakawa et al. (1997)	S2	R	0	600	600	0	38,00	30,00	2,90	3,284E+04	240000	0,015833	3800	W	C	0,167	1	1	90	242
	S3	R	0	600	600	0	38,00	30,00	2,90	3,284E+04	240000	0,015833	3800	W	C	0,334	1	1	90	346
	S4	R	0	600	600	0	38,00	30,00	2,90	3,284E+04	240000	0,015833	3800	W	C	0,501	1	1	90	493
Miyauchi et al. (1997)	1/5 Z-3	R	0	125	200	0	43,10	35,10	3,22	3,410E+04	230000	0,0151	3473	W	D	0,111	50	250	90	18,75
	1/2 Z-3	R	0	125	200	0	40,40	32,40	3,05	3,345E+04	230000	0,0151	3473	W	D	0,111	50	100	90	29,5
	1/L Z-2	R	0	125	200	0	47,10	39,10	3,46	3,502E+04	230000	0,0151	3473	W	D	0,111	50	100	90	34,55
Kamiharako et al. (1997)	2	R	0	250	500	0	32,60	24,60	2,54	3,136E+04	244000	0,016352	3990	W	D	0,11	40	100	90	28,1
	7	R	0	400	700	0	34,60	26,60	2,67	3,193E+04	244000	0,016352	3990	W	D	0,11	64	100	90	174,7
Taerwe et al. (1997)	BS2	R	0	200	450	0	43,10	35,10	3,22	3,410E+04	280000	0,0125	3500	U	D	0,11	100	400	90	41,2
	BS4	R	0	200	450	0	46,40	38,40	3,41	3,486E+04	280000	0,0125	3500	U	C	0,11	1	1	90	115,4
	BS5	R	0	200	450	0	44,80	36,80	3,32	3,450E+04	280000	0,0125	3500	U	D	0,11	50	400	90	33,4
	BS6	R	0	200	450	0	43,80	35,80	3,26	3,427E+04	280000	0,0125	3500	U	D	0,11	50	600	90	30
	BS7	R	0	200	450	0	42,70	34,70	3,19	3,401E+04	280000	0,0125	3500	W	D	0,11	50	200	90	98,9
Umezu et al. (1997)	CS1	R	0	300	300	0	48,50	40,50	3,54	3,533E+04	244000	0,017213	4200	W	C	0,111	1	1	90	86,6
	CS2	R	0	300	300	0	48,50	40,50	3,54	3,533E+04	244000	0,017213	4200	W	D	0,111	100	200	90	31,6
	CS3	R	0	150	300	0	52,80	44,80	3,78	3,624E+04	244000	0,017213	4200	W	D	0,111	100	200	90	52,3

Chaallal et al. (1998)	RS90a	R	0	150	250	0	35,00	27,00	2,70	3,204E+04	150000	0,016	2400	S	D	1	50	100	90	34,25
	RS90b	R	0	150	250	0	35,00	27,00	2,70	3,204E+04	150000	0,016	2400	S	D	1	50	100	90	41,75
	RS135a	R	0	150	250	0	35,00	27,00	2,70	3,204E+04	150000	0,016	2400	S	D	1	50	150	45	40,75
	RS135b	R	0	150	250	0	35,00	27,00	2,70	3,204E+04	150000	0,016	2400	S	D	1	50	150	45	46,25
Mitsui et al. (1998)	A	R	0	150	250	0	36,50	28,50	2,80	3,244E+04	230000	0,015	3450	W+	C	0,2775	1	1	90	40,2
	B	R	0	150	250	0	36,50	28,50	2,80	3,244E+04	230000	0,015	3450	W+	C	0,2775	1	1	90	43,2
	C	R	0	150	250	0	36,50	28,50	2,80	3,244E+04	230000	0,015	3450	W+	C	0,2775	1	1	90	34,5
	D	R	0	150	250	0	36,50	28,50	2,80	3,244E+04	230000	0,015	3450	W+	C	0,2775	1	1	90	55,4
	E	R	0	150	250	0	36,50	28,50	2,80	3,244E+04	230000	0,015	3450	W+	C	0,2775	1	1	90	38
	F	R	0	150	250	0	36,50	28,50	2,80	3,244E+04	230000	0,015	3450	W+	C	0,2775	1	1	90	18
Triantafillou (1998)	S1A	R	0	70	110	0	30,00	22,00	2,36	3,059E+04	235000	0,014043	3300	S	D	0,155	30	60	90	13,55
	S1B	R	0	70	110	0	30,00	22,00	2,36	3,059E+04	235000	0,014043	3300	S	D	0,155	30	60	90	11,25
	S145	R	0	70	110	0	30,00	22,00	2,36	3,059E+04	235000	0,014043	3300	S	D	0,155	30	60	45	14,05
	S2A	R	0	70	110	0	30,00	22,00	2,36	3,059E+04	235000	0,014043	3300	S	D	0,155	45	60	90	15,85
	S2B	R	0	70	110	0	30,00	22,00	2,36	3,059E+04	235000	0,014043	3300	S	D	0,155	45	60	90	12,9
	S245	R	0	70	110	0	30,00	22,00	2,36	3,059E+04	235000	0,014043	3300	S	D	0,155	30	60	45	15,45
	S3A	R	0	70	110	0	30,00	22,00	2,36	3,059E+04	235000	0,014043	3300	S	C	0,155	1	1	90	13,2
	S3B	R	0	70	110	0	30,00	22,00	2,36	3,059E+04	235000	0,014043	3300	S	C	0,155	1	1	90	10,55
	S345	R	0	70	110	0	30,00	22,00	2,36	3,059E+04	235000	0,014043	3300	S	C	0,155	1	1,4	45	12,15
Khalifa et al. (1999)	CW2	R	0	150	305	0	35,50	27,50	2,73	3,217E+04	228000	0,015351	3500	U+	C	0,165	1	1	90	39
	CO2	R	0	150	305	0	28,50	20,50	2,25	3,012E+04	228000	0,015351	3500	U	D	0,165	50	125	90	40
	CO3	R	0	150	305	0	28,50	20,50	2,25	3,012E+04	228000	0,015351	3500	U	C	0,165	1	1	90	65
Khalifa and Nanni (2000)	BT2	T	380	150	405	100	35,00	27,00	2,70	3,204E+04	228000	0,016623	3790	U	C	0,165	1	1	90	65,0
	BT3	T	380	150	405	100	35,00	27,00	2,70	3,204E+04	228000	0,016623	3790	U+	C	0,165	1	1	90	67,5
	BT4	T	380	150	405	100	35,00	27,00	2,70	3,204E+04	228000	0,016623	3790	U	D	0,165	50	125	90	72,0
	BT5	T	380	150	405	100	35,00	27,00	2,70	3,204E+04	228000	0,016623	3790	S	D	0,165	50	125	90	31,5
	BT6	T	380	150	405	100	35,00	27,00	2,70	3,204E+04	228000	0,016623	3790	U+	C	0,165	1	1	90	131,0
Täljsten and Elfgren (2000)	S4	R	0	180	500	0	56,50	48,50	3,99	3,699E+04	70800	0,012147	860	U	C	0,8	1	1,41	45	211
	SR1	R	0	180	500	0	61,80	53,80	4,28	3,799E+04	70800	0,012147	860	U	D	0,8	50	141,42	45	89
	SR2	R	0	180	500	0	60,70	52,70	4,22	3,779E+04	70800	0,012147	860	U	C	0,8	1	1,41	45	123
Deniaud and Cheng (2001)	T6NS-C45	T	400	140	600	150	44,10	36,10	3,28	3,434E+04	230000	0,014783	3400	U	D	0,11	50	100	45	103,5
	T6S4-C90	T	400	140	600	150	44,10	36,10	3,28	3,434E+04	230000	0,014783	3400	U	D	0,11	50	100	90	85,25
	T6S2-C90	T	400	140	600	150	44,10	36,10	3,28	3,434E+04	230000	0,014783	3400	U	D	0,11	50	100	90	0
Park et al. (2001)	2	R	0	100	250	0	33,40	25,40	2,59	31589,78	240000	0,014167	3400	U	C	0,16	1	1	90	39,3
	3	R	0	100	250	0	33,4	25,40	2,59	31589,78	155000	0,015484	2400	S	D	1,2	25	75	90	18,1

	5	T	300	100	300	50	33,4	25,40	2,59	31589,78	240000	0,014167	3400	U	C	0,16	1	1	90	38,1
	6	T	300	100	300	50	33,4	25,40	2,59	31589,78	155000	0,015484	2400	S	D	1,2	25	75	90	25,1
Li et al. (2002)	B80_1	R	0	130	300	0	38,00	30,00	2,90	3,284E+04	42400	0,011085	470	S+	C	1,5	1	1,41	45	12
	B80_2	R	0	130	300	0	38,00	30,00	2,90	3,284E+04	42400	0,011085	470	S+	C	1,5	1	1,41	45	23,5
	B80_3	R	0	130	300	0	38,00	30,00	2,90	3,284E+04	42400	0,011085	470	S+	C	1,5	1	1,41	45	22
	B40_1	R	0	130	300	0	38,00	30,00	2,90	3,284E+04	42400	0,011085	470	S+	C	1,5	1	1,41	45	10,5
	B20_1	R	0	130	300	0	38,00	30,00	2,90	3,284E+04	42400	0,011085	470	S+	C	1,5	1	1,41	45	7,5
	B20_2	R	0	130	300	0	38,00	30,00	2,90	3,284E+04	42400	0,011085	470	S+	C	1,5	1	1,41	45	13,5
	B20_3	R	0	130	300	0	38,00	30,00	2,90	3,284E+04	42400	0,011085	470	S+	C	1,5	1	1,41	45	13
	B10_1	R	0	130	300	0	38,00	30,00	2,90	3,284E+04	42400	0,011085	470	S+	C	1,5	1	1,41	45	0
	B'80_2	R	0	130	300	0	38,00	30,00	2,90	3,284E+04	42400	0,011085	470	S+	C	1,5	1	1,41	45	20,5
	B'20_2	R	0	130	300	0	38,00	30,00	2,90	3,284E+04	42400	0,011085	470	S+	C	1,5	1	1,41	45	30,5
Chaallal et al. (2002)	G5.5_1L	T	584,2	122,174	444,5	88,9	37,90	29,90	2,89	3,281E+04	231000	0,015801	3650	U+	C	0,145	1	1	90	31,1374
	G5.5_2L	T	584,2	122,174	444,5	88,9	37,90	29,90	2,89	3,281E+04	231000	0,015801	3650	U+	C	0,29	1	1	90	53,3784
	G8.0_1L	T	584,2	122,174	444,5	88,9	37,90	29,90	2,89	3,281E+04	231000	0,015801	3650	U+	C	0,145	1	1	90	31,1374
	G8.0_2L	T	584,2	122,174	444,5	88,9	37,90	29,90	2,89	3,281E+04	231000	0,015801	3650	U+	C	0,29	1	1	90	62,2748
	G8.0_3L	T	584,2	122,174	444,5	88,9	37,90	29,90	2,89	3,281E+04	231000	0,015801	3650	U+	C	0,435	1	1	90	84,5158
	G16_1L	T	584,2	122,174	444,5	88,9	37,90	29,90	2,89	3,281E+04	231000	0,015801	3650	U+	C	0,145	1	1	90	40,0338
	G16_2L	T	584,2	122,174	444,5	88,9	37,90	29,90	2,89	3,281E+04	231000	0,015801	3650	U+	C	0,29	1	1	90	84,5158
	G24_1L	T	584,2	122,174	444,5	88,9	37,90	29,90	2,89	3,281E+04	231000	0,015801	3650	U+	C	0,145	1	1	90	53,3784
	G24_2L	T	584,2	122,174	444,5	88,9	37,90	29,90	2,89	3,281E+04	231000	0,015801	3650	U+	C	0,29	1	1	90	48,9302
	G24_3L	T	584,2	122,174	444,5	88,9	37,90	29,90	2,89	3,281E+04	231000	0,015801	3650	U+	C	0,435	1	1	90	53,3784
Khalifa and Nanni (2002)	SW3-2	R	0	150	305	0	27,30	19,30	2,16	2,974E+04	228000	0,016623	3790	U+	C	0,165	1	1	90	50,5
	SW4-2	R	0	150	305	0	27,30	19,30	2,16	2,974E+04	228000	0,016623	3790	U+	C	0,165	1	1	90	80,5
	SO3-2	R	0	150	305	0	35,50	27,50	2,73	3,217E+04	228000	0,016623	3790	U	D	0,165	50	125	90	54
	SO3-3	R	0	150	305	0	35,50	27,50	2,73	3,217E+04	228000	0,016623	3790	U	D	0,165	75	125	90	56,5
	SO3-4	R	0	150	305	0	35,50	27,50	2,73	3,217E+04	228000	0,016623	3790	U	C	0,165	1	1	90	67,5
	SO3-5	R	0	150	305	0	35,50	27,50	2,73	3,217E+04	228000	0,016623	3790	U+	C	0,165	1	1	90	92,5
	SO4-2	R	0	150	305	0	35,50	27,50	2,73	3,217E+04	228000	0,016623	3790	U	D	0,165	50	125	90	62,5
	SO4-3	R	0	150	305	0	35,50	27,50	2,73	3,217E+04	228000	0,016623	3790	U	C	0,165	1	1	90	90
Pellegrino and Modena (2002)	TR30C2	R	0	150	300	0	27,50	19,50	2,17	2,980E+04	234000	0,015171	3550	S	C	0,165	1	1	90	45,3
	TR30C3	R	0	150	300	0	27,50	19,50	2,17	2,980E+04	234000	0,015171	3550	S	C	0,495	1	1	90	38,1
	TR30C4	R	0	150	300	0	27,50	19,50	2,17	2,980E+04	234000	0,015171	3550	S	C	0,495	1	1	90	65,5
	TR30D10	R	0	150	300	0	31,40	23,40	2,45	3,101E+04	234000	0,015171	3550	S	C	0,33	1	1	90	31,5
	TR30D2	R	0	150	300	0	31,40	23,40	2,45	3,101E+04	234000	0,015171	3550	S	C	0,495	1	1	90	51,8

	TR30D20	R	0	150	300	0	31,40	23,40	2,45	3,101E+04	234000	0,015171	3550	S	C	0,495	1	1	90	86
	TR30D3	R	0	150	300	0	31,40	23,40	2,45	3,101E+04	234000	0,015171	3550	S	C	0,165	1	1	90	0
	TR30D4	R	0	150	300	0	31,40	23,40	2,45	3,101E+04	234000	0,015171	3550	S	C	0,33	1	1	90	47,3
	TR30D40	R	0	150	300	0	31,40	23,40	2,45	3,101E+04	234000	0,015171	3550	S	C	0,33	1	1	90	50,5
Beber (2003)	V9_A	R	0	150	300	0	32,80	24,80	2,55	3,142E+04	230000	0,014783	3400	S	D	0,111	50	100	90	41,2
	V9_B	R	0	150	300	0	32,80	24,80	2,55	3,142E+04	230000	0,014783	3400	S	D	0,111	50	100	90	47,37
	V21_A	R	0	150	300	0	32,80	24,80	2,55	3,142E+04	230000	0,014783	3400	S	D	0,111	50	100	90	58,27
	V10_A	R	0	150	300	0	32,80	24,80	2,55	3,142E+04	230000	0,014783	3400	U	D	0,111	50	100	90	50,57
	V10_B	R	0	150	300	0	32,80	24,80	2,55	3,142E+04	230000	0,014783	3400	U	D	0,111	50	100	90	49,07
	V17_A	R	0	150	300	0	32,80	24,80	2,55	3,142E+04	230000	0,014783	3400	U	D	0,111	50	100	90	45,87
	V11_A	R	0	150	300	0	32,80	24,80	2,55	3,142E+04	230000	0,014783	3400	U	D	0,111	50	100	90	41,51
	V11_B	R	0	150	300	0	32,80	24,80	2,55	3,142E+04	230000	0,014783	3400	U	D	0,111	50	100	90	67,88
	V17_B	R	0	150	300	0	32,80	24,80	2,55	3,142E+04	230000	0,014783	3400	U	D	0,111	50	100	90	36,01
	V12_A	R	0	150	300	0	32,80	24,80	2,55	3,142E+04	230000	0,014783	3400	W	D	0,111	50	100	90	59,44
	V18_A	R	0	150	300	0	32,80	24,80	2,55	3,142E+04	230000	0,014783	3400	W	D	0,111	50	100	90	70,37
	V20_A	R	0	150	300	0	32,80	24,80	2,55	3,142E+04	230000	0,014783	3400	W	D	0,111	50	100	90	83,2
	V12_B	R	0	150	300	0	32,80	24,80	2,55	3,142E+04	230000	0,014783	3400	S	D	0,111	50	141,4	45	44,73
	V14_B	R	0	150	300	0	32,80	24,80	2,55	3,142E+04	230000	0,014783	3400	S	D	0,111	50	141,4	45	34,73
	V19_A	R	0	150	300	0	32,80	24,80	2,55	3,142E+04	230000	0,014783	3400	U	D	0,111	50	141,4	45	61,5
	V19_B	R	0	150	300	0	32,80	24,80	2,55	3,142E+04	230000	0,014783	3400	U	D	0,111	50	141,4	45	58,21
	V13_A	R	0	150	300	0	32,80	24,80	2,55	3,142E+04	230000	0,014783	3400	S	C	0,111	1	1	90	65,09
	V13_B	R	0	150	300	0	32,80	24,80	2,55	3,142E+04	230000	0,014783	3400	S	C	0,111	1	1	90	68,83
	V15_B	R	0	150	300	0	32,80	24,80	2,55	3,142E+04	230000	0,014783	3400	U	C	0,111	1	1	90	81,45
	V16_B	R	0	150	300	0	32,80	24,80	2,55	3,142E+04	230000	0,014783	3400	U	C	0,111	1	1	90	55,51
	V14_A	R	0	150	300	0	32,80	24,80	2,55	3,142E+04	230000	0,014783	3400	S	C	0,111	1	1,41	45	71,47
	V15_A	R	0	150	300	0	32,80	24,80	2,55	3,142E+04	230000	0,014783	3400	S	C	0,111	1	1,41	45	63,64
	V20_B	R	0	150	300	0	32,80	24,80	2,55	3,142E+04	205000	0,012195	2500	S	D	1,4	50	100	90	85,99
	V22_B	R	0	150	300	0	32,80	24,80	2,55	3,142E+04	205000	0,012195	2500	S	D	1,4	50	100	90	55,59
	V21_B	R	0	150	300	0	32,80	24,80	2,55	3,142E+04	205000	0,012195	2500	S	D	1,4	50	141,4	45	78,78
	V22_A	R	0	150	300	0	32,80	24,80	2,55	3,142E+04	205000	0,012195	2500	S	D	1,4	50	141,4	45	68,68
Deniaud and Cheng (2003)	T4S2-C45	T	400	140	400	150	37,40	29,40	2,86	3,268E+04	230000	0,014783	3400	U	D	0,11	50	141	45	17,8
Diagana et al. (2003)	PU1	R	0	130	450	0	38,00	30,00	2,90	3,284E+04	105000	0,013333	1400	U	D	0,43	40	200	90	32,5
	PU2	R	0	130	450	0	38,00	30,00	2,90	3,284E+04	105000	0,013333	1400	U	D	0,43	40	250	90	20
	PU3	R	0	130	450	0	38,00	30,00	2,90	3,284E+04	105000	0,013333	1400	U	D	0,43	40	300	45	44,5
	PU4	R	0	130	450	0	38,00	30,00	2,90	3,284E+04	105000	0,013333	1400	U	D	0,43	40	350	45	40

	PC1	R	0	130	450	0	38,00	30,00	2,90	3,284E+04	105000	0,013333	1400	W	D	0,43	40	200	90	67,5
	PC2	R	0	130	450	0	38,00	30,00	2,90	3,284E+04	105000	0,013333	1400	W	D	0,43	40	250	90	45
	PC3	R	0	130	450	0	38,00	30,00	2,90	3,284E+04	105000	0,013333	1400	W	D	0,43	40	300	45	35,5
	PC4	R	0	130	450	0	38,00	30,00	2,90	3,284E+04	105000	0,013333	1400	W	D	0,43	40	350	45	22
Täljsten (2003)	RC1	R	0	180	500	0	67,40	59,40	4,57	3,900E+04	234000	0,019231	4500	S	C	0,07	1	1,41	45	182
	C1	R	0	180	500	0	67,40	59,40	4,57	3,900E+04	234000	0,019231	4500	S	C	0,11	1	1,41	45	122,6
	C2	R	0	180	500	0	71,40	63,40	4,77	3,968E+04	234000	0,019231	4500	S	C	0,11	1	1,41	45	133,15
	C3	R	0	180	500	0	58,70	50,70	4,11	3,741E+04	234000	0,019231	4500	S	C	0,11	1	1	90	136,55
	C5	R	0	180	500	0	71,40	63,40	4,77	3,968E+04	234000	0,019231	4500	S	C	0,165	1	1,41	45	210,25
Adhikary et al. (2004)	C1	R	0	300	300	0	45,20	37,20	3,34	3,459E+04	230000	0,014783	3400	U	C	0,167	1	1	90	53
	C2	R	0	300	300	0	49,10	41,10	3,57	3,546E+04	230000	0,014783	3400	U+	C	0,167	1	1	90	116,5
	C3	R	0	300	300	0	49,10	41,10	3,57	3,546E+04	230000	0,014783	3400	U+	C	0,167	1	1	90	125,5
Feng Xue Song et al. (2004)	SB1_3	R	0	150	360	0	32,50	24,50	2,53	3,133E+04	235000	0,017872	4200	U	C	0,22	1	1	90	63,5
	SB1_4	R	0	150	360	0	32,50	24,50	2,53	3,133E+04	235000	0,017872	4200	U	C	0,22	1	1	90	76,5
	SB1_5	R	0	150	360	0	32,50	24,50	2,53	3,133E+04	235000	0,017872	4200	U	D	0,22	40	120	90	69,5
	SB1_6	R	0	150	360	0	32,50	24,50	2,53	3,133E+04	235000	0,017872	4200	U	D	0,22	40	120	90	53,5
	SB1_7	R	0	150	360	0	32,50	24,50	2,53	3,133E+04	235000	0,017872	4200	U+	D	0,22	40	120	90	63,5
	SB1_8	R	0	150	360	0	32,50	24,50	2,53	3,133E+04	235000	0,017872	4200	U+	D	0,22	40	120	90	62,5
	SB1_9	R	0	150	360	0	32,50	24,50	2,53	3,133E+04	235000	0,017872	4200	U	D	0,44	40	120	90	63,5
	SB1_10	R	0	150	360	0	32,50	24,50	2,53	3,133E+04	235000	0,017872	4200	U	D	0,44	40	120	90	66,5
	SB2_2	R	0	150	360	0	32,50	24,50	2,53	3,133E+04	235000	0,017872	4200	U+	D	0,22	40	120	90	72
	SB2_3	R	0	150	360	0	32,50	24,50	2,53	3,133E+04	235000	0,017872	4200	U	D	0,22	40	120	90	52
	SB3_2	R	0	150	360	0	32,50	24,50	2,53	3,133E+04	235000	0,017872	4200	U	D	0,22	40	120	90	35
	SB3_3	R	0	150	360	0	32,50	24,50	2,53	3,133E+04	235000	0,017872	4200	U+	D	0,22	40	120	90	54
Carolin and Täljsten (2005)	A145	R	0	180	500	0	67,00	59,00	4,55	3,893E+04	234000	0,019231	4500	S	C	0,07	1	1,41	45	128
	A245a	R	0	180	500	0	71,00	63,00	4,75	3,961E+04	234000	0,019231	4500	S	C	0,11	1	1,41	45	138
	A245b	R	0	180	500	0	53,00	45,00	3,80	3,628E+04	234000	0,019231	4500	S	C	0,11	1	1,41	45	186
	A245W	R	0	180	500	0	46,00	38,00	3,39	3,477E+04	234000	0,019231	4500	W	C	0,11	1	1,41	45	219
	A245Ra	R	0	180	500	0	67,00	59,00	4,55	3,893E+04	234000	0,019231	4500	S	C	0,11	1	1,41	45	187
	A245Rb	R	0	180	500	0	47,00	39,00	3,45	3,500E+04	234000	0,019231	4500	S	C	0,11	1	1,41	45	132
	A290a	R	0	180	500	0	59,00	51,00	4,13	3,747E+04	234000	0,019231	4500	S	C	0,11	1	1	90	137
	A290b	R	0	180	500	0	52,00	44,00	3,74	3,608E+04	234000	0,019231	4500	S	C	0,11	1	1	90	179
	A290W	R	0	180	500	0	52,00	44,00	3,74	3,608E+04	234000	0,019231	4500	W	C	0,11	1	1	90	248
	A290WR	R	0	180	500	0	46,00	38,00	3,39	3,477E+04	234000	0,019231	4500	W	C	0,11	1	1	90	269
	A345	R	0	180	500	0	71,00	63,00	4,75	3,961E+04	234000	0,019231	4500	S	C	0,17	1	1,41	45	215

	B290	R	0	180	400	0	46,00	38,00	3,39	3,477E+04	234000	0,019231	4500	S	C	0,11	1	1	90	61
	B390	R	0	180	400	0	46,00	38,00	3,39	3,477E+04	234000	0,019231	4500	S	C	0,17	1	1	90	61
Miyajima et al. (2005)	case2	R	0	340	440	0	29,90	21,90	2,35	3,056E+04	253000	0,01913	4840	W	D	0,111	50	150	90	81,3
	case3	R	0	340	440	0	29,90	21,90	2,35	3,056E+04	253000	0,01913	4840	W	D	0,111	75	150	90	122
	case4	R	0	340	440	0	29,90	21,90	2,35	3,056E+04	253000	0,01913	4840	W	D	0,111	87,5	150	90	132
	case5	R	0	340	440	0	29,90	21,90	2,35	3,056E+04	253000	0,01913	4840	W	D	0,111	100	150	90	162
Monti and Liota (2005)	SS90*	R	0	250	450	0	10,65	2,65	0,57	2,242E+04	390000	0,007692	3000	S	D	0,22	150	300	90	5
	SS45	R	0	250	450	0	10,65	2,65	0,57	2,242E+04	390000	0,007692	3000	S	D	0,22	150	300	45	6
	SSVA	R	0	250	450	0	10,65	2,65	0,57	2,242E+04	390000	0,007692	3000	S	D	0,22	150	300	45	10
	SF90	R	0	250	450	0	10,65	2,65	0,57	2,242E+04	390000	0,007692	3000	S	C	0,22	1	1	90	17,5
	US90*	R	0	250	450	0	10,65	2,65	0,57	2,242E+04	390000	0,007692	3000	U	D	0,22	150	300	90	0
	US60	R	0	250	450	0	10,65	2,65	0,57	2,242E+04	390000	0,007692	3000	U	D	0,22	150	300	60	16
	USVA	R	0	250	450	0	10,65	2,65	0,57	2,242E+04	390000	0,007692	3000	U	D	0,22	150	300	45	25
	USVA+	R	0	250	450	0	10,65	2,65	0,57	2,242E+04	390000	0,007692	3000	U+	D	0,22	150	300	60	40
	US45+	R	0	250	450	0	10,65	2,65	0,57	2,242E+04	390000	0,007692	3000	U+	D	0,22	150	300	45	31
	US90(2)*	R	0	250	450	0	10,65	2,65	0,57	2,242E+04	390000	0,007692	3000	U	D	0,22	150	300	90	0
	UF90	R	0	250	450	0	10,65	2,65	0,57	2,242E+04	390000	0,007692	3000	U	C	0,22	1	1	90	30
	US45++	R	0	250	450	0	10,65	2,65	0,57	2,242E+04	390000	0,007692	3000	U+	D	0,22	50	100	45	38,5
	US45+A	R	0	250	450	0	10,65	2,65	0,57	2,242E+04	390000	0,007692	3000	U+	C	0,22	1	1,41	45	63,5
	UF45++B	R	0	250	450	0	10,65	2,65	0,57	2,242E+04	390000	0,007692	3000	U+	C	0,22	1	1,41	45	72
	UF45++C	R	0	250	450	0	10,65	2,65	0,57	2,242E+04	390000	0,007692	3000	U+	C	0,22	1	1,41	45	77
	US45++F	R	0	250	450	0	10,65	2,65	0,57	2,242E+04	390000	0,007692	3000	U+	D	0,22	150	225	45	87,85
	US45++E	R	0	250	450	0	10,65	2,65	0,57	2,242E+04	390000	0,007692	3000	U+	D	0,22	150	225	45	55,15
	US45+D	R	0	250	450	0	10,65	2,65	0,57	2,242E+04	390000	0,007692	3000	U	D	0,22	150	225	45	68,45
	WS45++	R	0	250	450	0	10,65	2,65	0,57	2,242E+04	390000	0,007692	3000	W+	D	0,22	50	100	45	19,5
Bousselham and Chaallal (2006)	DBS01L	T	270	95	220	55	25,50	17,50	2,02	2,913E+04	231000	0,015801	3650	U+	C	0,066	1	1	90	15,4
	DBS02L	T	270	95	220	55	25,50	17,50	2,02	2,913E+04	231000	0,015801	3650	U+	C	0,132	1	1	90	13,8
	DBS11L	T	270	95	220	55	25,50	17,50	2,02	2,913E+04	231000	0,015801	3650	U+	C	0,066	1	1	90	12,7
	DBS12L	T	270	95	220	55	25,50	17,50	2,02	2,913E+04	231000	0,015801	3650	U+	C	0,132	1	1	90	17
	SBS01L	T	270	95	220	55	25,50	17,50	2,02	2,913E+04	231000	0,015801	3650	U+	C	0,066	1	1	90	23,2
	SBS02L	T	270	95	220	55	25,50	17,50	2,02	2,913E+04	231000	0,015801	3650	U+	C	0,132	1	1	90	32,4
	SBS11L	T	270	95	220	55	25,50	17,50	2,02	2,913E+04	231000	0,015801	3650	U+	C	0,066	1	1	90	2,8
	SBS12L	T	270	95	220	55	25,50	17,50	2,02	2,913E+04	231000	0,015801	3650	U+	C	0,132	1	1	90	12,2
Dias and Barros (2006)	2S_4M(1)	T	450	180	400	100	38,10	30,10	2,90	3,286E+04	240000	0,015	3600	U	D	0,176	60	180	90	4,38
	2S_7M(1)	T	450	180	400	100	38,10	30,10	2,90	3,286E+04	240000	0,015	3600	U	D	0,176	60	114	90	12,78

	2S_7M(2)	T	450	180	400	100	38,10	30,10	2,90	3,286E+04	240000	0,015	3600	U	D	0,352	60	114	90	39,78
	4S_4M(1)	T	450	180	400	100	41,00	33,00	3,09	3,359E+04	240000	0,015	3600	U	D	0,176	60	180	90	27,6
	4S_7M(1)	T	450	180	400	100	41,00	33,00	3,09	3,359E+04	240000	0,015	3600	U	D	0,176	60	114	90	30,96
De Lorenzis and Rizzo (2006)	UW90	R	0	200	210	0	29,30	21,30	2,31	3,037E+04	230000	0,014913	3430	U	C	0,165	1	1	90	19,3
Dias and Barros (2008)	A10_M	R	0	150	300	0	49,20	41,20	3,58	3,548E+04	390000	0,007692	3000	U	D	0,334	25	190	90	10,83
	A12_M	R	0	150	300	0	49,20	41,20	3,58	3,548E+04	390000	0,007692	3000	U	D	0,334	25	95	90	31,52
	B10_M	R	0	150	150	0	56,20	48,20	3,97	3,693E+04	390000	0,007692	3000	U	D	0,334	25	80	90	18,56
	B12_M	R	0	150	150	0	56,20	48,20	3,97	3,693E+04	390000	0,007692	3000	U	D	0,334	25	40	90	33,65

Note: $B_{slab\ T}$=width of flange for T section beams; b_{web}=beam's cross section width; h=height of the beam; $h_{slab\ T}$=thickness of the flange for T section beams; f_{cm}=mean value of concrete compressive cylinder strength; f_{ck}=characteristic compressive cylinder strength of concrete at 28 days; f_{ctm}= mean value of concrete cylinder compressive strength; E_c= elastic modulus of concrete; E_{frp}= elastic modulus of fibres; $e_{frp,u}$= ultimate design strain of the FRP; $f_{frp,u}$= ultimate design stress of the FRP; t_{frp}= thickness of the FRP; w_{frp}=width of the FRP; s_{frp}= spacing of the FRP; β=inclination angle of the FRP with respect to the longitudinal axis of the beam; $r_{frp,shear}$=shear reinforcement ration of the FRP; C=continuous; D= discontinuous; S=side bonded; S+=side bonded with anchorage; U= U wrapped; U= U wrapped with anchorage; W= fully wrapped bonded; W= fully wrapped; V_{frp}=contribution of the FRP to the shear capacity of the beam.

Paper II

"A model for predicting shear bearing capacity of FRP strengthened beams"

By:
G. Sas, A. Carolin and B. Täljsten

Published in:
Mechanics of Composite Materials, Vol. 44, No. 3, 2008.

Mechanics of Composite Materials, Vol. 44, No. 3, 2008

A MODEL FOR PREDICTING THE SHEAR BEARING CAPACITY OF FRP-STRENGTHENED BEAMS

G. Sas,* A. Carolin,* and B. Täljsten**

Keywords: *FRP, shear, concrete, beams, strengthening, strain, anchorage, debonding, fracture mechanics*

The shear failure of reinforced concrete beams needs more attention than the bending failure since no or only small warning precedes the failure. For this reason, it is of utmost importance to understand the shear bearing capacity and also to be able to undertake significant rehabilitation work if necessary. In this paper, a design model for the shear strengthening of concrete beams by using fiber-reinforced polymers (FRP) is presented, and the limitations of the truss model analogy are highlighted. The fracture mechanics approach is used in analyzing the bond behavior between the FRP composites and concrete. The fracture energy of concrete and the axial rigidity of the FRP are considered to be the most important parameters. The effective strain in the FRP when the debonding occurs is determined. The limitations of the anchorage length over the cross section are analyzed. A simple iterative design method for the shear debonding is finally proposed.

Introduction

The use of a fiber-reinforced polymer (FRP) for retrofitting concrete structures has been shown to be a reliable and competitive method regarding both the structural and the economic performance. Even though the method has been used for more than a decade, the main part of the research is focused on the flexural behavior of strengthened elements, while the shear behavior has not been studied to the same extent. The shear failure of beams, since it emerges almost without any forewarning and has a brittle character, needs more attention than the flexural failure. Some failure modes of a reinforced concrete beam are presented in Fig. 1.

The existing models for predicting the shear failure of reinforced concrete beams are limited in accuracy. Most analytical models for predicting the shear capacity of a structural element have their origin in the truss model (Fig. 2) and the modified theory of compression field. Owing to the ease of its employment, the truss model has become the most widely used one. The current study is a merger and development of the previous investigations presented in [1-4]. By using the principle of summation, the total shear capacity V_{Rd} of a beam can be expressed as

$$V_{Rd} = V_c + V_s + V_p + V_i + V_f,$$

where V_c is the contribution from concrete, which often includes the dowel action from the longitudinal steel reinforcement and is determined by relationships found empirically, V_s is the contribution from steel stirrups, calculated by the truss model, and

*Luleå University of Technology, SE - 971 87 Luleå, Sweden. ** Technical University of Denmark, DK – 2800 Lyngby, Denmark. Russian translation published in Mekhanika Kompozitnykh Materialov, Vol. 44, No. 3, pp. 357-372, May-June, 2008. Original article submitted August 20, 2007; revision submitted April 4, 2008.

0191-5665/08/4403-0245

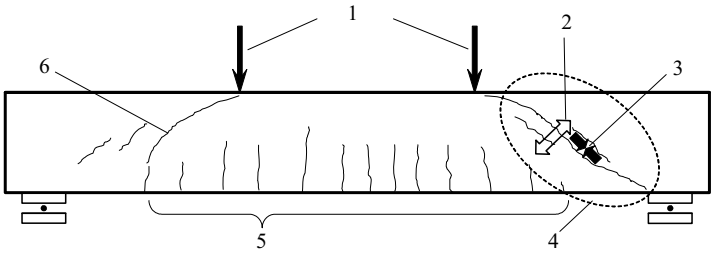

Fig. 1. Typical failure modes of rainforced concrete beams: 1 — loads; 2 — tension; 3 — compression; 4 — shear cracks/failure; 5 — flexural cracks; 6 — shear-bending crack/failure.

V_p is the contribution from axial forces, for example, prestressed tendons. V_i represents additional contributions, such as from inclined compression cords. The focus of our study will be the quantity V_f — the contribution from the externally bonded composite. Considering the fiber alignment (Fig. 3) and the nonuniform distribution of stresses over the cross section (Fig. 4), V_f can be calculated as

$$V_f = \eta \varepsilon_{cr} E_{frp} t_{frp} r_{frp} z \frac{\cos\theta}{\sin\alpha}, \tag{1}$$

where z is the length of a vertical tension tie in the truss (when composites are bonded over the whole cross section, it becomes equal to the beam height), α is the crack inclination angle, β is the fiber direction angle, and θ is the angle between the principal tensile stress and the fiber direction, i.e., $\theta = \alpha + \beta - 90°$. The factor r_{frp} depends on the strengthening scheme. The factor η considers the nonuniform distribution of strains over the cross section and is assumed equal to 0.6 [3].

The critical strain ε_{cr} can be defined as

$$\varepsilon_{cr} = \min\begin{Bmatrix} \varepsilon_{fu} \\ \varepsilon_{c\max} \\ \varepsilon_{bond} \end{Bmatrix}, \tag{2}$$

where ε_{fu} is the ultimate allowable fiber capacity, $\varepsilon_{c\max}$ is the maximum allowable strain to achieve the contribution from concrete, and ε_{bond} is the maximum allowable strain not causing the anchorage failure.

The ultimate fiber capacity and the maximum strain are material parameters. The contribution of concrete has been treated elsewhere [4] and will not be further discussed in this paper. In the case where the FRP is wrapped over all cross section, the shear capacity is not influenced by the anchorage limitation. When small amounts of fibers are used, a sufficient bond may nevertheless be achieved without wrapping [3]. Compared to the flexural strengthening, the shear strengthening, in most cases, cannot provide a sufficient anchorage length for side bonding and U wrapping due to the limitations imposed by beam geometry. When the anchorage is lost, the maximum strain depends on the amount of fibers and the fiber stiffness, which is also known as the axial rigidity [5].

In this study, the bond between FRP and concrete for reinforced concrete beams strengthened in shear is evaluated by using the principles of fracture mechanics. The shear stress in concrete and the maximum relative slip in the joint are considered to be the key parameters.

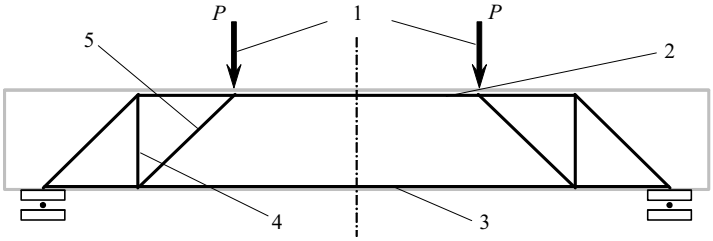

Fig.2. Truss model for reinforced concrete: 1 — load; 2 — compression chord; 3 — tension chord; 4 — tension tie; 5 — compression strut.

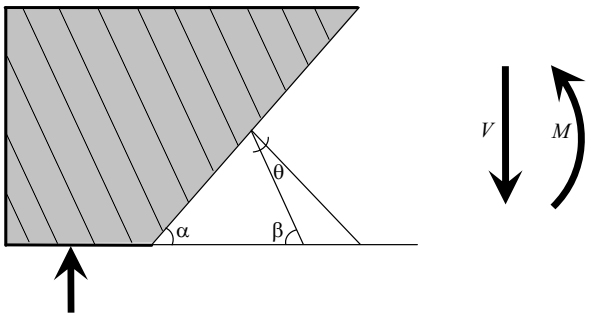

Fig. 3. Fiber alignment β and crack α angles.

Shear Design Models in the Literature

During the 1990s, the studies on shear strengthening with fiber-reinforced polymers intensified. At that time, the majority of researchers assumed that FRP materials behave like internal stirrups. Later, studies included the linearly elastic properties and the distribution of shear strains. Although many theoretical investigations have been carried out, the design models proposed are almost as many as researches in the field of mechanics, and the predictions of shear strength are discordant to some extent.

The equation for calculating the shear contribution of FRP proposed by Chaallal et al. [6] is based on the assumption that the composite and the stirrups behave in a similar manner. The model assumes that the tensile strength of FRP is reached for all fibers when the composite is intersected by a shear crack unless the bond is insufficient. The model does not cover the actual behavior of the strengthening systems, which includes the linearly elastic material response and a nonuniform distribution of strains.

Malek and Saadatmanesh [7, 8] considered the anisotropic behavior of FRP and examined how the crack inclination angle was affected by the plate thickness, the fiber orientation angle, and the vertical spacing of reinforcement.

Based on empirical data, Triantafillou and Antonopoulos [5, 9] derived a model that includes the effective FRP strain. This strain was found to be dependent on both the axial rigidity of the composite and the “effective bond length.” Khalifa et al. modified Triantafillou’s model by introducing the strain limitations due to opening of a shear crack and the loss of aggregate interlock. The model was developed by considering great number of tests [10, 11]. Pellegrino and Modena [12] suggested a modified reduction factor for the model. The new model includes the ratio between the stiffnesses of the transverse steel shear reinforcement and the FRP shear reinforcement.

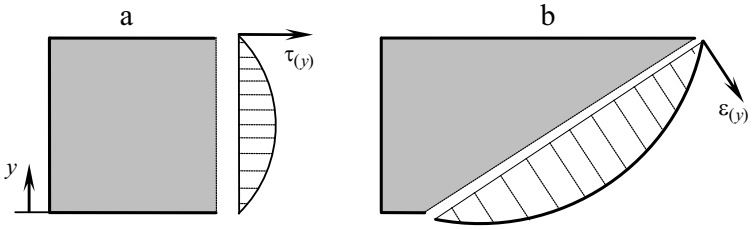

Fig. 4. Nonuniform distribution of stresses in transverse (a) and inclined (b) sections of a beam.

Deniaud and Cheng derived a model on the assumption that the FRP strains are distributed uniformly among the fibers crossing a crack. Based on empirical data, a design model was developed by combining the strip method and the shear friction approach [13, 14]. Later on, a refined and simplified model was also proposed [15].

Using the tensile strain of fibers, Täljsten [16] presented expressions for the contribution from the externally bonded composite to the shear bearing capacity. A comparison between the tests performed and the theory gave a good agreement for the overall bearing capacity. The nonuniform distribution of strains in the FRP over the cross section was considered. A reduction factor of 0.60 for the maximum strains in fibers was suggested.

Chen and Teng [17-19] analyzed the shear failure of reinforced concrete beams strengthened with FRP and arrived at the conclusion that the stress distribution in the FRP along the crack was nonuniform. They presented a model of shear strength, based on the rupture of fibers, for reinforced concrete beams strengthened with FRP. Owing to the lack of information on the actual distribution of strains in the FRP, a linear distribution was used. A stress limitation was introduced by using the coefficients of bond length and strip width. Design proposals were formulated with the use of reduction factors for the ultimate tensile strength (0.8 of the maximum tensile stress), the strip space (≤ 300 mm), and the maximum allowable strain (1.5%).

Aprile and Benedetti [20] presented a model based on a variable-angle truss model for the FRP. The bond strength of a sheet bridging over a diagonal crack was also analyzed taking into account the geometry of ties. As important factors, the crack pattern, the shear force transmitted by concrete across the cracks, and a reduction factor for the strength of FRP ties were considered.

Ianniruberto and Imbimbo [21] developed a model based on the theory of compression field. This model does not consider the debonding failure mechanism. The theoretical predictions were compared with experimental results, but, unfortunately, the agreement was not good.

Another model for the contribution of shear strength of CFRP was given by Saenz et al. [22]. The theory is founded on a strut-and-tie model for the shear friction strength of concrete and concrete– CFRP interaction. A simplified design method based on experimental results was also developed. From experimental results, an effective tensile strain for CFRP was defined, which takes into account the material properties and the CFRP reinforcement ratio.

Cao et al. [23] modified the Chen and Teng model and proposed an empirical model to predict the contribution of FRP to the shear strength of RC beams. The model takes into account the debonding in FRP-wrapped RC beams. The modification of the strain distribution factor gave uncertain results because of a great scatter of test data.

The shear bond model proposed by Zhang and Hsu [24] is based on employing two approaches: model calibration by curve fitting and bond mechanism. The smallest reduction factor for the effective strain obtained by the two methods is suggested for use.

Aspects regarding the lateral peeling failure of concrete under shear loading of FRP were studied by Pelegrino and Modena [25]. The model follows the truss model approach and describes the concrete, steel, and FRP contributions to the shear capacity of RC beams based on experimental observations.

Monti and Liotta [26] proposed a debonding model for the shear strengthening of RC beams with FRP. The model is based on the use of a generalized constitutive law for the FRP layer bonded to concrete, a function of the strengthening scheme

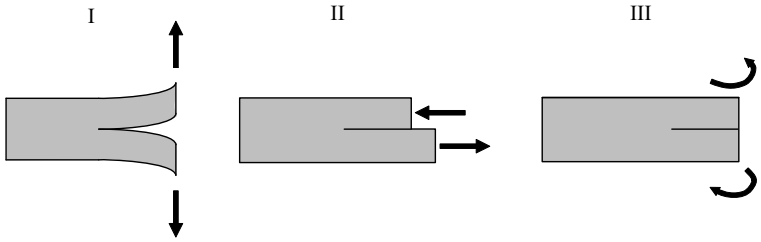

Fig. 5. Fracture modes: I — opening mode; II — shearing mode; III — tearing mode.

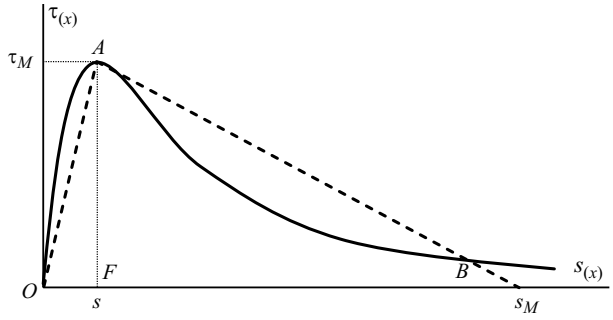

Fig. 6. Shear stress–slip behavior. Explanation in the text.

and shear crack opening provisions, and the stress field in the FRP crossing a shear crack, which is determined analytically. A generalized failure criterion for FRP strips/sheets is introduced. Two cases are considered: straight strips/sheets and strips/sheets wrapped around a corner.

Bond Concepts

Method. Two methods are employed in fracture mechanics to describe the propagation of cracks: the stress approach and the energy approach [1]. To determine the maximum strain in the FRP at the onset of bond failure, the energy approach will be used. Considering a crack that splits the material, the following three fracture modes are defined [1, 27], as shown in Fig. 5. Mode I (opening): crack faces are displaced perpendicularly to the crack plane; a tensile stress is assumed to develop. Mode II (shearing): crack faces are shifted parallel to the crack plane; a shear stress is assumed to develop. Mode III (tearing): crack faces are displaced laterally and parallel to the crack plane; a shear stress is assumed to develop.

Materials. Three materials are considered in modeling the FRP debonding process: the composite material, the adhesive, and concrete. Except for the rupture of fibers, most experimental tests have reported the failure of concrete in the vicinity of adhesive. In this study, the concrete is assumed as the failing material, and the failure of adhesive is neglected Two types of analysis are used in fracture mechanics considering the parameters of materials. The elastic fracture mechanics is suitable for analyzing materials with a linearly elastic behavior up to failure, e.g., glass. The nonlinear fracture mechanics is used when analyzing the behavior of materials with a pronounced yield zone, e.g., steel. Concrete has a different deformation behavior characterized by linearly elastic and nonlinear phases, as seen from the continuous curve in the stress–slip diagram in Fig. 6.

Deformation phases. To facilitate analytical studies, the actual deformation curve is replaced with a bilinear one, as shown by the dashed lines in Fig. 6. The elastic phase is described by the first section of the diagram. The maximum energy

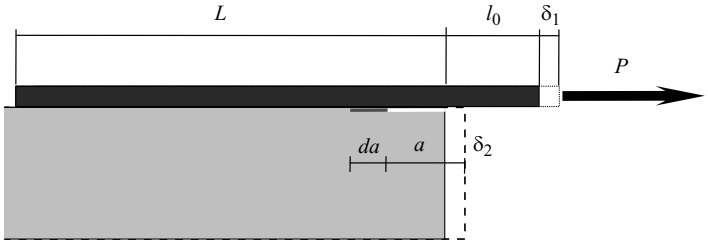

Fig. 7. Bond model.

stored in the bonded joint is given by the area of the triangle *OAB*. When the maximum shear stress τ_{max} is reached at a value of slip *s*, the limit of the elastic phase is reached, and the softening phase starts. Microcracks appear in the joint during the softening. The energy at this phase is determined by the area approximated by the triangle *FAB*. The shear stress decreases as the slip increases. When the slip reaches the value s_{max}, a macrocrack opens, and no more energy is needed for a further slip or displacement.

Fracture energy. The total energy defined by the stress–slip curve and approximated by the triangle *OAB* is the energy necessary to bring the bonded area to fracture. Several methods to determine the fracture energy have been suggested [1, 28-30]. In the empirically determined formulation of fracture energy proposed in [30], the total fracture energy is computed by the formula

$$G_f \approx 0.644 f_c^{0.19}.$$

From the same experimental data set, the expression for the maximum shear stress

$$\tau_{max} = 3.5 f_c^{0.19}$$

was obtained, where f_c is the compressive strength of concrete in MPa.

Bond Failure Strain

Derivation of the effective strain. The model is based on the following assumptions: only the shear force acts on the adhesive, the thickness of the FRP and adhesive are constant, and the bending effects can be neglected. Let us consider an overlap joint of unit width (see Fig. 7), and derive an expression for the Mode II fracture of the single-lap joint. The condition for the crack extending from *a* to $a + da$ is given by the elastic energy release in the concrete under the mechanical work done by an external load *P*. Mathematically, this can be expressed as

$$\frac{d}{da}(U_e - P) \geq \frac{dW}{da}, \tag{3}$$

where U_e is the elastic energy, *P* is the external load, and dW/da is the crack resistance force. Taking as a reference point the load point, the relative displacement is $\delta = \delta_1 + \delta_2$. By a geometrical analogy, we assume that the displacement increases by $d\delta$ when the crack increases by *da*. Hence, the external mechanical work is incremented by $Pd\delta$. Equation (3) can be rewritten in the form

$$G = \frac{d}{da}(P - U_e) = P\frac{d\delta}{da} - \frac{dU_e}{da}, \tag{4}$$

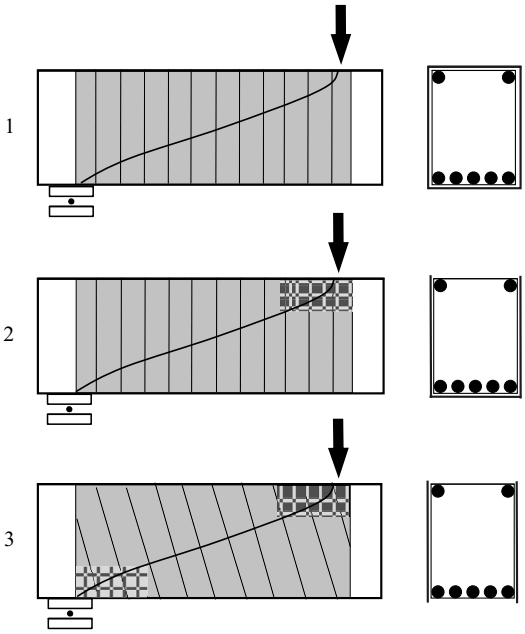

Fig. 8. Shear strengthening schemes: 1 — fully wrapped; 2 — U-wrapped; 3 — side-bonded.

where G is the energy release rate. Under the assumption of elastic behavior of the materials, the relative displacement can be written as $\delta = PC$, where C is the compliance of the lap joint. The elastic energy stored in the structure is

$$U_e = \frac{1}{2} P\delta = \frac{1}{2} P^2 C. \tag{5}$$

Inserting Eq. (5) in Eq. (4), after some mathematical manipulations, the energy release rate for the unit-width overlap joint is expressed as

$$G_f = \frac{P^2}{2} \cdot \frac{\partial C}{\partial a}.$$

The compliance can be determined by using the beam theory and taking the inverse of the stiffness:

$$C = \frac{l_0 + a}{E_{frp} A_{frp}} + \frac{a}{E_C A_C}, \quad \frac{\partial C}{\partial a} = \frac{1}{E_{frp} A_{frp}} + \frac{1}{E_C A_C} = 1 + \frac{E_{frp} t_{frp}}{E_C t_C} = 1 + \alpha,$$

where $A_{frp} = 1 t_{frp}$, $A_C = 1 t_C$ and $\alpha = \dfrac{E_{frp} t_{frp}}{E_C t_C}$. Here E_{frp} is the elastic modulus of FRP, E_C is the elastic modulus of concrete, t_{frp} is the thickness of FRP, and t_C is the thickness of concrete. The maximum strain in the FRP can be found from the equilibrium condition for the overlap joint:

$$\varepsilon_{frp} = \frac{1}{E_{frp} t_{frp}} \sqrt{\frac{2 E_{frp} t_{frp} G_f}{1 + \alpha}}.$$

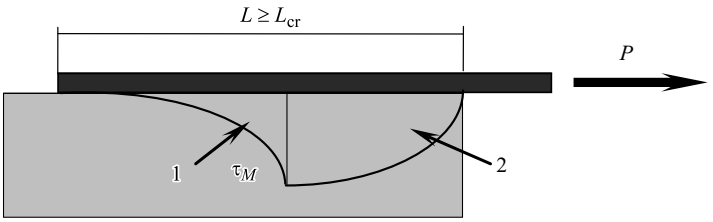

Fig. 9. Long bond length: elastic (1) and softening (2) phases.

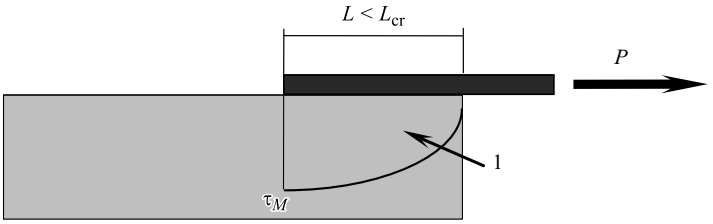

Fig. 10. Short bond length: 1 — softening phase.

A parametric study was performed in order to evaluate the influence of the parameters. The thickness of concrete is much larger than the thickness of FRP. Therefore, the factor α is a very small quantity, and even for high-modulus fibers and low-quality concrete, the influence of α can be neglected:

$$\varepsilon_{frp} = \sqrt{\frac{2E_{frp}t_{frp}G_f}{E_{frp}t_{frp}}}.$$

The bonded region of a strengthened beam can be divided into two parts — long and short with respect to the anchorage length. The anchorage length can be defined as the length of the bonded area outside which the strain in fibers will not increase with load. Different authors [2, 18, 23, 26, 27, 28, 31] have given different expressions for this length. Most of them were derived from shear-lap joint tests. Since the efficiency of strengthening of a beam in shear is limited by beam geometry, the slope of a crack, and the alignment of fibers with respect to the cracks pattern (see also Fig. 3) [4], limitations on the strain will be introduced considering the anchorage length. The common schemes of shear strengthening are presented in Fig. 8. The side-bonded and the U-wrapped beams are most liable to debonding due to the limited anchorage length. The most critical regions are shaded in the figure.

Effective anchorage length. A long bond length (Fig. 9) is defined as the length for which the shear stress is zero at the free end, with both the elastic and the softening phases still present in the joint. The coordinate s of the maximum shear stress (see Fig. 6) is smaller than the bonded length.

A short bond length (Fig. 10) is the length for which the maximum shear stress is at the end of the bonded length, while at the loaded end, the shear is stress greater than zero. The limit between the two situations (the maximum shear stress at the free end of the bonded length and the zero value at the loaded end) gives us the critical length. To evaluate the influence of bond length on the effective strain, the model from [27] is adopted and modified for shear strengthening.

Introducing a limit between the long and short bond lengths, the critical length is obtained as $L_{cr} = \pi/2\omega$. The effective strain is found by considering a one-dimensional unit shear lap joint, but the effective length is given in the direction perpendicular to the crack, as shown in Fig. 11. When the anchorage length is smaller than the critical length, the debonding process will

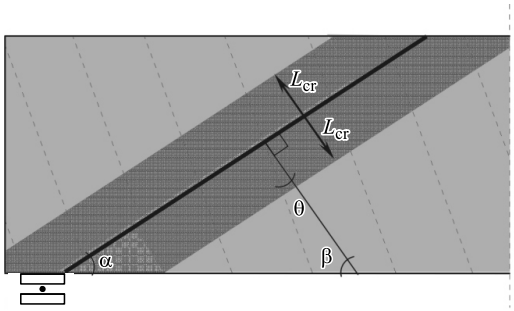

Fig. 11. Critical length over a shear crack.

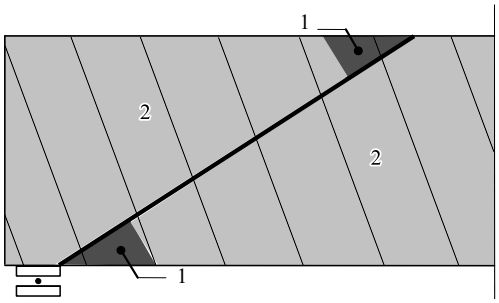

Fig. 12. Critical regions: 1— unsafe anchorage; 2 — fully developed anchorage.

be activated. The shaded highlighted regions in Fig. 12 show the critical regions for a beam of rectangular cross section. The strain in the FRP at debonding is affected by a limiting factor dependent on the available length. The strengthening contribution V_f given by Eq. (1) already contains the limitation due to crack inclination and fiber alignment, and thus the effective strain, given by the equation

$$\varepsilon_{\text{bond}} = \frac{1}{E_{frp} t_{frp}} \sqrt{2E_{frp} t_{frp} G_f} \begin{cases} \sin(\omega L_{\text{cr}}) & \text{at} \quad L_{\text{cr}} \le \dfrac{\pi}{2\omega}, \\ 1 & \text{at} \quad L_{\text{cr}} > \dfrac{\pi}{2\omega}, \end{cases}$$

where

$$\omega = \sqrt{\frac{\tau_{\max}^2}{2E_{frp} t_{frp} G_f}}$$

is already affected by these variables, where the new limitation imposed by the critical length is considered.

Notice that it is not ensured that the fiber rupture will be reached just because the anchorage length is greater than that described here as critical. For design purposes, the total bearing capacity of a beam that should be achieved by the strengthening must be known. The other contributions to the shear force (i.e., from concrete, stirrups, etc) should be computed according to national standards. The contribution of the FRP strengthening is determined using an iterative method. A strengthening system is chosen, and a value for the FRP thickness is assumed. A value of 0.17 mm is suggested for an initial computation. Equation (1) is used for checking, paying attention to the values of the critical strain defined by Eq. (2). If V_f is smaller than the value needed, a new value for the FRP thickness must be chosen. Two cases with the critical strain defined by Eq. (2) may be

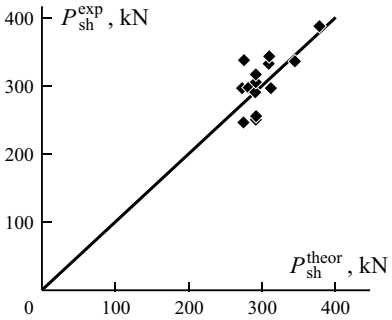

Fig. 13. Experimental shear load P_{sh}^{exp} versus the theoretical prediction P_{sh}^{theor}.

distinguished. If the ultimate strain of fibers ε_{fu} is exceeded, the fiber rupture occur. In this case, the thickness of FRP should be increased. In the second case, the bond strain is too small because of the excessive thickness of FRP, and the thickness of FRP must be decreased. When a sufficient contribution from FRP cannot be attained due to the loss of bond (i.e., the anchorage length is insufficient), the strengthening scheme with wrapping should be considered.

Comparison with Experimental Data

The results of four-point bending tests performed on rectangular RC beams were analyzed. The tests are described in detail in [3]. A series of twenty tests had been carried out on $4.50 \times 0.50 \times 0.18$-m beams with a span of 1.25 m without stirrups, and three tests were run on $3.50 \times 0.40 \times 0.18$-m beams with a span of 1.00 m and 6-mm stirrups spaced 200 mm apart. A tensile reinforcement with a 4% steel-to-concrete ratio and 500-MPa yield strength was provided to avoid the bending failure. Hand lay-up shear strengthening was performed using unidirectional fibers with a stiffness of 234 GPa and ultimate elongation of 1.6 %. Carbon-fiber fabrics of weight 125, 200, and 300 g/m^2, with fiber thickness of 0.07, 0.11, and 0.17 mm, respectively, were used. With the fabrics wapped around and bonded on the vertical sides only, the fibers were oriented in the 45° and 90° directions. The theoretical total shear capacity of all the beams was computed for a 30° crack. For the wrapped beams, the contribution was calculated assuming a uniform strain distribution ($\eta = 1$), since the initial failure was controlled by debonding, and the wrapping still kept the fibers in place, allowing for the redistribution of strains. The experimental and theoretical plots presented in Fig. 13 demonstrate a fairly good agreement.

Conclusions

The initiation of debonding in shear strengthening of concrete beams is important. With the model proposed, it is possible to estimate the critical strain in fibers at which the debonding is initiated. The iterative method for predicting the strain at bond failure is a technique which can be used in design with good results. When debonding occurs, the effective strain in fibers is small compared with their ultimate strain.

It is necessary to consider the nonuniform strain distribution when undertaking the design of shear strengthening with linearly elastic materials. Due to their anisotropic behavior, the fiber capacity is influenced by their orientation with respect to the crack and the longitudinal axis.

On the whole, the modified truss model for shear strengthening FRP gives an acceptable estimate for the contribution to the shear capacity. Still, when the principal strain in concrete is limiting the allowable strain, the different directions of the principle strain in concrete and the fiber alignment should be considered.

The wrapped strengthening configurations are as sensitive to the initiation of debonding as the side-bonded ones. The debonding is directly related to the properties of concrete through the fracture energy. Even after debonding, the wrapping ensures anchorage at the expense of unaffected bonded regions, hence it still contributes to the shear capacity and allows a further loading. Wrappings or other special anchorage solutions are essential in developing a sufficient force transfer for a higher amount of externally bonded reinforcement when the strengthening is undertaken in the ultimate state. For an efficient shear strengthening, wrapping is the best solution, because the debonding failure cannot be avoided in most cases of side bonding. Debonding starts from a possible shear crack and propagates outwards. When a high amount of fibers is used, i.e., FRP plates, debonding may occur whatever the anchorage length, due to their high stiffness and the high concentration of stresses at the end of the plates.

When calculating anchorage by using the fracture mechanics approach, the fracture energy plays an important role. It is not clear which fracture mode dominates in the shear strengthening when the principal strain and the fiber direction do not coincide. This could be a reason why the existing calculation models cannot describe the debonding process well enough. Therefore, further investigations into the fracture of FRP-strengthened concrete beams are necessary.

REFERENCES

1. B. Täljsten, Plate Bonding: Strengthening of Existing Concrete Structures with Epoxy Bonded Plates of Steel or Fibre Reinforced Plastics, Doctoral Thesis, Luleå University of Technology, Sweden (1994).
2. B. Täljsten, "Defining anchor lengths of steel and CFRP plates bonded to concrete," Int. J. Adhes. Adhesiv., **17**, No. 4, 319-327 (1997).
3. A. Carolin and B. Täljsten, "Experimental study of strengthening for increased shear bearing capacity," J. Compos. Construct., **9**, No. 6, 488-496 (2005).
4. A. Carolin and B. Täljsten, "Theoretical study of strengthening for increased shear bearing capacity," J. Compos. Construct., **9**, No. 6, 497-506 (2005).
5. T. C. Triantafillou, "Shear strengthening of reinforced concrete beams using epoxy-bonded FRP composites," ACI Struct. J., **95**, No. 2, 107-115 (1998).
6. O. Chaallal, M.-J. Nollet, and D. Perraton, "Strengthening of reinforced concrete beams with externally bonded fiber-reinforced plastic plates: design guidelines for shear and flexure," Canad. J. Civil Eng., **25**, 692-708 (1998).
7. A. M. Malek and H. Saadatmanesh, "Analytical study of reinforced concrete beams strengthened with web-bonded fiber reinforced plastic plates or fabrics," ACI Struct. J., **95**, No. 3, 343-352 (1998).
8. A. M. Malek and H. Saadatmanesh, "Ultimate shear capacity of reinforced concrete beams strengthened with web-bonded fiber-reinforced plastic plates," ACI Struct. J., **95,** No. 4, 391-399 (1998).
9. T. C. Triantafillou and C. P. Antonopoulos, "Design of concrete flexural members strengthened in shear with FRP," J. Compos. Construct., **4**, No. 4, 198-205 (2000).
10. A. Khalifa, W. Gold, A. Nanni, and M. J. Abdel Aziz, "Contribution of externally bonded FRP to shear capacity of RC flexural members," J. Compos. Construct., **2**, No. 4, 195-202 (1998).
11. A. Khalifa, and A. Nanni, "Improving the shear capacity of existing RC T-section beams using CFRP composites," Cement Concr. Compos., **22**, No. 3, 165-174 (1999).
12. C. Pellegrino and C. Modena, "Fiber-reinforced polymer shear strengthening of reinforced concrete beams with transverse steel reinforcement," J. Compos. Construct., **6**, No. 2, 104-111 (2002).
13. C. Deniaud and J. J. Roger Cheng, "Shear behavior of reinforced concrete T-beams with externally bonded fiber-reinforced polymer sheets," ACI Struct. J., **98,** No. 3, 396-394 (2001).
14. C. Deniaud and J. J. Roger Cheng, "Reinforced concrete T-beams strengthened in shear with fiber-reinforced polymer sheets," J. Compos. Construct., **7,** No. 4, 302-310 (2003).
15. C. Deniaud and J. J. Roger Cheng, "Simplified shear design method for concrete beams strengthened with fiber-reinforced polymer sheets," J. Compos. Construct., **8**, No. 5, 425-433 (2004).

16. B. Täljsten, “Strengthening concrete beams for shear with CFRP sheets,” Construct. Build. Mater., **17**, 15-26 (2003).
17. J. F. Chen and J. G. Teng, “Shear capacity of fiber-reinforced polymer-strengthened reinforced concrete beams. Fiber-reinforced polymer rupture,” J. Struct. Eng., **129,** No. 5, 615-625 (2003).
18. J. F. Chen and J. G. Teng, “Shear capacity of FRP-strengthened RC beams: FRP debonding,” Construct. Build. Mater., **17**, 27-41 (2003).
19. J. F. Chen and J. G. Teng, “Shear strengthening of RC beams with FRP composites,” Progress Struct. Eng. Mater., **6**, 173-184 (2004).
20. A. Aprile and A. Benedetti, “Coupled flexural-shear design of R/C beams strengthened with FRP,” Compos., Pt. B, **35,** 1-25 (2004).
21. U. Ianniruberto and M. Imbimbo, “Role of fiber-reinforced plastic sheets in shear response of reinforced concrete beams. Experimental and analytical results,” J. Compos. Construct., **8**, No. 5, 415-424 (2004).
22. N. Saenz, C. P. Pantelides, and L. D. Reaveley, “Strut-and-tie model for shear friction of concrete with fiber-reinforced polymer composites,” ACI Struct. J., **101**, No. 6, 863-871 (2004).
23. S. Y. Cao, J. F. Chen, J. G. Teng, Z. Hao, and J. Chen, “Debonding in RC beams shear strengthened with complete FRP wraps,” J. Compos. Construct., **9**, No. 5, 417-428 (2005).
24. Z. Zhang and C.-T. T. Hsu, “Shear strengthening of reinforced concrete beams using carbon-fiber-reinforced polymer laminates,” J. Compos. Construct., **9,** No.2, 158-169 (2005).
25. C. Pellegrino and C. Modena, “Fiber-reinforced polymer shear strengthening of reinforced concrete beams. Experimental study and analytical modeling,” ACI Structural J., **103**, No. 5, 720-728 (2006).
26. G. Monti and M.’A. Liotta, “Tests and design equations for FRP-strengthening in shear,” Construct. Build. Mater. (2006), doi:10.1016/j.conbuildmat.2006.06.023.
27. E. Oller, Pelling Failure in Beams Strengthened by Plate Bonding. A Design Proposal, Doctoral Thesis, Barcelona, Spain (2005).
28. K. Brosens, Anchorage of Externally Bonded Steel Plates and CFRP Laminates for the Strengthening of Concrete Elements, PhD Dissertation, Department of Civil Engineering, Katholieke Universiteit Leuven (2001).
29. H. Yuan, Z. S. Wu, and H. Yoshizawa, “Theoretical solutions on interfacial stress transfer of externally bonded steel/composite laminates,” J. Struct. Mech. Earthquake Eng., **18**, No. 1, 27-39, (2001).
30. K. Nakaba, T. Kanakubo, T. Furuta, and H. Yoshizawa, “Bond behavior between fiber-reinforced polymer laminates and concrete,” ACI Struct. J., **98**, No. 3, 359-367 (2001).
31. L. P. Ye , X. Z. Lu, and J. F. Chen, “Design proposals for debonding strengths of FRP strengthened RC beams in the Chinese design code,” in: Proc. Int. Symp. on Bond Behavior of FRP in Structures, Hong Kong, China (2005).

Paper III

"Research Results on RC Walls and Dapped Beam Ends Strengthened with FRP Composites"

By:

T. Nagy-György, V. Stoian, D. Dan, C. Dãescu, D. Diaconu, G. Sas and, M. Mosoarcã

Published in:

Proceedings: FRPRCS-8, Patras, Greece, July, 2007, ISBN 978-960-89691-0-0.

RESEARCH RESULTS ON RC WALLS AND DAPPED BEAM ENDS STRENGTHENED WITH FRP COMPOSITES

Tamas NAGY-GYORGY [1] Valeriu STOIAN [1] Daniel DAN [1] Cosmin DAESCU [1]
Dan DIACONU [1] Gabriel SAS [1] Marius MOSOARCA [2]

[1] Department of Civil Engineering, Politehnica University of Timisoara, Romania
[2] H.I. STRUCT SRL, Timisoara, Romania

Keywords: beams, dapped ends, FRP, strengthening, walls.

1 INTRODUCTION

The paper presents a description of the theoretical studies and the results of the experimental tests carried out on specific reinforced concrete structural elements strengthened with FRP composites. All the experimental work has been carried out in the Civil Engineering Laboratory of the "Politehnica" University of Timisoara, Romania. In the first part of the article, there are described several investigations done on RC plane shear walls with monotonic and staggered openings, while the second part is dedicated to beams with dapped ends strengthened with composites. In both cases there have been performed theoretical and experimental studies.

2 RETROFIT OF RC SHEAR WALLS WITH CFRP COMPOSITES

2.1 Literature review

FPR composite materials have been used in numerous applications worldwide, in order to retrofit structural reinforced concrete (RC) elements, like beams, columns or walls. Despite of this, less attention has been given to the research on the in-plane behaviour of RC wall members with FRP composites. In fact, few teams have carried out proper RC wall experiments. Lombard et al. have applied carbon FRP (CFRP) sheets on vertical and horizontal directions on the side faces of the walls, and then tested them under a predetermined in-plane quasi-static cyclic loading sequence in load control up to the yield load, and then in displacement control at predetermined steps up to failure. Antoniades et al. have used for strengthening both CFRP and glass FRP (GFRP) sheets, applied laterally on vertical direction and in the form of horizontal jacketing, the walls being tested in the displacement control mode. Other similar cases have been studied by Iso et al. in the form of wing walls, by Sugiyama et al. as infill walls and by Paterson and Mitchell for walls strengthening combined with other techniques.

2.2 Objectives

The objectives of the present experimental programme were to investigate the effectiveness of CFRP composites for the seismic retrofit of reinforced concrete shear walls with staggered openings. The application field of this procedure could be the restoring, improving and/or supplying the load bearing capacity of such structural elements before or after an earthquake. There have been studied the behaviour of the strengthened elements, the specific anchorage detail, the strengthening system, the stiffness, the ductility and the collapse mechanism.

2.3 Research programme

In the first part of the study, there have been performed numerical analyses on RC shear walls with staggered openings in the elastic and nonlinear range, in order to determine practical reinforcing solutions for this kind of elements and to obtain better values of their real load bearing capacity. In the design of the retrofitting solution and then in the analyses made on strengthened elements, the contribution of the FRP composites was taken into account in a simplified way, as an equivalent steel reinforcement.

For the experimental test five structural shear walls with staggered door openings were considered. The specimens were 1:4 scale models of typical RC walls designed according to the Romanian prescriptions. The walls were of the cantilever type, had the height of 260cm, width of 125cm, storey height of 65cm and a thickness of 8cm. The opening had the dimensions of 25cm x 50cm. The experimental model foundations and the walls were cast simultaneously. The concrete

compression strength was f_{cm}=50N/mm^2. All the reinforcing bars had a 6 mm diameter, with characteristic strength of f_{sk}=355N/mm^2. There were studied five types of structural walls with different values of α angle (Figure 1).

The elements were subjected to a constant vertical load V=50kN at the top. The horizontal load (H) was applied monotonically for the wall without openings and cyclically for the rest of the elements, in a displacement-controlled mode. The top displacements were increased with an average drift (horizontal top displacement divided by wall height) (details in [14], [15], [16]).

During the first phase, the simple wall (SW) specimens were tested up to failure (concrete crushing, steel reinforcement yielding). By comparing the results, the conclusion might be that all the walls showed a ductile behaviour, only with different failure modes.

The SW1 wall (without openings) failed ductile, in a typical bending way, whereas at the SW8 wall in the first phase appear plastic hinge in the coupling beams and then at the base of the wall. At the SW23, SW45 and SW67 walls, witch have staggered openings, the failure is produced by concrete crushing at the base of the small sidewall, with cantilever-like behaviour of the bigger sidewall.

The conclusion which could be drawn is that the behaviour of the walls with staggered openings is very close to the behaviour of solid walls (without openings) and there is no need for special reinforcing details or increasing of the ductility.

The next phase was the wall retrofitting. The damaged or crushed parts of the walls were replaced with an epoxy based repairing mortar and the existing cracks were filled with an epoxy resin. The next step was the surface cleaning and the creation of the anchorage zone, which was very simple, but as was demonstrated after the test, was very efficient and not presented any degradation. All the walls have been strengthened with unidirectional CFRP composite fabric, on one side. The role of the vertical sheets was to increase the bending capacity, while the horizontal sheets' to restore the shear capacity. The nominal tensile strength of the fabrics was f_{frp}=3900N/mm^2, the nominal Young's modulus E_{frp}=231000N/mm^2 with the strain at failure ε_{frp}=1.7%.

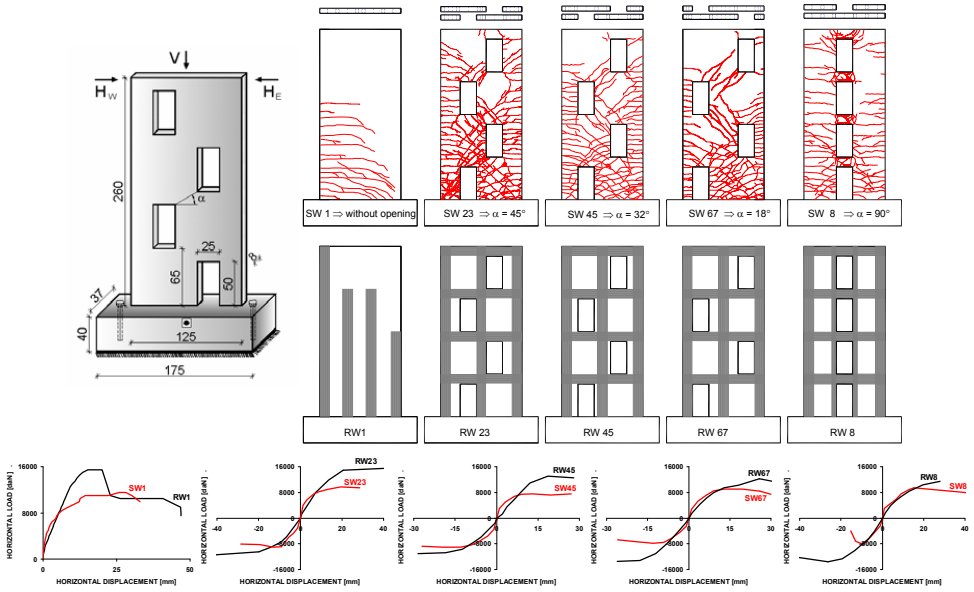

Fig. 1 Geometrical parameters, crack pattern and retrofitting schemes of the specimens.

The SW specimens after the retrofitting were renamed as RW (Retrofitted Wall). For the SW1, the behaviour and the capacity increase was unknown, therefore there were applied 4 vertical aligned sheets with a 150mm width. That was enough to increase the load bearing capacity by 35%, compared with the baseline specimen. Knowing this, for the rest of the walls there was modified the amount of the FRP used. Thus, 3 sheets of 150mm wide were aligned vertically (two in the wall edge and one in its middle) and 4 of a 150mm width were placed horizontally (at the floor level).

The test set-up and the principles of the tests (loading schemes, value of the loads, cycles) for the retrofitted wall specimens (RW) were identical with the baseline specimens' ones (SW). Additional strain gages were attached to the composite in the maximum stress zones and were aligned in the direction of the carbon fibres. By using these instruments, the strain levels could be monitored on the surface of the composite material. The recorded data were the horizontal load, the horizontal displacement, the strain in the composite and the specimens' failure modes.

2.4 Observations regarding to the failure modes of the retrofitted wall (RW) elements

The RW1 element (without openings) was subjected to a monotonic increasing load up to failure, which was produced through CFRP tension failure followed by the debonding of the composite in the compression zone, simultaneously with concrete crushing. The load bearing capacity increased by 35% and the displacement by 42%, but the stiffness decreased by 54%. The measured maximum strain in the FRP was 0.54%.

Failure of the RW23 element subjected to cyclic loads appeared in more steps. First, a small area of composite from the bigger sidewall debonded in compression. The following cycles brought the extension of this area, by producing a horizontal crack close to the anchorage zone. The failure of the specimen was caused by gradual opening of the existing cracks in the concrete, by the debonding in compression of the composite and by the tension failure of the cracked composite. The capacity increased by 58%, respectively by 22%, the displacements increased by over 40% on both directions and the maximum strain in the composite reached 0.63%.

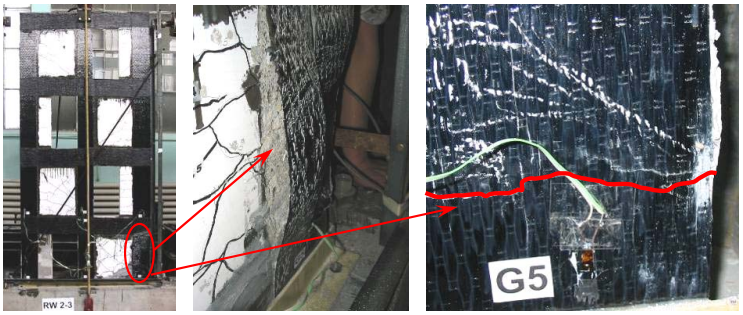

Fig. 2 RW23 wall failure modes.

The failure mode of the RM45 specimen was similar to RW23. In the beginning, the composite from the bigger sidewall debonded under compression, while in the next cycle the FRP failed under tension on a width of 10cm, simultaneously with the composite debonding under compression in the smaller sidewall. During the next two cycles, the crack openings widened and finally there was noticed the tension failure of the composite in the small sidewall, with concrete crushing under compression in the wide sidewall. The capacity increased by 71%, respectively by 19%, the displacements were identical with the baseline specimen and the maximum strain in the composite reached 0.79%.

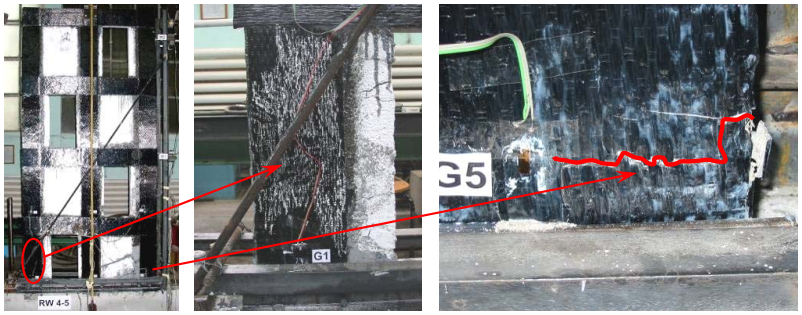

Fig. 3 RW45 wall failure modes.

The specimen RW67 behaved similarly to the previous two walls. The composite began to debond under compression in the bigger sidewall and in the same time a horizontal crack appeared in the composite. During the next cycle, the debonded area continued to extend, in the same time developing a compression crack in the FRP from the smaller sidewall. During the following steps, the major part of the FRP from the biggest sidewall failed under compression, the cracks in the concrete widened, half of the composite from the smaller sidewall also failed under compression and the other half fully debonded. Finally, the entire FRP sheet failed under tension and the concrete crushed under compression. The capacity increased by 48%, respectively by 57%, the displacements were identical with the ones of the baseline specimen and the maximum strain measured in the composite was 0.58%.

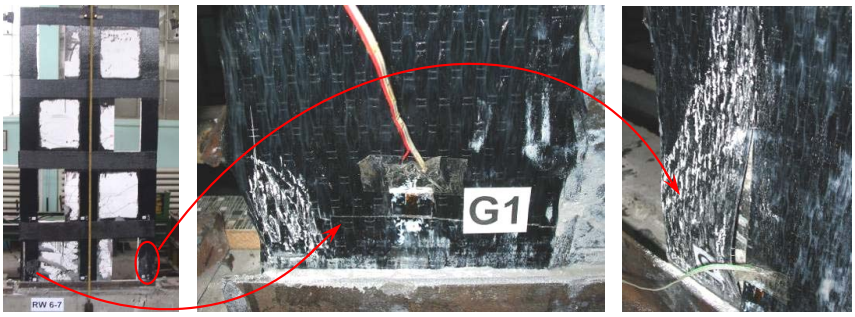

Fig. 4 RW67 wall failure modes.

The SW8 specimen was a coupled shear wall. The failure mode of the wall was different from the previous specimens, due to the coupling beams. During the first phase, it was noticed the debonding of the composite under compression on the right side of the wall, then, after 2 more cycles there became visible a number of X-shaped cracks in the coupling beams at levels 1 and 2, both in the concrete (its back side) and in the resin. The failure of the wall occurred by shearing of the coupling beam after the FRP debonding and the tension failure of the composite in the upper-right side of the wall, followed by the concrete crushing. The capacity increased by 21%, respectively by 63%, the displacements were asymmetric, on one direction decreasing by 33% and on the other increasing by 180%. The maximum strain measured in the composite was 0.83%.

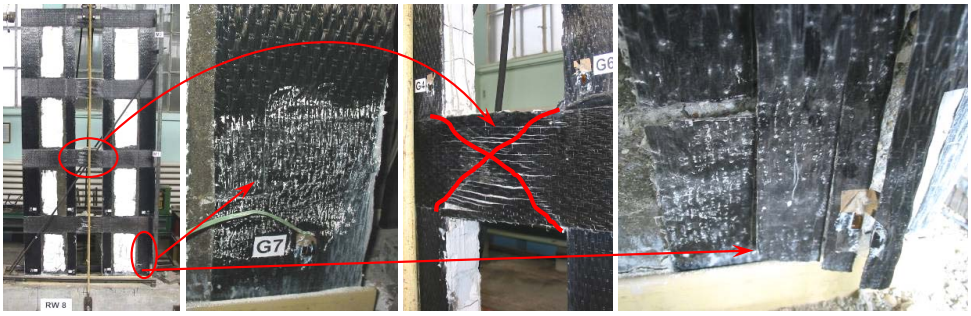

Fig. 5 RW8 wall failure modes.

3 STRENGTHENING DAPPED BEAM ENDS WITH CFRP COMPOSITES

3.1 Literature review

Huang, Nanni et al. accorded a special attention to the behaviour and performance of beams support zones retrofitted with FRP composite materials, by studying dapped-ends strengthened using externally bonded CFRP sheets with and without end anchors in two different configurations. There was demonstrated that the externally bonded FRP strengthening systems represent a viable solution

in retrofitting / repairing applications. Gold et al. have obtained successful practical uses of carbon FRP to strengthen dapped beam ends. Several methods for strengthening the double tees were investigated including external post-tensioning, steel plate and steel angle bonding, as well as externally bonded FRP reinforcement. In order to verify the addition of shear strength to the double tees, a load testing program was carried out. Tan studied several schemes for strengthening in shear of dapped beams in order to increase the imposed loads. Tests were carried out on beams strengthened with carbon FRP plates, carbon fibre sheets or glass fibre fabrics. The results indicated an increase in the ultimate load, with the observation that the use of anchorage bolts in the carbon plate system at the critical location could lead to further enhancement. Similar experimental tests were performed on corbels by Elgwady et al. Within an experimental program, they studied the effectiveness of using CFRP laminates in order to increase the load bearing capacity of corbels. Six elements were tested, with different strengthening configurations. The results indicated the potential of improving the capacity of these types of elements.

3.2 Objectives

The research program was carried out in order to study the pre-stressed concrete beam support zone with dapped-ends, retrofitted with different externally bonded FRP composite systems, based on several specific theoretical and experimental investigations. The theoretical calculus for the un-retrofitted elements was made both in the linear and nonlinear ranges, correlated with the results of the strut-and-tie models. The strengthening was designed so as to increase the service load of the dapped-ends by 20%, in terms of displacement and strain level in steel reinforcement, without a significant modification of the stiffness. For this reason, four full scale dapped beam ends were tested.

3.3 Research programme

Preliminary dimensioning and detailing of the studied dapped beam end were performed according to the Romanian standards and verified with those from EC2, ACI318 and PCI, in order to reach the bearing capacity of 800kN. The beam height was 150cm, the dapped zone had 80/80cm and the element width was 66cm. The dapped-end was reinforced by using horizontal and vertical stirrups.

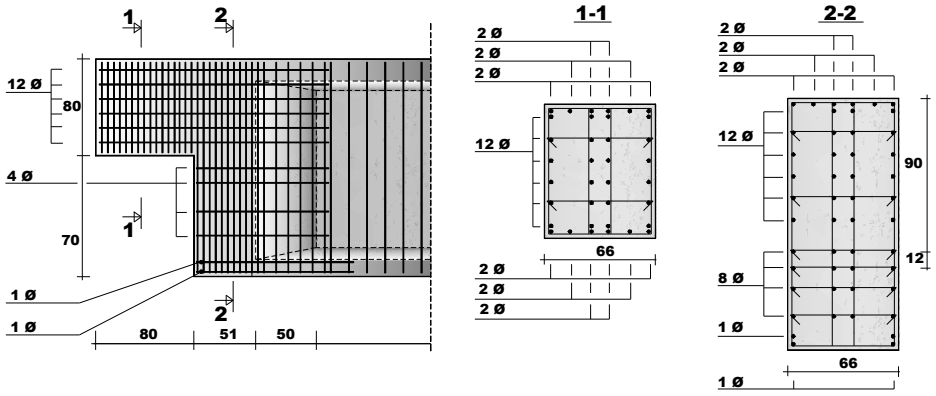

Fig. 6 Details and dimensions of the studied element**.**

In the theoretical model, the characteristic strengths of the concrete and of the steel reinforcement were used. The elastic analysis was performed so as to obtain the level and the distribution of stresses in the concrete. The load level corresponding to the yielding limit in the horizontal reinforcement resulted in 1150kN. The nonlinear analysis gave the crack pattern at different load levels, the failure load and the collapse mechanism of the element. The yielding level in the horizontal reinforcement was achieved at the load level of 900kN. In order to check the obtained results, there was used an alternative strut-and-tie modelling, which also allowed the determination of the necessary steel reinforcement. Since the steel reinforcement was known, the analysis was performed just to determine the maximum force applied on the element at the moment when the dapped-end's horizontal bars started to yield.

Within the experimental phase of the programme, two dapped beams with the same dimensions

and internal reinforcement were manufactured for the experimental tests. Since the research focused on the dapped beam ends, the mid-span was over-reinforced. Before casting, two strain gages were added near the re-entrant corner, one to the horizontal reinforcement (S1) and the other to the vertical stirrup (S2). The dapped-ends were tested one by one in an experimental stand, as shown in Fig. 7.

The first element C1 was tested prior to the failure, this being considered the reference element, while the other elements (C2, C3, C4) were tested up to 800kN, this being the yielding level of the horizontal reinforcements from the cantilever zone. The monotonic increasing load was applied through a hydraulic system, in the force-control mode.

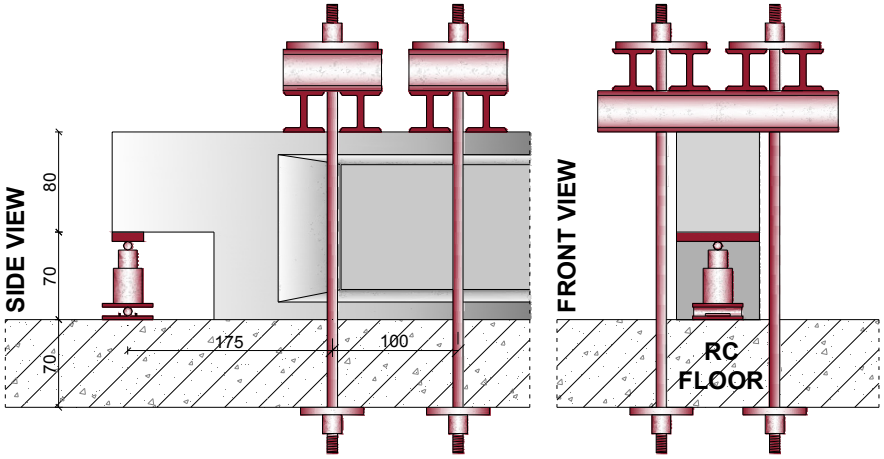

Fig. 7 The specimens test setup – side and front view.

The strengthening of the elements was done by using three systems of CFRP composites, in four different retrofitting solutions, in order to increase the service load by 20%. After the hardening of the composite, strain gages (G3÷G5) were attached in order to evaluate the stresses. The data recorded during the tests were: the vertical load and the displacements, the strains in the composite and in the steel reinforcements, as well as the elements' failure modes. An identical test set-up was used for both the un-strengthened specimens (C) and the retrofitted ones (RC).

The strengthening of the C1 element was performed by using the system (1), the system (3) for C3, and both solutions were composed of 30cm wide unidirectional carbon fibre fabric, applied in 3 layers on both sides, on the 45°/0° /90° directions. The strengthening of the C2 and C4 elements was made by using system (2), composed by pairs of 10cm wide carbon fibre plates, applied on both sides. For specimen C2, the plates were applied on the 45° and 90° directions, while for C2 on the 0° and 90° directions. The length of the horizontal and the inclined plates was limited by the sectional change of the web.

Table 1 Characteristics of the composite systems used.

System (Element)	Components	Tensile Strength [N/mm^2]	Tensile Modulus [N/mm^2]	Strain at Failure [‰]
System 1 (RC1)	Fabric	4100	231000	17
	Resin	30	3800	-
System 2 (RC2/RC4)	Plate	2800	165000	17
	Resin	30	12800	-
System 3 (RC3)	Fabric	2600	640000	4
	Resin	45	3500	15

During the first phase, the elements showed similar behaviour with respect to the maximum force and deflection. The design value of the serviceability limit state was of 800kN. For this value of the experimental load, we have observed the following: (a) the stress level recorded in the reinforcement

was comparable for all the experimental elements; (b) a good similarity was noted between the crack patterns of all specimens, and the general aspect was identical.

Specimen C1 was tested close to failure and later referred to as a control element. The final crack pattern was distributed uniformly around the re-entrant corner, as expected. Unfortunately, the strain gages attached to the reinforcement did not function. The peak load was 1600kN. After that, the specimen was retrofitted and retested. The specimen RC1 showed a linear behaviour up to 1600kN, when there were observed the first fibre ruptures. The maximum load reached was of 1780kN and then, until the collapse, a long yielding level (approx. 14mm) followed. The failure was ductile, produced by successive breaking of the carbon fibres along a principal crack, and not due to fibre debonding or delamination. In the same time, in the compressed area, the concrete crushed at the maximum load.

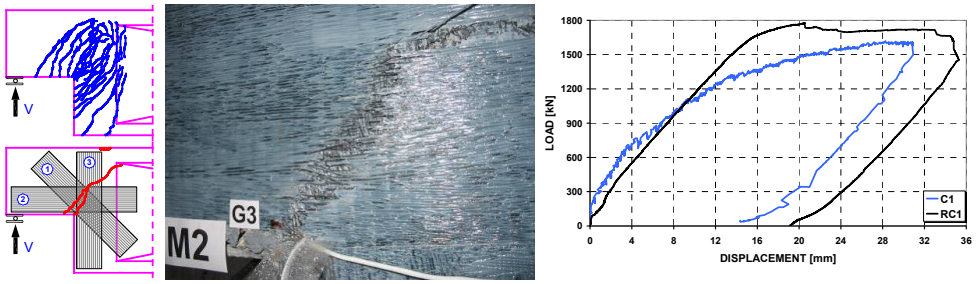

Fig. 8 Crack patterns, failure detail and load-displacement curves of the C1 and RC1 elements

Specimen C2 was tested up to 800kN. Strain gages attached to the steel reinforcement (S1) indicated 1.87‰, which meant that it was at the yielding level. After that the specimen was retrofitted and retested. The specimen RC2 showed a linear behaviour up to 1300kN, when, except for some cracks, it developed a crack around the inclined plates, which, for a small increase in load (1430kN), lead to the peeling-off. The element resisted up to 1760kN, when the vertical plates failed brittle through peeling-off, too. The maximum measured strain in the steel reinforcement was 2.59‰ at 1480kN and 1.87‰ at 1160kN, which indicated an increase of the service load by 45%, compared with the same strain level of the reference specimen (C2). The maximum strain in the composite reached the percentage of 7‰, which corresponds to 41% of the composite's ultimate value.

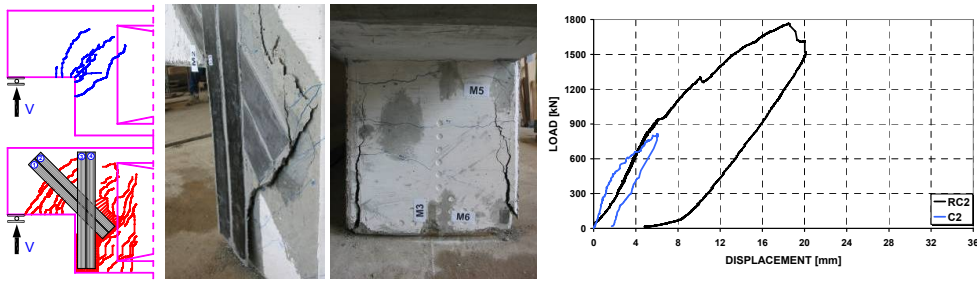

Fig. 9 Crack patterns, failure detail and load-displacement curves of the C2 and RC2 elements.

Specimen C3 was tested up to 800kN. Strain gages attached to the steel reinforcement (S1) indicated 1.95‰, which meant that it was at the yielding level. After that, the specimen was retrofitted and retested. The specimen RC3 showed a linear behaviour up to 900kN, but, starting with 640kN, there was observed the composite's step-by-step failure through an inclined crack, which could be observed also in the load-displacement curve. The curve aspect is very close to the one of the C1 specimen, without significant differences over 1000kN. The strain gages attached to the composite were out of work after 500kN. However, comparing the maximum strain in the steel reinforcements in C3 at 800kN with the same level in RC3, it could be noticed an increase of the service load by 25÷50%. The maximum load and remnant displacement were identical with the one from C1. The

failure was ductile, produced by successive breaking of the carbon fibres along the main crack.

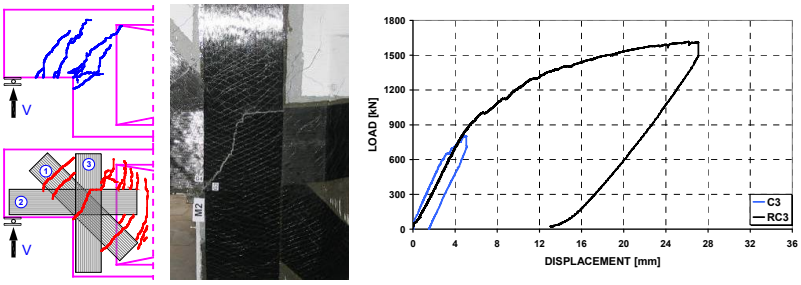

Fig. 10 Crack patterns, failure detail and load-displacement curves of the C3 and RC3 elements.

Specimen C4 was tested up to 800kN. Strain gages attached to the steel reinforcement (S1) indicated 1.44‰, showing that it was at the yielding level. After that the specimen was retrofitted and retested. The specimen RC4 showed a linear behaviour up to 980kN, when the first new crack appeared. At 1190kN, a crack developed around the horizontal plates. The element failed at 1690kN, through de-bonding of the vertical plates, followed by an immediate peeling-off of the horizontal plates. The maximum measured strain in the steel reinforcement was 3.78‰ at 1530kN and 1.44‰ at 1000kN, which indicated an increase of the service load by 25%, compared with the same strain level of the reference specimen (C2). The maximum strain in the composite reached 6.72‰, which corresponded to 40% of the composite's ultimate value.

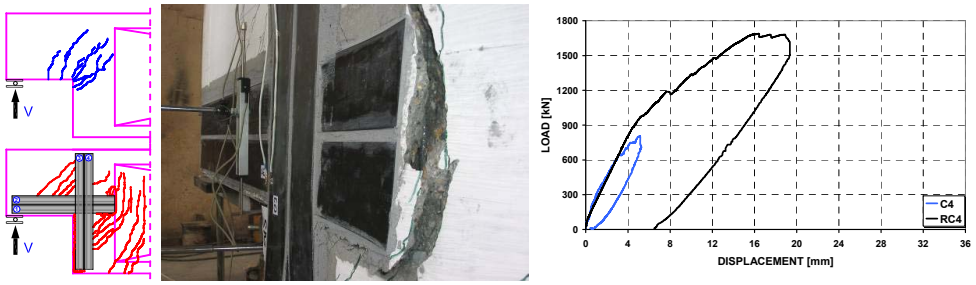

Fig. 11 Crack patterns, failure detail and load-displacement curves of the C4 and RC4 elements.

4 CONCLUSIONS

4.1 Conclusions regarding RC wall retrofitted with composite

Based on the studies performed and on the behaviour of the tested specimens, the following conclusions have been drawn:

- The load bearing capacity of the damaged walls retrofitted on one side with CFRP increased considerably over the baseline value (practically, the load bearing capacity of the pre-tested walls was negligible), it being completely restored.
- The strain in the composite indicates the major contribution of the CFRP in the load bearing capacity of the walls, the average recorded value being 0.54 ÷ 0.84%.
- The failure of the retrofitted wall was caused by the gradual opening of the existing cracks, by debonding of the FRP under compression followed by tension, or in some cases by compression of the FRP.
- The maximum horizontal displacements of the retrofitted walls were generally higher, or at least equal with those of the baseline specimens.
- The results highly depended on the initial state of the un-retrofitted element (width and number of cracks, yielded steel reinforcement, rehabilitation method and material), and on the evaluation

method. Based on the used method for the characteristics' evaluation (such as the stiffness, ductility, elastic limit), the following results were obtained (Tab. 1):
  - the elastic limit of the walls increased, in average, by 47%;
  - the failure load of the walls increased, in average, by 45%;
  - the stiffness of the elements decreased, in average, by 53%;
  - the ductility of the elements decreased, in average, by 60%;
- The anchorage system behaved excellently, without degradations.
- RC walls subjected to seismic forces showed ductile failure. Retrofitting such structural elements with composites preserves the characteristic ductile behaviour, but at the maximum load they fail brittle.

4.2 Conclusions regarding dapped beam ends retrofitted with composite

Based on the studies performed, respectively on the behaviour of the tested specimens, the following conclusions were drawn:

- The used theoretical models approximate with sufficient accuracy the un-strengthened elements' behaviour;
- The FRP systems used for the retrofitting of the elements proved to be viable for these kinds of applications, increasing the service load by 25% for RC3, 40% for RC4 and 45% for RC2 (compared with the reference strain in the steel reinforcement at 800kN), consequently demonstrating the effectiveness of the solutions used.
- The maximum load bearing capacity of the elements increased by 11% for RC1, 10% for RC2, 6% for RC4 and 0% for RC3. Further increase of the ultimate load could have been reached by supplementing the fabric cross-sectional area in the case of RC1 and RC3 and by using anchorages for plates in the case of RC2 and RC4.
- Elements strengthened with fabrics failed more ductile compared to those retrofitted with plates.
- The strengthened elements show a delay in cracking, the failure occurring by peeling-off the horizontal or inclined plates, of by fibre rupture along the main diagonal crack in the case of fabric strengthening.
- With respect to the baseline specimen (C1), the maximum displacement had a very close value for fabric retrofitted elements, but a decreased value, by more than 30%, in the case of plate retrofitted elements.

ACKNOWLEDGEMENTS

The research work was granted to some extent by the National University Research Council, Romania. The authors would also like to thank SIKA Romania Corporation for the composite systems offered to be used in the experimental tests.

REFERENCES

[1] Antoniades, K.K., Salonikios, T.N. and Kappos, A.J., "Cyclic Tests on Seismically Damaged R/C Walls Strengthened Using FRP Reinforcement", *ACI Structural Journal*, 100, 4, 2003, pp. 510-518.

[2] Antoniades, K.A., Salonikios, T.N. and Kappos, A.J., "Tests on seismically damaged R/C walls repaired and strengthened using FRP's", *Journal of Composites for Construction*, ASCE, 9, 3, 2005, pp. 236-246.

[3] Antoniades, K.K., Salonikios, T.N. and Kappos, A.J., "Inelastic Behaviour of FRP-Strengthened R/C Walls with Aspect Ratio 1.5, Subjected to Cyclic Loading", *Concrete Structures in Seismic Regions - fib Symposium*, Athens, Greece, 2003.

[4] Antoniades, K.A., Kappos, A.J. and Salonikios, T.N., "Inelastic Response Characteristics of Repaired R/C Walls Strengthened with FRPs", *Proceedings of the Second fib Congress*, Naples, Italy, 2006.

[5] Antoniades, K.A., Salonikios, T.N. and Kappos, A.J., "Estimating strength of FRP-strengthened RC walls, *fib Symposium - Keep Concrete Attractive*, Budapest, Hungary, 2005, pp. 436-443

[6] Chen, B.S., Hagenberger, M.J. and Breen, J.E., "Evaluation of Strut-and-Tie Modeling Applied to Dapped Beam with Opening", *ACI Structural Journal*, 99, 4, 2002, pp. 445-450.

[7] Elgwady, M.E., Rabie, M. and Mustafa, M.T., "Strengthening of Corbels Using CFRP - an experimental program", *3rd International Conference for Composite in Infrastructure (ICCI'02)*,

San Francisco, USA, 2002, paper no. 013.

[8] Gold, W.J., Blaszak, G.J., Mettemeyer, M., Nanni, A. and Wuerthele, M.D., "Strengthening Dapped Ends of Precast Double Tees with Externally Bonded FRP Reinforcement", *ASCE Structures Congress*, Philadelphia, USA, 2000.

[9] Huang, P.C. and Nanni, A., "Dapped-End Strengthening in Precast Prestressed Concrete Double Tee Beams with FRP Composites", *Report CIES 99-15*, University of Missouri-Rolla, 1999.

[10] Huang, P.C., Myers, J.J. and Nanni, A., "Dapped-End Strengthening in Precast Prestressed Concrete Double Tee Beams with FRP Composites", *Proceeding, 3rd International Conference on Advanced Composite Materials in Bridges and Structures*, Ottawa, Canada, 2000, pp. 545-552.

[11] Hwang, S.J. and Lee, H.J., "Strength Prediction for Discontinuity Regions by Softened Strut-and-Tie Model", *Journal of Structural Engineering*, 2002; 12(128), pp. 1519-1526.

[12] Iso, M., Matsuzaki, Y., Sonobe Y., Nakamura H. and Watanabe M., "Experimental study on reinforced concrete columns having wing walls retrofitted with continuous fiber sheets", *Proceedings of the 12th World Conference on Earthquake Engineering*, New Zealand, 2000, paper no. 1865.

[13] Lombard, J., Lau, D., Humar, J., Foo, S. and Cheung M., "Seismic strengthening and repair of reinforced concrete shear walls", *Proceedings of the 12th World Conference on Earthquake Engineering*, New Zealand, 2000, paper no. 2032.

[14] Moşoarcă, M., "Contributions in design and detailing of reinforced concrete structural walls", *Ph.D. Thesis*, "Politehnica" University of Timişoara, Romania, 2004.

[15] Nagy-György, T., "Using the FRP Composite Materials for Strengthening of Brick Masonry and Reinforced Concrete Elements", *Ph.D. Thesis*, "Politehnica" University of Timişoara, Romania, 2004.

[16] Nagy-György, T., Moşoarcă, M., Stoian, V., Gergely, J. and Dan D., "Retrofit of reinforced concrete shear walls with CFRP composites", *fib Symposium - Keep Concrete Attractive*, Budapest, Hungary, 2005, pp. 897-902.

[17] Paterson, J. and Mitchell, D., "Seismic retrofit of shear walls with headed bars and carbon fiber wrap", *Journal of Structural Engineering*, 129, 5, 2003, pp. 606-614.

[18] Stoian, V., Nagy-György, T., Dăescu, C. and Diaconu, D., "Theoretical and experimental study of prestressed concrete beam support zone strengthened with composite materials", *Proceedings of the Second fib Congress*, Naples, Italy, 2006.

[19] Stoian, V., Nagy-György, T., Dan, D., Gergely, J. and Dăescu, C., "Composite Materials for Constructions", *Ed. Politehnica*, Timişoara, Romania (in Romanian), 2004.

[20] Sugiyama, T., Uemura, M., Fukuyama, H., Nakano, K. and Matsuzaki Y., "Experimental study on the performance of the RC frame infilled cast-inplace non- structural RC walls retrofitted by using carbon fiber sheets", *Proceedings of the 12th World Conference on Earthquake Engineering*, New Zealand, 2000, paper no. 2153 (CD-ROM).

[21] Lu, W.Y., Lin, I.J., Hwang, S.J. and Lin, Y.H., "Shear Strength of High-Strength Concrete Dapped-end Beams", *Journal of the Chinese Institute of Engineers*, 5, 26, 2003.

[22] Tan, K.H., "Shear strengthening of dapped beams using FRP systems", *Fifth International Symposium on Fibre Reinforced Plastics for Reinforced Concrete Structures (FRPRCS-5)*, Cambridge, UK, 2001, 1, pp. 249-258.

Paper IV

"FRP strengthened RC panels with cut-out openings"

By:

G. Sas, I. Demeter, A. Carolin, T. Nagy-György, V. Stoian and B. Täljsten

Published in:

Proceedings: Challenges for Civil Construction, Porto, Portugal, ISBN: 978-972-752-100-5, April 2008.

CCC 2008 - Challenges for Civil Construction
Torres Marques et al. (Eds)

FRP STRENGTHENED RC PANELS WITH CUT-OUT OPENINGS

Gabriel Sas[*], István Demeter[†], Anders Carolin[*], Tamás Nagy-György[†], Valeriu Stoian[†] and Björn Täljsten[**]

[*] Division of Structural Engineering (SHB)
Luleå University of Technology
971 87 Luleå, Sweden
e-mail: gabriel.sas@ltu.se, web page: http://www.ltu.se

[†] Faculty of Civil Engineering (CCIA)
Politehnica University of Timişoara
2A T. Lalescu 300223 Timişoara, Romania
e-mail: istvan.demeter@ct.upt.ro, web page: http://www.ct.upt.ro

[**] Division of Structural Engineering (BYG)
Technical University of Denmark
DK-2800 Kgs. Lyngby, Denmark
e-mail: bt@byg.dtu.dk, web page: http://www.byg.dtu.dk

Keywords: Strengthening, FRP, Reinforced Concrete, Shear Walls, Cut-out Openings.

Summary: *A strengthening solution for multi-storey buildings in seismically active regions is considered. The Precast Reinforced Concrete Large Panel (PRCLP) structural system is described. Besides earthquakes, different problems during the last decades were identified in the PRCLP structural behaviour: design mistakes, neglected health monitoring, construction problems, change of use for example cut-out openings. The presented study is a part of an ongoing research program which deals with the influence of the Fibre Reinforced Polymer (FRP) strengthening on the behaviour of Precast RC Wall Panels (PRCWP) with cut out openings subjected to cyclic (seismic) and normal (gravity) loading. In this paper a brief literature survey concerning RC walls strengthened by FRP is presented and the experimental tests setup is discussed. The wall specimens were designed according to the 1981 Romanian code. Tests are described and a discussion based on previous experimental work on shear walls is undertaken and future research is suggested.*

1 INTRODUCTION

Precast Reinforced Concrete Large Panel structures are one of the most common structural systems in seismically designed buildings constructed in Romania from nineteen fifty to late nineteen ninety [1]. Nowadays, functionality modifications of the structures are often encountered. New windows, doors or paths for ventilation or heating systems demands openings in walls. Small openings do normally not create any effect on the structural behaviour, mainly due to the stress redistribution capability. However, in the case of larger openings the stress distribution induced by lateral (in-plane) or vertical loads may change. This happens when considerable amount of concrete and reinforcing steel have to be removed, so that the structural wall is no more capable to transfer forces. Thus, a strengthening of the structure is imposed to recover the initial capacity. Traditional strengthening methods, such as bordering of reinforced concrete/steel frame system, may not be architecturally convenient or fulfil the functionality of the opening. It is therefore suggested that FRP systems are used for shear wall retrofitting when openings are made.

2 LITERATURE REVIEW

FRP, epoxy bonded on the surface of reinforced concrete structures, has been proved in time to be an efficient and viable strengthening method [2,3,4,5]. The major advantage of the FRP strengthening of walls comes from the high speed application, low weight-strength ratio and low costs. Special attention must be given when strengthening an already made opening since a strain field already exists around the opening.

One of the first FRP strengthening of RC walls was reported by Ehsani and Saadatmanesh [6]. A concrete building was retrofitted using glass fibres following the '94 Northridge earthquake. Out-of-plane flexural failure was recorded immediately after the earthquake. The major cause of the failure was considered the horizontal forces acting perpendicular to the plane of the wall while stiffness redistribution of the structure occurred.

Bond properties between Carbon Fibre Reinforced Polymer (CFRP) and concrete on adjacent RC wall panels connected through CFRP were experimentally studied by Volnyy and Pantelides [7]. A series of nine tests on full scale precast RC wall under in-plane horizontal cyclic quasi-static load was conducted. Three main modes of failure were reported: fibre failure of the composites, "cohesive failure" (delamination of the fabric from the concrete surface) and concrete surface shear failure. The measurements showed a low utilization of the fibres i.e. 1200 micro strains. The strains had a zero value at a length of 125 mm measured in the direction perpendicular to the crack from the tip of the crack. This value was defined as experimental effective anchorage length and considered in good agreement with the theoretical values.

The feasibility of CFRP strengthening and rehabilitation of reinforced concrete shear walls was studied by Lombard et al [8]. Four walls were tested in a quasi static cyclic load sequence in load control up to yielding and displacement control up to failure, respectively. Based on the experimental observations an empirical theoretical model was developed to predict the load – displacement envelope of reinforced concrete shear walls strengthened with CFRP. The flexural and shear deflection at the top of the wall are considered as the most important parameters. A correlation between the cantilever beam behaviour and the shear wall behaviour is considered to derive the model. A partial factor is introduced to account the inelastic behaviour of the concrete, the non-linear distribution in the wall and the load resistant effect of the carbon fibre sheets. Model predictions were in good agreement with experimental result performed.

Sixteen scaled specimens of RC columns with wing walls were tested in simulated seismically loading (in-plane cyclic displacement control and vertical load) to investigate the shear reinforcing effect of the externally bonded carbon and aramid FRP sheets by Iso et al. [9]. Authors reported a linear increase of the shear capacity with the increase of composites layers. However, a limitation of the retrofitting effects of FRP sheets on the element's ultimate shear capacity was found.

Seismic behaviour of non-structural reinforced concrete walls with openings, strengthened using FRP composite sheets, was studied by Sugiyama et al. [10]. A series of tests were conducted on eight 1:3 scale specimens. Shear failure was reported as governing mechanism of collapse followed by debonding of CFRP at approximately 15 mm lateral displacement. The non-structural reinforced concrete walls were compared with a structural RC shear wall and an independent RC frame. Authors concluded that even if the load bearing capacity of the non-structural walls was not increased, the overall behaviour of the frame-wall assemblies was improved in terms of serviceability limit state parameters.

In two series of tests Antoniades et al. [11,12] analyzed the results of seismic loading on reinforced concrete walls strengthened with FRP. A series of different anchorage methods were used to provide the force transfer from the applied FRP strengthening system to the foundation. The walls, designed according to modern code provisions, were subjected to in plane cyclic loading up to failure. The dominant failure mode in all cases was flexural with local anchorage failure.

Paterson and Mitchell [13] conducted an experimental program on four cantilever reinforced concrete walls in order to investigate the effectiveness of the combined strengthening using FRP wrapping, headed reinforcement and reinforced concrete collars. Test showed a flexural failure in all

four cases. Difference was made in the type of failure; unstrengthened walls by brittle lap splice failure while companion i.e. strengthened specimens had gradual strength degradation.

An innovative strengthening method of reinforced concrete walls using aramid fiber reinforced polymers (AFRP) was performed by Kobayasi [14]. AFRP bundles were passed through drilled holes on a diagonal path. Shear failure was reported in all the cases. A 25% increase of the shear load was noted. The author considered the research as having a valuable significance also from economical point of view i.e. reduced consumption of material and easier to apply.

In order to validate finite element analysis (FEA) Li et al. [15] tested a 1:5 scale reinforced concrete shear wall strengthened with Glass Fibre Reinforced Polymers (GFRP). After an initial test of the wall the strengthening was applied and subjected to a cyclic loading. The FEA was based on three key parameters for the material behaviour. Concrete was defined using damaged plasticity criterion. GFRP was implemented using SPRING elements. The reinforcing steel rebars were supposed to behave as a perfect elasto-plastic material. The material parameters were determined from tests. Good correlation between FEA and experimental test was reported. Shear failure was observed as dominant failure mode followed by GFRP debonding and rupture. As secondary failure mode flexure at the toe edges were reported in the real test represented by concrete spalling, concrete crushing and horizontal cracks development.

Following a pattern of a real four stories building arrangement (i.e. different positions of doors and windows), five 1:4 scale reinforced concrete walls specimens, strengthened with FRP were tested by Nagy-György et al. [16]. Since three out of five specimens had an unsymmetrical geometry the test results were dependent on the loading direction. The effect of the strengthening was evaluated by average values (relative to baseline records). The elastic limit increased by 47%, average failure load increased by 45%, average stiffness decreased by 53% and average ductility decreased by 60%.

3 EXPERIMENTAL PROGRAM

3.1 General description

A typical construction of precast reinforced concrete large panels is presented in Figure 1. The shear walls panels are distributed in both transversal and longitudinal directions at span range between 3 to 5.4 m (Figure 2). Their height varies from four to eight stories. The main destination of these buildings is private housing. Changes of society imposed modifications in their original purpose i.e. commercial activities started to develop primarily at the ground floor of the buildings imposing structural modifications of the walls. The internal space reconfiguration and new access ways demand were achieved by cutting out new or enlarging existing openings in the structural walls. All the modifications affected the global behaviour of the entire structure, causing load redistribution toward the adjacent members. This affects the load bearing capacity of the structure when subjected to seismic loadings.

Figure 1: Typical PRCLP building

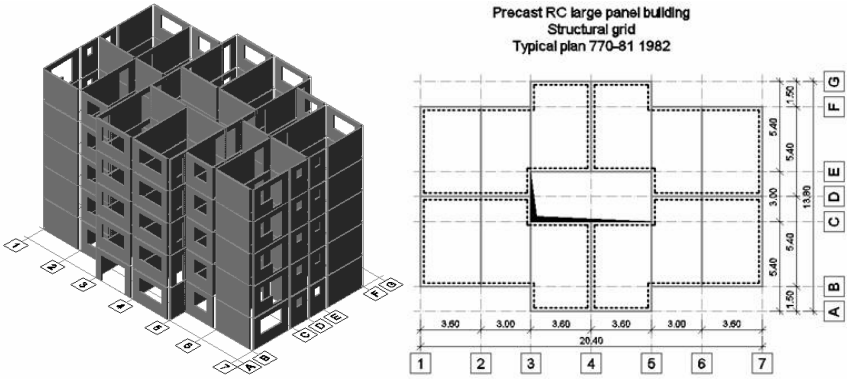

Figure 2: Distribution and arrangement of the walls and the structural grid of the typical plan

3.2 Experimental elements description

A selection of 50 different practical configurations of existing and possible openings in walls was found. From all specimens two sets were selected, according to the proposed loading configurations. The first set, consisting of 8 wall panels, is aimed to be tested with loads that reproduce the seismic action, i.e. horizontal loading. The elements are highlighted in red in the Figure 3. The second set highlighted in blue, includes 4 wall panels, and is intended to be loaded only with vertical loads.

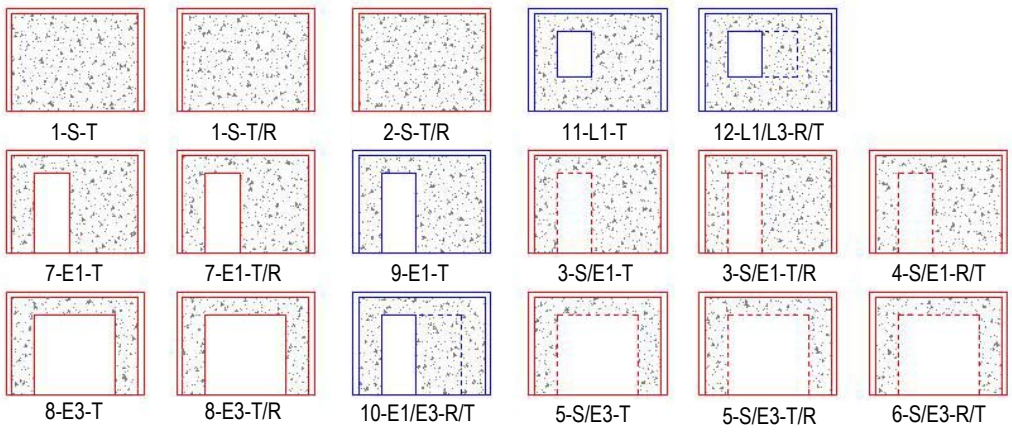

Figure 3: Experimental walls

The denominations of the experimental elements are including the next set of variables (Figure 4):

a) Opening type: solid wall-"S", narrow door-"E1", narrow window-"L1" wide door-"E3", wide window "L3"
b) Opening nature: original or cut-out. For example element 12 is obtained from a specimen with initial narrow window by enlarging to a wide window (L1/L3)
c) Strengthening order: not strengthened-"T", prior damage-"R/T" and post damage-"T/R".

These variables generate a total of 13 tests for the 1st set and 4 tests for the 2nd set respectively. As elements nr 1, 3, 5, 7 and 8 are tested twice and nr 2, 4, 6, 9, 10, 11, 12 only once.

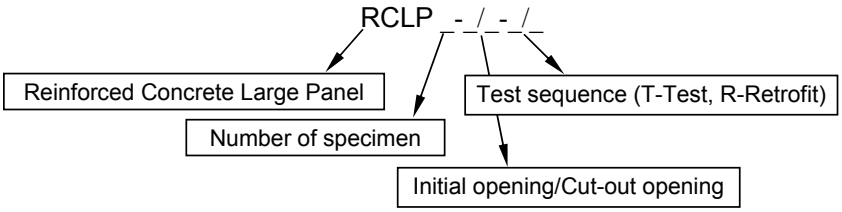

Figure 4: Denomination of the experimental elements

Due to economical, technical and loading limitations the walls were designed and executed at 1:1.2 scale. All the walls had the same dimensions 2.75x2.15x0.10 m. The reinforcement details were provided by a typical plan (Figure 5), using steel welded wire mesh and steel reinforcement. The diameters of steel reinforcements varied for different types of wall from 6 millimetres to 16 millimetres, respectively. The welded mesh contained steel rebars of 4 millimetres diameter. A normal concrete class, C20, was chosen for casting the elements having a characteristic compressive strength of 20.5 N/mm^2. The proposed strengthening system is the externally bonded carbon FRP fabrics. Further details regarding the strengthening arrangement will be available when the failure mode of plain specimens is assessed. Configurations of the detailing are given in Figure 5. Please note that the FRP strengthening is only for qualitative purpose.

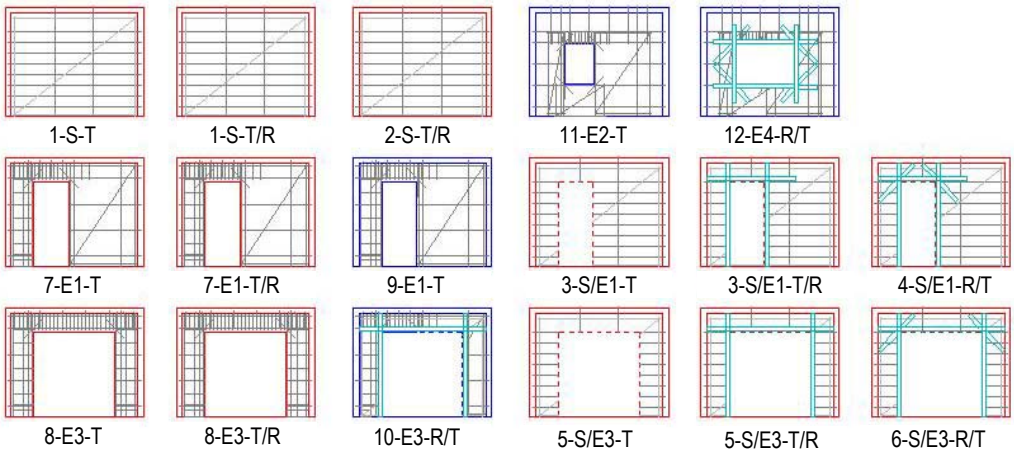

Figure 5: Detailing of the walls

3.3 Test procedure and test set-up

To simulate the earthquake loading, a standard cyclic in plane loading procedure has been defined [17]. The walls will be tested in load control up to the first yielding of the steel reinforcement. Then a displacement control will be applied in three cycles for each ductility level (defined relative to yield or cracking displacement) up to failure. The effect of the gravity load on the walls will be determined considering a monotonic vertical loading up to failure.

The experimental program is divided in two main directions based on the opening's nature. The

first series of experiments contain walls with initial openings tested up to failure. The damaged specimens will be repaired and retrofitted and then retested. The objective of this procedure is to analyze the efficiency of a post earthquake FRP strengthening. The second series of experiments will be focused on the tests of the walls with cut out openings. The walls will be strengthened in the following sequence: prior to damage (i.e. unstrengthened state) and post damage (similar to the first set). The effect of the strengthening on the reinforced concrete walls subjected to earthquake excitation will be monitored.

In order to consider the effect of the adjacent walls, two vertical reinforced concrete boarding elements were designed.

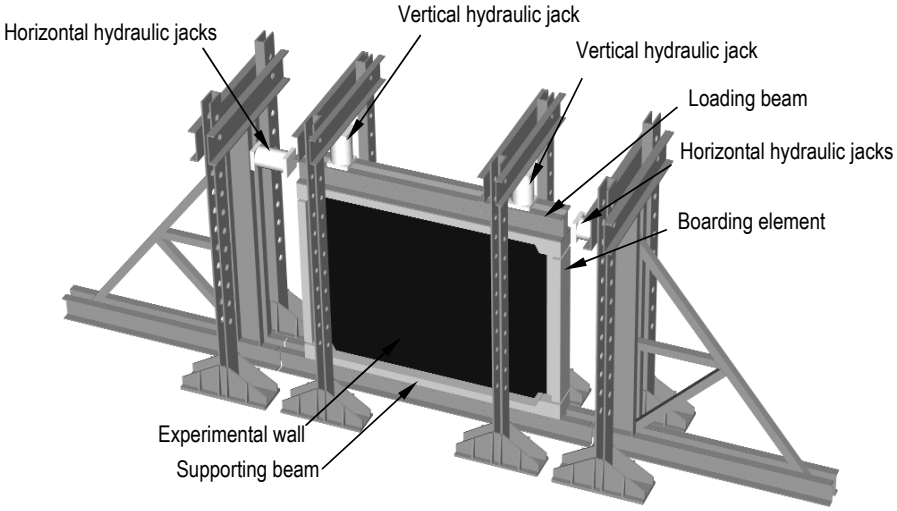

Figure 6: Detailed element assembly

The specimens are supported, on a heavily reinforced concrete beam. The cyclic horizontal loading and the constant vertical pressure is applied by means of hydraulic jacks using a composite steel reinforced concrete beam at the top of the walls. The force transfer between the wall and the loading beam is provided by the discontinuous surface of the elements. High strength mortar is casted in-between the walls the loading beam and supporting beam, respectively. The experimental element assembly and the stand set-up are presented in Figure 6.

Monitoring of the behaviour of the experimental elements is performed. The position of the devices and the measurement equipment differs from element to element. Strain gages are placed on the steel reinforcement surrounding the openings. Strains will be measured on the FRP at the position corresponding to the reinforcement strain measurement. In this way a comparison can be performed between the utilization of the fibres and the steel reinforcement. The global behaviour is monitored using displacement sensors. The vertical and horizontal displacement is recorded in the key regions: bottom of the wall, top of the wall, inferior and superior edges of the openings, respectively.

A preliminary FEA was carried out using BIOGRAF program [18], in order to predict the behaviour of the unstrengthened experimental specimens. The horizontal load-displacement curves presented in the Figure 7 shows the differences between the initial stiffness and the stiffness corresponding to ultimate shear capacity of the wall assemblies when subjected to monotonic horizontal forces.

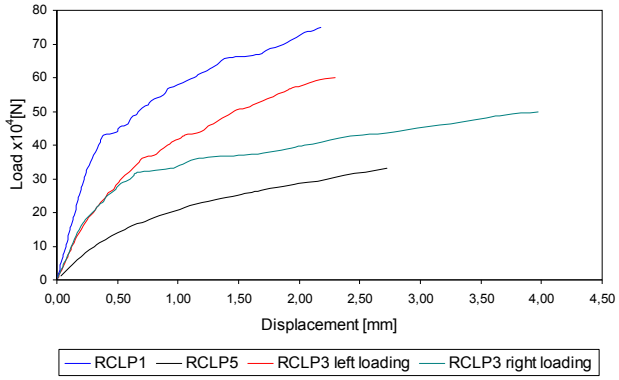

Figure 7: Load displacement curves

4 DISCUSSION AND FUTURE RESEARCH

Reinforced concrete walls have two major failure modes when loaded in their plane. Shear failure is associated with the development of diagonal cracks perpendicular to the maximum tensile stress. The flexural failure is generally described by horizontal parallel cracks and the corresponding compressive force in concrete.

The behaviour of reinforced concrete walls with cut-out openings and strengthened with FRP is not fully covered up to this moment. The previous experimental investigations performed during the years are covering a wide range of variables i.e. mechanical properties of the concrete and reinforcement steel bars, geometric shape of the element, the reinforcement ratio and configuration, the confinement of the concrete, restraints of the element and the position and evolution of loadings. Unfortunately few specifications are given for critical parameters as the anchorage length, the position of the strengthening with respect to the opening, the type of the FRP used (sheets, laminates or near surface mounted reinforcement) and their material characteristics (high strength, high modulus).

The classical methods for monitoring i.e. strain measurements and displacement recording are offering a good view of the behaviour just in local regions. Global distribution of the strains cannot be captured using these methods. Photometric measurement is intended to be used [19] to overcome the above inconvenient.

Although finite element programs are limited in presenting the real behaviour of the reinforced concreted under cyclic loading after cracking, a nonlinear finite element analysis will be used to capture critical aspects as: cracking pattern, yielding of reinforcement, crushing of concrete, and rupture of the fibres.

Analytical theoretical models for RC walls with openings strengthened with FRP are missing. The only models developed up to this moment are not referring to the present subject of study and are based on empirical methods. Using an analytical approach, a theoretical model will be derived to account the effectiveness of the FRP strengthening on reinforced concrete large panels with cut-out openings.

REFERENCES

[1] I. Demeter, “Short history of large panel structures in Romania”, *Scientific Bulletin of The “Politehnica” University of Timişoara*, Vol. 51(65), No. 1, 87-94, (2005).

[2] FIB Bulletin 14, *Externally bonded FRP reinforcement for RC structures*, Technical Report. Task

Group 9.3 FRP (Fibre Reinforced Polymer) reinforcement for concrete structures: ISBN 2-88394-054-1, (2001).
[3] K. Neale, *Strengthening reinforced concrete structures with externally bonded fibre reinforced polymers*, Design Manual No. 4, ISIS Canada: ISBN 0-9689007-0-4, (2001).
[4] J.G.Teng, J.F. Chen, S.T. Smith and L. Lam, *FRP strengthened RC structures*, Chichester: Wiley, ISBN 0 471-48706-6, (2002).
[5] B. Täljsten, *FRP strengthening of existing concrete structures – design guidelines (fourth edition)*, Luleå, Sweden: Luleå University of Technology; ISBN 91-89580-03-6, (2006).
[6] M. M. Ehsani and H. Saadatmanesh, "Fiber composites: An economical alternative for retrofitting earthquake-damaged precast-concrete walls", *Earthquake Spectra*, Vol. 13, No. 2, 225-241, (1997).
[7] V. Volnyy and C. P. Pantelides, "Bond length of CFRP composites attached to precast concrete walls", *Journal of Composites for Constructions*, Vol. 3, No. 4, 168-176, (1999).
[8] J. Lombard, D. T. Lau, J. L. Humar, S. Foo and M. S. Cheung, "Seismic strengthening and repair of reinforced concrete shear walls", *Proceedings, Twelfth World Conference on Earthquake Engineering*, New Zealand Society for Earthquake Engineering, Silverstream, New Zeeland, Paper No. 2032, (2000).
[9] M. Iso, Y. Matsuzaki, Y. Sonobe, H. Nakamura and M. Watanabe, "Experimental study on reinforced concrete columns having wing walls retrofitted with continuous fiber sheets", *Proceedings, Twelfth World Conference on Earthquake Engineering*, New Zealand Society for Earthquake Engineering, Silverstream, New Zeeland, Paper No. 1865, (2000).
[10] T. Sugiyama, M. Uemura, H. Fukuyama, K. Nakano and Y. Matsuzaki, "Experimental study on the performance of the RC frame infilled cast-in-place non-structural RC walls retrofitted by using carbon fiber sheets", *Proceedings, Twelfth World Conference on Earthquake Engineering*, New Zealand Society for Earthquake Engineering, Silverstream, New Zealand, Paper No. 2153, (2000).
[11] K. K. Antoniades, T. N. Salonikios and A. J. Kappos, "Cyclic tests on seismically damaged reinforced concrete walls strengthened using fiber-reinforced polymer reinforcement", *ACI Structural Journal*, Vol. 100, No. 4, 510-518, (2003).
[12] K. K. Antoniades, T. N. Salonikios and A. J. Kappos, "Tests on seismically damaged reinforced concrete walls repaired and strengthened using fiber-reinforced polymers", J*ournal of Composites for Constructions*, Vol. 9, No. 3, 236-246, (2005).
[13] J. Paterson and D. Mitchell, "Seismic retrofit of shear walls with headed bars and carbon fiber wrap", *Journal of Structural Engineering*, Vol. 129, No. 5, 606- 614, (2003).
[14] K. Kobayashi, "Innovative application of FRPs for seismic strengthening of RC shear wall", *Proceeding, Fiber-Reinforced Polymer (FRP) Reinforcement for Concrete Structures,* ACI, Farmington Hills, Mi., Paper No. 72, (2005).
[15] Z. J. Li, T. Balendra, K. H. Tan and K. H. Kong, "Finite element modeling of cyclic behaviour of shear wall structure retrofitted using GFRP", *Proceeding, Fiber-Reinforced Polymer (FRP) Reinforcement for Concrete Structures*, ACI, Farmington Hills, Mi., Paper No. 74, (2005).
[16] T. Nagy-György, M. Mosoarca, V. Stoian, J. Gergely and D. Dan, "Retrofit of reinforced concrete shear walls with CFRP composites", *Proceedings, Keep Concrete Attractive*, Hungarian Group of fib, Budapest, Hungary, vol. 2, 897-902, (2005).
[17] ICC-ES, AC125, "Interim criteria for concrete and reinforced and unreinforced masonry strengthening using fiber-reinforced polymer (FRP) composite system", CC EVALUATION SERVICE INC, (2003).
[18] BIOGRAF, *Finite Element Analysis Program*, Faculty of Civil Engineering, Politehnica University of Timisoara, (1998).
[19] A. Carolin, T. Olofsson, B. Täljsten, "Photographic Strain Monitoring for Civil Engineering", *Proceedings, FRP Composites in Civil Engineering, CICE 2004*, Adelaide, Australia, 593-600, (2004).

Doctoral and Licentiate Theses

Division of Structural Engineering
Luleå University of Technology

Doctoral Theses

(Some are downloadable from: http://epubl.ltu.se/1402-1544/index.shtml)

1980 Ulf Arne Girhammar: *Dynamic Fail-Safe Behaviour of Steel Structures*. Doctoral Thesis 1980:060D. pp. 309.

1983 Kent Gylltoft: *Fracture Mechanics Models for Fatigue in concrete Structures*. Doctoral Thesis 1983:25D. pp. 210.

1985 Thomas Olofsson: *Mathematical Modelling of Jointed Rock Masses*. In collaboration with the Division of Rock Mechanics. Doctoral Thesis 1985:42D. pp. 143.

1988 Lennart Fransson: *Thermal ice pressure on structures in ice covers*. Doctoral Thesis 1988:67D. pp. 161.

1989 Mats Emborg: *Thermal stresses in concrete structures at early ages*. Doctoral Thesis 1989:73D. pp. 285.

1993 Lars Stehn: *Tensile fracture of ice. Test methods and fracture mechanics analysis*. Doctoral Thesis 1993:129D, September 1993. pp. 136.

1994 Björn Täljsten: *Plate Bonding. Strengthening of existing concrete structures with ep oxy bonded plates of steel or fibre reinforced plastics*. Doctoral Thesis 1994:152D, August 1994. pp. 283.

1994 Jan-Erik Jonasson: *Modelling of temperature, moisture and stresses in young concrete*. Doctoral Thesis 1994:153D, August 1994. pp. 227.

1995 Ulf Ohlsson: *Fracture Mechanics Analysis of Concrete Structures*. Doctoral Thesis 1995:179D, December 1995. pp. 98.

1998 Keivan Noghabai: *Effect of Tension Softening on the Performance of Concrete Structures*. Doctoral Thesis 1998:21, August 1998. pp. 150.

1999 Gustaf Westman: *Concrete Creep and Thermal Stresses. New creep models and their effects on stress development*. Doctoral Thesis 1999:10. pp. 301. May 1999.

1999 Henrik Gabrielsson: *Ductility in High Performance Concrete Structures. An experimental investigation and a theoretical study of prestressed hollow core slabs and prestressed cylindrical pole elements*. Doctoral Thesis 1999:15,.pp. 283.May 1999.

2000 Patrik Groth: *Fibre Reinforced Concrete - Fracture Mechanics Methods Applied on Self-Compacting Concrete and Energetically Modified Binders*. Doctoral Thesis 2000:04, January 2000. pp. 214. ISBN 978-91-85685-00-4.

2000 Hans Hedlund: *Hardening concrete. Measurements and evaluation of non-elastic deformation and associated restraint stresses*. Doctoral Thesis 2000:25, December 2000. pp. 394. ISBN 91-89580-00-1.

2003 Anders Carolin: *Carbon Fibre Reinforced Polymers for Strengthening of Structural Members*. Doctoral Thesis 2003:18, June 2003. pp. 190. ISBN 91-89580-04-4.

2003 Martin Nilsson: *Restraint Factors and Partial Coefficients for Crack Risk Analyses of Early Age Concrete Structures*. Doctoral Thesis 2003:19, June 2003. pp. 170. ISBN: 91-89580-05-2.

2003 Mårten Larson: *Thermal Crack Estimation in Early Age Concrete – Models and Methods for Practical Application*. Doctoral Thesis 2003:20, June 2003. pp. 190. ISBN 91-86580-06-0.

2005 Erik Nordström: *Durability of Sprayed Concrete. Steel fibre corrosion in cracks*. Doctoral Thesis 2005:02, January 2005. pp. 151. ISBN 978-91-85685-01-1.

2006 Rogier Jongeling: *A Process Model for Work-Flow Management in Construction. Combined use of Location-Based Scheduling and 4D CAD*. Doctoral Thesis 2006:47, October 2006. pp. 191. ISBN 978-91-85685-02-8.

2006 Jonas Carlswärd: *Shrinkage cracking of steel fibre reinforced self compacting concrete overlays - Test methods and theoretical modelling*. Doctoral Thesis 2006:55, December 2006. pp. 250. ISBN 978-91-85685-04-2.

2006 Håkan Thun: *Assessment of Fatigue Resistance and Strength in Existing Concrete Structures*. Doctoral thesis 2006:65, December 2006. pp. 169. ISBN 978-91-85685-03-5.

2007 Lundqvist Joakim: *Numerical Analysis of Concrete Elements Strengthened with Carbon Fiber Reinforced Polymers*. Doctoral thesis 2007:07, March 2007. pp. 50+58. ISBN 978-91-85685-06-6.

2007 Arvid Hejll: *Civil Structural Health Monitoring - Strategies, Methods and Applications*. Doctoral Thesis 2007:10, March 2007. pp. 189. ISBN 978-91-85685-08-0.

2007 Stefan Woksepp: *Virtual reality in construction: tools, methods and processes*. Doctoral thesis 2007:49, November 2007. pp. 191. ISBN 978-91-85685-09-7.

2007 Romuald Rwamamara: *Planning the Healty Construction Workplace through Risk assessment and Design Methods*. Doctoral thesis 2007:74, November 2007. pp. 179. ISBN 978-91-85685-11-0.

2008 Björnar Sand: *Nonlinear finite element simulations of ice forces on offshore structures*. Doctoral Thesis 2008:39, September 2008. pp. 241. ISSN 1402-1544

2008 Bengt Toolanen: *Lean contracting : relational contracting influenced by lean thinking*.Doctoral Thesis 2008:41. October 2008. pp. 190. ISSN 1402-1544

Licentiate Theses

(Some are downloadable from: http://epubl.ltu.se/1402-1757/index.shtml)

1984 Lennart Fransson: *Bärförmåga hos ett flytande istäcke. Beräkningsmodeller och experimentella studier av naturlig is och av is förstärkt med armering*. Licentiate Thesis 1984:012L. pp. 137.

1985 Mats Emborg: *Temperature stresses in massive concrete structures. Viscoelastic models and laboratory tests*. Licentiate Thesis 1985:011L, May 1985. rev. November 1985. pp. 163.

1987 Christer Hjalmarsson: *Effektbehov i bostadshus. Experimentell bestämning av effektbehov i små- och flerbostadshus*. Licentiate Thesis 1987:009L, October 1987. pp. 72.

1990 Björn Täljsten: *Förstärkning av betongkonstruktioner genom pålimning av stålplåtar*. Licentiate Thesis 1990:06L, May 1990. pp. 205.

1990 Ulf Ohlsson: *Fracture Mechanics Studies of Concrete Structures*. Licentiate Thesis 1990:07L, May 1990. pp. 66.

1990 Lars Stehn: *Fracture Toughness of sea ice. Development of a test system based on chevron notched specimens*. Licentiate Thesis 1990:11L, September 1990. pp. 88.

1992 Per Anders Daerga: *Some experimental fracture mechanics studies in mode I of concrete and wood*. Licentiate Thesis 1992:12L, 1ed April 1992, 2ed June 1992. pp. 81.

1993 Henrik Gabrielsson: *Shear capacity of beams of reinforced high performance concrete*. Licentiate Thesis 1993:21L, May 1993. pp. 109.

1995 Keivan Noghabai: *Splitting of concrete in the anchoring zone of deformed bars. A fracture mechanics approach to bond*. Licentiate Thesis 1995:26L, May 1995. pp. 123.

1995 Gustaf Westman: *Thermal cracking in high performance concrete. Viscoelastic models and laboratory tests*. Licentiate Thesis 1995:27L, May 1995. pp. 125.

1995 Katarina Ekerfors: *Mognadsutveckling i ung betong. Temperaturkänslighet, hållfasthet och värmeutveckling*. Licentiate Thesis 1995:34L, October 1995. pp. 137.

1996 Patrik Groth: *Cracking in concrete. Crack prevention with air-cooling and crack distribution with steel fibre reinforcement*. Licentiate Thesis 1996:37L, October 1996. pp. 128.

1996 Hans Hedlund: *Stresses in High Performance Concrete due to Temperature and Moisture Variations at Early Ages*. Licentiate Thesis 1996:38L, October 1996. pp. 240.

2000 Mårten Larson: *Estimation of Crack Risk in Early Age Concrete. Simplified methods for practical use*. Licentiate Thesis 2000:10, April 2000. pp. 170.

2000 Stig Bernander: *Progressive Landslides in Long Natural Slopes. Formation, potential extension and configuration of finished slides in strain- softening soils*. Licentiate Thesis 2000:16, May 2000. pp. 137.

2000 Martin Nilsson: *Thermal Cracking of young concrete. Partial coefficients, restraint effects and influences of casting joints*. Licentiate Thesis 2000:27, October 2000. pp. 267.

2000 Erik Nordström: *Steel Fibre Corrosion in Cracks. Durability of sprayed concrete*. Licentiate Thesis 2000:49, December 2000. pp. 103.

2001 Anders Carolin: *Strengthening of concrete structures with CFRP – Shear strengthening and full-scale applications*. Licentiate thesis 2001:01, June 2001. pp. 120. ISBN 91-89580-01-X.

2001 Håkan Thun: *Evaluation of concrete structures. Strength development and fatigue capacity*. Licentiate thesis 2001:25, June 2001. pp. 164. ISBN 91-89580-08-2.

2002 Patrice Godonue: *Preliminary Design and Analysis of Pedestrian FRP Bridge Deck*. Licentiate thesis 2002:18. pp. 203.

2002 Jonas Carlswärd: *Steel fibre reinforced concrete toppings exposed to shrinkage and temperature deformations*. Licentiate thesis 2002:33, August 2002. pp. 112.

2003 Sofia Utsi: *Self-Compacting Concrete - Properties of fresh and hardening concrete for civil engineering applications*. Licentiate thesis 2003:19, June 2003. pp. 185.

2003 Anders Rönneblad: *Product Models for Concrete Structures - Standards, Applications and Implementations*. Licentiate thesis 2003:22, June 2003. pp. 104.

2003 Håkan Nordin: *Strengthening of Concrete Structures with Pre-Stressed CFRP*. Licentiate Thesis 2003:25, June 2003. pp. 125.

2004 Arto Puurula: *Assessment of Prestressed Concrete Bridges Loaded in Combined Shear, Torsion and Bending*. Licentiate Thesis 2004:43, November 2004. pp. 212.

2004 Arvid Hejll: *Structural Health Monitoring of Bridges. Monitor, Assessand Retrofit*. Licentiate Thesis 2004:46, November 2004. pp. 128.

2005 Ola Enochsson: *CFRP Strengthening of Concrete Slabs, with and without Openings. Experiment, Analysis, Design and Field Application*. Licentiate Thesis 2005:87, November 2005. pp. 154.

2006 Markus Bergström: *Life Cycle Behaviour of Concrete Structures – Laboratory test and probabilistic evaluation*. Licentiate Thesis 2006:59, December 2006. pp. 173. ISBN 978-91-85685-05-9.

2007 Thomas Blanksvärd: *Strengthening of Concrete Structures by Mineral Based Composites*. Licentiate Thesis 2007:15, March 2007. pp. 300. ISBN 978-91-85685-07-3.

2007 Alann André: *Strengthening of Timber Structures with Flax Fibres*. Licentiate Thesis 2007:61, November 2007. pp. 154. ISBN 978-91-85685-10-3.

2008 Peter Simonsson: *Industrial bridge construction with cast in place concrete: New production methods and lean construction philosophies*. Licentiate thesis 2008:17, May 2008. pp. 164. ISBN 978-91-85685-12-7.

2008 Anders Stenlund: *Load carrying capacity of bridges: three case studies of bridges in northern Sweden where probabilistic methods have been used to study effects of monitoring and strengthening*. Licentiate thesis 2008:18, May 2008. pp. 306. ISBN 978-91-85685-13-4.

2008 Anders Bennitz: *Mechanical Anchorage of Prestressed CFRP Tendons - Theory and Tests*. Licentiate thesis 2008:32, November 2008. pp. 319.